

**EVALUATING SHRINKAGE AND CRACKING BEHAVIOR OF
CONCRETE USING RESTRAINED RING
AND FREE SHRINKAGE TESTS**

By

Nathan Tritsch

David Darwin

JoAnn Browning

A Report on Research Sponsored by

THE TRANSPORTATION POOLED FUND PROGRAM
Project No. TPF-5(051)

Structural Engineering and Engineering Materials
SM Report No. 77

**THE UNIVERSITY OF KANSAS CENTER FOR RESEARCH, INC.
LAWRENCE, KANSAS**

January 2005

ABSTRACT

Free shrinkage and restrained ring tests are used to evaluate concrete mixes designed for use in bridge decks. The study consists of a series of preliminary tests and three test programs. In each program, the concrete is exposed to drying conditions of about 21°C (70°F) and 50% relative humidity. The concrete mixes include a typical concrete bridge deck mix from both the Kansas (KDOT) and Missouri (MoDOT) Departments of Transportation, plus seven laboratory mixes, including a basic mix used as a control, a mix similar to the control but made with Type II coarse-ground cement, the control mix cured for 7 and 14 days, a mix with a shrinkage-reducing admixture, a mix with a reduced cement content compared to that of the control, and a mix with quartzite in place of the limestone coarse aggregate used for the other mixes. The free shrinkage specimens were 76 x 76 x 286 mm (3 x 3 x 11_ in.). The concrete ring specimens were 76 mm (3 in.) or 57 mm (2_ in.) thick and 76 mm (3 in.) tall and were cast around a 13 mm (_ in.) thick steel ring with an outside diameter of 324 mm (12_ in.).

The results show that as the paste content of the concrete increases, the ultimate free shrinkage also increases. Replacing Type I/II Portland cement with Type II coarse-ground cement lowers the free shrinkage and shrinkage rate, and adding a shrinkage-reducing admixture significantly reduces these values. Extending the curing time lowers free shrinkage at early ages due to delayed drying and expansion during curing, but does not affect the restrained shrinkage rate at the start of drying. The free shrinkage and restrained shrinkage decrease as the surface to volume ratio of the concrete decreases. One out of 39 restrained rings cracked during testing, and the mix that did crack, MoDOT, had the highest paste content and highest shrinkage rate of all the mixes.

Key Words: concrete; shrinkage; cracking; free shrinkage; restrained shrinkage; ring test; cement; shrinkage-reducing admixture (SRA); curing

ACKNOWLEDGEMENTS

This report is based on research performed by Nathan Tritsch in partial fulfillment of the requirements of the MSCE degree from the University of Kansas. Funding for this research was provided by the Transportation Pooled Fund Program, Project No. TPF-5(051). Participants included the Kansas Department of Transportation, serving as the lead sponsor, and the Delaware Department of Transportation, the Idaho Transportation Department, the Indiana Department of Transportation, the Michigan Department of Transportation, the Minnesota Department of Transportation, the Mississippi Department of Transportation, the Missouri Department of Transportation, the Montana Department of Transportation, the New Hampshire Department of Transportation, the North Dakota Department of Transportation, the Oklahoma Department of Transportation, the South Dakota Department of Transportation, the Texas Department of Transportation, the Wyoming Department of Transportation, and the U.S. Department of Transportation, Federal Highway Administration (FHWA).

Heather McLeod and Maria Voelker assisted by developing the concrete mixes and casting specimens. Lien Gong, Guohui Guo, and Swapnil Deshpande assisted by taking data. Scott Brannon assisted in obtaining the steel pipe. Havens Steel Co., Ottawa, KS, sandblasted the pipe sections, and Louis Voelker polished the steel rings. LRM, Inc. provided concrete materials, and Marty Smith and Jim Weaver assisted in the laboratory and shop. Evan Tritsch and Nathan Marshall assisted during the fabrication of the test facilities and by taking data.

TABLE OF CONTENTS

	<u>Page</u>
ABSTRACT	ii
ACKNOWLEDGEMENTS	iv
LIST OF TABLES	viii
LIST OF FIGURES	xi
CHAPTER 1: INTRODUCTION	1
1.1 General.....	1
1.2 Types of Shrinkage	2
1.3 Factors that Affect Shrinkage	3
1.4 Restraint	5
1.5 Ring Tests	6
1.5.1 Ring Test Background	6
1.5.2 AASHTO Ring Test.....	7
1.5.3 ASTM Ring Test.....	8
1.5.4 Geometry of the Ring Test.....	9
1.6 Free Shrinkage Test	10
1.7 Previous Work	11
1.7.1 Plate Tests	11
1.7.2 Linear Tests.....	14
1.7.3 Ring Tests	20
1.7.4 Variations of the Ring Test.....	29
1.7.5 Summary of Previous Work.....	32
1.8 Objective and Scope	33

CHAPTER 2: EXPERIMENTAL PROGRAM	34
2.1 General.....	34
2.2 Restrained Ring Test.....	34
2.2.1 Construction of Forms	35
2.2.2 Restraining Ring Preparation.....	36
2.2.3 Instrumentation	37
2.2.4 Data Acquisition	38
2.3 Free Shrinkage Test	38
2.4 Temperature and Humidity	38
2.5 Materials	39
2.6 Concrete Mixes	41
2.7 Preliminary Testing.....	42
2.7.1 Mixes.....	43
2.8 Program 1.....	43
2.8.1 Mixes.....	44
2.9 Replicate Free Shrinkage Tests from Program 1	45
2.9.1 Mixes.....	46
2.10 Program 2.....	46
2.10.1 Mixes.....	48
2.11 Mixing.....	50
2.12 Casting	51
2.13 Curing	51
2.14 Drying.....	52
CHAPTER 3: RESULTS AND EVALUATION	53
3.1 Preliminary Testing.....	53
3.2 Program 1.....	55

3.3	Replication of Program 1 Free Shrinkage Tests	61
3.4	Program 2.....	62
3.5	Additional Analyses of Results.....	69
3.5.1	Number of Drying Surfaces	70
3.5.2	Statistical Certainty of Results.....	71
3.5.3	Free Shrinkage as a Prediction of Restrained	74
	Shrinkage Rate	
	CHAPTER 4: SUMMARY AND CONCLUSIONS	75
4.1	Summary.....	75
4.2	Conclusions.....	76
4.3	Recommendations.....	77
	REFERENCES.....	78
	TABLES.....	82
	FIGURES.....	96
	APPENDIX A	128

LIST OF TABLES

<u>Table</u>	<u>Page</u>
2.1 Sand Gradations	82
2.2 Pea Gravel Gradations	82
2.3 Limestone Gradations	83
2.4 Quartzite Gradation.....	83
2.5 Mix Proportions for Preliminary Testing.....	84
2.6 Mix Proportions and Concrete Properties for Program 1	85
2.7 Mix Proportions and Concrete Properties for Replication of Program 1 Free Shrinkage Tests	86
2.8a Mix Proportions and Concrete Properties for Program 2	87
2.8b Mix Proportions and Concrete Properties for Program 2 (cont.).....	88
3.1 Summary of Free Shrinkage Data for Program 1	89
3.2 Summary of Slope Analysis for Program 1 Ring Test	89
3.3 Summary of Free Shrinkage Data for the Replication of Program 1.....	89
3.4a Summary of Free Shrinkage Data for Program 2	90
3.4b Summary of Free Shrinkage Data for Program 2 (cont.).....	90
3.5 Summary of Slope Analysis for Program 2 Ring Test	91
3.6 Student's t-test Results for Program 1 30-day Free Shrinkage Data	92
3.7 Student's t-test Results for Program 1 150-day Free Shrinkage Data	92
3.8 Student's t-test Results for Program 1 Ring Test Data.....	93
3.9 Student's t-test Results for the Replication of Program 1 30-day Free Shrinkage Data	93

3.10	Student's t-test Results for the Replication of Program 1 150-day Free Shrinkage Data	93
3.11	Student's t-test Results for Program 2 30-day Free Shrinkage Data	94
3.12	Student's t-test Results for Program 2 150-day Free Shrinkage Data	94
3.13	Student's t-test Results for Program 2 Ring Test Data	95
A3.1	Control, Batch 55: Slope Analysis of Shrinkage Versus Square Root of Time Data for Ring Tests	128
A3.2	Type II coarse-ground, Batch 56: Slope Analysis of Shrinkage Versus Square Root of Time Data for Ring Tests	128
A3.3	MoDOT, Batch 57: Slope Analysis of Shrinkage Versus Square Root of Time Data for Ring Tests	129
A 3.4	KDOT, Batch 58: Slope Analysis of Shrinkage Versus Square Root of Time Data for Ring Tests	129
A3.5	KDOT, Batch 130: Slope Analysis of Shrinkage Versus Square Root of Time Data for Ring Tests	130
A3.6	MoDOT, Batch 132: Slope Analysis of Shrinkage Versus Square Root of Time Data for Ring Tests	130
A3.7	Control, Batch 138: Slope Analysis of Shrinkage Versus Square Root of Time Data for Ring Tests	131
A3.8	7-day cure, Batch 140: Slope Analysis of Shrinkage Versus Square Root of Time Data for Ring Tests	131
A3.9	14-day cure, Batch 143: Slope Analysis of Shrinkage Versus Square Root of Time Data for Ring Tests	132
A3.10	Type II coarse-ground, Batch 145: Slope Analysis of Shrinkage Versus Square Root of Time Data for Ring Tests	132
A3.11	SRA, Batch 147: Slope Analysis of Shrinkage Versus Square Root of Time Data for Ring Tests	133
A3.12	497, Batch 149: Slope Analysis of Shrinkage Versus Square Root of Time Data for Ring Tests	133

A3.13 Quartzite, Batch 159: Slope Analysis of Shrinkage Versus Square134
Root of Time Data for Ring Tests

LIST OF FIGURES

<u>Figure</u>		<u>Page</u>
2.1	Ring Specimen Form Layout.....	96
2.2	Clamping Device Detail.....	96
2.3	Hold-down Bolt Detail.....	97
2.4	Schematic of Data Acquisition	97
2.5	Free Shrinkage Specimen Mold.....	98
2.6	Cross-section of Free Shrinkage Specimen	98
2.7	Ring Details for Preliminary Testing and Program 1	99
2.8	Ring Details for Program 2.....	99
3.1	Free Shrinkage Test. Preliminary free shrinkage, P1.	100
3.2	Restrained Ring Test. Strain gage data for preliminary ring, P1.....	100
3.3	Free Shrinkage Test. Preliminary free shrinkage, P2.	101
3.4	Restrained Ring Test. Strain gage data for preliminary ring, P2.....	101
3.5	Free Shrinkage Test. Preliminary free shrinkage, P3.	102
3.6	Restrained Ring Test. Strain gage data for preliminary ring, P3.....	102
3.7	Crack observed in ring P2 on day 27	103
3.8	Crack observed in ring P3 on day 6.....	103
3.9	Average free shrinkage curves for preliminary tests	104
3.10	Average restrained shrinkage curves for preliminary tests.....	104
3.11	Free Shrinkage Test, Program 1. Control mix, Batch 55.....	105

3.12	Free Shrinkage Test, Program 1. Type II coarse-ground cement mix, ...	105
	Batch 56.	
3.13	Free Shrinkage Test, Program 1. MoDOT mix, Batch 57.	106
3.14	Free Shrinkage Test, Program 1. KDOT mix, Batch 58.	106
3.15	Free Shrinkage Test, Program 1. Average free shrinkage curves for	107
	all specimens in a batch. First 30 days.	
3.16	Free Shrinkage Test, Program 1. Average free shrinkage curves for	107
	all specimens in a batch.	
3.17	Ring Test, Program 1. Control mix, Batch 55. Average adjusted	108
	curve for each ring.	
3.18	Ring Test, Program 1. Type II C.G. mix, Batch 56. Average	108
	adjusted curve for each ring.	
3.19	Ring Test, Program 1. MoDOT mix, Batch 57. Average adjusted.....	109
	curve for each ring.	
3.20	Ring Test, Program 1. KDOT mix, Batch 58. Average adjusted	109
	curve for each ring.	
3.21	Free Shrinkage Test, Replication of Program 1. Control mix, Batch.....	110
	81.	
3.22	Free Shrinkage Test, Replication of Program 1. Type II coarse-	110
	ground cement mix, Batch 82.	
3.23	Free Shrinkage Test, Replication of Program 1. MoDOT mix, Batch ...	111
	83.	
3.24	Free Shrinkage Test, Replication of Program 1. KDOT mix Batch.....	111
	84.	
3.25	Free Shrinkage Test, Replication of Program 1. Average free.....	112
	shrinkage curves for all specimens in a batch. First 30 days.	
3.26	Free Shrinkage Test, Replication of Program 1. Average free.....	112
	shrinkage curves for all specimens in a batch.	

- 3.27 Free Shrinkage Test, Program 2. Average free shrinkage curves for113
all specimens in a batch.
- 3.28 Free Shrinkage Test, Program 2. Average free shrinkage curves for114
all specimens in a batch. First 30 days of drying.
- 3.29 Free Shrinkage Test, Program 2. Average free shrinkage curves for115
all specimens in a batch.
- 3.30 Free Shrinkage test, Program 2. Average free shrinkage curves for116
all specimens in a batch. Drying begins on day 0.
- 3.31 Ring Test, Program 2. KDOT mix, Batch 130. Average adjusted117
curve for each ring.
- 3.32 Ring Test, Program 2. MoDOT mix, Batch 132. Average adjusted.....117
curve for each ring.
- 3.33 Ring Test, Program 2. Control mix, Batch 138. Average adjusted118
curve for each ring.
- 3.34 Ring Test, Program 2. 7-day cure mix, Batch 140. Average adjusted....118
curve for each ring.
- 3.35 Ring Test, Program 2. 14-day cure mix, Batch 143. Average.....119
adjusted curve for each ring.
- 3.36 Ring Test, Program 2. Type II C.G. mix, Batch 145. Average119
adjusted curve for each ring.
- 3.37 Ring Test, Program 2. SRA mix, Batch 147. Average adjusted.....120
curve for each ring.
- 3.38 Ring Test, Program 2. 497 mix, Batch 149. Average adjusted.....120
curve for each ring.
- 3.39 Ring Test, Program 2. Quartzite mix, Batch 159. Average adjusted.....121
curve for each ring.
- 3.40 Crack observed in MoDOT Ring A on day 103.121
- 3.41 Comparison of the number of drying sides (2 or all) versus free122
shrinkage at 7, 30, 90, and 150 days for the MoDOT mix.

3.42	Comparison of the number of drying sides (2 or all) versus free shrinkage at 7, 30, 90, and 150 days for the KDOT mix.	122
3.43	Comparison of the number of drying sides (2 or all) versus free shrinkage at 7, 30, 90, and 150 days for the control mix.	123
3.44	Comparison of the number of drying sides (2 or all) versus free shrinkage at 7, 30, 90, and 150 days for the Type II coarse-ground mix.	123
3.45	Comparison of the average shrinkage rate versus drying surfaces for the restrained ring test.	124
3.46	Restrained shrinkage rate versus 30-day free shrinkage for Program 1.	125
3.47	Restrained shrinkage rate versus 30-day free shrinkage for Program 1. KDOT data excluded.	125
3.48	Restrained shrinkage rate versus 30-day free shrinkage for Program 1 rings and the replication of Program 1 free shrinkage specimens.	126
3.49	Restrained shrinkage rate versus 30-day free shrinkage for Program 2.	127
A3.1a	Ring Test, Program 1. Control, Batch 55, Ring A.	135
A3.1b	Ring Test, Program 1. Control, Batch 55, Ring A. Shrinkage versus the square root of time.	135
A3.2a	Ring Test, Program 1. Control, Batch 55, Ring B.	136
A3.2b	Ring Test, Program 1. Control, Batch 55, Ring B. Shrinkage versus the square root of time.	136
A3.3a	Ring Test, Program 1. Control, Batch 55, Ring C.	137
A3.3b	Ring Test, Program 1. Control, Batch 55, Ring C. Shrinkage versus the square root of time.	137
A3.4a	Ring Test, Program 1. Type II C.G., Batch 56, Ring A.	138
A3.4b	Ring Test, Program 1. Type II C.G., Batch 56, Ring A. Shrinkage versus the square root of time.	138
A3.5a	Ring Test, Program 1. Type II C.G., Batch 56, Ring B.	139

A3.5b	Ring Test, Program 1. Type II C.G., Batch 56, Ring B. Shrinkage.....	139
	versus the square root of time.	
A3.6a	Ring Test, Program 1. Type II C.G., Batch 56, Ring C	140
A3.6b	Ring Test, Program 1. Type II C.G., Batch 56, Ring C. Shrinkage.....	140
	versus the square root of time.	
A3.7a	Ring Test, Program 1. MoDOT, Batch 57, Ring A.....	141
A3.7b	Ring Test, Program 1. MoDOT, Batch 57, Ring A. Shrinkage versus ...	141
	the square root of time.	
A3.8a	Ring Test, Program 1. MoDOT, Batch 57, Ring B.....	142
A3.8b	Ring Test, Program 1. MoDOT, Batch 57, Ring B. Shrinkage versus ...	142
	the square root of time.	
A3.9a	Ring Test, Program 1. MoDOT, Batch 57, Ring C.....	143
A3.9b	Ring Test, Program 1. MoDOT, Batch 57, Ring C. Shrinkage versus ...	143
	the square root of time.	
A3.10a	Ring Test, Program 1. KDOT, Batch 57, Ring A	144
A3.10b	Ring Test, Program 1. KDOT, Batch 57, Ring A. Shrinkage versus.....	144
	the square root of time.	
A3.11a	Ring Test, Program 1. KDOT, Batch 57, Ring B	145
A3.11b	Ring Test, Program 1. KDOT, Batch 57, Ring B. Shrinkage versus.....	145
	the square root of time.	
A3.12a	Ring Test, Program 1. KDOT, Batch 57, Ring C	146
A3.12b	Ring Test, Program 1. KDOT, Batch 57, Ring C. Shrinkage versus.....	146
	the square root of time.	
A3.13	Free Shrinkage Test, Program 2. KDOT mix, Batch 130.....	147
A3.14	Free Shrinkage Test, Program 2. MoDOT mix, Batch 132	147
A3.15	Free Shrinkage Test, Program 2. Control mix, Batch 138.....	148

A3.16	Free Shrinkage Test, Program 2. 7-day cure mix, Batch 140.....	148
A3.17	Free Shrinkage Test, Program 2. 14-day mix, Batch 143.....	149
A3.18	Free Shrinkage Test, Program 2. Type II coarse-ground cement mix, ... Batch 145	149
A3.19	Free Shrinkage Test, Program 2. SRA mix, Batch 147.....	150
A3.20	Free Shrinkage Test, Program 2. 497 mix, Batch 149.....	150
A3.21	Free Shrinkage Test, Program 2. Quartzite mix, Batch 159.....	151
A3.22a	Ring Test, Program 2. KDOT mix, Batch 130, Ring A.....	152
A3.22b	Ring Test, Program 2. KDOT mix, Batch 130, Ring A. Shrinkage..... versus the square root of time.	152
A3.23a	Ring Test, Program 2. KDOT mix, Batch 130, Ring B.....	153
A3.23b	Ring Test, Program 2. KDOT mix, Batch 130, Ring B. Shrinkage..... versus the square root of time.	153
A3.24a	Ring Test, Program 2. KDOT mix, Batch 130, Ring C.....	154
A3.24b	Ring Test, Program 2. KDOT mix, Batch 130, Ring C. Shrinkage..... versus the square root of time.	154
A3.25a	Ring Test, Program 2. MoDOT mix, Batch 132, Ring A.....	155
A3.25b	Ring Test, Program 2. MoDOT mix, Batch 132, Ring A. Shrinkage.... versus the square root of time.	155
A3.26a	Ring Test, Program 2. MoDOT mix, Batch 132, Ring B.....	156
A3.26b	Ring Test, Program 2. MoDOT mix, Batch 132, Ring B. Shrinkage.... versus the square root of time.	156
A3.27a	Ring Test, Program 2. MoDOT mix, Batch 132, Ring C.....	157
A3.27b	Ring Test, Program 2. MoDOT mix, Batch 132, Ring C. Shrinkage.... versus the square root of time.	157
A3.28a	Ring Test, Program 2. Control mix, Batch 138, Ring A.....	158

A3.28b	Ring Test, Program 2. Control mix, Batch 138, Ring A. Shrinkage158 versus the square root of time.	158
A3.29a	Ring Test, Program 2. Control mix, Batch 138, Ring B	159
A3.29b	Ring Test, Program 2. Control mix, Batch 138, Ring B. Shrinkage.....159 versus the square root of time.	159
A3.30a	Ring Test, Program 2. Control mix, Batch 138, Ring C	160
A3.30b	Ring Test, Program 2. Control mix, Batch 138, Ring C. Shrinkage.....160 versus the square root of time.	160
A3.31a	Ring Test, Program 2. 7-day cure, Batch 140, Ring A	161
A3.31b	Ring Test, Program 2. 7-day cure, Batch 140, Ring A. Shrinkage.....161 versus the square root of time.	161
A3.32a	Ring Test, Program 2. 7-day cure, Batch 140, Ring B.....	162
A3.32b	Ring Test, Program 2. 7-day cure, Batch 140, Ring B. Shrinkage162 versus the square root of time.	162
A3.33a	Ring Test, Program 2. 7-day cure, Batch 140, Ring C.....	163
A3.33b	Ring Test, Program 2. 7-day cure, Batch 140, Ring C. Shrinkage163 versus the square root of time.	163
A3.34a	Ring Test, Program 2. 14-day cure, Batch 143, Ring A	164
A3.34b	Ring Test, Program 2. 14-day cure, Batch 143, Ring A. Shrinkage.....164 versus the square root of time.	164
A3.35a	Ring Test, Program 2. 14-day cure, Batch 143, Ring B.....	165
A3.35b	Ring Test, Program 2. 14-day cure, Batch 143, Ring B. Shrinkage165 versus the square root of time.	165
A3.36a	Ring Test, Program 2. 14-day cure, Batch 143, Ring C.....	166
A3.36b	Ring Test, Program 2. 14-day cure, Batch 143, Ring C. Shrinkage166 versus the square root of time.	166

A3.37a	Ring Test, Program 2. Type II C.G., Batch 145, Ring A.....	167
A3.37b	Ring Test, Program 2. Type II C.G., Batch 145, Ring A. Shrinkage versus the square root of time.	167
A3.38a	Ring Test, Program 2. Type II C.G., Batch 145, Ring B.....	168
A3.38b	Ring Test, Program 2. Type II C.G., Batch 145, Ring B. Shrinkage..... versus the square root of time.	168
A3.39a	Ring Test, Program 2. Type II C.G., Batch 145, Ring C.....	169
A3.39b	Ring Test, Program 2. Type II C.G., Batch 145, Ring C. Shrinkage..... versus the square root of time.	169
A3.40a	Ring Test, Program 2. SRA mix, Batch 147, Ring A.....	170
A3.40b	Ring Test, Program 2. SRA mix, Batch 147, Ring A. Shrinkage..... versus the square root of time.	170
A3.41a	Ring Test, Program 2. SRA mix, Batch 147, Ring B.....	171
A3.41b	Ring Test, Program 2. SRA mix, Batch 147, Ring B. Shrinkage..... versus the square root of time.	171
A3.42a	Ring Test, Program 2. SRA mix, Batch 147, Ring C.....	172
A3.42b	Ring Test, Program 2. SRA mix, Batch 147, Ring C. Shrinkage..... versus the square root of time.	172
A3.43a	Ring Test, Program 2. 497 mix, Batch 149, Ring A.....	173
A3.43b	Ring Test, Program 2. 497 mix, Batch 149, Ring A. Shrinkage..... versus the square root of time.	173
A3.44a	Ring Test, Program 2. 497 mix, Batch 149, Ring B.....	174
A3.44b	Ring Test, Program 2. 497 mix, Batch 149, Ring B. Shrinkage..... versus the square root of time.	174
A3.45a	Ring Test, Program 2. 497 mix, Batch 149, Ring C.....	175
A3.45b	Ring Test, Program 2. 497 mix, Batch 149, Ring C. Shrinkage..... versus the square root of time.	175

A3.46a	Ring Test, Program 2. Quartzite mix, Batch 159, Ring A	176
A3.46b	Ring Test, Program 2. Quartzite mix, Batch 159, Ring A. Shrinkage... versus the square root of time.	176
A3.47a	Ring Test, Program 2. Quartzite mix, Batch 159, Ring B	177
A3.47b	Ring Test, Program 2. Quartzite mix, Batch 159, Ring B. Shrinkage... versus the square root of time.	177
A3.48a	Ring Test, Program 2. Quartzite mix, Batch 159, Ring C	178
A3.48b	Ring Test, Program 2. Quartzite mix, Batch 159, Ring C. Shrinkage... versus the square root of time.	178

CHAPTER 1: INTRODUCTION

1.1 GENERAL

Shrinkage cracking of concrete is a significant problem in bridge decks. Cracking diminishes the structural integrity, reduces the durability, increases the maintenance costs, and shortens the service life of bridges. Cracks provide a path for ingress of water and deicing chemicals to penetrate the concrete, which can bring about corrosion of the reinforcing steel or freeze-thaw problems. Cracks may also extend through the entire depth of the deck, which can lead to deterioration of the girders. In the 1960s, the Portland Cement Association investigated the durability of bridge decks, and subsequently, attempts have been made to ameliorate the degree of cracking. While the concrete industry has experienced changes in design specifications, construction techniques, and materials over the years, cracking remains a difficult problem. A 2002 Federal Highway Administration report, with deck condition being a primary factor, concluded that 25% of the bridges in Kansas were structurally deficient or obsolete. In 2002, a study estimated that, each year, the direct costs associated with corrosion of highway bridges totaled \$8.3 billion. The indirect costs to the users were ten times that value (Yunovich et al. 2002).

Shrinkage cracking occurs when the tensile stresses due to restrained volume contraction exceed the tensile strength of the concrete. Cracking in service depends on many variables, including shrinkage potential, degree of restraint, construction methods, and environmental conditions. Many researchers have performed laboratory studies to evaluate the shrinkage and cracking potential of concrete and cement-based materials. This report reviews some of this work and describes an experimental study that uses the restrained ring and free shrinkage prism tests to evaluate a series of mix designs, some of which were optimized to reduce shrinkage and shrinkage induced cracking.

1.2 TYPES OF SHRINKAGE

Concrete can experience volume changes at different ages and under a variety of conditions. Plastic, drying, and autogenous shrinkage, to various degrees, contribute to cracking in concrete structures.

Plastic shrinkage occurs in fresh concrete. In this semi-fluid or plastic state, water fills the voids between cement particles. At exposed surfaces, this water can be removed by exterior forces such as evaporation. When the rate of removal exceeds the rate at which bleed water rises to the surface, menisci are formed. The menisci exert negative capillary pressures on the cement skeleton, and these negative pressures result in a net volume reduction in the cement (Mindess, Young, and Darwin 2003). Since the volume reduction occurs only at the exposed surface, tensile stresses result that cause cracks to form in the plastic concrete.

Drying shrinkage is the strain caused by the loss of adsorbed water from the network of capillary pores within hardened cement paste. The three mechanisms by which this loss of water causes volume changes are capillary stress, disjoining pressure, and surface free energy. Capillary stress occurs at relative humidities between 45 and 95% when a meniscus forms on the adsorbed water between cement surfaces. The meniscus is under hydrostatic tension and places the cement in hydrostatic compression. This compressive stress reduces the size of the capillary pores, and thus causes a reduction in the overall volume of the cement paste. Capillary stress is a function of the capillary pore size, surface tension of the water, and the relative humidity. Disjoining pressure is the pressure caused by adsorbed water confined within the small spaces of the capillary pores. In this narrow space, the water exerts pressure on the adjacent cement surfaces. When the adsorbed water is lost, the disjoining pressure is reduced and the cement particles are drawn closer together, which results in shrinkage. Changes in surface energy are the cause of shrinkage at relative humidities below 45%. The last molecular layers of water

surrounding cement particles are the most strongly adsorbed. This water has a high surface tension and exerts a compressive force on the cement particle, causing a net reduction in volume (Mindess, Young, and Darwin 2003).

Autogenous shrinkage is another type of concrete shrinkage that primarily occurs in concrete with low water-cement ratios. It occurs due to self-desiccation, a process where the cement continues to hydrate under conditions that do not allow the addition of more water to the paste. Except for concretes with low water-cement ratios, autogenous shrinkage is generally small and is commonly included as part of the drying shrinkage (Neville 1996).

1.3 FACTORS THAT AFFECT SHRINKAGE

Cement paste (water and cementitious materials) is the portion of concrete that most commonly experiences volume changes. Therefore, the quantities of water and cementitious materials, and thus the water-cement ratio, are important factors that influence shrinkage behavior. Shrinkage increases with increasing water-cement ratios. The water-cement ratio controls the evaporable water content per unit volume of paste and the rate at which water can reach the surface. For mixes with the same water-cement ratio, shrinkage increases with increases in cement content because the volume of hydrated cement, or paste, also increases (Shoya 1979). The water content, however, may not be as influential on shrinkage. At a constant water content, increasing the cement content may have no effect or may even decrease shrinkage due to reduced permeability caused by the reduced water-cement ratio (Shoya 1979). However, the water content is important in that it affects the volume of aggregate in a mix (Neville 1996). Shrinkage increases at a much greater rate with decreasing aggregate volumes than it does with increasing water-cement ratios (Ödman 1968).

Cement fineness can affect the drying shrinkage of concrete. Larger cement particles that do not undergo full hydration can provide a restraining effect similar to that of aggregates. For this reason, shrinkage values tend to be greater for finer cements (Mehta 1994). Chariton and Weiss (2002) observed that mortar made with finer cement experienced lower weight loss due to drying than mortar made with coarser cement. They explained that the increased surface area of the finer cement increased the amount of pore water that was hydrated, and therefore decreased the amount of evaporable water. They also stated that the finer cement resulted in a finer pore structure, which caused higher capillary stresses and increased shrinkage.

Powers (1959) argues that the length of curing is relatively unimportant in regard to overall concrete shrinkage. Longer curing times reduce the amount of unhydrated cement particles, which previously restrained the paste from shrinking. Curing also increases the modulus of elasticity and reduces the rate of creep of the paste. These effects lead to greater cracking potential when the paste is severely restrained. Microcracking of the paste around the aggregates, however, can diminish the total shrinkage in the concrete.

Neville (1996) argues that the most important influence on shrinkage is the aggregate. The aggregate restrains shrinkage of the cement paste, and the use of more aggregate allows for a mix with less paste. Aggregates provide restraint because they do not undergo volume changes due to changing moisture conditions. The amount, size, and stiffness of an aggregate determine how much restraint it provides (Mindess, Young, and Darwin 2003). Pickett (1956) reports that shrinkage was reduced by 20% for mixes with the same water-cement ratio in which the aggregate content was increased from 71% to 74%. The amount of restraint provided by the aggregate depends on its elastic properties. Reichard (1964) observed that concrete shrinkage was directly related to the modulus of elasticity and compressibility of the aggregate. Granite, limestone, and quartzite typically do not shrink (Neville 1996).

Lightweight aggregates with low moduli of elasticity exhibit higher shrinkage (Mindess, Young, and Darwin 2003).

Mehta (1994) states that drying shrinkage tends to increase when admixtures that increase the water requirement of a mix are used. However, drying shrinkage is not reduced by using water-reducing admixtures that reduce the water content. Brooks and Neville (1992) report that shrinkage has been found to increase by 10 to 20% with the use of superplasticizers. Air entrainment is believed to have no influence on shrinkage (Neville 1996).

Many researchers (Karagular and Shah (1990), Shah, Karaguler, and Sarigaphuti (1992), Folliard and Berke (1997), Shah, Weiss, and Yang (1998), Weiss and Shah (2002), See, Attiogbe, and Miltenberger (2003)) have observed improved shrinkage resistance and cracking behavior by using a shrinkage-reducing admixture (SRA) in concrete. SRAs work by reducing the surface tension of the mix water, which in turn reduces the stresses in the capillary pores (Shah, Weiss, and Yang 1998). Shah et al. (1992) found that free shrinkage decreased with increasing amounts of SRA and that crack widths were reduced compared to mixes of plain concrete.

1.4 RESTRAINT

Concrete in bridge decks is not allowed to shrink freely. Fixed ends, reinforcing bars, and the girder system can all restrain the concrete deck from shrinking, which may ultimately lead to cracking. In a crack survey of forty bridge decks in northeast Kansas, Schmitt and Darwin (1995) observed an increase in cracking near the abutments in bridges with fixed-end girders. Krauss and Rogalla (1996) reported that it is widely accepted that deck cracking is greater in continuous bridges versus simply-supported structures. Also, steel girders are believed to provide the greatest restraint because they do not shrink. In addition, steel has a

higher coefficient of thermal expansion than concrete. In the case of restraint provided by girders, differential shrinkage movement can occur between the top and bottom surfaces of the deck due to thermal effects or drying conditions. The bottom surface of the deck is restricted from shrinking by the girders, while the top surface is relatively unrestrained. Tensile stresses then develop at the top surface of the concrete as it dries, and if they exceed the tensile strength of the concrete, cracks may form.

1.5 RING TESTS

As will be discussed in more detail in Section 1.7, many researchers have attempted to evaluate the shrinkage and cracking behavior of concrete and cement-based materials under restrained conditions. The most common procedure is the restrained ring test. Flat panel specimens and linear specimens have also been used and these are discussed later in the section on Previous Work.

1.5.1 RING TEST BACKGROUND

The ring test was designed to restrict concrete shrinkage and induce cracking so that the cracking tendencies of different mixes could be compared under similar conditions. Weiss and Shah (2002) assumed that the concrete ring simulated an infinitely long pavement restrained from shrinking freely. Krauss and Rogalla (1996) summarized the usefulness of the ring test. First, it is simple and the test apparatus is relatively inexpensive to construct. Analysis does not require the use of complex calculations or assumptions of early-age concrete behavior. The effects of stress development, volume deformation, and creep at early ages can all be considered simultaneously, and the stresses are similar to in-service stresses. Thus, the most important factor is that all of the material variables affecting cracking can be

evaluated together using a single procedure. The ring test also produces easily visible cracks.

In the restrained ring test, a concrete ring is cast around an inner steel ring. The steel ring restrains the shrinking concrete, producing an internal pressure on the concrete ring, which causes tensile hoop stresses to develop in the concrete. When the tensile stresses minus the relaxation due to creep exceed the tensile strength of the concrete, cracking will occur. The steel ring can be instrumented to monitor the strain development and determine time to cracking.

The first ring tests were conducted by Carlson and Reading (1988) between 1939 and 1942. For many years, no standard procedure existed for conducting the test. The American Association of State Highway and Transportation Officials proposed AASHTO PP34-98 “Practice for Estimating the Crack Tendency of Concrete” (AASHTO Provisional 1998), but it has not yet been approved. The American Society of Testing and Materials (ASTM) recently approved the “Standard Test Method for Determining Age at Cracking and Induced Tensile Stress Characteristics of Mortar and Concrete under Restrained Shrinkage (ASTM C 1581-04).”

1.5.2 AASHTO RING TEST

This test method is used to compare concrete mixes for restrained shrinkage cracking potential. Factors such as aggregate source and gradation, aggregate-paste bond, cement type, cement content, water content, mineral admixtures, fiber reinforcement, and chemical admixtures can be evaluated. The test does not predict concrete cracking in actual service, but rather compares the relative cracking potential of different mixes. The steel ring used in this test is 9.5 ± 0.4 mm ($1/2 \pm 1/64$ in.) thick, 152 mm (6 in.) high, and has an outside diameter of 305 mm (12 in.). The outer surface is machined and polished to be round and true. A 457 mm (18 in.)

diameter outer mold produces a concrete ring that is 76 mm (3 in.) thick. Four strain gages are mounted on the inner surface of the steel ring at equidistant points at midheight. The outer forms are removed from the concrete 24 ± 1 hour after casting, and after curing, the top and bottom surfaces of the ring are sealed. The specimens are dried at 69.8 ± 0.9 °C (21 ± 1.7 °F) and $50 \pm 4\%$ relative humidity. Strain gage data is recorded every 30 minutes beginning as soon after casting as possible. Every 2 to 3 days, the rings are visually inspected for cracks. After the concrete cracks, the time-to-cracking is recorded and the crack width is measured at three locations along its length.

1.5.3 ASTM RING TEST

This test can be used to evaluate and select cement-based materials on the basis of potential for early age cracking. Concrete mix parameters that can be tested include aggregate source and gradation, cement type, cement content, water content, and additional cementitious materials. The mixes can be evaluated by comparing the age of cracking or the rate of stress development at the end of the test in cases where the ring does not crack. This test method uses a 13 mm ($\frac{1}{2}$ in.) thick, 152 mm (6 in.) high steel ring with an outside diameter of 330 mm (13 in.). The ring is machined and polished to make it round and true. The outer mold has a diameter of 406 mm (16 in.), producing a concrete ring 38 mm ($1\frac{1}{2}$ in.) thick. This restricts the maximum aggregate size to 13 mm ($\frac{1}{2}$ in.). Two strain gages are mounted at the midheight of the inner surface of the steel ring. Data is recorded every 30 minutes using a data acquisition (DA) system. Within 10 minutes after casting, the rings are moved to the testing environment, and the strain gages are connected to the DA within the next two minutes. The specimens are demolded after 24 hours and then cured. After curing, the top surface of the rings is sealed to allow drying from the outer circumference only. The testing environment is maintained at 22.8 ± 1.7 °C (73 ± 3 °F) and $50 \pm$

4% relative humidity. The rings are monitored by examining the strain gage data and visually inspecting the rings every 3 days. The test should continue for at least 28 days of drying.

1.5.4 GEOMETRY OF THE RING TEST

The dimensions of the ring test play a large role in the behavior of the concrete. Krauss and Rogalla (1996) performed a finite element analysis on the ring test. They evaluated the geometry of both the steel and concrete rings by subjecting the concrete to either a uniform shrinkage stress or a shrinkage stress that increased linearly from the steel-concrete interface; simulating drying from either the top and bottom surface or the circumferential surface. They found that the concrete shrinkage stresses and cracking tendency were not significantly different for steel ring thicknesses between 13 mm (½ in.) and 25 mm (1 in.). They also observed increased steel stresses for thinner steel rings and increasing concrete stresses with larger ring diameters. As the height of the rings increased from 76 mm (3 in.) to 152 mm (6 in.), the concrete shrinkage stresses decreased.

See et al. (2003) used concrete rings where the height was four times the radial thickness and drying occurred on the circumferential surface. They assumed that drying shrinkage was uniform along the height of the ring because of this geometry. They also assumed that the concrete rings were under uniaxial tensile stress due to the internal pressure applied to the concrete by the steel ring. For a 152 mm (6 in.) tall, 12.5 mm (½ in.) thick steel ring and concrete rings with inner and outer radii of 165 mm (6½ in.) and 203 mm (8 in.), respectively, and subjected to an internal pressure, the hoop stresses at both the inner and outer edges were within 10% of the average hoop stress. The average radial compressive stress was about 10% of the average hoop stress, compared to about 25% for the dimensions of the AASHTO test.

See et al. (2003) also calculated the degree of restraint R , the ratio of the stiffness of the steel ring to the combined stiffness of the steel and concrete rings.

$$R = \frac{A_{st} E_{st}}{A_{st} E_{st} + A_c E_c} \quad (1.1)$$

where A_{st} and A_c are the cross-sectional areas of the steel and concrete, respectively, and E_{st} and E_c are the corresponding moduli of elasticity. Depending on the modulus of elasticity of the concrete, the authors calculated a degree of restraint of 70 to 75% for their setup. For the AASHTO geometry, the degree of restraint is between 55 and 60%, indicating that, under similar conditions, it will take longer for the rings to crack in the AASHTO test. Krauss and Rogalla (1996) stated that the amount of restraint increased as the diameter of the steel ring increased. They believed that a 305 mm (12 in.) diameter steel ring was a good approximation of the in-service case of large steel girders.

Attigbe et al. (2004) determined that the time-to-cracking was related to the thickness of the concrete ring. Based on a ring dried from the circumference, they first established that the depth of drying increased proportionally with the square root of drying time. Through reanalysis of previous ring data, they also observed that the time-to-cracking was linearly proportional to the square of the concrete ring thickness. Combining these two observations, they concluded that the depth of drying at cracking was proportional to the thickness of the ring, and suggested that thicker rings could develop larger flaws before failure occurred.

1.6 FREE SHRINKAGE TEST

Tests to measure the unrestrained shrinkage of concrete are widely used and often performed simultaneously with restrained shrinkage tests. Several test methods have been developed, including those that use rectangular and ring-shaped specimens.

The most common procedure is described in ASTM C 157, “Standard Test Method for Length Change of Hardened Hydraulic-Cement Mortar and Concrete.” In this test method, rectangular concrete prisms are cast with gage studs at either end. A length comparator is used to measure shrinkage relative to an initial reading.

In a study for the Pennsylvania Department of Transportation, Babaei and Purvis (1996) developed a bridge deck cracking prediction procedure and limiting requirements for results from the free shrinkage test. In an analysis on crack surveys for several bridge decks, they found that, at early ages, thermal shrinkage in excess of 228 microstrain due to temperature differences between the concrete deck and steel girders can cause cracking. They also found that cracks would initiate when the long-term deck shrinkage (thermal plus drying shrinkage) exceeded 400 microstrain. To limit the spacing of 4 μm (0.01 in.) wide cracks to a minimum of 10 m (30 ft) on bridge decks, they recommended a limitation on the ultimate specimen drying free shrinkage to 700 microstrain, which they stated was equivalent to a 28-day free shrinkage of 400 microstrain.

1.7 PREVIOUS WORK

Many researchers have evaluated the shrinkage and cracking behavior of concrete using a variety of test procedures and specimens. The most common restrained shrinkage tests have used flat, plate-type specimens, long and thin linear specimens, or the aforementioned ring specimens. In many of the studies, free shrinkage tests have accompanied the restrained shrinkage test.

1.7.1 PLATE TESTS

Kraai (1985) proposed a cracking potential test in which flat concrete specimens were exposed to severe drying conditions, thereby increasing the cracking tendency of the concrete. In this test, two concrete specimens, one control and one

with a single property altered, were concurrently subjected to harsh drying conditions for 24 hours. Nineteen millimeter ($\frac{3}{4}$ in.) thick plate specimens were cast in 61 x 91 cm (2 x 3 ft) wood forms with the bottom lined with plastic to prohibit absorption and reduce restraint. Evaporation and shrinkage rates were accelerated by the low thickness and large surface area. Edge restraint was provided by 13 x 25 mm ($\frac{1}{2}$ x 1 in.) mesh hardware cloth bent in a L-shape and attached to the base of the mold. Fresh concrete was placed in the mold, screeded, and troweled, and then the specimens were immediately placed in front of fans producing air speeds of 4.5 to 5.4 m/s (10 to 12 mph). After 24 hours of drying, the concrete panels were inspected and crack lengths and widths were measured. Relative cracking potential was determined by comparing the test panel with the control panel. The mixes Kraai tested contained 418 kg/m^3 (705 lb/yd^3) of cement and a high water-cement ratio, 0.70. For this test, the suggested proportion of cement to aggregate was 1:4 by weight and no coarse aggregate was used due to the 19 mm ($\frac{3}{4}$ in.) thickness of the panel. Kraai found that cracking began around one hour after drying was initiated and most of the cracking occurred within 4 hours.

Shaeles and Hover (1987) used a similar test procedure to that of Kraai to evaluate how mix proportions and construction practices affect plastic shrinkage in concrete. To improve durability and prevent absorption, the authors used plexiglass forms to produce the same 91 cm x 61 cm x 19 mm (3 ft x 2 ft x $\frac{3}{4}$ in.) specimens as Kraai. Edge restraint was improved with the use of expanded metal lath attached to the inside perimeter of the form. After casting, the concrete panels were subjected to air speeds of 3.1 to 3.6 m/s (10.3 to 11.7 ft/s), temperatures ranging from 25 to 35 °C (77 to 95 °F), and relative humidities between 10 and 25 percent. The concretes used in this test were proportioned to have cement-sand ratios of 1:2.2 to 1:3.3 using Type I cement. The water-cement ratios varied between 0.50 and 0.70, and the cement contents ranged from 294 to 347 kg/m^3 (495 to 585 lb/yd^3). Again, no coarse

aggregate was used because of the small thickness of the panel. The authors observed that cracking initiated earlier and stopped quicker in stiffer mixes and when the air temperature was higher. Crack widths and total crack areas were lower for stiff mixes compared to fluid and semi-plastic mixes. The effect of paste volume was also investigated, and it was found that cracking was significantly less for mixes with lower paste contents.

Padron and Zollo (1990) studied the effects of adding synthetic fibers to concrete and mortar mixes with a plate-type test. Their specimens were 30.5 x 30.5 cm (1 x 1 ft) with a thickness of either 13 mm (½ in.) for mixes with small aggregates or 25 mm (1 in.) for mixes with large aggregates. A steel ring in the center of the specimen provided restraint. The ring, which was cut from standard steel pipe, was 114 mm (4½ in.) in diameter for the 13 mm (½ in.) specimens and 140 mm (5½ in.) in diameter for the 25 mm (1 in.) specimens. After casting, the concrete samples were placed in a wind tunnel and subjected to a drying environment of 31 °C (88 °F) and 50% relative humidity for 16 hours. The specimens were kept in the molds so that only the top surface was exposed. The wind tunnel produced air speeds of 2.7 m/s (9 ft/s) for the mortar samples and 6.1 m/s (20 ft/s) for the concrete specimens. After 16 hours of drying, the top surfaces were polished with a series of coarse to fine sandpapers so that the cracks could be seen more readily. These cracks were then measured for length and width to calculate overall shrinkage and crack area. The authors tested both mortar and concrete mixes. The mortar mixes contained 584 kg/m³ (985 lb/yd³) of cement with a cement-sand ratio of 1:2 by weight and a water-cement ratio of 0.65. For the concrete mixes, the largest aggregate was 9.5 mm (3/8 in.) pea gravel. These mixes consisted of a cement to sand screenings to pea gravel ratio of 1:2:3. The cement content was 408 kg/m³ (687 lb/yd³), and the water-cement ratio was 0.65. Padron and Zollo observed that cracks began to form in the mortar samples 1¼ to 2 hours after drying started. Cracks initiated in the concrete specimens

1½ to 2 hours after drying began, and most cracking occurred within the first 6 hours for both types of mixes.

The Missouri Department of Transportation (MoDOT 2002) tested a number of their concrete bridge deck mixes for shrinkage and cracking behavior. They used the *Slab Cracking Potential Test Method* developed by the New York State Department of Transportation to evaluate plastic shrinkage cracking in concrete panel specimens. In this test, a 56 cm x 36 cm x 102 mm (22 x 14 x 4 in.) specimen is cast in a form with angled sheet metal stress risers on the bottom. A 6 x 360 mm (¼ x 14 in.) triangular stress riser is located 89 mm (3½ in.) from either end and a 64 x 360 mm (2½ x 14 in.) triangular stress riser is located in the middle. Severe environmental conditions, such as increased mixing temperatures, increased air temperatures, low relative humidity, and wind, are applied to increase the cracking tendency. Thirty minutes after mixing is completed, the concrete slabs are placed in a chamber with fans blowing, where they are dried for 24 hours. Crack lengths are first measured 4½ hours into the drying regime and a total length per unit area is reported. After the 24-hour drying period, the forms are removed, crack lengths are measured, and total length per unit area is calculated again. MoDOT observed inconsistent results that made repeatability of this test a concern. They determined that comparisons of their mixes could not be made with this test because conflicting results were observed for identical mixes. In some cases, one mix would crack and an identical one would not under the same drying conditions.

1.7.2 LINEAR TESTS

Paillère, Buil, and Serrano (1989) studied the restrained autogenous shrinkage behavior of concrete with steel fibers. They performed a self-cracking test on concrete using a Laboratoire Central des Ponts et Chaussées (LCPC) cracking-test bench. With this apparatus, a concrete specimen is cast in a mold on a horizontal

bench. The specimen is placed in a vertical position after the concrete sets to prevent any bending effects. The specimen has a cross section of 8.5 x 12 cm (3.4 x 4.7 in.) and a total length of 1.50 m (59 in.). The ends of the specimen are enlarged to fit into grips on the testing apparatus. One end is fixed, while the other is mobile to allow for shrinkage. A monitoring system at the mobile end controls a dynamometer that applies and records the force required to keep the specimen at a constant length. The restrained shrinkage stress is calculated from this force and the cross-sectional area. To measure and compare the free shrinkage behavior of the concrete, a companion specimen with the same geometry is cast in a mold that allows it to shrink freely at one end. The authors tested six concrete mixes with water-cement ratios between 0.26 and 0.44 and a constant cement content of 425 kg/m³ (716 lb/yd³). The maximum size of coarse aggregate was 20 mm (0.8 in.). Five mixes contained varying amounts of superplasticizer, and four of those mixes included 63.75 kg/m³ (107.5 lb/yd³) of silica fume. Two different sizes of steel fibers were used, one size at a time, in three of the mixes. The addition of steel fibers to concrete was found to increase the time to cracking and restrict crack width development in silica fume concretes.

Bloom and Bentur (1995) modeled their restrained shrinkage test after the one developed by Paillère, Buil, and Serrano. In their test, Bloom and Bentur reduced the cross section of the concrete specimen to 40 x 40 mm (1.6 x 1.6 in.) and the length to 1000 mm (39.4 in.). The ends of the specimen were enlarged and held in grips; one was free to move and the other was fixed. The mobile grip was connected to a screw assembly that was used to manually return the specimen to its initial length whenever its shrinkage reached 2 µm. Therefore, full restraint was maintained in a step-wise manner. The load applied in each step was determined through the use of a load cell that was connected inline with the screw assembly. The restrained shrinkage stress was then calculated from these loads. This test was designed so that the specimens

were cast horizontally and testing could begin immediately after casting. The forms could be removed from the sides so the specimen can be dried from any combination of three sides. The six mixes in this test were considered “microconcrete” because the maximum aggregate size was 7 mm (0.3 in.). Cement contents and water to binder (w/b) ratios ranged from 465 to 510 kg/m³ (784 to 860 lb/yd³) and 0.33 to 0.50, respectively. Superplasticizer use ranged from 1.5 to 3.0 percent of the cement by weight. Three of the six mixes contained 15% silica fume. The mixes with low w/b ratios, both with and without silica fume, exhibited plastic shrinkage cracking, while the one with no silica fume and a w/b of 0.50 did not. Plastic shrinkage cracking occurred in the 0.40 w/b mix with silica fume, but not in a similar mix without silica fume. The 0.40 w/b mix without silica fume exhibited cracking in the hardened concrete after 36 hours. Plastic shrinkage in unrestrained specimens was significantly increased by the addition of silica fume.

Kovler and Bentur (1997) studied shrinkage in steel fiber reinforced concrete at early ages under hot climate conditions. They used a closed-loop, computer-controlled uniaxial-restrained shrinkage (CLCCURS) testing device that was developed at the Technion – Israel Institute of Technology. This automated testing apparatus is used to measure strain components, and determine shrinkage induced stresses, modulus of elasticity, and tensile strength of the concrete. The effect of creep was determined by simultaneously evaluating twin specimens, one free and one restrained. The creep strain was the difference between the free shrinkage and restrained shrinkage strains. The concrete specimens were 40 x 40 mm (1.6 x 1.6 in.) in cross section and had a gage length of 1000 mm (39.4 in.). After one day of curing, the specimens were placed in a 32 ± 1 °C (89.6 ± 1.8 °F), $35 \pm 2\%$ relative humidity drying environment. With a maximum size aggregate of 7 mm (0.3 in.), the mixes in this test were considered “microconcretes.” The mixes had proportions of 1:2:2 of cement to sand to gravel by mass, and the water-cement ratio was 0.7. Steel

fibers were added in percentages of 0 to 2% by volume. The major conclusions from this test were that the steel fiber reinforced concrete maintained load carrying capacity after initial cracking and that the cracks were distributed along the length of the specimens. Crack widths were also found to be small in this type of concrete. The test ran for only 42 hours.

Pigeon et al. (2000) investigated the early age behavior of concrete restrained from shrinking. They modeled their testing device after the CLCCURS apparatus used by Kovler and Bentur (1997). In this study, the concrete specimens were cast in an aluminum mold that was attached to a steel frame. The specimen cross section was increased to 50 x 50 mm (2 x 2 in.), while the 1 m (39.4 in.) gage length remained the same. The ends of the specimen were enlarged to 50 x 150 mm (2 x 6 in.) to provide restraint with the end grips. After the specimen reached a specified shrinkage, a computer-controlled motor at the free end applied a tensile load to return the specimen to its original length. Companion free shrinkage specimens, 500 mm (20 in.) long and with the same cross section as the restrained specimens, were cast in a similar apparatus where only one end was fixed. These specimens were monitored simultaneously with the restrained specimens. The authors tested a mortar mix with a water-cement ratio of 0.27 and a cement to fine aggregate ratio of 1:2 by weight. The free shrinkage was about 450 microstrain and the tensile stress was around 2.5 MPa (0.36 ksi) after 10 days of testing. The authors concluded that creep is very important when analyzing shrinkage and cracking, because it results in relaxation of the restrained shrinkage stresses. They found that creep in the restrained specimens was about 67% of the free shrinkage strain.

Collins and Sanjayan (2000) studied restrained shrinkage cracking of alkali-activated slag concrete. They designed a restrained beam test after experiencing difficulties using the restrained ring test to evaluate cracking potential. The concrete beam specimen was 75 mm wide (3 in.), 150 mm (6 in.) deep, and 1000 mm (39.4

in.) long. Mild steel rods, 25 mm (1 in.) in diameter, provided restraint from within the beam. The rods were machined smooth in the middle 600 mm (24 in.) and greased to reduce bond. After the first series of beams did not crack, PVC electrical insulation sheathing was added to further reduce the bond between the rods and the concrete. Coarse threads were machined on the remaining 200 mm (8 in.) at each end of the rod for anchorage. Additional restraint was provided by four anchor nuts, two fastened to either end of each rod. The beam specimens were cured for 24 hours at 23 °C (73 °F) and then dried at 23 °C (73 °F) and 50% relative humidity on roller supports in the middle and at the two ends. Collins and Sanjayan tested beams with one to three restraining rods to examine the effect they had on shrinkage cracking. They found that two rods provided the best results as one rod did not provide enough restraint and three rods caused congestion within the beam. The two-rod beams cracked at random locations along the sheathed portion of the rod. To ensure that the beam cracked at the center, a 50 x 120 x 2 mm (2 x 4.7 x 0.08 in.) steel plate wrapped in PVC film was added at the center of the specimen as a stress magnifier. The authors evaluated two cementitious binders, portland cement and ground granulated blast furnace slag, in four different mixes. For all mixes, the total binder content was 360 kg/m³ (607 lb/yd³) and the w/b ratio was 0.50. Three of the mixes used 14 mm (0.6 in.) basalt coarse aggregate. Of these three mixes, one used a binder that consisted of only portland cement. The binder for the other two mixes contained equal parts of portland cement and slag; one of the mixes included 1.5% SRA by weight of cement. A fourth mix used 14 mm (0.6 in.) blast furnace slag coarse aggregate, and the binder was entirely slag. The calculated volume percentages of paste for the four mixes were within 1.5% of each other. The authors compared the results of the restrained beam tests by using the time-to-cracking and measuring crack widths. The beams with the all portland cement binder cracked within 9 days of drying, while the beams with slag and portland cement and no SRA cracked within a

day. At 175 days, the average crack width for the three beams with slag and portland cement was almost three times the average crack width for the portland cement beams. The authors found that 3 and 14-day curing for the slag cement beams reduced the crack width. Shrinkage reducing admixtures did not delay time to cracking for the slag mix, but did restrict crack growth. The best cracking behavior was found in the slag cement mix with blast furnace slag coarse aggregate. This mix cracked at 10 days and had lower crack widths than the portland cement beams.

Chariton and Weiss (2002) evaluated shrinkage in mortar specimens using acoustic emission technology. In each test, two specimens were monitored, one free and one restrained. Both specimens were 25 x 25 mm (1 x 1 in.) in cross section. The free shrinkage specimen was 275 mm (11 in.) long with a gage length of 250 mm (10 in.). The restrained specimen was barbell-shaped, with enlarged ends that hooked around two steel pegs at each end that prevented it from shrinking; this specimen was 250 mm (10 in.) long from center to center of the pegs, with the 25 x 25 mm (1 x 1 in.) cross section widening to a cross section of 50 x 25 mm (2 x 1 in.) at each end. After curing for 24 hours, the specimens were demolded and the sides sealed with aluminum tape to prevent loss of moisture. This allowed drying from only the top and bottom surfaces. The restrained specimens were also sealed at the ends to ensure they had the same drying surface to volume ratio as the free shrinkage specimens. The concrete specimens were dried at 23 ± 1 °C (73 ± 1.8 °F) and $50 \pm 2\%$ relative humidity. The authors conducted this test on mortar mixes containing either Type I or Type III cement; both obtained from the same source and having essentially the same chemical composition (56 to 60% C_3S , 11 to 13% C_2S , 8 to 9% C_3A , and 0.5 to 0.6% Na_2O equivalent alkali content). The Type I cement had a Blaine fineness of 360 m^2/kg , while the Type III cement had a fineness of 535 m^2/kg . The portion of fine aggregate by volume was 45% and the water-cement ratio was 0.5. Acoustic emission (AE) technology was used to monitor the specimens. Two AE sensors were

attached to each specimen to record acoustic events and acoustic energy as the concrete dried. The AE results showed a sudden increase in acoustic events just before cracking was observed. The Type I mix, with coarser cement, exhibited lower free shrinkage than the Type III mix. Cracking occurred at 3 days for the Type III mix and at 4 days for the Type I mix.

1.7.3 RING TESTS

Carlson and Reading (1988) discussed the first restrained ring tests, which they performed between 1939 and 1942. These tests were used to examine the influence of cracking resistance on shrinkage cracking in concrete walls. The authors cast a 25 mm (1 in.) thick concrete ring around a 25 mm (1 in.) thick, 175 mm (7 in.) diameter steel ring. The height of the specimen was 38 mm (1½ in.). Drying was limited to the outer circumference of the concrete ring by sealing the top and bottom surfaces. The rings were dried at relative humidities of 25, 50, or 75 percent. Time of cracking was determined by periodical visual observation. Companion free shrinkage bars were used to establish the strain at the time of cracking. These rectangular specimens had the same cross section as the ring and were 305 mm (12 in.) long. To simulate the shrinkage at the circumferential surface of the concrete ring, the free shrinkage specimens were sealed to allow drying from one side only. Free shrinkage measurements were made on the exposed surface, as well as the opposite surface. Carlson and Reading used the strain from free shrinkage bars to determine the strain in the rings at time of cracking. They found that the stresses at the time of cracking for specimens dried in the harshest environment were the highest. In the harshest environment, the specimens also experienced shorter times to cracking.

Grzybowski and Shah (1990) investigated shrinkage cracking of fiber reinforced concrete using a restrained ring test. In this test, the steel ring had inside

and outside diameters of 254 and 305 mm (10 and 12 in.), respectively. The concrete ring cast around the steel ring had an outside diameter of 375 mm (15 in.) and was formed with a cardboard tube. The height of the specimen was 140 mm (5½ in.). The top surface of the concrete ring was sealed with silicone-rubber and the bottom surface remained on the form to permit drying from the circumferential surface only. The authors assumed that uniform drying occurred along this surface since the concrete height was four times the thickness. One day after casting, the rings were demolded and cured for four days at 20 °C (68 °F) and 100% relative humidity. Early age specimens were demolded at 2.5 hours and immediately placed in the drying environment. All specimens were dried at 20 °C (68 °F) and 40% relative humidity. Two companion free shrinkage specimens were cast for each ring test, a 225 x 75 x 25 mm (9 x 3 x 1 in.) prism and a concrete ring with the same dimensions as the restrained ring. The free shrinkage rings were produced by casting the concrete around a steel ring that had been cut into four pieces. The ring pieces were removed one day after casting, and the top and inner surfaces of the concrete ring were sealed. The concrete mix proportions were 1:2:2:0.5 by weight of cement, sand, coarse aggregate, and water. A 9 mm (0.4 in.) maximum size aggregate was used. Steel or polypropylene fibers were also added to the test mixes. The rings were monitored with three strain gages that were attached to the outside of the concrete ring at midheight. Crack widths were measured with a specially designed microscope that moved vertically and rotated around the ring. Each crack was illuminated and then measured at three locations along its height. To monitor free shrinkage, a dial gage extensometer was used on the prisms, and a single strain gage was attached to the outer surface of the unrestrained rings. The authors observed that the addition of fibers did not significantly affect drying shrinkage in the free shrinkage test. They found, however, that fibers did reduce the crack widths, and steel fibers performed the better than polypropylene fibers. They also determined that geometry did not

influence the free shrinkage, since both the rings and the prisms produced similar results.

Karaguler and Shah (1990) studied shrinkage cracking in concretes with either welded wire reinforcement, steel fibers, or a shrinkage reducing admixture (SRA) added. They used the same restrained ring test, microscope setup, and drying regime as Grzybowski and Shah. For this testing, however, the specimens were demolded after only 4 hours. Also, free shrinkage was evaluated on 100 x 100 x 285 mm (4 x 4 x 11.2 in.) companion specimens. These specimens were measured every day for length change using a dial gage extensometer. The authors tested concrete mixes containing Type I portland cement, sand, coarse aggregate, and water with proportions of 1:2:2:0.5 by weight. The coarse aggregate consisted of a 9 mm (0.4 in.) pea gravel. Hooked-end steel fibers, welded wire fabric, or an SRA were added to each mix to study their effect on shrinkage and cracking. The authors found that the addition of fibers did not affect free shrinkage, but the addition of SRA reduced shrinkage by 16 to 37%. In terms of cracking, the plain mix cracked after 4 days of drying, the wire mesh mix within 9 days, the fiber mix within 14 days, and the SRA mixes after 8 days. All additions to the concrete reduced the width of the cracks compared to plain concrete.

Folliard and Berke (1997) studied the effect of an SRA on the properties of high performance concrete. Their restrained ring test consisted of a steel ring with inside and outside diameters of 250 and 300 mm (10 and 12 in.), respectively, and a concrete ring, cast around the steel with a thickness of 50 mm (2 in.) and a height of 150 mm (6 in.). After 24 hours of moist curing, the specimens were demolded and the top surface was sealed with polyurethane, exposing only the outer circumference. The ring specimens, along with 75 x 75 x 285 mm (3 x 3 x 11.2 in.) free shrinkage prisms, were dried at 20 °C (68 °F) and 50% relative humidity. Four mixes were used in this test, all with a cement or binder content of 457 kg/m³ (770 lb/yd³). A

paste volume fraction of 32.5% was selected in the design of these mixes, and the calculated paste volumes based on their mix proportions ranged from 30.0 to 31.1%. In two of the mixes, silica fume replaced 34 kg/m^3 (57 lb/yd^3) of the cement. Shrinkage reducing admixture replaced water at 1.5% by weight of the binder in two mixes, one with silica fume and one without. The water-binder ratio was 0.34 for mixes with SRA and 0.35 for the mixes without SRA. A 12.5 mm (1/2 in.) maximum size coarse aggregate was used in these mixes. The authors observed cracking in the control mix after 44 days of drying. The similar mix with SRA added cracked at 120 days. The plain silica fume mix cracked at 38 days, while the silica fume mix with SRA cracked at 95 days.

Hossain, Pease, and Weiss (2002) investigated restrained shrinkage cracking in concretes with low water-cement ratios. The concrete ring they tested was 75 mm (3 in.) thick, 75 mm (3 in.) high, with a 300 mm (12 in.) inside diameter. Rather than use a height of 150 mm (6 in.) (AASHTO Provisional 1998), a height of 75 mm (3 in.) was chosen to increase the shrinkage rate and to allow direct comparisons with the results of the free shrinkage specimens. To examine the degree of restraint provided by the steel rings, the authors used rings with thicknesses of 3.1 mm (0.12 in.), 9.5 mm (0.37 in.), and 19 mm (0.75 in.). The concrete specimens were sealed for 24 hours and then demolded. The outer circumference of the concrete ring was sealed with aluminum tape to allow drying from the top and bottom surfaces at $23 \text{ }^\circ\text{C}$ ($23 \text{ }^\circ\text{F}$) and 50% relative humidity. By allowing drying from the top and bottom surfaces only, moisture loss in the concrete ring is uniform along the radial direction, producing uniform shrinkage in the radial direction. In this case, the stress calculations are simpler than those for rings dried from the circumference. The latter causes a drying gradient from the exposed surface and, therefore, differential shrinkage in the radial direction. For comparison, rings were also tested with the top and bottom surfaces sealed to allow drying from the outer circumference only. Four

strain gages were attached to the steel ring at midheight, and readings began 30 minutes after mixing. Subsequent readings were recorded every 10 minutes with a data acquisition system. A single acoustic emission sensor was coupled directly with the concrete on the circumference of each restrained ring as well. Free shrinkage was tested by using both the standard length-change prisms and unrestrained ring specimens. The standard specimens consisted of 75 x 75 x 250 mm (3 x 3 x 10 in.) prisms dried from either two sides only or all sides and 75 x 150 x 250 mm (3 x 6 x 10 in.) prisms dried from the 75 mm (3 in.) sides. The different drying regimes were studied to determine which one most closely matched the shrinkage of the unrestrained ring specimens. Testing was conducted on mortar mixes made with Type I cement, a water-cement ratio of 0.3 or 0.5, and a sand volume of 50%. The mortars with the 0.3 w/c included a high range water reducer at 3.0% by weight of cement. The authors observed that shrinkage increased as the surface to volume ratio of the specimens increased. Comparing the free shrinkage rings to the free shrinkage prisms, they determined that a 75 x 75 x 250 mm (3 x 3 x 10 in.) prism with two-sided drying provided similar results to the ring dried from the top and bottom. The authors also proposed the calculation of *cracking potential*, expressed as the ratio of the residual stress in the concrete ring (calculated from the strain in the concrete and the geometry of the concrete and steel rings) to the time-dependent splitting tensile strength. Their results showed that failures occurred at cracking potentials between 0.7 for highly restrained specimens and 1.0 for lightly restrained specimens.

See, Attiogbe, and Miltenberger (2003) studied the shrinkage characteristics of different concrete mixes using the restrained ring test. They used a thin, tall concrete ring. The steel ring had inside and outside diameters of 305 and 330 mm (12 and 13 in.), respectively, and the 152 mm (6 in.) tall concrete ring had an outside diameter of 406 mm (16 in.). A 152 mm (6 in.) tall section of PVC pipe was used as the outer mold. The bond between the steel and concrete rings was reduced by

applying mold release spray to the steel ring. Strain in the ring specimens was monitored using two strain gages attached to the inner surface of the steel ring. One strain gage and a precision resistor formed one leg of a full bridge and a strain conditioner formed the other leg. The strain conditioner improved the accuracy of the readings by reducing noise. Strain readings were recorded every 30 minutes from the time of casting until the rings cracked. The concrete rings were sealed on the top and bottom surfaces with paraffin, producing a volume to surface area of drying ratio of 34 mm (1.3 in.) and a surface to volume ratio of 0.29 cm^{-1} (0.74 in.^{-1}). The concrete specimens were dried at $22 \pm 1 \text{ }^\circ\text{C}$ ($71.6 \pm 1.8 \text{ }^\circ\text{F}$) and $50 \pm 5\%$ relative humidity after being moist cured for 24 hours. Free shrinkage data was collected by measuring $75 \times 75 \times 285 \text{ mm}$ ($3 \times 3 \times 11 \text{ in.}$) specimens that had the same volume to surface area of drying ratio as the rings. This was done by sealing 64 mm (2.5 in.) lengths from each end of the prism, exposing 157 mm (6.2 in.) at the center. It should be noted that sealing the ends of the free shrinkage specimens did not allow uniform drying along the entire 285 mm (11 in.) length, possibly altering the effective gage length. Free shrinkage was evaluated only during drying and continued until the companion restrained rings cracked. The authors tested two normal-strength concrete mixes and two “high-performance” concrete mixes with one of each containing an SRA. The normal-strength mix had a cement content of 363 kg/m^3 (612 lb/yd^3) and a w/c ratio of 0.45, while the high-performance mix had 475 kg/m^3 (801 lb/yd^3) of cement and a 0.35 w/c. Air contents were maintained at $5 \pm 1\%$. Three ring specimens were cast for each mix. The normal strength mixes had lower steel ring and free shrinkage strains than the high-performance mixes. The SRA increased the time-to-cracking for both concretes. The plain, normal-strength mix without the SRA cracked at 17 days, while the mix with the SRA cracked at 32 days. For the high-performance concrete, the time to cracking was 5 days for the plain mix and 19 days for the SRA mix. The authors found that tensile creep played a significant role in cracking behavior. They

predicted times to cracking by performing an analysis on free shrinkage strains and found that the predicted times were between one-seventh and one-half of the times observed in testing. The longer times to cracking in the testing was attributed to tensile creep.

The Missouri Department of Transportation (MoDOT 2003) intended to use the AASHTO provisional ring test (AASHTO Provisional 1998), discussed in Section 1.5.2, as one method to evaluate concrete mix designs for use in bridge decks. They tested eleven concrete mixes, including two MoDOT standard B-2 mixes as control. The control mixes had 432 kg/m^3 (728 lb/yd^3) cement. The other nine mixes were developed to evaluate the effect of supplementary cementitious materials, including Class C flyash, ground granulated blast furnace slag, and silica fume. These nine mixes had total cementitious contents of 357 kg/m^3 (602 lb/yd^3). The coarse aggregate was a 25 mm (1 in.) maximum size gradation D limestone, and the fine aggregate was Class A Missouri River sand (MoDOT 2002). MoDOT's results were inconclusive since the concrete rings did not crack during the two weeks they were monitored. The authors concluded that more research was needed on this test and cited other researchers who had used it successfully.

Xi, Shing, and Xie (2001) performed a laboratory study for the Colorado Department of Transportation to develop optimized concrete mix designs for bridge decks. The authors used the AASHTO Provisional Standard PP34-98 ring test in an attempt to evaluate various mix designs. Two ring specimens were cast for each concrete mix. The specimens were cured for one day at room temperature before being dried in a $22 \text{ }^\circ\text{C}$ ($72 \text{ }^\circ\text{F}$) and 35% relative humidity environment. The concrete rings were monitored visually and using strain gages attached to both the inside of the steel ring and the outside of the concrete ring. Two $25 \times 25 \times 305 \text{ mm}$ ($3 \times 3 \times 12 \text{ in.}$) free shrinkage prisms were also cast for some of the mixes. The specimens were cured for 7 days at $20 \text{ }^\circ\text{C}$ ($68 \text{ }^\circ\text{F}$) in a fog room. During testing, the authors observed

no change in strain in the gages mounted on the steel ring. The strain readings for the gages attached to the concrete surface began to drop after about seven days, which the authors concluded was due to microcracking. Time-to-cracking, determined by visual inspection and not strain gage readings, ranged from 10 to 67 days for the mixes that cracked. In all, cracking was observed for 36 of the 39 mixes that were tested. As the cement content increased, the time to cracking decreased. Time to cracking also increased with decreasing 28 and 56-day compressive strength. The results also showed that cracking resistance can be correlated to aggregate content, improving as the coarse aggregate content was increased and when some sand was replaced with larger aggregate. Cracking resistance decreased when smaller coarse aggregate was used. The free shrinkage testing was inconclusive due to large scatter in the data. However, the data shows that all of the specimens experienced shrinkage greater than 600 microstrain at 90 days after casting.

Krauss and Rogalla (1996) performed an extensive study on transverse cracking in bridge decks. Part of the study involved using the restrained ring test to evaluate the factors in concrete mix design that affect cracking tendency. The mix design factors they examined included cement content, water-cement ratio, cement type, silica fume, fly ash, aggregate type, superplasticizers, and entrained air. Aggregate types included ASTM C 33 size No. 56 limestone, 9.5 mm (3/8 in.) lightweight expanded shale, No. 8 trap rock, and No. 7 Eau Claire gravel. The effects of curing times, temperature, evaporation rate, casting time, and insulation were also considered. They used a custom-machined steel ring with inside and outside diameters of 286 and 305 mm (11¼ and 12 in.), respectively, and a height of 152 mm (6 in.). [The authors noted that the custom-machined rings were more expensive than standard pipe and suggested 305 mm (12 in.) extra strong pipe as an alternative. The pipe is 13 mm (½ in.) thick and has an outside diameter of 12¾ in. (324 mm).] The concrete ring cast around the steel was 75 mm (3 in.) thick. Two rings and two 75 x

75 x 280 mm (3 x 3 x 11 in.) free shrinkage prisms were cast for each batch. After casting, the rings were moved to their final testing location and the strain gages were immediately connected to the monitoring equipment. All of the specimens were demolded 24 hours after casting and stored at 23 °C (73 °F) and 50% relative humidity, producing an evaporation rate of 0.15 kg/m²/hr (0.03 lb/ft²/hr) for drying. The ring specimens remained on the bottom form and the top surface was sealed with polyethylene or rubber to permit only circumferential surface drying. The strain readings were measured hourly, and the rings were carefully examined when a significant change in readings occurred. When a crack was detected, its width was measured and the ring was monitored for another week. Krauss and Rogalla found that the mixes that performed best had a low water-cement ratio, low cement content, and low slump. However, these mixes were difficult to consolidate and not practical. For the other mixes, cracking generally decreased as cement content decreased and the water-cement ratio increased. Free shrinkage was directly proportional to the paste volume, and some mixes with higher paste contents had a greater tendency for cracking. For rings made with No. 56 crushed limestone with a moderately high modulus of elasticity, cracking was marked by a gradual decrease in the strain readings and not a sharp drop. Surface cracks extending 25 mm (1 in.) into the specimen were observed instead of well-defined cracks. Testing on the limestone specimens stopped after 280 days. For rings with lightweight aggregate, large external cracks were found, but strain readings only showed a change in slope rather than a sharp drop in strain. Rings that received no curing after final set cracked sooner than control specimens that had been cured for 24 hours. For high cracking tendency mixes, 60-day wet curing delayed cracking by an average of 9 days. The authors also saw earlier cracking in rings exposed to higher evaporation rates.

1.7.4 VARIATIONS OF THE RING TEST

Kovler, Sikuler, and Bentur (1993) tested plain concrete and fiber-reinforced concrete. They tried to improve the crack sensitivity and achieve quicker results with the restrained ring test by replacing the inner steel ring with a material with a high coefficient of thermal expansion. They tested concrete rings with an outer diameter of 236 mm (9.3 in.) and a height of 43 mm (1.7 in.). The inner diameter ranged from 125 to 187 mm (4.9 to 7.4 in.). Increased crack sensitivity was achieved by casting the rings around a solid Perspex core, a Plexiglas material that has a coefficient of thermal expansion of 70 to $80 \times 10^{-6} \text{ }^\circ\text{C}^{-1}$, compared to steel, which has a coefficient of thermal expansion of 10 to $15 \times 10^{-6} \text{ }^\circ\text{C}^{-1}$. Perspex is also more sensitive to the pressure caused by shrinking concrete because of its low modulus of elasticity, 2.7 to 2.9 GPa (390 to 420 ksi), which is less than that of both steel (200 GPa, 29000 ksi) and hardened concrete (~ 25 GPa, 3600 ksi). After the concrete hardened, the specimens were subjected to a temperature increase, which caused the Perspex core to expand and increase the stress in the concrete. The concrete mixes in this test consisted of cement, sand, and gravel in proportions of 1:2:2 and a water-cement ratio of 0.57. The coarse aggregate had a maximum size of 6 mm (0.2 in.). The reinforcing fibers were made of polypropylene or steel. By subjecting the specimens with a Perspex core to an increase in temperature, the authors were able to produce cracks in the hardened concrete in as little as 20 to 60 minutes. They were unable to produce cracks in rings subjected to drying immediately after casting. The authors then added a Perspex wedge to the outside of the Perspex core to produce a stress concentration. Cracks then appeared in the hardened concrete within 1 to 2 minutes of drying and in fresh concrete within 20 to 30 minutes.

Holt and Janssen (1998) attempted to replicate the restraint on a concrete overlay provided by a concrete pavement. They evaluated the use of steel fiber reinforcement in concrete. By equating the horizontal shrinkage stress in a concrete

slab to the hoop stress in the concrete ring specimen, the authors derived an equation to determine the required thickness of steel ring. These calculations produced an 83 mm (3.3 in.) high, 83 mm (3.3 in.) thick concrete ring with an outside diameter of 465 mm (18.3 in.). The steel ring was 50 mm (2 in.) thick. The specimens were cured at 20 °C (68 °F) and 100% relative humidity for 7 days and then dried from the outer circumference at 23 °C (73 °F) and 55% relative humidity. Two concrete mixes were tested and they consisted of Type I portland cement, Class C fly ash, and a 32 mm (1¼ in.) maximum size coarse aggregate. The water-cement ratio was 0.54 and the water-binder ratio was 0.46. One of the mixes included steel fibers. Sixty days after casting, the plain concrete mix developed a crack that extended down the side of the ring and continued across the top and bottom surfaces. The ring cast with a steel fiber mix showed hairline cracking 300 days after casting.

Weiss and Shah (2002) compared different geometries of the restrained ring test and used it to evaluate SRAs. The authors performed two series of ring tests, a tall ring series and a short ring series. In both series, concrete rings were cast around a 150 mm (6 in.) diameter solid steel core. In the tall ring series, the height of the specimen was held at 150 mm (6 in.) while thicknesses of 25, 75, and 150 mm (1, 3, and 6 in.) were used to simulate varying slab thicknesses. These rings were exposed to drying from the outer circumference, causing a moisture gradient between the inner and outer edges of the concrete ring. For the short ring series, specimens were 30 mm (1.2 in.) tall with concrete wall thicknesses of 30, 75, and 150 mm (1.2, 3, and 6 in.). These rings were dried from the top and bottom surfaces and experienced a uniform moisture gradient along the radial direction of the concrete ring. All specimens were cured at 30 °C (86 °F) for 24 hours and dried at 30 °C (86 °F) and 40% relative humidity. Companion 100 x 100 x 400 mm (4 x 4 x 16 in.) free shrinkage prisms were dried from two surfaces only. Two concrete mixes were evaluated in the study, one a normal strength mix and the other a similar mix with 4% of the water replaced

with a shrinkage-reducing admixture. The mixes were 65% aggregate by volume, with equal parts of fine aggregate and a 9 mm (0.4 in.) coarse aggregate. For both mixes, the liquid-binder ratio (approximately water-cement ratio) was 0.5. The results of the tall ring series showed that time to cracking is delayed as ring thickness increases. In the mixes without SRA, cracking occurred between 7 and 23 days. Two mixes with SRA in the 25 mm (1 in.) thick rings cracked between 70 and 77 days, while the rest of the SRA mixes did not crack during the 150 day test period in the tall ring series. The short ring series showed that cracking potential decreased with increased ring thickness and that the SRA delayed or prevented cracking. For mixes without the SRA, cracking occurred at 8 days for the 25 mm (1 in.) thick rings, and $10\frac{2}{3}$ days for the 75 mm (3 in.) thick rings. The 150 mm (6 in.) thick rings did not crack within 70 days, the maximum length of the test. The mixes with SRA had no cracks in the two thicker rings, while the 25 mm (1 in.) thick ring cracked at 17.3 days. They concluded that thicker concrete rings are more resistant to cracking, with or without a uniform moisture profile.

He, Zhou, and Li (2004) developed a new method to assess cracking potential of cement-based materials, specifically those with varying alkali contents. Instead of using a conventional circular ring, they constructed an ellipse-shaped ring to provide restraint. They noted that for the conventional geometry, cracks might not occur due to low steel stiffness, high concrete toughness, or the absence of locations of increased stress in the circular ring. The elliptical ring causes higher stresses at certain locations, which leads to cracking at a predictable location around the concrete ring. The authors constructed an inner steel ellipse and an outer PVC mold to form the concrete. The specimens were 50 mm (2 in.) high, and the concrete thickness varied from 18.75 to 20 mm (0.74 to 0.79 in.) around the ellipse. The 20 mm (0.79 in.) thickness was used at the four locations along the principle axes. The length of the half major principle axis of the steel mold was 105 mm (4.1 in.), while

the length of the half minor principle axis was 45 mm (1.8 in.). The base of the mold was covered with Teflon to reduce friction, as it remained in place during the tests. The top surface was sealed with epoxy to restrict drying to the outer circumference of the ellipse. The specimens were cured for 18 hours at 28 ± 1 °C (82.4 ± 1.8 °F) and greater than 95% relative humidity. Drying conditions were held at 28 ± 1 °C (82.4 ± 1.8 °F) and $50 \pm 5\%$ relative humidity. An electroconductive material was used to monitor the elliptical rings for cracking; a loop of this zero-strength material was attached on the circumference of the specimen. Electrodes from a universal meter were connected to each end to close the circuit and provide a voltage source. During the tests, the resistance of the material was monitored. When a crack formed, the conductive loop was broken and the resistance jumped abruptly. The authors stated that this was a reliable monitoring system. The specimens were cast with mortar mixes with a w/c ratio of either 0.40 or 0.50. NaOH or KOH was added to some of the mixes to increase the alkalinity of the mortar. The proportions of binder and sand by mass were 1:2. Time-to-cracking for the mixes in this test ranged from 40 to 140 hours. Under the testing conditions, the mortar with increased alkalinity showed higher crack sensitivity at early ages than plain mortar.

1.7.5 SUMMARY OF PREVIOUS WORK

A wide variety of tests have been implemented to evaluate the shrinkage and cracking behavior of concrete. Due to its simplicity, the ring test is the most widely used for cracking tendency. Plate tests are used to evaluate plastic shrinkage in fresh concrete immediately exposed to drying. Except for the NYSDOT test, the geometry of the plates limits the mixes to a small coarse aggregate or none at all. The small cross sections in the linear tests also restrict the size of the coarse aggregate. Some of the linear tests require complicated instrumentation that monitors shrinkage and applies a tensile force to restrain the specimen. In contrast to other tests, ring tests

allow actual concrete mixes to be evaluated under restraint that is similar to the restraint caused by girder systems on bridge decks. Instrumenting the rings with strain gages allows the strain development to be monitored and provides an accurate indication of time-to-cracking. With the ring test, several mixes can be evaluated under the same conditions to determine which mix exhibits the best shrinkage and cracking behavior.

1.8 OBJECTIVE AND SCOPE

The goal of this study is to evaluate the shrinkage and cracking potential of optimized concrete mixes for use in bridge decks. The restrained ring test is used to determine the relative cracking potential of several concrete mixes exposed to drying conditions. Free shrinkage tests are run simultaneously to further evaluate the shrinkage behavior of these mixes.

Three preliminary trials, consisting of one restrained ring and two free shrinkage prisms per mix, are conducted to check the procedure and test setup.

A series of concrete mixes is evaluated in two test programs. Program 1 consists of four concrete mixes, including a typical bridge deck mix from both the Missouri (MoDOT) and the Kansas (KDOT) Departments of Transportation. The other two mixes are a control mix and a mix containing coarse-ground cement. Program 2 repeats the four mixes from Program 1 and includes an additional five mixes. These additional mixes are used to evaluate the curing period (3, 7, and 14 days), the addition of a shrinkage-reducing admixture, lower cement content, and coarse aggregate type (quartzite versus limestone). Three restrained rings and three free shrinkage specimens are cast for each mix. Three cylinders are also cast for each mix to determine the compressive strength of the concrete.

CHAPTER 2: EXPERIMENTAL PROGRAM

2.1 GENERAL

This report covers the evaluation of restrained concrete ring specimens and free shrinkage prism specimens to compare the shrinkage and cracking properties of several concrete mixes. Three individual preliminary tests were performed to evaluate the experimental procedures. Two testing programs, each involving a series of concrete mixes, were conducted to evaluate several mixes subjected to the same environmental conditions. Most specimens used concrete cast with a Type I/II portland cement and limestone coarse aggregate that were cured for three days prior to the initiation of drying. Program 1 involves four mixes; a control mix, a mix similar to the control mix but with Type II coarse-ground cement, and typical bridge deck mixes from both the Kansas Department of Transportation (KDOT) and the Missouri Department of Transportation (MoDOT). Program 2 includes these four mixes plus five more, including the control mix cured for 7 and 14 days, a mix using a shrinkage-reducing admixture, a mix with reduced cement content, and a mix with quartzite coarse aggregate.

2.2 RESTRAINED RING TEST

The restrained ring test is similar to the one used by Hossain, Pease, and Weiss (2002) in which they used a 76 mm (3 in.) thick, 76 mm (3 in.) high concrete ring cast around a steel ring with an outside diameter of 305 mm (12 in.). The steel ring used in the current study had an outside diameter of 324 mm (12³/₄ in.) and a wall thickness of 13 mm (1/2 in.). In preliminary tests and Program 1, the concrete ring was 76 mm (3 in.) thick, 76 mm (3 in.) high, and dried from the top and bottom surfaces. In Program 2, the concrete thickness was reduced to 57 mm (2¹/₄ in.), and the concrete was dried from the circumferential surface.

2.2.1 CONSTRUCTION OF FORMS

The concrete ring molds consist of a flat base and a circular outer mold, as shown in Fig. 2.1. The base is cut from a 16 mm (5/8 in.) thick sheet of medium density fiberboard (MDF) to an approximate size of 60 cm (2 ft) square. The center point of the base is located and a circle equal to the circumference of the steel ring is drawn around this point. Lines are drawn from the center of the circle at angles of 0, 45, 135, 150, 210, 225, and 315 degrees for use in laying out the locations of hold-down bolts and strain gages. A clamping device (Fig. 2.2), constructed from a machined aluminum block and a horizontal bolt, is attached to the base with the bolt aligned with the 0 degree line. The horizontal bolt, located at a height of 38 mm (1½ in.), is tightened to hold the steel ring in place during casting. The other components of the clamping mechanism are two vertical bolts with loose washers attached at points on the 150 and 210 degree lines (Fig. 2.3). These bolts are located so that the steel ring is held in place concentrically around the center point. After the clamping mechanism is in place, the base is sealed with several coats of polyurethane.

The ring molds are constructed out of 76 mm (3 in.) strips cut from a sheet of 3 mm (1/8 in.) thick Eucaboard, a high density composite wood panel with one smooth, finished side. These strips are cut to length to match the outer circumference of the desired concrete ring. A clamping jig matching the circumference of the concrete ring is made from plywood and four wooden blocks. The unfinished sides of two Eucaboard strips are glued together and clamped around the jig, forming a circular ring. After the glue dries, five 38 mm (1½ in.), 90 degree angle brackets are attached with small, countersunk bolts to the outside of the ring form. One bracket is attached on either side of the inside seam on the ring, and the other three are evenly spaced around the remainder of the ring. The ring is then cut along its height at the inner seam between the two brackets to allow for adjustments when aligning it around the steel ring, as discussed next.

To attach the ring mold to the base, a steel ring is first clamped to the base. The mold is placed on the board and clamped to the steel ring using spacers matching the thickness of the desired concrete ring. The use of spacers maintains proper concentricity with the steel ring and helps form a true circle. Holes are drilled into the base at the bracket locations, and the mold is held in place with bolts. The mold is then removed and sealed with several coats of polyurethane.

2.2.2 RESTRAINING RING PREPARATION

Two 1.2 m (4 ft) sections of steel pipe are used to fabricate the restraining rings. The pipe has an inside diameter of 298 mm (11¾ in.) and an outside diameter of 324 mm (12¾ in.). Using a horizontal bandsaw, the tubes are cut into 28 rings approximately 83 mm (3¼ in.) tall. The rings are then sandblasted with steel shot to remove corrosion products from the inner and outer surfaces. Next, the rings are machined on a lathe so the sides are square and the rings are 76 mm (3 in.) high. In the process, the outer surface is smoothed and any remaining rust is removed. Care is taken to reduce the ring thickness as little as possible. The outer surface is then polished at a professional shop.

The steel rings are then instrumented with strain gages. Using a tri-square as a straightedge, each ring is marked with a 0 degree line by inscribing a line on the inner surface along the height of the ring. The ring is then clamped on the wooden base with the 0 degree line on the ring aligned with the 0 degree line on the base. Lines are inscribed halfway along the height of the ring at the 45, 135, 225, and 315 degree locations (Fig. 2.1) around the inside of the ring. At these locations, the four strain gage positions are marked along the midheight. These locations are then smoothed and polished using a Dremel[®] rotary tool. First, a grinding bit (Dremel[®] #8193) is used to smooth a 50 mm (2 in.) long, 25 mm (1 in.) high area around the marked locations. After this area is sufficiently free of surface imperfections, a

polishing wheel (Dremel[®] #425) is used to deburr and polish the ground area to a finish suitable for strain gage installation.

2.2.3 INSTRUMENTATION

The strain gages and terminal strips for attaching the wires are installed according to the manufacturer's instructions (Vishay-Measurements Group, Inc. 1991). Type CEA-06-250UW-120 strain gages from Measurements Group, Inc. are used. The terminal strips are type CPF-75C and are cut into sections, each with two soldering tabs. Each strain gage is mounted with a two-tab terminal strip about 3 mm (1/8 in.) directly behind it. Jumper wires approximately 13 mm (1/2 in.) long and cut from individual strands of stranded 26 gage wire connect the strain gage to the terminal strip. Terminal strips are used to avoid disturbing the strain gage in a case where the wires are accidentally pulled.

Two different types of wiring were used over the course of testing. For the preliminary rings, 3.7 m (12 ft) lengths of M-Line Accessories three conductor cable (326 DFV 6503) were used. The individual conductor cables were 26 gage wires. For Programs 1 and 2, 3.7 m (12 ft) lengths of three conductor shielded cable (#8771 060) from Belden were used. Only two of the three wires in each cable are needed. Spade terminals are soldered to the ends these wires to simplify the connection with the terminal boxes. The other end of each wire is soldered to the tabs on the terminal strips. Once all the wires are connected, the resistance through each cable and strain gage circuit is checked with a digital multimeter. If the measured resistance is equal to the specified strain gage resistance, then the gage and terminal strip are covered with DAP[®] Aquarium Sealant to protect them from moisture.

2.2.4 DATA ACQUISITION

Data acquisition is conducted using a Vishay Measurements Group P-3500 strain indicator with digital readout. A series of switchboxes allows numerous strain gages to be monitored with this indicator box (Fig. 2.4). The instrumented rings are connected to switchboxes that can accommodate input from 20 or 22 gages. Each switchbox is connected to one of ten terminals on a Vishay Measurements Group SB-10 switch and balance unit. The switch and balance unit is connected to the indicator box so that the individual strain gages are treated in a quarter bridge configuration and bridge completion is completed internally within the indicator box.

Strain gage readings begin immediately after the rings are cast and the wires are connected. Subsequent readings are taken daily for the duration of the test.

2.3 FREE SHRINKAGE TEST

The free shrinkage specimens are cast in steel molds, as specified in ASTM C 157, from Humboldt Manufacturing Co. (Fig. 2.5). These molds produce 76 x 76 x 286 mm (3 x 3 x 11¼ in.) prisms with gage studs at each end providing a gage length of 254 mm (10 in.) (Fig. 2.6). Free shrinkage measurements are made with a dial gage length comparator from Humboldt. Using a calibration bar, the comparator is zeroed prior to taking a set of readings. The subsequent measurements on the specimens are based on the zero reading to obtain the specimen length each day. The overall change in length for each specimen is calculated by subtracting the initial length after demolding from the daily measurements. Shrinkage strain is calculated as the ratio of this change in length to the 254 mm (10 in.) gage length.

2.4 TEMPERATURE AND HUMIDITY

Two methods were used for maintaining temperature and humidity during the test. For both methods, the drying environment was located within a larger

temperature-controlled room. For the preliminary testing, Program 1, and the replication of the Program 1 free shrinkage test, the specimens were dried in two small tents that hold either six or nine ring specimens and their companion free shrinkage prisms. These tents are framed with wood and sealed with plastic sheeting. The specimens rest on wooden racks that allow drying from all sides. The humidity is maintained within the tents using a saturated magnesium nitrate salt solution placed in plastic containers on the floor of the tent. In theory, the salt solution maintains 53% humidity at 25 °C (CRC 2003).

For Program 2, the drying environment was maintained within a 3.7 x 3.7 m (12 x 12 ft) room framed with wood and sealed with plastic sheeting. In this method, a humidistat controls the humidity in the surrounding room at close to 50%. A humidifier in the drying room provides air moisture, as needed, to maintain the humidity near 50%. This room is large enough to house all 27 ring specimens and the companion free shrinkage prisms in one environment. Again, the specimens rest on wooden racks that allow drying from all sides.

2.5 MATERIALS

The concrete materials include Type I/II cement, Type II coarse-ground cement, sand and pea gravel fine aggregates, limestone and quartzite coarse aggregates, superplasticizers, air-entraining agents, and a shrinkage-reducing admixture. The materials were provided by a local concrete producer, with the exception of some of the chemical admixtures and the Type II coarse-ground cement.

Cement:

The **Type I/II portland cement** has a Blaine Fineness of 378 m²/kg and is produced by Lafarge North America in Sugar Creek, MO. The specific gravity is 3.2. The Bogue composition is 55% C₃S, 18% C₂S, 7% C₃A, and 10% C₄AF.

The **coarse-ground Type II cement** has a Blaine Fineness of 306 m²/kg and is produced by the Ash Grove Cement Co. in Seattle, WA. The specific gravity is 3.2. The Bogue composition is 61.50% C₃S, 13.44% C₂S, 7.69% C₃A, and 8.94% C₄AF.

Fine Aggregate:

The **sand** is Kansas River sand from the Victory Sand and Gravel Co. in Topeka, KS. The specific gravity saturated surface (SSD) is 2.63 and the absorption (dry) is 0.35%. Sand gradations for each program are listed in Table 2.1.

The **pea gravel** is KDOT classification UD-1 from Midwest Concrete Materials in Manhattan, KS. The specific gravity (SSD) is 2.62 and the absorption (dry) is 0.7%. The pea gravel has the same maximum size as the sand, but there are more coarse particles. Pea gravel gradations for each program are listed in Table 2.2.

Coarse aggregate:

The 19 mm (¾ in.) **limestone** is KDOT approved Class 1 durable from Hunt-Midwest Mining's Sunflower Quarry in De Soto, KS. The specific gravity (SSD) is 2.58 and the absorption (dry) is 3.0%. Limestone gradations for each program are listed in Table 2.3.

The 19 mm (¾ in.), No. 67 **quartzite** is from L. G. Everist Inc., in Dell Rapids, SD. The specific gravity (SSD) is 2.64 and the absorption (dry) is 0.44%. The quartzite gradation is listed in Table 2.8. The quartzite was only used in Program 2.

Superplasticizer:

Glenium[®] 3000 NS, produced by Master Builders, Inc., conforms to the requirements in ASTM C 494 for a Type A and a Type F admixture. It contains 30% solids, and the specific gravity is 1.08.

Adva[®] 100, produced by Grace Construction Products, conforms to the requirements in ASTM C 494 for a Type F admixture. It contains 27.5 to 32.5% solids, and the specific gravity is about 1.1.

Air-entraining Agent:

Micro Air[®], produced by Master Builder's, Inc., conforms to ASTM C 260. It contains 13% solids, and the specific gravity is 1.01.

Daravair[®] 1000, produced by Grace Construction Products, conforms to ASTM C 260. It contains 4.5 to 6.0% solids, and the specific gravity is 1.0 to 1.1.

Shrinkage-Reducing Admixture:

Tetraguard AS20, is produced by Master Builders, Inc. The specific gravity is 0.985.

2.6 CONCRETE MIXES

A variety of concrete mixes are used to evaluate the effects of cement fineness, curing time, aggregate type, cement content, and the use of a shrinkage-reducing admixture on shrinkage and cracking. The preliminary testing used a basic concrete mix and two mixes expected to have a high cracking tendency. In Programs 1 and 2, the MoDOT and KDOT mixes represent typical concrete mixes for bridge decks used by those two agencies. The rest of the mixes in those programs were developed in the laboratory. The water-cement ratio (w/c) is held constant at 0.45 for all of the mixes, except values of 0.37 and 0.44 are used for the MoDOT and KDOT

mixes, respectively. The mixes developed in the laboratory have a desired air content of 7 to 9%, a desired slump of 75 mm (3 in.), and contain optimized aggregate gradations based on the Shilstone (1990) method. Shilstone developed a method of blending two or more aggregates together to produce an optimized aggregate gradation to minimize the paste content of the concrete while providing good workability. In this study, the optimized gradation contains individual aggregate contents (as a percentage of total aggregate content by weight) of 30.5% for sand, 12.4% for pea gravel, and 57.1% for coarse aggregate. The cement content is 317 kg/m³ (535 lb/yd³) for all the mixes in Programs 1 and 2, except for the MoDOT and KDOT mixes and a mix with 295 kg/m³ (497 lb/yd³). Details on mixing, casting, curing, and drying are presented in Sections 2.11 through 2.14.

2.7 PRELIMINARY TESTING

Three preliminary rings were fabricated to determine if the procedure and apparatus would successfully indicate cracking in the concrete rings. The preliminary ring tests were not performed simultaneously. Subsequent tests were performed only after an earlier series had been completed. Three different mixes were used. A single restrained ring was cast for the first mix. One restrained ring and two free shrinkage prisms were cast for the second and third preliminary mixes. The specimens were demolded after 24 hours and subjected to drying without any additional curing.

The concrete rings in the preliminary tests were 75 mm (3 in.) thick and 75 mm (3 in.) high (Fig. 2.7). This geometry results in a degree of restraint R from Eq. (1.1) of 0.57, based on $E_s = 200$ GPa (29,000 ksi) and $E_c = 25$ GPa (3,600 ksi). The rings were sealed on the circumferential surface, exposing the top and bottom faces. The drying surface to volume ratio (S/V) of these rings is 0.26 cm⁻¹ (0.67 in.⁻¹). The free shrinkage prisms were sealed on two sides and the ends, producing a S/V value of 0.26 cm⁻¹ (0.67 in.⁻¹).

2.7.1 MIXES

The material proportions for the mixes used in the preliminary tests are listed in Table 2.5.

Preliminary 1: This mix was selected for a ring test to practice acquiring data from the strain gages. It contains 355 kg/m³ (598 lb/yd³) of Type I/II cement, 852 kg/m³ (1436 lb/yd³) of sand, 874 kg/m³ (1473 lb/yd³) of limestone, and 88 mL/m³ (2.3 oz/yd³) of Daravair[®] 1000 air entraining agent. The w/c is 0.45 and an air content of 6.5% was assumed in the design.

Preliminary 2: This mix was based on of a mix used by See, Attiogbe, Miltenberger (2003). It is assumed to be a mix with high cracking potential and was selected to determine if the strain gage readings would indicate the time-to-cracking. This mix consists of 479 kg/m³ (807 lb/yd³) of Type I/II cement, 665 kg/m³ (1121 lb/yd³) of sand, and 1020 kg/m³ (1719 lb/yd³) of pea gravel. The w/c is 0.40 and an air content of 1.5% was assumed in the design.

Preliminary 3: This mortar mix was also selected because it is assumed to have a high cracking potential. This mix is used to determine if the strain gage readings would indicate time-to-cracking. This mix has a 2:1 sand to Type I/II cement ratio by weight and a 0.50 w/c. An air content of 1.5% was assumed in the design.

2.8 PROGRAM 1

Program 1 involves the evaluation of four concrete mixes that are simultaneously exposed to similar drying conditions. All of the mixes were cast over the course of two days. For each mix, three restrained ring specimens and three free shrinkage specimens were cast. Two 152 mm (6 in.) diameter, 305 mm (12 in.) long

cylinders were also cast with each batch to determine the compressive strength. The rings and free shrinkage prisms were demolded after 24 hours and cured for two more days in sealed plastic bags. The compressive strength cylinders were demolded after 24 hours and cured in lime-saturated water for 27 days.

The geometry and drying regime for both the rings and the free shrinkage prisms was the same as used for the preliminary testing, giving $R = 0.57$, and $S/V = 0.26 \text{ cm}^{-1}$ (0.67 in.^{-1}). The details of the ring specimen are shown in Fig. 2.7.

2.8.1 MIXES

The proportions and properties for the mixes used in Program 1 are listed in Table 2.6.

Control, Batch 55: This concrete mix is used as the control. The aggregate content is blended to achieve an optimum gradation, and the Type I/II cement content is 317 kg/m^3 (535 lb/yd^3). This mix contains 538 kg/m^3 (906 lb/yd^3) of sand, 218 kg/m^3 (368 lb/yd^3) of pea gravel, and 1006 kg/m^3 (1695 lb/yd^3) of limestone. The mix has a w/c of 0.45. Adva[®] 100 superplasticizer and Daravair[®] 1000 air-entraining agent were mixed with a portion of the mix water and added to the mix at a rate of 621 mL/m^3 (16 oz/yd^3) and 186 mL/m^3 (4.8 oz/yd^3), respectively. An additional 805 mL/m^3 (20.8 oz/yd^3) of the superplasticizer was added straight to the mix during mixing.

Type II coarse-ground cement, Batch 56: This mix is similar to Batch 55, except the cement is Type II coarse-ground. The amount of cement remains at 317 kg/m^3 (535 lb/yd^3). This mix contains 538 kg/m^3 (906 lb/yd^3) of sand, 218 kg/m^3 (368 lb/yd^3) of pea gravel, 1007 kg/m^3 (1697 lb/yd^3) of limestone, and the w/c is 0.45. Adva[®] 100 superplasticizer and Daravair[®] 1000 air-entraining agent were mixed with a portion of

the mix water and added to the mix at a rate of 785 mL/m³ (20.3 oz/yd³) and 235 mL/m³ (6.1 oz/yd³), respectively.

MoDOT, Batch 57: This mix was adapted from a MoDOT bridge deck mix. It contains 432 kg/m³ (729 lb/yd³) of Type I/II cement, 640 kg/m³ (1078 lb/yd³) of sand, 1059 kg/m³ (1785 lb/yd³) of limestone, and the w/c is 0.37. Adva[®] 100 superplasticizer and Daravair[®] 1000 air-entraining agent were mixed with a portion of the mix water and added to the mix at a rate of 392 mL/m³ (10.1 oz/yd³) and 262 mL/m³ (6.8 oz/yd³), respectively. An additional 2515 mL/m³ (65.0 oz/yd³) of the superplasticizer was added straight to the mix during mixing.

KDOT, Batch 58: This mix was adapted from a KDOT bridge deck mix. It contains 357 kg/m³ (602 lb/yd³) of Type I/II cement, 872 kg/m³ (1469 lb/yd³) of sand, 874 kg/m³ (1474 lb/yd³) of limestone, and the w/c is 0.44. Adva[®] 100 superplasticizer and Daravair[®] 1000 air-entraining agent were mixed with a portion of the mix water and added to the mix at a rate of 229 mL/m³ (5.9 oz/yd³) and 233 mL/m³ (6.0 oz/yd³), respectively. An additional 1006 mL/m³ (26.0 oz/yd³) of the superplasticizer was added straight to the mix during mixing.

2.9 REPLICATE FREE SHRINKAGE TESTS FROM PROGRAM 1

The free shrinkage tests for the mixes in Program 1 were repeated. The specimens were demolded after 24 hours and cured for two more days in lime-saturated water. In this program, the free shrinkage prisms were not sealed, allowing drying to occur from all surfaces of the specimens. The S/V value is 0.60 cm⁻¹ (1.51 in.⁻¹) for these prisms.

2.9.1 MIXES

The material quantities for the mixes used in the replication of the Program 1 free shrinkage tests are listed in Table 2.7.

Control, Batch 81: This mix is a replication of Batch 55. An additional 872 mL/m³ (22.5 oz/yd³) of the superplasticizer was added straight to the mix during mixing.

Type II coarse-ground cement, Batch 82: This mix is a replication of Batch 56, except for the admixture quantities. Adva[®] 100 superplasticizer and Daravair[®] 1000 air-entraining agent were mixed with a portion of the mix water and added to the mix at a rate of 748 mL/m³ (19.3 oz/yd³) and 203 mL/m³ (5.2 oz/yd³), respectively.

MoDOT, Batch 83: This mix is a replication of Batch 57, except for the admixture quantities. Adva[®] 100 superplasticizer and Daravair[®] 1000 air-entraining agent were mixed with a portion of the mix water and added to the mix at a rate of 504 mL/m³ (13.0 oz/yd³) and 242 mL/m³ (6.3 oz/yd³), respectively. An additional 2725 mL/m³ (70.4 oz/yd³) of the superplasticizer was added straight to the mix during mixing.

KDOT, Batch 84: This mix is a replication of Batch 58, except for the admixture quantities. Adva[®] 100 superplasticizer and Daravair[®] 1000 air-entraining agent were mixed with a portion of the mix water and added to the mix at a rate of 196 mL/m³ (5.1 oz/yd³) and 209 mL/m³ (5.4 oz/yd³), respectively. An additional 1090 mL/m³ (28.2 oz/yd³) of the superplasticizer was added straight to the mix during mixing.

2.10 PROGRAM 2

Program 2 involves the evaluation of nine concrete mixes, four of which are repeated from Program 1. These mixes include the typical KDOT and MoDOT

mixes, a control mix, the control mix cured for 7 and 14 days, a mix similar to the control, but with Type II coarse-ground cement, a mix with a shrinkage-reducing admixture, a mix with reduced cement content, and a mix with quartzite coarse aggregate instead of limestone. The rings and free shrinkage specimens are exposed to similar drying conditions. The mixes represented by Batches 130, 132, 138, 140, 143, 145, 147, and 149, were cast over a span of 8 days. Batch 159, the ninth and final batch, was cast 14 days after Batch 149. Three restrained ring specimens and three free shrinkage specimens were cast for each mix. Three 152 mm (6 in.) diameter, 305 mm (12 in.) long cylinders are also cast with each batch to determine the compressive strength [Batch 130 only had two cylinders]. The rings and free shrinkage prisms were demolded after 24 hours and cured for two more days, except Batch 143 (six days) and Batch 145 (13 days). The rings cured in sealed plastic bags, and the prisms cured in lime-saturated water. The compressive strength cylinders were demolded after 24 hours and cured in lime-saturated water for 27 days.

The concrete rings in Program 2 are 57 mm (2¼ in.) thick and 76 mm (3 in.) high. The thickness was reduced to increase the potential for cracking and the 57 mm (2¼ in.) thickness was chosen because it is three times the 19 mm (¾ in.) maximum size aggregate. This ring geometry results in a degree of restraint R from Eq. (1.1) of 0.64, with $E_s = 200$ GPa (29,000 ksi) and $E_c = 25$ GPa (3,600 ksi), compared to 0.57 for the preliminary tests and Program 1 [for the 76 mm (3 in.) thick concrete ring]. The rings were sealed on the top and bottom surfaces, exposing only the circumferential surface, similar to the ASTM (2003) and AASHTO (1998) procedures. The S/V value of these rings is 0.20 cm^{-1} (0.51 in.^{-1}), reduced from the S/V value of 0.26 cm^{-1} (0.67 in.^{-1}) for the previous tests. Ring geometry is shown in Fig. 2.8. The free shrinkage prisms were exposed to drying on all sides, producing an S/V value of 0.60 cm^{-1} (1.51 in.^{-1}).

2.10.1 MIXES

The proportions and properties for the mixes used in Program 2 are listed in Table 2.8.

KDOT, Batch 130: This is the KDOT bridge deck mix. It has the same w/c, cement type and content, and aggregate types and contents as Batch 58. Adva[®] 100 superplasticizer and Daravair[®] 1000 air-entraining agent were mixed with a portion of the mix water and added to the mix at a rate of 327 mL/m³ (8.5 oz/yd³) and 157 mL/m³ (4.1 oz/yd³), respectively.

MoDOT, Batch 132: This is the MoDOT bridge deck mix. It has the same w/c, cement type and content, and aggregate types and contents as Batch 57. Adva[®] 100 superplasticizer and Daravair[®] 1000 air-entraining agent were mixed with a portion of the mix water and added to the mix at a rate of 379 mL/m³ (9.8 oz/yd³) and 412 mL/m³ (10.7 oz/yd³), respectively.

Control, Batch 138: This mix is the basic concrete mix used as control. It has the same w/c, cement type and content, and aggregate types and contents as Batch 55. Adva[®] 100 superplasticizer and Daravair[®] 1000 air-entraining agent were mixed with a portion of the mix water and added to the mix at a rate of 523 mL/m³ (13.5 oz/yd³) and 170 mL/m³ (4.4 oz/yd³), respectively.

7-day cure, Batch 140: This is a replication of Batch 138, but subjected to drying after seven, rather than three, days of curing.

14-day cure, Batch 143: This is a replication of Batch 138, but subjected to drying after 14, rather than three, days of curing.

Type II coarse-ground cement, Batch 145: This mix is similar to the control mix (Batch 138), except that the cement is Type II coarse-ground. It has the same w/c, cement type and content, and aggregate types and contents as Batch 56. Glenium[®] 3000 NS superplasticizer and Micro Air[®] air-entraining agent were mixed with a portion of the mix water and added to the mix at a rate of 360 mL/m³ (9.3 oz/yd³) and 213 mL/m³ (5.5 oz/yd³), respectively.

Batch 147: This mix is similar to the control mix but with a shrinkage-reducing admixture (SRA) included. It has the same w/c, cement type and content, and aggregate types and contents as Batch 55. Glenium[®] 3000 NS superplasticizer and Micro Air[®] air-entraining agent were mixed with a portion of the mix water and added to the mix at 490 mL/m³ (12.7 oz/yd³) and 1046 mL/m³ (27.1 oz/yd³), respectively. After all of the materials had been mixed, Tetraguard AS20 SRA was added straight to the mix at a rate of 6.3 kg/m³ (10.7 lb/yd³).

Reduced Cement (RC), Batch 149: In this mix, the Type I/II cement content is reduced to 295 kg/m³ (497 lb/yd³). It contains 551 kg/m³ (929 lb/yd³) of sand, and 224 kg/m³ (377 lb/yd³) of pea gravel, 1031 kg/m³ (1738 lb/yd³) of limestone, and the w/c is 0.45. Adva[®] 100 superplasticizer and Daravair[®] 1000 air-entraining agent were mixed with a portion of the mix water and added to the mix at a rate of 1341 mL/m³ (34.7 oz/yd³) and 92 mL/m³ (2.4 oz/yd³), respectively.

Quartzite, Batch 159: In this mix, quartzite is used for the coarse aggregate. It contains 317 kg/m³ (535 lb/yd³) of Type I/II cement, 545 kg/m³ (918 lb/yd³) of sand, and 221 kg/m³ (373 lb/yd³) of pea gravel, and 1019 kg/m³ (1718 lb/yd³) of quartzite. Adva[®] 100 superplasticizer and Daravair[®] 1000 air-entraining agent were mixed with

a portion of the mix water and added to the mix at a rate of 497 mL/m^3 (12.8 oz/yd^3) and 111 mL/m^3 (2.9 oz/yd^3), respectively.

2.11 MIXING

The batches were cast in a counter-current pan mixer according to the following procedure: First, the coarse aggregate is soaked with 80% of the mix water in the mixing pan for 30 minutes. The sand, pea gravel, and cement are added, and the materials are mixed for one minute. Next, the air-entraining agent is mixed with 10% of the mix water and added to the concrete. After another minute of mixing, the superplasticizer is mixed with the remaining 10% of mix water and added to the concrete. The concrete is then mixed for three minutes, and, when necessary, liquid nitrogen is poured in while the concrete is being mixed to lower the temperature of the concrete to about 21°C (70°F). After mixing, the concrete is allowed to rest for three minutes and the temperature is measured. The concrete is then mixed for a final two minutes and more liquid nitrogen is added, as needed. Following mixing, the concrete is immediately tested for slump and air content. Batch 138 rested an additional 30 minutes before casting to allow the air content to drop to a desirable level. Batch 147 with the SRA was allowed to rest for 45 minutes, per the manufacturer's recommendation, to allow the air content to stabilize.

For Batch 159, the quartzite coarse aggregate was not soaked for 30 minutes prior to casting. Instead, it is washed thoroughly to remove excess fines and then used in the mix. The trial batches for this mix were stiff and it was attributed to high water demand from the excess fines.

Liquid nitrogen was used for all of the mixes in Program 2. It was not used for other mixes. Concrete temperatures are given in Tables 2.6 through 2.8.

2.12 CASTING

The ring and free shrinkage specimens were cast immediately after the slump and air content tests were completed. Mineral oil was applied to all of the molds and the steel ring to prevent bond with the concrete. The specimens were cast in two layers and consolidated on a vibrating table at a frequency of 60 Hz and amplitude of 20 seconds for each layer. After vibrating, excess concrete was struck off the top and the surface made smooth with a 178 mm (7 in.) long, 38 x 32 mm (1½ x 1¼ in.) metal angle.

2.13 CURING

Immediately after casting, the specimens were sealed with plastic sheeting and moved to the testing room. Once the ring specimens were in place, the plastic sheeting was temporarily removed to loosen the clamping bolt holding the steel ring in place. The strain gage wires were connected to the switchboxes at this time. After 24 hours, the plastic sheeting was removed from the specimens, and they were demolded. An initial measurement was recorded for the free shrinkage specimens immediately after demolding and prior to any additional curing.

The specimens in the preliminary testing were not cured after removing the molds.

For Program 1, both the rings and free shrinkage specimens were cured for an additional two days by spraying with water and sealing them in plastic bags.

In the replication of the free shrinkage prisms of Program 1, the specimens were cured for an additional two days in lime-saturated water.

In Program 2, the ring specimens were sprayed with water and sealed in plastic bags for additional curing. The free shrinkage specimens were further cured in a lime-saturated water bath. Except for Batches 140 and 143, the specimens were cured for a total of three days. Batch 140 was removed after six days for a total

curing period of 7 days, and Batch 143 was removed after 13 days for a total curing period of 14 days.

2.14 DRYING

In the preliminary tests and Program 1, the ring specimens were sealed on the circumferential surface before being placed in a drying tent. The free shrinkage prisms were sealed on two sides and the ends and placed in the same tent as the companion rings. In the replication of the free shrinkage specimens from Program 1, the prisms were not sealed before being placed in a tent. In Program 2, the rings are sealed on the top and bottom surfaces and dried in the drying room. The free shrinkage prisms in Program 2 were exposed to drying on all sides.

CHAPTER 3: RESULTS AND EVALUATION

This chapter presents the results of the free shrinkage and restrained ring tests from the preliminary testing and the two evaluation programs. The results are evaluated to compare the relative shrinkage and cracking behavior of the concrete mixes within each program.

3.1 PRELIMINARY TESTS

The preliminary tests used a basic concrete mix (P1), and two mixes, one concrete (P2), and one mortar (P3), designed to have higher cracking tendencies through the use of increased paste contents. The mix proportions are presented in Table 2.5.

Figures 3.1 through 3.6 present the free shrinkage and restrained ring data for the three preliminary tests. Each test consisted of two free shrinkage prisms exposed to drying on two sides and one restrained ring specimen exposed to drying on the top and bottom surfaces. In the plots for the ring tests, the specimens were cast on day 0 and were demolded on day 1, the day drying was initiated. For the free shrinkage results, day 1 indicates the day of demolding and the day that drying began. None of the specimens in the preliminary tests were cured after they were demolded. For P1, the ring test ran for 73 days, while the free shrinkage test lasted 72 days. The free shrinkage and ring tests ran for 26 and 27 days, respectively for P2, and for 8 and 7 days for P3.

Preliminary Test 1:

The free shrinkage results for the first preliminary mix, P1 (27.1% cement paste by volume), are shown in Figure 3.1. The two prisms exhibited similar shrinkage, except during the first day of drying. After one day, the shrinkage of

prism 1 exceeded that of prism 2 by $190 \mu\epsilon$. The shrinkage of both prisms gradually increased until day 72, the final day of testing, on which the difference in shrinkage between the two prisms was still $190 \mu\epsilon$ and the average shrinkage was $605 \mu\epsilon$.

The results for the restrained ring test for mix P1 are shown in Figure 3.2. The data from the four strain gages on the restrained ring provided similar results, including increasing strains on the first two days. After two days, the strain readings dropped and gradually decreased until day 28. After day 28, the strain gradually increased, likely due to creep in the concrete. The strain leveled off near zero around day 60 and remained there until testing was stopped on day 73. No cracks were observed in this ring.

Preliminary Test 2:

The free shrinkage results for the second preliminary mix, P2 (34.7% cement paste), are shown in Figure 3.3. The data for both prisms were very similar throughout the duration of the test. On the final day of testing, day 26, the average shrinkage was $350 \mu\epsilon$.

The results for the restrained ring test for mix P2 are shown in Figure 3.4. The four strain gages produced similar shrinkage curves, with a slight increase in strains on the first day. After the first day, the strains decreased until day 10, when they began to gradually increase. All of the strain gages showed a sharp increase in strain, between 72 and $75 \mu\epsilon$, between day 24 and day 27, indicating cracking of the concrete. A crack extending radially outward from the steel ring was observed in the concrete on day 27, as shown in Figure 3.7.

Preliminary Test 3:

The free shrinkage results for the third preliminary mix, P3 (51.7% cement paste), are shown in Figure 3.5. The data for both prisms were very similar

throughout the duration of the test. On the final day of testing, day 8, the average shrinkage was $315 \mu\epsilon$.

The results for the restrained ring test for mix P3 are shown in Figure 3.6. Again, the results from the four strain gages were similar. All of the gages showed a sharp increase in strain of from day 3 to day 6, indicating cracking of the concrete. A crack extending radially outward from the steel ring was observed in the concrete on day 6, as shown in Figure 3.8.

Summary of Preliminary Testing

Plots summarizing the preliminary free shrinkage and restrained ring tests are shown in Figures 3.9 and 3.10. The preliminary testing showed that the procedure and test apparatus could successfully indicate cracking in the concrete rings. The strain gages on the steel rings appeared to give reliable data, as data from the four gages were consistent for each ring. In the free shrinkage testing, aside from the initial shrinkage difference in P1, the measurements for the two prisms for a given test did not vary greatly, and they produced smooth shrinkage curves.

As expected, the two mixes assumed to have a high cracking tendency cracked quickly, while the basic concrete mix did not crack. P3, the mortar mix with 51.7% paste and only sand as an aggregate, cracked within 6 days of casting. P2, a concrete mix in which the largest aggregate was pea gravel and the paste content was 34.7%, cracked within 27 days. The basic concrete mix, P1, with a paste content of 27.1%, did not crack within the 73 day testing period.

3.2 PROGRAM 1

Program 1 involved four concrete mixes. The control mix (Batch 55) had a 0.45 w/c and contains 317 kg/m^3 (535 lb/yd^3) of cement. Batch 56 was identical to the control mix, except the cement was Type II coarse-ground. Both of these mixes

had optimized aggregate contents. The MoDOT mix (Batch 57) had a 0.37 w/c and a cement content of 432 kg/m³ (729 lb/yd³), and the KDOT mix (Batch 58) had a 0.44 w/c and a cement content of 357 kg/m³ (602 lb/yd³). The mix proportions are presented in Table 2.6.

The data for the free shrinkage tests in Program 1 are presented in Figures 3.11 through 3.14, with the average presented in Figures 3.15 and 3.16. The individual strain gage readings for the restrained ring tests are presented in Figures A3.1 through A3.12 in Appendix A, and adjusted average strain data are presented in Figures 3.17 through 3.20. The tests in Program 1 included three free shrinkage prisms exposed to drying on two sides and three restrained ring specimens exposed to drying on the top and bottom surfaces for each mix, as used in the preliminary tests. All of the specimens were cured for three days. In the plots for the ring tests, the specimens were cast on day 0, and drying was initiated on day 3. For the free shrinkage results, the specimens were demolded on day 1 and drying began on day 3. For the control and Type II coarse-ground mixes, the free shrinkage tests ran for 356 days and the ring tests ended after 161 days. For the MoDOT and KDOT mixes, the free shrinkage and ring tests lasted 354 days and 159 days, respectively.

Free Shrinkage Tests:

The results from Batch 55, the control mix, are given in Figure 3.11. Prism 3 was the only specimen to expand during curing (indicated by negative strain). Upon drying, the shrinkage increased rapidly for about 60 days before leveling off. Prism 2 exhibited the greatest shrinkage for most of the test, while Prism 3 showed the least. The largest difference for these two specimens was 80 $\mu\epsilon$ on day 206.

The results from Batch 56, the Type II coarse-ground cement mix, are given in Figure 3.12. All three prisms expanded during curing, and all three produced similar shrinkage curves. As shown in the plot of the first 30 days (Figure 3.15),

between days 7 and 16, the data fluctuated but did not ultimately increase during a period where the shrinkage is normally rapidly increasing. After day 16, the shrinkage increased sharply until around day 75 before leveling off.

The results from Batch 57, the MoDOT mix, are given in Figure 3.13. All three prisms expanded during curing, and all three produced similar shrinkage curves. Similar to Batch 56, the shrinkage fluctuated but did not ultimately increase between days 6 and 14. After day 14, the shrinkage increased rapidly until around day 100 before beginning to level out.

The results from Batch 58, the KDOT mix, are given in Figure 3.14. In Prisms 1 and 2, the gage studs did not extend out of the concrete far enough to take accurate readings. After curing (day 3), some concrete was chiseled away to expose more of the gage studs in these specimens. The reading on that day was then taken to be the “zero” reading. Prisms 1 and 2 produced similar shrinkage curves, while Prism 3 exhibited greater shrinkage throughout the test. Upon drying, the shrinkage increased rapidly for about 60 days before leveling off. The largest difference between Prisms 2 and 3, $90 \mu\epsilon$, occurred on day 354.

Average curves for each mix over the first 30 days are shown in Figure 3.15. The KDOT mix had the highest 30-day free shrinkage with a value of $297 \mu\epsilon$. The control mix followed with a free shrinkage of $200 \mu\epsilon$. The MoDOT and Type II coarse-ground mixes had the lowest free shrinkage with values of 170 and $160 \mu\epsilon$, respectively.

Figure 3.16 presents the average shrinkage curves for each mix for the duration of the test. The values for each of these curves on days 3, 7, 30, 90, 180, and the end of the test are summarized in Table 3.1. Interpolated values are identified. The KDOT and MoDOT mixes clearly exhibit greater ultimate shrinkage than the laboratory mixes. The shrinkage on day 354 for the KDOT and MoDOT mixes was 570 and $520 \mu\epsilon$, respectively. For the control mix and the Type II coarse-ground

cement mix, the shrinkage was 400 and 350 $\mu\epsilon$, respectively, on day 355. Comparing the data in Figure 3.15, the KDOT mix had the highest early shrinkage rate. After 14 days, MoDOT had the next highest shrinkage rate. The shrinkage rate of the control mix was greater than that of the Type II coarse-ground mix.

Restrained Ring Tests:

The restrained shrinkage curves, plotted for each strain gage on each ring specimen, are presented in Figures A3.1a through A3.12a in Appendix A. Plots of restrained shrinkage versus the square root of time are presented in Figures A3.1b through A3.12b. Plotting the restrained shrinkage data versus the square root of time gives a nearly linear relationship during initial drying, a period during which the strain reading is growing increasingly negative. [Attiogbe et al. (2004) determined that the average shrinkage stress, which is a function of the shrinkage strain, in the cross section of the concrete ring was proportional to the square root of drying time.]

For some of the strain gages, the initial reading varied significantly from the rest of the readings for the ring. To observe the data for all of the gages on a similar scale, the strain was adjusted by adding a strain value (in parentheses next to the strain gage designation) to all of the readings for that gage. The adjustment was calculated using the best-fit line for the near linear portion of the data in the shrinkage versus square root of time plots as follows: For each strain gage on each ring, an initial day and final day bounding the portion of the data where the curve is most linear are selected. The slope and intercept of the linear best-fit line through this portion of the data is calculated using the SLOPE and INTERCEPT functions in Microsoft Excel. Using these values, an adjustment number is calculated for each strain gage so that, when this number is added to the data, the best-fit line crosses $\epsilon=0$ on day 3.

Plots of the average adjusted shrinkage data for each ring are presented in Figures 3.17 through 3.20 for the four concrete mixes. Overall, the results for the restrained ring tests were inconclusive in regards to cracking tendency. None of the twelve concrete rings cracked during 159 days of testing. Most of the rings produced curves that showed shrinkage occurring (increasingly negative strain) until around day 70. From there, the strain increased for a period of time, likely due to creep, before eventually leveling off.

The data for three rings, Type II coarse-ground Ring C (Figure 3.18) and MoDOT Rings A and B (Figure 3.19), were highly variable and did not produce shrinkage curves similar to the other rings. Aside from gage 4 on MoDOT Ring B (Figure A3.8), all of the strain gages on these three rings were connected through the same dial on the same switchbox.

The slopes of the best-fit lines for the near linear portion of the shrinkage versus the square root of time plots provide an approximation of the rate of increase in shrinkage stress, which is a function of the shrinkage strain. The average slope is calculated from all of the strain gages on all of the rings for a given mix. The results for each mix are given in Tables A3.1 through A3.4 and summarized in Table 3.2. The slopes for Batch 56 (Type II coarse-ground) Ring C and Batch 57 (MoDOT) Ring A and Ring B, gages 1 through 3, are not included due to the variability of the data.

As shown in Table 3.2, the MoDOT mix had the highest shrinkage rate, with a slope of $-33 \mu\epsilon/d^{1/2}$ and a standard deviation of 1.0 for five strain gages. The KDOT mix had the lowest shrinkage rate at $-23 \mu\epsilon/d^{1/2}$, but it also had the highest variability, as evidenced by the standard deviation of 9.4 for twelve strain gages. The control mix had a higher shrinkage rate, $-27 \mu\epsilon/d^{1/2}$, than the Type II coarse-ground mix, $-24 \mu\epsilon/d^{1/2}$. The standard deviation and number of gages for these two mixes were 3.2 and 12, and 5.9 and eight, respectively.

Summary of Program 1:

In the free shrinkage tests, the KDOT mix had free shrinkage $50 \mu\epsilon$ greater than that of the MoDOT mix on day 353, even though the MoDOT mix had the higher cement content and paste volume. The cement and paste contents for the KDOT mix were 357 kg/m^3 (602 lb/yd^3) and 26.9%, while these values were 432 kg/m^3 (729 lb/yd^3) and 29.6% for the MoDOT mix. The MoDOT mix had a w/c ratio of 0.37, while the KDOT mix had a w/c ratio of 0.44. This difference in w/c ratios offers one explanation for the lower initial shrinkage of the MoDOT mix, since the MoDOT mix, in all likelihood, had a denser paste that did not allow the water to escape during drying as rapidly as it did for the KDOT mix.

Using the 30-day free shrinkage values, all of the concrete mixes in Program 1 met the PennDOT (Babaei and Purvis 1996) requirement that limits the free shrinkage to $400 \mu\epsilon$ at 28 days. The KDOT mix had the highest 30-day free shrinkage with a value of $297 \mu\epsilon$.

As expected, the laboratory mixes with lower cement contents and paste volumes performed better than the typical bridge deck mixes from KDOT and MoDOT. The control mix and Type II coarse-ground cement mix, both with paste volumes of 24.2%, experienced significantly less free shrinkage than the KDOT and MoDOT mixes. The coarse-ground cement mix had a free shrinkage of $350 \mu\epsilon$ on day 355, while the value for the control mix was $400 \mu\epsilon$.

The results of the ring test were inconclusive in terms of cracking tendency since none of the rings cracked. In comparing the approximate shrinkage rates, MoDOT had the highest value of $-33 \mu\epsilon/d^{1/2}$, followed by the control at $-27 \mu\epsilon/d^{1/2}$ and the coarse ground cement mix at $-24 \mu\epsilon/d^{1/2}$, similar to the free shrinkage results. The KDOT mix, which had the highest ultimate free shrinkage, had the lowest shrinkage rate at $-23 \mu\epsilon/d^{1/2}$.

3.3 REPLICATION OF PROGRAM 1 FREE SHRINKAGE TESTS

Figures 3.21 through 3.24 present the free shrinkage curves for the four concrete mixes in the replication of the Program 1 free shrinkage tests. In these tests, the specimens were cured for three days and allowed to dry from all sides, rather than two sides as done in Program 1. The reading on day 1 indicates the measurement made immediately after the specimens were demolded and prior to curing. The reading on day 3 indicates the measurement made immediately after curing ended and drying was initiated. For each mix, all three prisms expanded during curing, and all three prisms exhibited similar shrinkage behavior.

Average free shrinkage curves for each concrete mix through the first 30 days are presented in Figure 3.25. At 30 days, the control mix had a free shrinkage of 387 $\mu\epsilon$. The MoDOT and KDOT mixes exhibited similar shrinkage behavior throughout the first 30 days and had values of free shrinkage at 30 days of 350 and 340 $\mu\epsilon$, respectively. The Type II coarse-ground mix exhibited the lowest free shrinkage through 30 days, with a value of 257 $\mu\epsilon$.

The curves for the average shrinkage for each mix for the duration of the tests are given in Figure 3.26. The values for each of these curves on days 3, 7, 30, 90, 180, and the end of the test are summarized in Table 3.3. The Type II coarse-ground mix exhibited the lowest ultimate shrinkage. The control, MoDOT, and KDOT mixes initially had similar values of shrinkage. Starting about day 23, the control mix began to show greater shrinkage than the MoDOT and KDOT mixes (Fig. 3.25). The ultimate free shrinkage values for the four mixes were 507 $\mu\epsilon$ at day 278 for the control, 467 $\mu\epsilon$ at day 273 for MoDOT, 467 $\mu\epsilon$ at day 273 for KDOT, and 397 $\mu\epsilon$ at day 278 for Type II coarse-ground.

Summary:

The results of this test do not match those of the free shrinkage tests from Program 1. As in Program 1, the coarse ground cement mix had the lowest free shrinkage (397 $\mu\epsilon$ on day 278 in this case). In the replication, however, the control mix had the highest free shrinkage, 507 $\mu\epsilon$ on day 278, even though the paste content was less than that of the MoDOT and KDOT mixes. The MoDOT and KDOT mixes exhibited nearly identical shrinkage behavior, and both had free shrinkage values of 467 $\mu\epsilon$ on day 273.

As was the case with the original Program 1 free shrinkage tests, all of the mixes in this Program met the PennDOT (Babaei and Purvis, 1996) requirement that the 28-day free shrinkage be less than 400 $\mu\epsilon$. At 30 days, the control, MoDOT, and KDOT mixes were close to that free shrinkage, with values of 387, 350, and 340 $\mu\epsilon$, respectively.

Differences in free shrinkage between specimens dried on two sides, as done in Program 1, and specimens dried on all sides, as done in this replication, are discussed in Section 3.5.

3.4 PROGRAM 2

Program 2 involved the evaluation of nine concrete mixes, four of which were repeated from Program 1 and all but two of which were cured for three days. These mixes included the typical KDOT and MoDOT mixes, a control mix, the control mix cured for 7 and 14 days, a mix similar to the control, but with Type II coarse-ground cement, a mix with a shrinkage-reducing admixture, a mix with a cement content reduced below that of the control mix, and a mix with quartzite coarse aggregate instead of limestone. The mix proportions are presented in Table 2.8.

The data for the individual free shrinkage specimens in Program 2 are presented in Figures A3.13 through A3.21 in Appendix A, and the free shrinkage

curves are presented in Figures 3.27 through 3.30. The data for the individual strain gages in the test are given in Figures 3.31 through 3.39, and the average restrained ring data for each ring are given in Figures A3.22 through A3.48 in Appendix A. The tests in Program 2 consisted of three free shrinkage prisms exposed to drying on all sides and three restrained ring specimens exposed to drying on the circumferential surface for each mix, rather than the top and bottom as used in the preliminary tests and Program 1. All of the specimens were cured for three days, except for the 7-day and 14-day cure mixes. In the plots for the ring tests, the specimens were cast on day 0, and drying was initiated on day 3, except for the 7-day and 14-day cure mixes, for which drying began on day 7 and day 14, respectively. Similarly for the free shrinkage results, the specimens were demolded on day 1 and drying began on day 3, except for the 7-day and 14-day cure mixes. Data are presented for 146 to 168 days for the free shrinkage tests and 148 to 170 days for the ring tests.

Free Shrinkage Tests:

Figures A3.13 through A3.21 present the free shrinkage curves for the nine concrete mixes in Program 2. In contrast to the free shrinkage specimens in the preliminary tests in which the specimens were allowed to dry from two sides, the specimens were allowed to dry from all sides. The reading on day 1 indicates the measurement made immediately after the specimens were demolded and prior to curing. Except for Batches 140 (7-day curing) and 143 (14-day curing), the reading on day 3 indicates the measurement made immediately after curing ended and drying was initiated. For Batches 140 and 143, the first measurement after curing was made on day 7 and day 14, respectively. In Figure A3.16 for the 7-day cure mix, Batch 140, no curve is given for Prism 2 because one of the gage studs was embedded in the specimen and could not be recovered.

Average free shrinkage curves for each concrete mix through the first 30 days are presented in Figure 3.27. The KDOT and MoDOT mixes had the greatest free shrinkage at 30 days, with values of 413 and 357 $\mu\epsilon$, respectively. The quartzite, 497 (cement content was 497 lb/yd³), Type II coarse-ground, and control mixes exhibited similar free shrinkage behavior through the first 30 days. The 30-day free shrinkage values for these four mixes were 323, 320, 320, and 313 $\mu\epsilon$, respectively. The 7-day and 14-day cure mixes show early advantages due to extra curing, expansion during curing and a delayed start of drying. These two factors cause the 7 and 14-day cure mixes to have lower 30-day free shrinkage than the other mixes even though the rate of shrinkage, once drying begins, is similar. At 30 days, the free shrinkage was 260 $\mu\epsilon$ for the 7-day cure mix and 193 $\mu\epsilon$ for the 14-day cure mix. The SRA mix had the lowest 30-day free shrinkage, with a value of 143 $\mu\epsilon$.

Figure 3.28 presents the average free shrinkage curves through the first 30 days of drying. At this point, the KDOT and MoDOT mixes again had the highest free shrinkage, with values of 457 and 387 $\mu\epsilon$, respectively. The quartzite, 497, Type II coarse-ground, and control mixes were bunched together with values that ranged from 313 $\mu\epsilon$ for the control to 343 $\mu\epsilon$ for the quartzite mix. The 7 and 14-day cure mixes showed slightly better free shrinkage through 30 days of drying with values of 290 and 253 $\mu\epsilon$, respectively. Again, with a free shrinkage of 157 $\mu\epsilon$, the SRA showed the least free shrinkage.

Figure 3.29 presents the average free shrinkage curves for each mix with day 1 indicating the day the specimens were demolded. The values for each of these curves on days 3, 7, 30, 90, 150, the end of the test, and 30 days after the start of drying are summarized in Table 3.4. The KDOT, MoDOT, and 497 mixes did not exhibit expansion during the curing period. The Type II coarse-ground mix expanded 3 $\mu\epsilon$, the SRA mix expanded 10 $\mu\epsilon$, and the quartzite mix expanded 20 $\mu\epsilon$. The 3-day, 7-day, and 14-day mixes expanded 37, 20, and 37 $\mu\epsilon$, respectively.

The KDOT and MoDOT mixes exhibited the greatest free shrinkage, with values of 593 $\mu\epsilon$ and 517 $\mu\epsilon$, respectively, at 150 days. The SRA mix, with a value of 296 $\mu\epsilon$ at 150 days, had the lowest free shrinkage. The shrinkage curves for the Type II coarse-ground, quartzite, 497, and control mixes did not vary significantly from each other during the test. The free shrinkage values for these four mixes were 469, 457 (147-day), 442, and 439 $\mu\epsilon$, respectively, at 150 days.

With the benefit of extra curing, the 7-day cure mix initially showed slightly less shrinkage than the control mix. The 7-day cure curve fell about 35 $\mu\epsilon$ below the control curve until day 45. From that point on, the two mixes exhibited similar free shrinkage, with values on day 150 of 439 $\mu\epsilon$ for the control, and 443 $\mu\epsilon$ for the 7-day cure mix.

The 14-day cure mix showed lower shrinkage than the control mix for the duration of the test. At 30 days, the shrinkage of the control mix was 313 $\mu\epsilon$, while the shrinkage of the 14-day cure mix was 193 $\mu\epsilon$. At 90 days, these values were 402 $\mu\epsilon$ and 343 $\mu\epsilon$, respectively. The shrinkage of the control mix was 439 $\mu\epsilon$ at 150 days, while the shrinkage of the 14-day cure mix was 408 $\mu\epsilon$.

Figure 3.30 presents the average shrinkage curves for each mix with day 0 indicating the day that drying was initiated. On day 0, some values were negative, indicating expansion during curing. In this figure, the shrinkage curves for the control mix and the 7-day cure mix essentially overlap throughout the duration of the test. Although the 14-day cure mix produces a shrinkage curve similar to the control and 7-day mixes, its expansion during curing, and therefore lower initial reading, causes it to have a lower free shrinkage than the other two mixes throughout the test period. All of the other mixes were cured for three days, and the Type II coarse-ground, 497, and quartzite mixes showed similar shrinkage to the control mix, while the KDOT and MoDOT mixes had the highest shrinkage.

Restrained Ring Tests:

The restrained shrinkage curves for each strain gage on the ring specimens are presented in Figures A3.22a through A3.48a in Appendix A. Plots of the restrained shrinkage versus the square root of time are presented in Figures A3.22b through A3.48b. Day 0 indicates the day of casting, and day 3 indicates the start of drying for all of the mixes, except those with the 7 or 14-day cure.

In some cases, the initial strain gage reading varied significantly from the rest of the readings for a given strain gage. To observe the data for all of the rings on a similar scale, these data were adjusted as described for the specimens in Program 1.

Plots of the average adjusted shrinkage data for each ring for each concrete mix are presented in Figures 3.31 through 3.39. Only one of the 27 concrete rings cracked within 127 days of the date of casting. MoDOT Ring A cracked at 101 days, as indicated by the sharp increase of about 60 to 70 $\mu\epsilon$ in all four gages, as shown in Figures A3.25 and 3.32. A vertical crack extending the height of the ring was observed on the circumference of the concrete on day 103, as shown in Figure 3.40.

Most of the ring data shows a period of shrinkage, indicated by increasingly negative strain, before leveling off. The quartzite rings shrank for about 45 days and the control and 7-day rings shrank for about 50 days. The KDOT mix leveled off after about 55 days, while the MoDOT and 497 rings leveled off at 60 days. The 14-day cure rings shrank for about 65 days, and the Type II coarse-ground and SRA rings continued shrinking past 100 days.

Some of the strain gage data were not used in analyzing the ring tests because the strains were inconsistent with the results from the other gages. The gages that were excluded were control B3, 7-day C1, C2, and C4, 14-day C4, and 497 B2. In other cases, no reading could be obtained from the gage during testing (7-day A2 and B1). Gage A2 for the 14-day ring fell off the specimen.

The slopes of the best-fit lines for strain gage readings versus the square root of time are compared, as they were for Program 1, as an approximation of the rate of increase in shrinkage stress in the concrete. The average slope is calculated from all of the strain gages on all of the rings for a given mix. The results for each mix are given in Tables A3.5 through A3.13 and summarized in Table 3.5.

The MoDOT and 497 mixes had the highest shrinkage rate, both with slopes of $-22 \mu\epsilon/d^{1/2}$, as well as the highest standard deviations, with values of 5.1 and 4.9, respectively. The mixes to evaluate curing period had similar slopes, with shrinkage rates during drying for the control, 7-day, and 14-day cure mixes of -20 , -19 , and $-20 \mu\epsilon/d^{1/2}$, with standard deviations of 3.4, 2.0, and 2.0, respectively. The quartzite and KDOT mixes had the next highest shrinkage rates, with values of -17 and $-16 \mu\epsilon/d^{1/2}$ and standard deviations of 2.7 and 4.3. The two mixes that exhibited the best shrinkage behavior were the Type II coarse-ground mix and the SRA mix, both with shrinkage rates of $-12 \mu\epsilon/d^{1/2}$. The standard deviation was 2.3 for the Type II coarse-ground and 1.7 for the SRA specimens. All 12 gages were used in the analysis of the MoDOT, quartzite, KDOT, Type II coarse ground, and SRA rings. Only 11 gages were analyzed for the 497 and control specimens. Ten gages were used for the 14-day rings, and seven gages were used for the 7-day rings.

Summary of Program 2:

In the free shrinkage tests, the KDOT and MoDOT mixes had the highest shrinkage, similar to the results of Program 1. On day 150, the KDOT mix had the highest free shrinkage, at $593 \mu\epsilon$, followed by the MoDOT mix with a value of $517 \mu\epsilon$. Although the MoDOT mix had the higher cement and paste contents, its low w/c resulted in a denser paste that slowed the rate at which pore water could escape during drying.

Four mixes, Type II coarse-ground, quartzite, 497, and control, produced similar free shrinkage curves and had 150-day free shrinkage values of 469, 457 (147-day), 442, and 439 $\mu\epsilon$, respectively. Thus, contrary to expectations, no benefit was observed in reduced cement content (497 mix) or replacing the limestone coarse aggregate with quartzite.

The KDOT mix was the only mix that failed the PennDOT (Babaei and Purvis, 1996) requirement of limiting the 28-day free shrinkage to 400 $\mu\epsilon$. After 25 days, the KDOT free shrinkage exceeded 400 $\mu\epsilon$, and its 30-day free shrinkage was 413 $\mu\epsilon$. With a 30-day value of 357 $\mu\epsilon$, the MoDOT mix was the next closest to this limiting requirement.

For similar drying times, the 7 and 14-day cure mixes produced similar shrinkage curves to the control mix, with the 14-day cure mix showing slightly lower values. After 150 days of drying, the free shrinkage values for the 7-day cure and 14-day cure mixes were 443 $\mu\epsilon$ and 408 $\mu\epsilon$, respectively, compared to 439 $\mu\epsilon$ for the control. The benefit of extended curing can be seen by comparing these mixes from the day of casting (Table 3.4, Figures 3.27 and 3.28). For the first 45 days, the shrinkage of the 7-day cure mix was about 35 $\mu\epsilon$ less than the control. After 45 days, the two curves overlapped. The 14-day cure mix remained about 50 $\mu\epsilon$ lower than the control and 7-day cure mixes during the latter part of testing, due in part to expansion during curing.

The SRA mix displayed the best shrinkage behavior of all of the mixes. With a free shrinkage of 296 $\mu\epsilon$ on day 150, it was about 112 $\mu\epsilon$ below that of the 14-day cure mix, the mix with the next lowest free shrinkage. Using the shrinkage-reducing admixture reduced free shrinkage by about 33% at 150 days compared to the control mix at 439 $\mu\epsilon$. Although the SRA mix showed improved free shrinkage behavior, it was difficult to achieve consistent air content results with it in laboratory mixes. As discussed in Section 2.11, the air contents for laboratory trial batches were highly

variable immediately after casting and after the 45 minute rest recommended by the manufacturer.

Overall, all of the laboratory mixes showed improved free shrinkage behavior over both the KDOT and MoDOT mixes. The main differences between the laboratory mixes and the KDOT and MoDOT mixes are lower paste contents and optimized aggregate contents.

The results of the ring test were inconclusive in terms of cracking tendency since only one of the 27 rings cracked. MoDOT Ring A cracked 101 days after casting, as indicated by a sharp increase in the strain gage readings and confirmed by visual inspection. As was the case in Program 1, however, the MoDOT mix did have the greatest shrinkage rate (in this case tied with the 497 mix) at $-22 \mu\epsilon/d^{1/2}$, suggesting that the shrinkage rate might provide an indication of cracking tendency. Likewise, the KDOT mix behaved similar to that in Program 1, having a low shrinkage rate of $-16 \mu\epsilon/d^{1/2}$, ranking it as the seventh lowest out of the nine mixes. The three mixes used to compare curing times all exhibited similar shrinkage behavior, with values of $-20 \mu\epsilon/d^{1/2}$ for the control and 14-day mixes and $-19 \mu\epsilon/d^{1/2}$ for the 7-day mix. The quartzite mix had a shrinkage rate of $-18 \mu\epsilon/d^{1/2}$. As expected, the SRA and Type II coarse-ground mixes had the lowest shrinkage rates, both with values of $-12 \mu\epsilon/d^{1/2}$.

3.5 ADDITIONAL ANALYSES OF RESULTS

The test results were analyzed to evaluate the effect of number of drying surfaces on shrinkage, the statistical certainty, and the correlation between restrained shrinkage rate and free shrinkage. The analysis on drying surfaces compared the four mixes that were included in all three test programs (MoDOT, KDOT, control, and Type II coarse-ground). In this case, it should be noted that the mixes in the programs are not exact duplicates because they were cast on different dates, the

concrete properties differed, and the drying conditions were not identical (although they were controlled so as to be relatively close). The tests for statistical certainty and the correlation between restrained shrinkage and free shrinkage include all of the mixes for each test program.

3.5.1 NUMBER OF DRYING SURFACES

To evaluate the effect of the number of drying surfaces on free shrinkage, data for the MoDOT, KDOT, control, and Type II coarse-ground mixes for Program 1 (two sides), the replication of Program 1 (all sides), and Program 2 (all sides) are presented in Figures 3.41 through 3.44. The average free shrinkage is shown, along with the range of values for each mix, at 7, 30, 90, and 150 days.

For the MoDOT (Figure 3.41) and KDOT (Figure 3.42) mixes, the 7-day free shrinkage of the specimens dried from two sides was less than that of the other two programs. For the control (Figure 3.43) and Type II coarse-ground (Figure 3.44) mixes, the two-sided drying free shrinkage was in between the values for the specimens dried from all sides. At 30 days, the two-sided drying free shrinkage for each mix was less than the values for drying from all sides, with relatively large differences for the MoDOT, control, and Type II coarse-ground mixes. By 90 days, the free shrinkage of the two-sided drying specimens for the KDOT mix was between the values for the specimens dried from all sides, while the two-sided drying free shrinkage remained lowest for the other three mixes. At 150 days, the two-sided drying free shrinkage for the control and Type II coarse-ground mixes remained the lowest but were relatively close to the values for the specimens dried from all sides, while the values for the other two mixes were between those of the specimens dried from all sides. In general, the specimens dried from two sides showed lower early free shrinkage, but eventually reached ultimate free shrinkage levels close to those of the specimens dried from all sides.

Figure 3.45 presents a comparison of the restrained shrinkage rate in $\mu\epsilon/d^{1/2}$ for Program 1, in which the rings were dried from the top and bottom, and Program 2, in which the rings were dried from the circumference. The average shrinkage rate and range of values is presented for the four mixes that were included in both programs. In all four mixes, the rings dried from the top and bottom [$S/V = 0.26 \text{ cm}^{-1}$ (0.67 in.^{-1})] had higher shrinkage rates than the rings dried from the circumference [$S/V = 0.20 \text{ cm}^{-1}$ (0.51 in.^{-1})]. In addition to the differences in surface to volume ratios S/V , the concrete rings in Program 2 were only 57 mm ($2\frac{1}{2}$ in.) thick, compared to 76 mm (3 in.) thick for those in Program 1. Thus, for a given shrinkage in the concrete, the specimens in Program 1 would be expected to produce higher strain gage readings. Observing the ranges of values, the greatest shrinkage rate for each mix from Program 2 is less than or equal to the average shrinkage rate from Program 1.

3.5.2 STATISTICAL CERTAINTY OF RESULTS

The Student's t-test was used for some of the test results to determine if the observed differences are statistically significant. The Student's t-test is used when the sample groups are small to determine whether differences in the sample means, X_1 and X_2 , represent differences in the population means, μ_1 and μ_2 , at a specified level of significance, α . For example, $\alpha = 0.05$ indicates a five percent chance that the test will incorrectly identify (or a 95% chance of correctly identifying) a statistically significant difference in sample means when, in fact, there is no difference. A two-side test is used in the analyses performed in this study, meaning that there is a probability of $\alpha/2$ that $\mu_1 > \mu_2$ and $\alpha/2$ that $\mu_1 < \mu_2$ when, in fact, μ_1 and μ_2 are equal. The results of the Student's t-tests are presented in Tables 3.6 through 3.13. A "Y" indicates that there is a statistical difference between two samples at a confidence level of 98% ($\alpha = 0.02$), and an "N" indicates that there is no statistical

difference at the lowest confidence level, 80% ($\alpha = 0.2$). Statistical differences at confidence levels of, but not exceeding, 80%, 90%, and 95% are indicated by “80”, “90”, and “95”. The results of the Student’s t-tests are presented in Tables 3.6 through 3.13. In these tables, the mixes are listed in order of decreasing free shrinkage or decreasing shrinkage rate to compare the relative differences between mixes.

Tables 3.6 and 3.7 present the Student’s t-test results for Program 1 for the 30 and 150-day free shrinkage data. At 30 days, the difference in shrinkage of the KDOT mix from that of the other three mixes (which show only slight differences between themselves) is statistically significant at $\alpha = 0.02$. At 150 days, the differences between all four mixes is statistically significant at $\alpha = 0.02$, except the difference between the control and Type II coarse-ground mixes, which is significant at a value of $\alpha = 0.10$.

Table 3.8 presents the Student’s t-test results for the Program 1 restrained shrinkage rates. The difference in shrinkage rate of the MoDOT mix from that of the control and Type II coarse-ground mixes is statistically significant at $\alpha = 0.02$, but only at $\alpha = 0.10$ for the KDOT mix, even though the MoDOT mix has the highest shrinkage rate and the KDOT mix has the lowest shrinkage rate. The difference in shrinkage rate for the control mix from those of the Type II coarse-ground and KDOT mixes is statistically significant only at $\alpha = 0.20$. The shrinkage rate of the Type II coarse-ground mix is not statistically different from that of the KDOT mix.

Tables 3.9 and 3.10 present the Student’s t-test results for the replication of Program 1 for the 30 and 150-day free shrinkage data. At 30 days, the difference in the shrinkage of the control mix from that of the KDOT and Type II coarse-ground mixes is statistically significant at $\alpha = 0.02$, and from that of the MoDOT mix at $\alpha = 0.05$. The difference in the shrinkage of the Type II coarse-ground mix from that of the MoDOT and KDOT mixes is statistically significant at $\alpha = 0.02$, while the

difference in free shrinkage between the MoDOT and KDOT mixes is not statistically significant. At 150 days, the differences between the free shrinkage for the MoDOT and KDOT mixes is not statistically significant, but the differences in the free shrinkage of the control and MoDOT mixes and the KDOT and Type II coarse-ground mixes is statistically significant at $\alpha = 0.05$.

Tables 3.11 and 3.12 present the Student's t-test results for Program 2 for the 30 and 150-day free shrinkage data. At 30 days, the differences between the results for the mix with the highest free shrinkage, KDOT, and the mixes with the lowest free shrinkage, 14-day and SRA, from the rest of the mixes are statistically significant at $\alpha = 0.02$. The remaining six mixes, for the most part, exhibit values of free shrinkage that either do not differ significantly or exhibit differences that are significant at $\alpha = 0.05$, 0.10, or 0.20. Similarly at 150 days, the results for the mix with the highest free shrinkage, KDOT, and the mix with the lowest free shrinkage, SRA, exhibit differences from the rest of the mixes that are statistically significant at $\alpha = 0.02$. The remaining seven mixes, for the most part, are either not significantly different or exhibit differences that are significant at $\alpha = 0.05$ and 0.10.

Table 3.13 presents the Student's t-test results for the Program 2 restrained shrinkage rates. The differences between the shrinkage rates of the five mixes with the highest shrinkage rates, MoDOT, 497, control, 14-day, and 7-day are not statistically significant. The differences of the Type II coarse-ground and SRA mixes from all of the other mixes (but not each other) are statistically significant at $\alpha = 0.02$. The shrinkage rate of the quartzite mix is lower than that of the four mixes with the highest shrinkage rates at $\alpha = 0.02$ or 0.05, and the shrinkage rate of the KDOT mix is lower than that of the five mixes with the highest shrinkage rates at $\alpha = 0.02$ or 0.05. The difference between the quartzite and KDOT mixes is not statistically significant.

Overall, the observations made in Sections 3.2 through 3.4 based on relative differences in free shrinkage and restrained shrinkage rate are supported as being based on differences that are statistically significant.

3.5.3 FREE SHRINKAGE AS A PREDICTION OF RESTRAINED SHRINKAGE RATE

Figures 3.46 through 3.49 present plots of the average restrained shrinkage rate versus the average 30-day free shrinkage for the mixes in each test program. The ranges in the data are also included. Figure 3.47 is similar to 3.46 except the data from the KDOT mix were excluded. In Figure 3.46, the trend line for Program 1 shows decreasing restrained shrinkage with increasing free shrinkage due to the low restrained shrinkage of the KDOT mix. With the KDOT mix excluded (Figure 3.47), the trend is one of increasing restrained shrinkage with increasing free shrinkage, which is the case for both the comparison of the Program 1 rings with the replication of Program 1 free shrinkage tests (Figure 3.48) and the Program 2 tests (Figure 3.49). In each case, the R^2 value for the trend line is very low. Thus, while the trend is clear and, with one exception (Figure 3.46), consistent, the data in this study indicate that free shrinkage serves as only a weak predictor of the restrained shrinkage rate.

CHAPTER 4: SUMMARY AND CONCLUSIONS

4.1 SUMMARY

Free shrinkage and restrained ring tests are used to evaluate concrete mixes designed for use in bridge decks. The study consists of a series of preliminary tests and three test programs. In each program, the concrete is exposed to drying conditions of about 21°C (70°F) and 50% relative humidity.

The preliminary tests include one basic concrete mix and two mixes designed to have a high cracking tendency, one concrete and one mortar. For each mix, two 76 x 76 x 286 mm (3 x 3 x 11¼ in.) free shrinkage prisms and one restrained ring specimen are cast. The concrete ring is 76 mm (3 in.) tall, 76 mm (3 in.) thick, and is cast around a 13 mm (½ in.) thick steel ring with an outside diameter of 324 mm (12¾ in.). The free shrinkage specimens are sealed to expose two sides to drying, and the ring is sealed to allow drying from the top and bottom surfaces only. The specimens are exposed to drying after one day of curing.

Program 1 includes two concrete mixes representing typical bridge deck mixes from the Missouri (MoDOT) and Kansas (KDOT) Departments of Transportation, a basic mix used as a control, and a mix similar to the control but made with Type II coarse-ground cement. Three free shrinkage prisms and three restrained rings with the same geometry and exposed drying surfaces as the specimens from preliminary testing are cast for each mix. The specimens are exposed to drying after three days of curing.

The free shrinkage tests for the four mixes from Program 1 are replicated, but with the specimens exposed to drying from all sides.

Program 2 involves the evaluation of nine concrete mixes, including the four from Program 1, plus the control mix cured for 7 days, the control mix cured for 14 days, a mix with a shrinkage-reducing admixture, a mix with a reduced cement

content compared to that of the control, and a mix with quartzite replacing the limestone coarse aggregate. The free shrinkage specimens are the same size as Program 1 but are dried from all sides. The geometry of the concrete rings is similar to the geometry used in Program 1, except the radial thickness is reduced from 76 mm (3 in.) to 57 mm (2¼ in.) and the rings are sealed to allow drying from the circumferential surface.

4.2 CONCLUSIONS

The following conclusions are based on the test results and analyses presented in this report:

1. As the paste content of the concrete increases, the ultimate free shrinkage generally increases. The laboratory mixes with lower paste contents, generally exhibited lower free shrinkage values than the MoDOT and KDOT mixes.
2. Replacing Type I/II portland cement in the control mix with Type II coarse-ground cement results in slightly lower free shrinkage and a lower restrained shrinkage rate.
3. Adding a shrinkage-reducing admixture to the concrete significantly reduces the free shrinkage and restrained shrinkage rate, but also makes achieving consistent concrete properties (i.e., air content) difficult.
4. Longer curing times delay the start of drying (and initial shrinkage) and allow the concrete to initially expand, resulting in lower free shrinkage values at early ages (the first 45 days after casting). The restrained shrinkage rate at the start of drying is not affected when the curing time is increased from 3 to 14 days.
5. The restrained ring tests in this study are inconclusive in terms of cracking tendency since only one out of 39 concrete rings cracked during testing. The

ring that did crack, however, was made with the MoDOT mix, which had the highest paste content and highest shrinkage rate of all of the mixes in Programs 1 and 2.

6. The free shrinkage and restrained shrinkage rate decrease as the surface to volume ratio of the concrete specimens decrease.
7. The restrained shrinkage rate generally increases with increasing free shrinkage, although free shrinkage is found to be a weak predictor of actual restrained shrinkage rate.

4.3 RECOMMENDATIONS

1. To minimize shrinkage and cracking in concrete bridge decks, mixes with lower cement and paste contents should be used.
2. If available, Type II coarse-ground cement should be investigated for use in bridge decks to minimize shrinkage cracking.
3. Shrinkage-reducing admixtures can be used to reduce both the rate of shrinkage and the ultimate shrinkage when the concrete quality is sufficiently controlled by knowledgeable personnel.
4. The concrete curing time should be extended because it slightly reduces shrinkage, and promotes more hydration of cement particles, resulting in less permeable concrete.
5. In future restrained ring test studies, the thickness of the steel ring should be increased from 25 mm (½ in.) to increase the restraint and promote cracking in the concrete.

REFERENCES

- AASHTO PP34-98 (1998). "Standard Practice for Estimating the Crack Tendency of Concrete," AASHTO Provisional Standards, pp. 179-182.
- ASTM C 157-04, (2003). "Standard Test Method for Length Change of Hardened Hydraulic-Cement, Mortar, and Concrete," *2003 Annual Book of ASTM Standards*, Vol. 4.02, American Society for Testing and Materials, West Conshohocken, PA.
- ASTM C 1581-04, (2004). "Standard Test Method for Determining Age at Cracking and Induced Tensile Stress Characteristics of Mortar and Concrete under Restrained Shrinkage," ASTM International, West Conshohocken, PA.
- Attigobe, E. K., Weiss, W. J., and See, H. T., (2004). "A Look at the Stress Rate Versus Time of Cracking Relationship Observed in The Restrained Ring Test," *Advances in Concrete Through Science and Engineering*, Northwestern University, Evanston, IL, Mar., 14 pp.
- Babaei, K. and Purvis, R. L., (1996). "Prevention of Cracks in Concrete Bridge Decks – Summary Report," Research Project No. 89-01 for the Pennsylvania Department of Transportation, prepared by Wilbur Smith Associates, Falls Church, VA, Mar., 30 pp.
- Bloom, R. and Bentur, A., (1995). "Free and Restrained Shrinkage of Normal and High-strength Concretes," *ACI Materials Journal*, Vol. 92, No. 2, Mar.-Apr., pp. 211-217.
- Brooks, J. J. and Neville, A. (1992). "Creep and Shrinkage of Concrete as Affected by Admixtures and Cement Replacement Materials," *Creep and Shrinkage of Concrete: Effect of Materials and Environment*, ACI SP-135, pp. 19-36.
- Carlson, R. W. and Reading, T. J., (1988). "Model Study of Shrinkage Cracking in Concrete Building Walls," *ACI Structural Journal*, Vol. 85, No. 4, Jul.-Aug., pp. 395-404.
- Chariton, T. and Weiss, W. J., (2002). "Using Acoustic Emission to Monitor Damage Development in Mortars Restrained from Volumetric Changes," *Concrete: Material Science to Application, A Tribute to Surendra P. Shah*, ACI SP-206, pp. 205-218.
- Collins, F. and Sanjayan, J. G., (2000). "Cracking Tendency of Alkali-Activated Slag Concrete Subjected to Restrained Shrinkage," *Cement and Concrete Research*, Vol. 30, No. 5, pp. 791-798.

- CRC Handbook of Chemistry and Physics (2003). "Constant Humidity Solutions," pp. 15-25.
- Folliard, K. J. and Berke, N. S., (1997). "Properties of High-Performance Concrete Containing Shrinkage-reducing Admixture," *Cement and Concrete Research*, Vol. 27, No. 9, Sept., pp. 1357-1364.
- Grzybowski, M. and Shah, S. P., (1990). "Shrinkage Cracking of Fiber Reinforced Concrete," *ACI Materials Journal*, Vol. 87, No. 2, Mar.-Apr., pp. 138-148.
- He, Z., Zhou, X., and Li, Z., (2004). "New Experimental Method for Studying Early-age Cracking of Cement-based Materials," *ACI Materials Journal*, Vol. 101, No. 1, Jan.-Feb., pp. 50-56.
- Holt, E. E. and Janssen, D. J., (1998). "Influence of Early Age Volume Changes on Long-term Concrete Shrinkage," *Transportation Research Record*, No. 1610, Aug., pp. 28-32.
- Hossain, A. B., Pease, B., and Weiss, J., (2003). "Quantifying Early-Age Stress Development and Cracking in Low Water-to-Cement Concrete: Restrained-Ring Test with Acoustic Emission," *Transportation Research Record*, No. 1834, pp. 24-32.
- Karaguler, M. E. and Shah, S. P., (1990). "Test Method to Evaluate Shrinkage Cracking in Concrete," *Serviceability and Durability of Construction Materials – Proceedings of the First Materials Engineering Conference*, pp. 626-639.
- Kovler, K. and Bentur, A., (1997). "Shrinkage of Early Age Steel Fiber Reinforced Concrete," *Archives of Civil Engineering*, Vol. 43, No. 4, pp. 431-439.
- Kovler, K., Sikuler, J., and Bentur, A., (1993). "Restrained Shrinkage Tests of Fibre-reinforced Concrete Ring Specimens: Effect of Core Thermal Expansion," *Materials and Structures*, Vol. 26, No. 158, May, pp. 231-237.
- Kraai, P. P., (1985). "Proposed Test to Determine the Cracking Potential Due to Drying Shrinkage of Concrete," *Concrete Construction*, Vol. 30, No. 9, Sept., pp. 775-778.
- Missouri Department of Transportation (MoDOT), (2003). "Laboratory Study - Laboratory Testing of Bridge Deck Mixes," Report No. RDT03-004, Mar., 33 pp.
- Ödman, S. T. A. (1968). "Effects of Variations in Volume, Surface Area Exposed to Drying, and Composition of Concrete on Shrinkage," *RILEM/CEMBUREAU International Colloquium on the Shrinkage of Hydraulic Concretes*, Vol. 1, 20 pp.

Padron, I. and Zollo, R. F., (1990). "Effect of Synthetic Fibers on Volume Stability and Cracking of Portland Cement Concrete and Mortar," *ACI Materials Journal*, Vol. 87, No. 4, Jul.-Aug., pp. 327-332.

Paillère, A. M., Buil, M., and Serrano, J. J., (1989). "Effect of Fiber Addition on the Autogenous Shrinkage of Silica Fume Concrete," *ACI Materials Journal*, Vol. 86, No. 2, Mar.-Apr., pp. 139-144.

Pickett, G. (1956). "Effect of Aggregate on Shrinkage of Concrete and Hypothesis Concerning Shrinkage," *Journal of the American Concrete Institute*, Vol. 27, No. 5, Jan., pp. 581-590.

Pigeon, M., Toma, G., Delagrave, A., Bissonnette, B., Marchand, J., and Prince, J. C., (2000). "Equipment for the Analysis of the Behaviour of Concrete Under Restrained Shrinkage at Early Ages," *Magazine of Concrete Research*, Vol. 52, No. 4, Aug., pp. 297-302.

Powers, T. C. (1959). "Causes and Control of Volume Change," *Journal of the PCA Research and Development Laboratories*, Vol. 1, No. 1, Jan., pp. 29-39.

Reichard, T. W. (1964). "Creep and Drying Shrinkage of Lightweight and Normal-weight Concretes," *Monograph – United States Bureau of Standards*, No. 74, Mar., 30 pp.

See, H. T., Attiogbe, E. K., and Miltenberger, M. A., (2003). "Shrinkage Cracking Characteristics of Concrete Using Ring Specimens," *ACI Materials Journal*, Vol. 100, No. 3, May-Jun., pp. 239-245.

Shaeles, C. A. and Hover, K. C., (1988). "Influence of Mix Proportions and Construction Operations on Plastic Shrinkage Cracking in Thin Slabs," *ACI Materials Journal*, Vol. 85, No. 6, Nov.-Dec., pp. 495-504.

Shah, S. P., Karaguler, M. E., and Sarigaphuti, M., (1992). "Effects of Shrinkage-reducing Admixtures on Restrained Shrinkage Cracking of Concrete," *ACI Materials Journal*, Vol. 89, No. 3, May-Jun., pp. 291-295.

Shah, S. P., Weiss, W. J., and Yang, W., (1998). "Shrinkage Cracking – Can it be Prevented?," *Concrete International*, Vol. 20, No. 4, Apr., pp. 51-55.

Shilstone, Sr., J. M. (1990). "Concrete Mixture Optimization," *Concrete International: Design and Construction*, Vol. 12, No. 6, Jun., pp. 33-39.

Shoya, M. (1979). "Drying Shrinkage and Moisture Loss of Super Plasticizer Admixed Concrete of Low Water Cement Ratio," *Transactions of the Japan Concrete Institute*, II-5, pp. 103-110.

Vishay-Measurements Group, Inc., (1991). "Strain Gage Installations with M-Bond 200 and AE-10 Adhesive Systems," *Bulletin 309 C: Student Manual for Strain Gage Technology*," pp. 17-25.

Weiss, W. J. and Shah, S. P., (2002). "Restrained Shrinkage Cracking : The Role of Shrinkage Reducing Admixtures and Specimen Geometry," *Materials and Structures*, Vol. 34, No. 246, March, pp. 85-91.

Xi, Y., Shing, B., and Xie, Z. (2001). "Development of Optimal Concrete Mix Designs for Bridge Decks," Report No. CDOT-DTD-R-2001-11, sponsored by the Colorado Department of Transportation, Jun., 60 pp.

Yunovich, M., Thompson, N. G., Balvanyos, T., and Lave, L., (2002). "Highway Bridges," Appendix D, *Corrosion Cost and Preventive Strategies in the United States*, by G. H. Koch, M. PO, H. Broongers, N. G. Thompson, Y. P. Virmani, and J. H. Payer, Report No. FHWA-RD-01-156, Federal Highway Administration, McLean, VA, March, 773 pp.

Table 2.1 – Sand Gradations

	<i>% Retained</i>		
	Program 1	Replicate Program 1 Free Shrinkage Tests	Program 2
9.51 mm (3/8 in.)	0	0	0
4750 μm (No. 4)	1.2	1.4	1.6
2360 μm (No. 8)	12.6	13.1	12.7
1180 μm (No. 16)	22.0	21.3	20.9
600 μm (No. 30)	27.2	24.2	25.4
300 μm (No. 50)	27.1	28.6	29.5
150 μm (No. 100)	8.3	10.3	8.6
75 μm (No. 200)	1.1	1.0	1.0
Pan	0.5	0.1	0.2

Table 2.2 – Pea Gravel Gradations

	<i>% Retained</i>		
	Program 1	Replicate Program 1 Free Shrinkage Tests	Program 2
9.51 mm (3/8 in.)	0	0	0
4750 μm (No. 4)	11.8	10.3	12.5
2360 μm (No. 8)	41.0	41.0	40.5
1180 μm (No. 16)	32.4	32.9	30.2
600 μm (No. 30)	7.9	8.6	9.0
300 μm (No. 50)	4.2	4.9	5.6
150 μm (No. 100)	1.9	1.8	1.7
75 μm (No. 200)	0.5	0.4	0.4
Pan	0.3	0.1	0.2

Table 2.3 – Limestone Gradations

	<i>% Retained</i>		
	Program 1	Replicate Program 1 Free Shrinkage Tests	Program 2
38.1 mm	0	0	0
25.4 mm	0	0	0.1
19.0 mm	27.9	23.0	0.1
12.7 mm	28.2	26.5	11.3
9.51 mm	37.9	42.1	18.7
4750 µm (No. 4)	4.0	6.1	48.7
2360 µm (No. 8)	2.0	2.26	15.1
1180 µm (No. 16)	0	0	6.1

Table 2.4 – Quartzite Gradation

	<i>% Retained</i>
	Program 2
38.1 mm	0
25.4 mm	0
19.0 mm	1.6
12.7 mm	25.9
9.51 mm	28.4
4750 µm (No. 4)	36.8
2360 µm (No. 8)	3.5
1180 µm (No. 16)	3.9

Table 2.5 - Mix Proportions for Preliminary Testing

Batch	P1	P2	P3
w/c	0.45	0.4	0.5
Cement, kg/m ³ (lb/yd ³): Type I/II Coarse-ground Type II	355 (598) - -	479 (807) - -	625 (1053) - -
Water, kg/m ³ (lb/yd ³)	160 (270)	192 (324)	313 (528)
Coarse Aggregate, kg/m ³ (lb/yd ³): Limestone Quartzite	874 (1473) - -	- - -	- - -
Fine Aggregate, kg/m ³ (lb/yd ³)	852 (1436)	665 (1121)	1250 (2107)
Pea Gravel, kg/m ³ (lb/yd ³)	-	1020 (1719)	-
Superplasticizer, mL/m ³ (oz/yd ³)	-	-	-
Air-Entraining Agent, mL/m ³ (oz/yd ³)	88.3 (2.3) ^a	-	-
SRA, kg/m ³ (lb/yd ³)	-	-	-

^a – Daravair® 1000 (Grace Construction Products)

Note: P1 was designed with 6.5% air, and P2 and P3 were designed with 1.5% air.

Table 2.6 – Mix Proportions and Concrete Properties for Program 1

Batch	Control, 55	Type II C.G., 56	MoDOT, 57	KDOT, 58
w/c	0.45	0.45	0.37	0.44
Cement, kg/m ³ (lb/yd ³): Type I/II Coarse-ground Type II	317 (535) - -	- 317 (535)	432 (729) -	357 (602) -
Water, kg/m ³ (lb/yd ³)	143 (241)	143 (241)	161 (271)	157 (265)
Coarse Aggregate, kg/m ³ (lb/yd ³): Limestone Quartzite	1006 (1695) - -	1007 (1697) - -	1059 (1785) - -	874 (1474) - -
Fine Aggregate, kg/m ³ (lb/yd ³)	538 (906)	538 (906)	640 (1078)	872 (1469)
Pea Gravel, kg/m ³ (lb/yd ³)	218 (368)	218 (368)	-	-
Superplasticizer, mL/m ³ (oz/yd ³) plus additional	621(16.1) ^a 805 (20.8)	785 (20.3) ^a -	392 (10.1) ^a -	229 (5.9) ^a -
Air-Entraining Agent, mL/m ³ (oz/yd ³)	186 (4.8) ^b	235 (6.1) ^b	262 (6.8) ^b	233 (6.0) ^b
SRA, kg/m ³ (lb/yd ³)	-	-	-	-
Slump, mm (in.)	115 (4.5)	120 (4.75)	150 (6)	57 (2.25)
Air Content, %	5.2	10.45	3	5.5
Unit Weight, kg/m ³ (lb/ft ³)	2355 (147.0)	2244 (140.1)	2355 (147.0)	2300 (143.6)
Temperature, °C (°F)	21 (70)	21 (70)	22 (72)	23 (73)
28 Day Compressive Strength, MPa (psi)	49 (7160)	33 (4820)	59 (8590)	46 (6680)

^a – Adva[®] 100 (Grace Construction Products)^b – Daravair[®] 1000 (Grace Construction Products)

Table 2.7 – Mix Proportions and Concrete Properties for Program 1 Replication of Free Shrinkage Tests

Batch	Control, 81	Type II C.G., 82	MoDOT, 83	KDOT, 84
w/c	0.45	0.45	0.37	0.44
Cement, kg/m ³ (lb/yd ³): Type I/II Coarse-ground Type II	317 (535) - -	- 317 (535) 143 (241)	432 (729) - 161 (271)	357 (602) - 157 (265)
Water, kg/m ³ (lb/yd ³)	143 (241)	143 (241)	161 (271)	157 (265)
Coarse Aggregate, kg/m ³ (lb/yd ³): Limestone Quartzite	1006 (1695) - -	1007 (1697) - -	1059 (1785) - -	874 (1474) - -
Fine Aggregate, kg/m ³ (lb/yd ³)	538 (906)	538 (906)	640 (1078)	872 (1469)
Pea Gravel, kg/m ³ (lb/yd ³)	218 (368)	218 (368)	-	-
Superplasticizer, mL/m ³ (oz/yd ³) plus additional	621 (16.1) ^a 872 (22.5)	748 (19.3) ^a -	504 (13.0) ^a 2725 (70.4)	196 (5.1) ^a 1090 (28.2)
Air-Entraining Agent, mL/m ³ (oz/yd ³)	186 (4.8) ^b	203 (5.2) ^b	242 (6.3) ^b	209 (5.4) ^b
SRA, kg/m ³ (lb/yd ³)	-	-	-	-
Slump, mm (in.)	90 (3.5)	70 (2.75)	145 (5.75)	145 (5.75)
Air Content, %	5.65	5.15	3.25	5.4
Unit Weight, kg/m ³ (lb/ft ³)	2250 (140.4)	2302 (143.7)	2354 (147.0)	2291 (143.0)
Temperature, °C (°F)	24 (75)	23 (74)	27 (80)	25 (77)

^a – Adva[®] 100 (Grace Construction Products)

^b – Daravair[®] 1000 (Grace Construction Products)

Table 2.8a – Mix Proportions and Concrete Properties for Program 2

Batch	KDOT, 130	MoDOT, 132	Control, 138	7-day, 140	14-day, 143
w/c	0.44	0.37	0.45	0.45	0.45
Cement, kg/m ³ (lb/yd ³): Type I/II Coarse-ground Type II	357 (602)	432 (729)	317 (535)	317 (535)	317 (535)
Water, kg/m ³ (lb/yd ³)	157 (265)	161 (272)	143 (241)	143 (241)	143 (241)
Coarse Aggregate, kg/m ³ (lb/yd ³): Limestone Quartzite	874 (1474)	1059 (1785)	1006 (1695)	1006 (1695)	1006 (1695)
Fine Aggregate, kg/m ³ (lb/yd ³)	872 (1469)	640 (1078)	538 (906)	538 (906)	538 (906)
Pea Gravel, kg/m ³ (lb/yd ³)	-	-	218 (368)	218 (368)	218 (368)
Superplasticizer, mL/m ³ (oz/yd ³)	327 (8.5) ^a	379 (9.8) ^a	523 (13.5) ^a	523 (13.5) ^a	523 (13.5) ^a
Air-entraining Agent, mL/m ³ (oz/yd ³)	157 (4.1) ^b	412 (10.7) ^b	170 (4.4) ^b	170 (4.4) ^b	170 (4.4) ^b
SRA, kg/m ³ (lb/yd ³)	-	-	-	-	-
Slump, mm (in.)	110 (4.25)	30 (1.25)	70 (2.75)	100 (4)	75 (3)
Air Content, %	7.25	5.15	6.15	9.25	9.0
Unit Weight, kg/m ³ (lb/ft ³)	2215 (138.3)	2291 (143.0)	2248 (140.3)	2237 (139.6)	2230 (139.2)
Temperature, °C (°F)	18 (64)	19 (66)	18 (65)	20 (68)	20 (68)
28 Day Compressive Strength, MPa (psi)	35 (5060)	40 (5801)	38 (5460)	35 (5050)	35 (5050)

^a – Adva[®] 100 (Grace Construction Products)^d – Micro Air[®] (Master Builders, Inc.)^b – Daravair[®] 1000 (Grace Construction Products)^e – Tetrargard AS20 (Master Builders, Inc.)^c – Glenium[®] 3000 NS (Master Builders, Inc.)

Table 2.8b – Mix Proportions and Concrete Properties for Program 2 (cont.)

Batch	Type II C.G., 145	SRA, 147	R.C., 149	Quartzite, 159
w/c	0.45	0.45	0.45	0.45
Cement, kg/m ³ (lb/yd ³): Type I/II Coarse-ground Type II	- 317 (535)	317 (535) -	295 (497) -	317 (535) -
Water, kg/m ³ (lb/yd ³)	143 (241)	143 (241)	133 (224)	143 (241)
Coarse Aggregate, kg/m ³ (lb/yd ³): Limestone Quartzite	1007 (1697) - -	1006 (1695) - -	1031 (1738) - -	- 1019 (1718)
Fine Aggregate, kg/m ³ (lb/yd ³)	538 (906)	538 (906)	551 (929)	545 (918)
Pea Gravel, kg/m ³ (lb/yd ³)	218 (368)	218 (368)	224 (377)	221 (373)
Superplasticizer, mL/m ³ (oz/yd ³)	360 (9.3) ^c	490 (12.7) ^c	1341 (34.7) ^a	497 (12.8) ^a
Air-entraining Agent, mL/m ³ (oz/yd ³)	213 (5.5) ^d	1046 (27.1) ^d	92 (2.4) ^b	111 (2.9) ^b
SRA, kg/m ³ (lb/yd ³)	-	6.3 (10.7) ^e	-	-
Slump, mm (in.)	55 (2.25)	120 (4.75)	200 (8)	70 (2.75)
Air Content, %	8.4	8.4	8.4	8.15
Unit Weight, kg/m ³ (lb/ft ³)	2216 (138.3)	2241 (139.9)	2235 (139.5)	2237 (139.7)
Temperature, °C (°F)	19 (66)	20 (68)	18 (65)	20 (68)
28 Day Compressive Strength, MPa (psi)	26 (3770)	31 (4430)	33 (4790)	28 (4050)

^a – Adva[®] 100 (Grace Construction Products)

^b – Daravair[®] 1000 (Grace Construction Products)

^c – Glenium[®] 3000 NS (Master Builders, Inc.)

^d – Micro Air[®] (Master Builders, Inc.)

^e – Tetrarguard AS20 (Master Builders, Inc.)

Table 3.1 – Summary of Free Shrinkage Data for Program 1 (in microstrain)

<u>Day</u>	Control, Batch 55	Type II C.G., Batch 56	MoDOT, Batch 57	KDOT, Batch 58
3	3	-13	-23	0
7	83	70	37	73
30	200	160	170 ⁱ	297 ⁱ
90	350 ⁱ	320 ⁱ	422 ⁱ	512 ⁱ
180	390	347	485 ⁱ	565
End of Test ^a	400	350	520	570

^a From 354 to 356 days

ⁱ Denotes interpolated values

Table 3.2 – Summary of Slope Analysis for Program 1 Ring Test

Mix	Batch	Number of Gages	Average Shrinkage Rate, $\mu\epsilon/d^{1/2}$	Standard Deviation, $\mu\epsilon/d^{1/2}$
MoDOT	57	4	-33	1.0
Control	55	12	-27	3.2
Type II C.G.	56	8	-24	5.9
KDOT	58	12	-23	9.4

Table 3.3 – Summary of Free Shrinkage Data for the Replication of Program 1 (in microstrain)

<u>Day</u>	Control, Batch 81	Type II C.G., Batch 82	MoDOT, Batch 83	KDOT, Batch 84
3	-30	-43	-37	-33
7	113	57	83	107
30	387	257	350	340
90	455 ⁱ	344 ⁱ	437 ⁱ	440 ⁱ
180	488 ⁱ	381 ⁱ	460 ⁱ	457 ⁱ
End of Test ^a	507	397	467	467

^a From 273 to 278 days

ⁱ Denotes interpolated values

Table 3.4a – Summary of Free Shrinkage Data for Program 2 (in microstrain)

Day	KDOT, Batch 130	MoDOT, Batch 132	Control, Batch 138	7-Day, Batch 140	14-Day, Batch 143
3	10	0	-37	-7 ⁱ	-6 ⁱ
7	157	113	63	-20	-17 ^{ij}
30	413	357	313	260	193
90	533	490 ⁱ	402 ⁱ	400	343
150	593 ⁱ	517 ⁱ	439 ⁱ	443 ⁱ	408 ⁱ
End of Test ^a	580	517	420	425	397
After 30 Days of Drying	457	387	313	290	253

^a From 166 to 170 days

ⁱ Denotes interpolated values

^j -37 $\mu\epsilon$ at 14 days

Table 3.4b – Summary of Free Shrinkage Data for Program 2, cont. (in microstrain)

Day	Type II C.G., Batch 145	SRA, Batch 147	497, Batch 149	Quartzite, Batch 159
3	-3	-10	7	-20
7	123	33	100	87
30	313	143	320	323
90	408 ⁱ	242 ⁱ	407	433 ⁱ
150	469 ⁱ	296 ⁱ	442 ⁱ	457 ^b
End of Test ^a	457	283	440	457
After 30 Days of Drying	327	157	333	343

^a From 148 to 165 days

^b On day 148

ⁱ Denotes interpolated values

Table 3.5 – Summary of Slope Analysis for Program 2 Ring Test

Mix	Batch	Number of Gages	Average Shrinkage Rate, $\mu\epsilon/d^{1/2}$	Standard Deviation, $\mu\epsilon/d^{1/2}$
MoDOT	132	12	-22	5.1
497	149	11	-22	4.9
Control	138	11	-20	3.4
14-day	143	10	-20	2.0
7-day	140	7	-19	2.0
Quartzite	159	12	-17	2.7
KDOT	130	12	-16	4.3
Type II C.G.	145	12	-12	2.3
SRA	147	12	-12	1.7

Note: For the results of the Student's t-tests (Tables 3.6 through 3.13),

“Y” indicates a statistical difference between the two samples at a confidence level of 98% ($\alpha = 0.02$),

“N” indicates that there is no statistical difference at the lowest confidence level, 80% ($\alpha = 0.2$),

Statistical differences at confidence levels at, but not exceeding 80%, 90%, and 95% are indicated by “80”, “90”, and “95”.

Table 3.6 – Student's t-test Results for Program 1 30-day Free Shrinkage Data

Free Shrinkage, $\mu\epsilon$		KDOT	Control	MoDOT	Type II C.G.
302	KDOT		Y	Y	Y
197	Control			80	90
170	MoDOT				95
160	Type II C.G.				

Table 3.7 – Student's t-test Results for Program 1 150-day Free Shrinkage Data

Free Shrinkage, $\mu\epsilon$		KDOT	MoDOT	Control	Type II C.G.
568	KDOT		Y	Y	Y
486	MoDOT			Y	Y
389	Control				90
359	Type II C.G.				

Table 3.8 – Student’s t-test Results for Program 1 Ring Test Data

Shrinkage Rate, $\mu\epsilon/d^{1/2}$		MoDOT	Control	Type II C.G.	KDOT
-33	MoDOT		Y	Y	90
-27	Control			80	80
-24	Type II C.G.				N
-23	KDOT				

Table 3.9 – Student’s t-test Results for the Replication of Program 1 30-day Free Shrinkage Data

Free Shrinkage, $\mu\epsilon$		Control	MoDOT	KDOT	Type II C.G.
389	Control		95	Y	Y
353	MoDOT			N	Y
340	KDOT				Y
256	Type II C.G.				

Table 3.10 – Student’s t-test Results for the Replication of Program 1 150-day Free Shrinkage Data

Free Shrinkage, $\mu\epsilon$		Control	MoDOT	KDOT	Type II C.G.
486	Control		95	Y	Y
461	MoDOT			N	95
459	KDOT				Y
373	Type II C.G.				

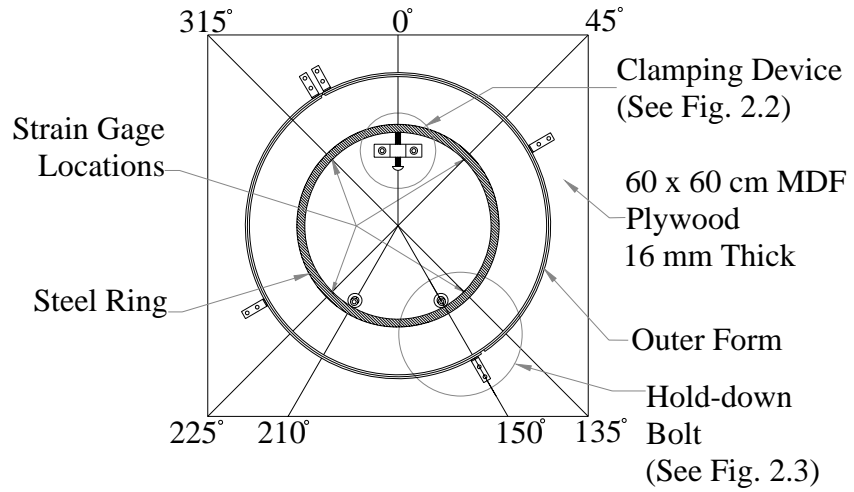


Figure 2.1 – Ring Specimen Form Layout

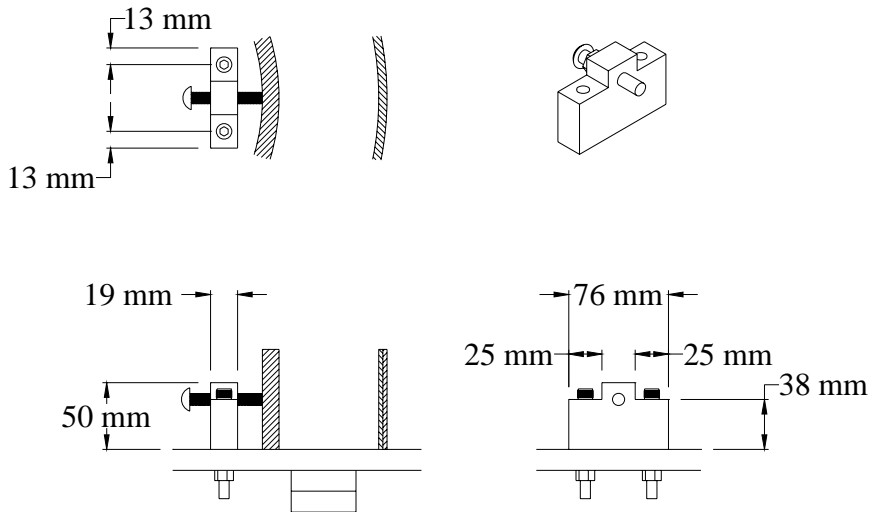


Figure 2.2 – Clamping Device Detail

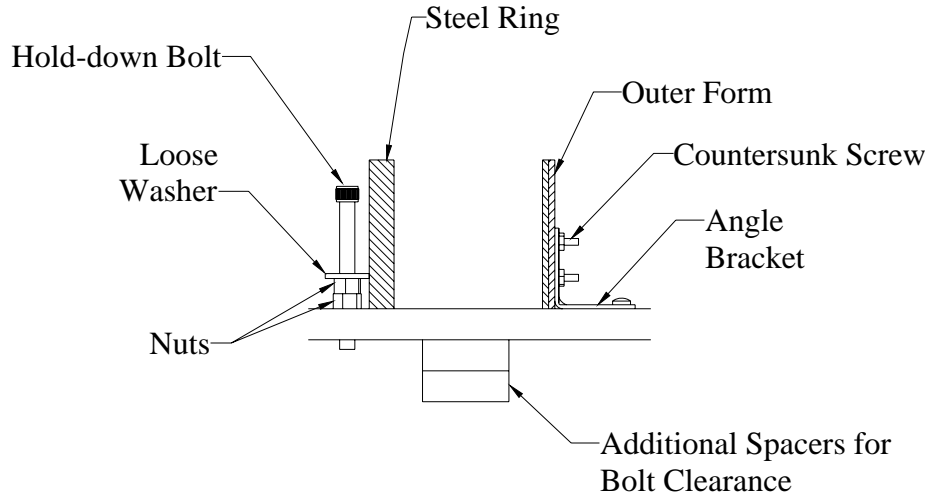


Figure 2.3 – Hold-down Bolt Detail

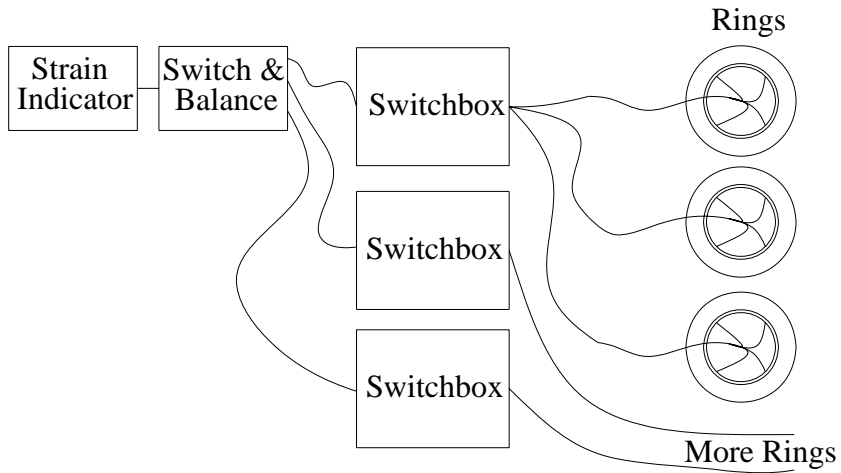


Figure 2.4 – Schematic of Data Acquisition

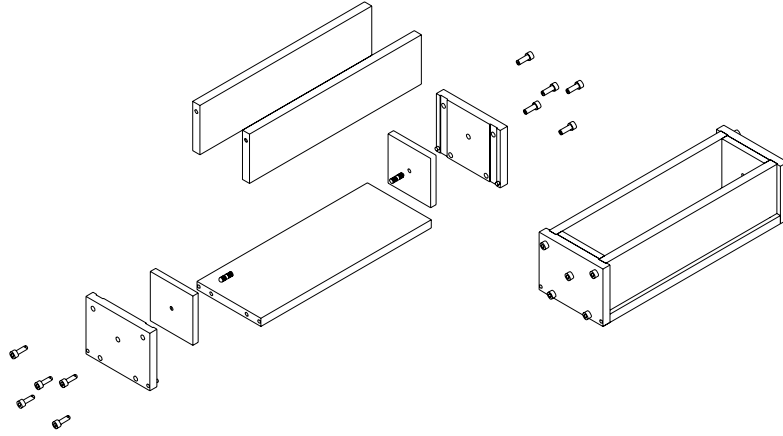


Figure 2.5 – Free Shrinkage Specimen Mold

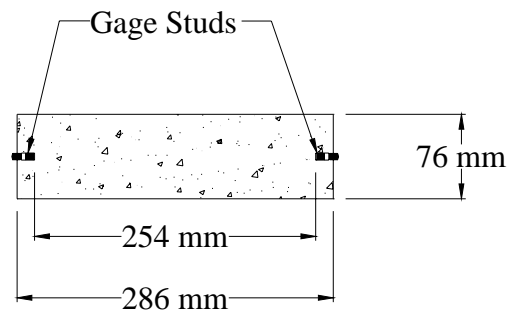


Figure 2.6 – Cross-section of Free Shrinkage Specimen

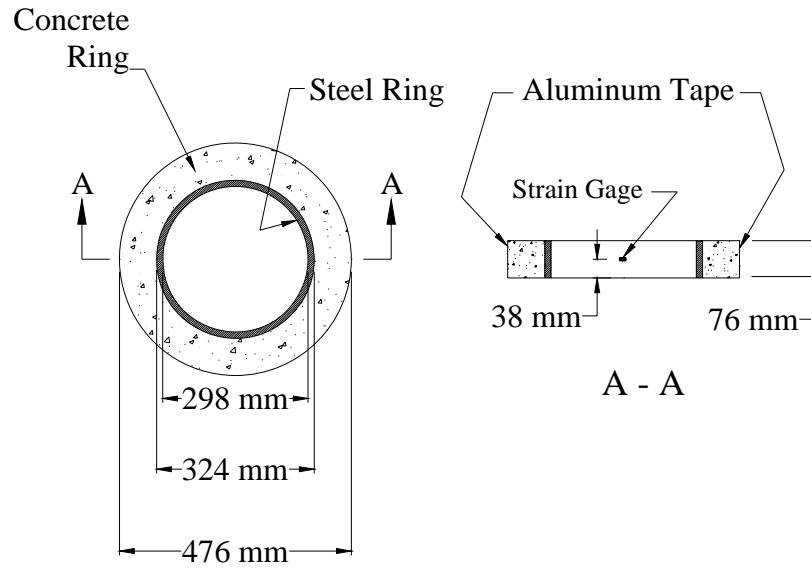


Figure 2.7 – Ring Details for Preliminary Testing and Program 1

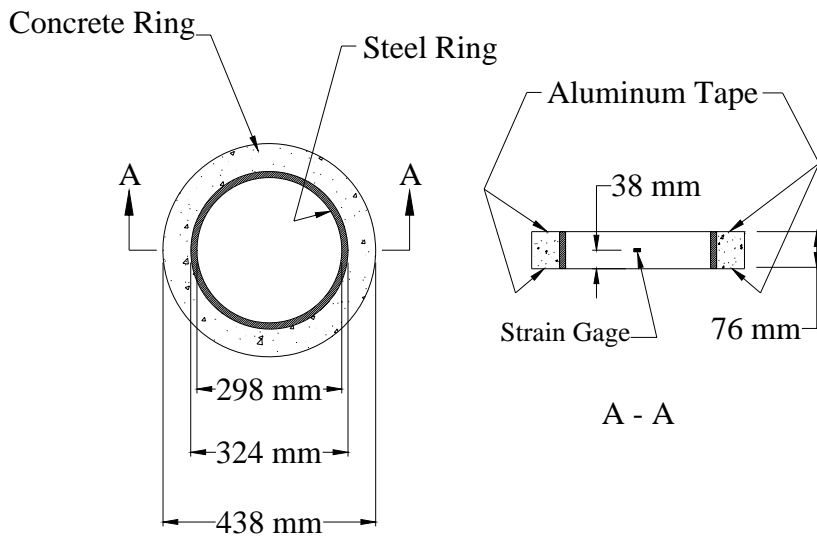


Figure 2.8 – Ring Details for Program 2

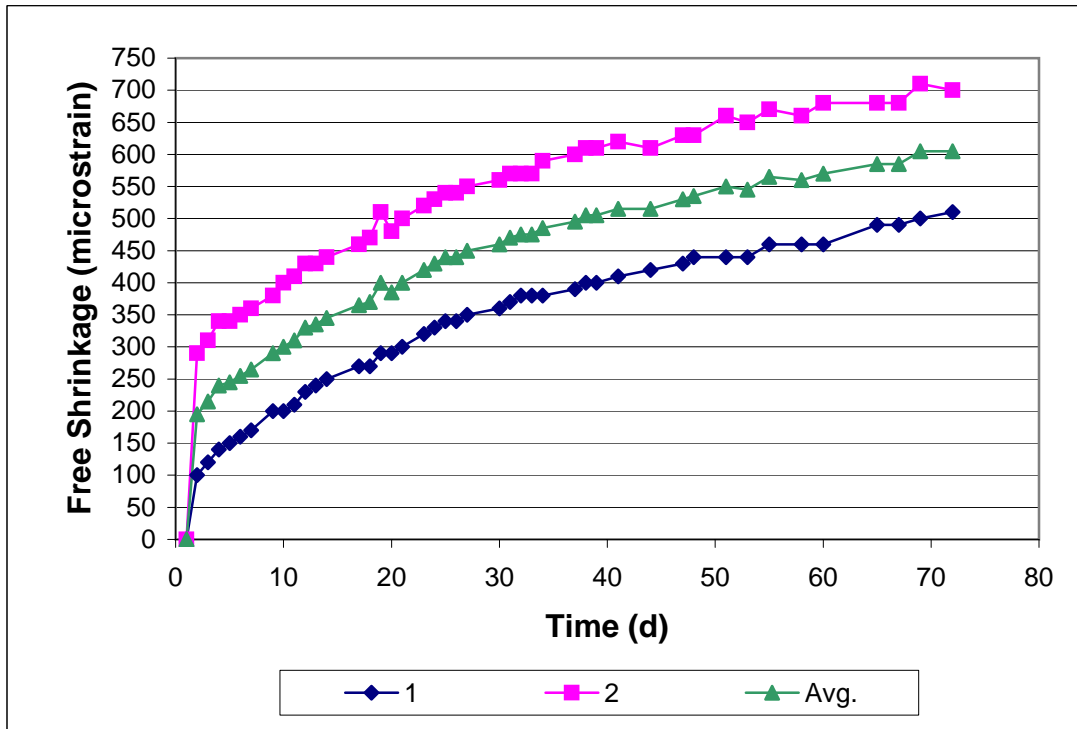


Figure 3.1 - Free Shrinkage Test. Preliminary free shrinkage, P1. No curing, drying begins on day 1.

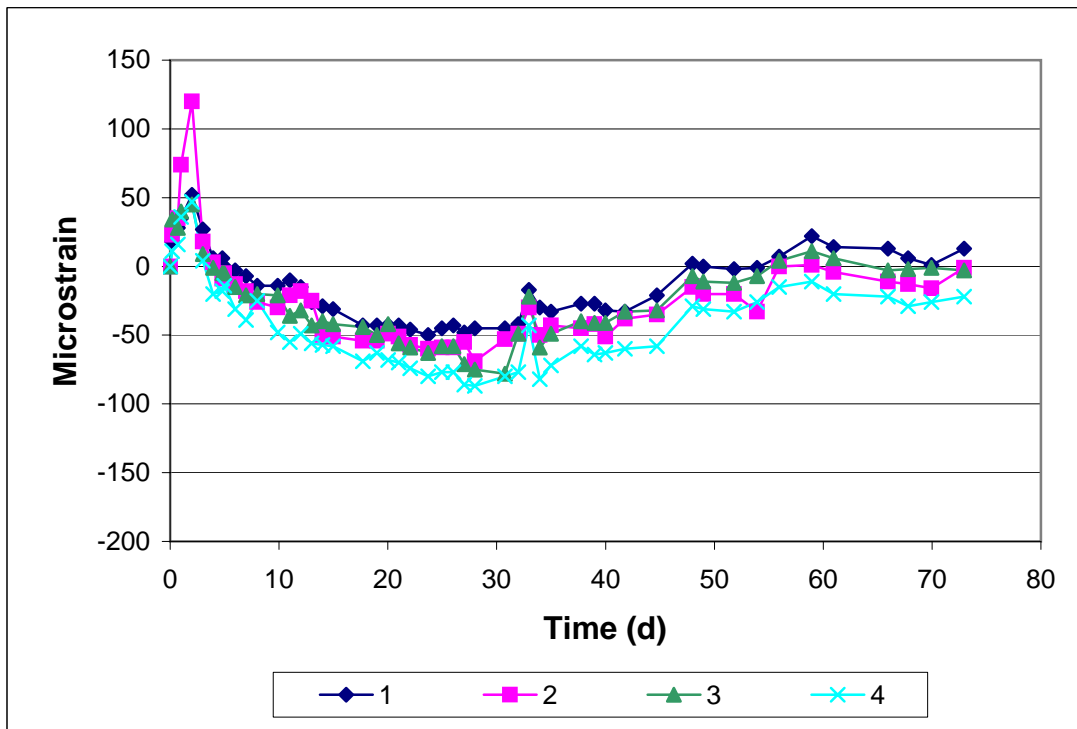


Figure 3.2 - Restrained Ring Test. Strain gage data for preliminary ring, P1. No curing, drying begins on day 1.

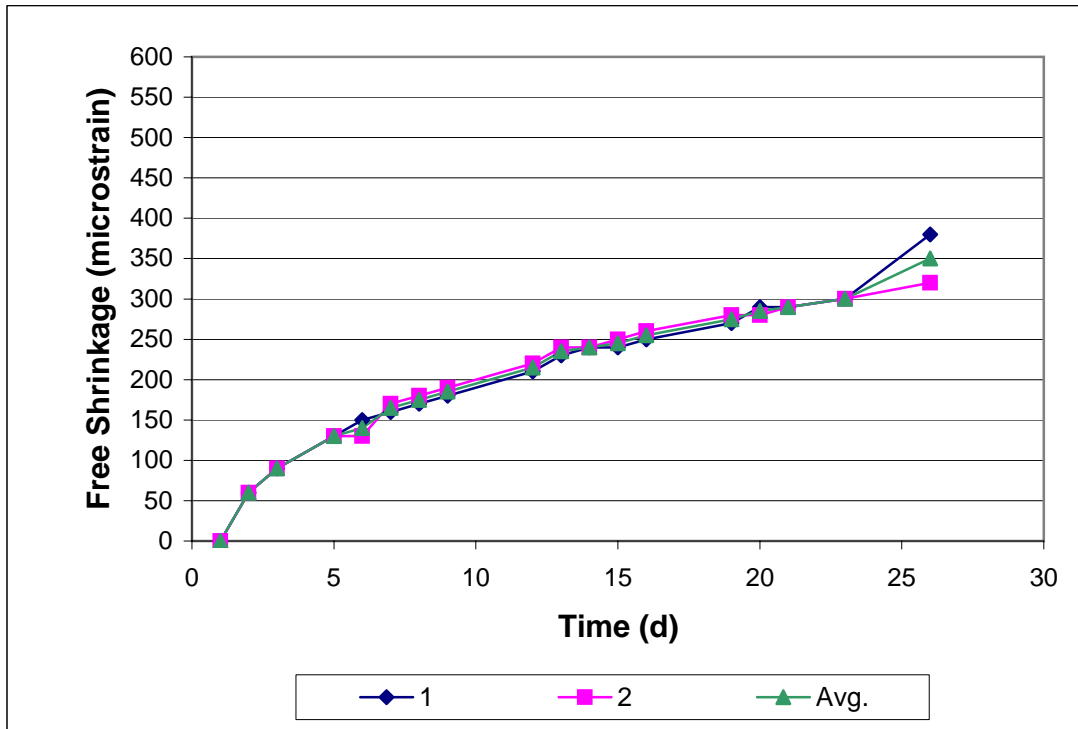


Figure 3.3 - Free Shrinkage Test. Preliminary free shrinkage, P2. No curing, drying begins on day 1.

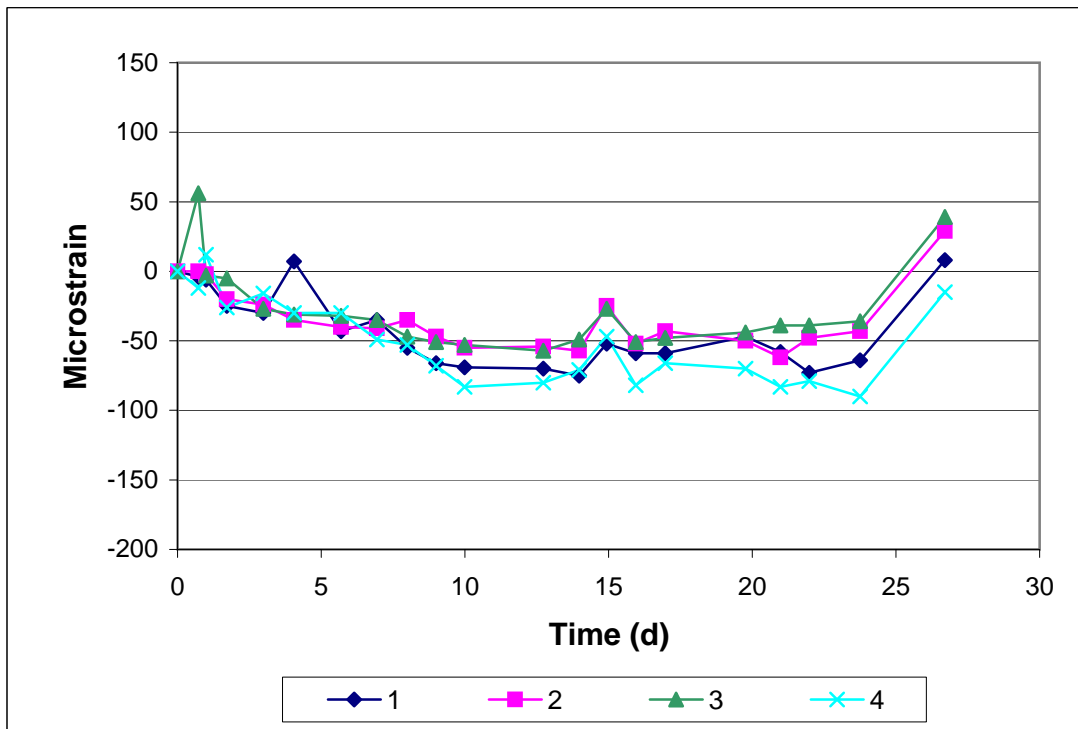


Figure 3.4 - Restrained Ring Test. Strain gage data for preliminary ring, P2. No curing, drying begins on day 1.

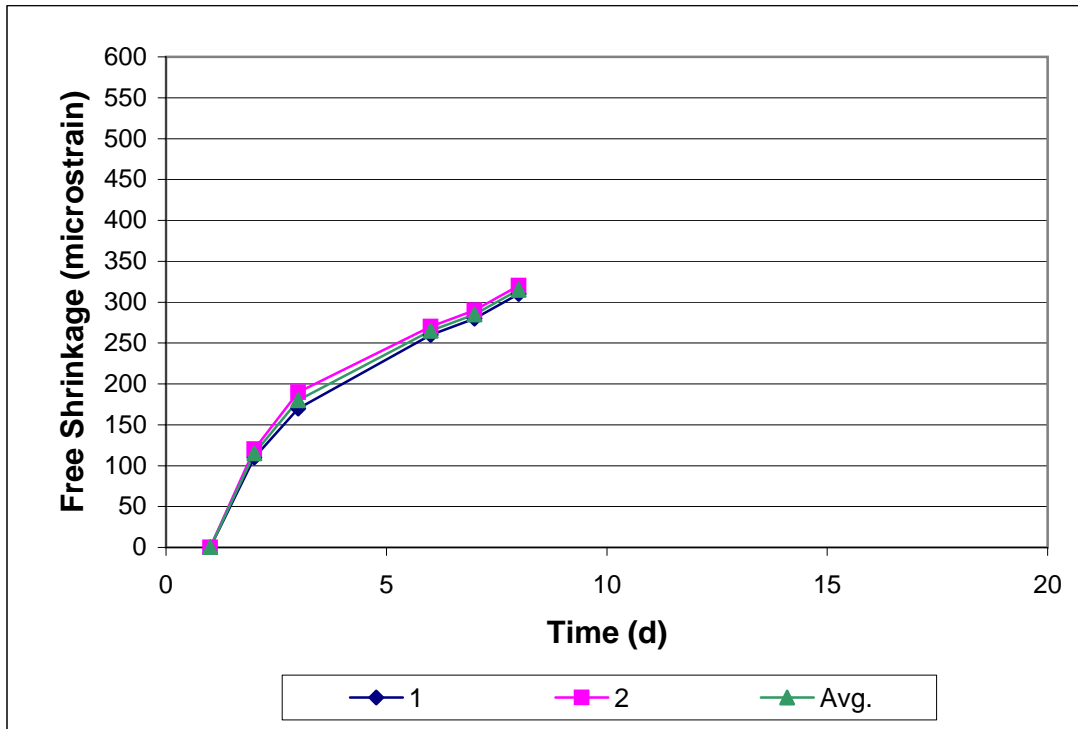


Figure 3.5 - Free Shrinkage Test. Preliminary free shrinkage, P3. No curing, drying begins on day 1.

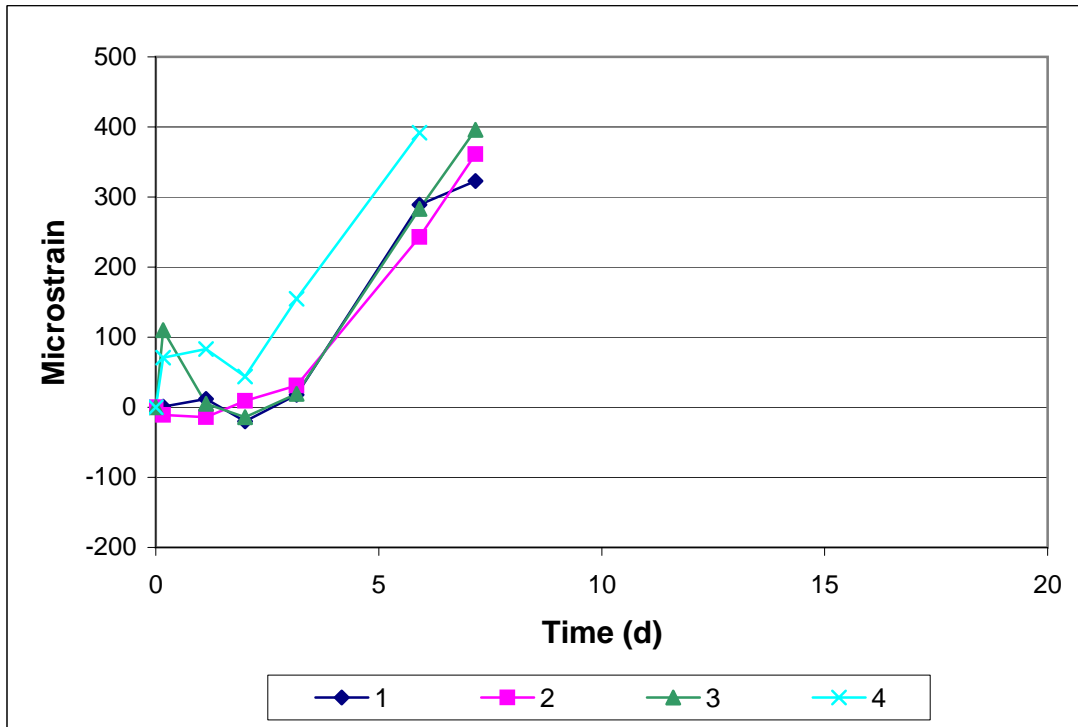


Figure 3.6 - Restrained Ring Test. Strain gage data for preliminary ring, P3. No curing, drying begins on day 1.



Figure 3.7 - Crack observed in ring P2 on day 27



Figure 3.8 - Crack observed in ring P3 on day 6

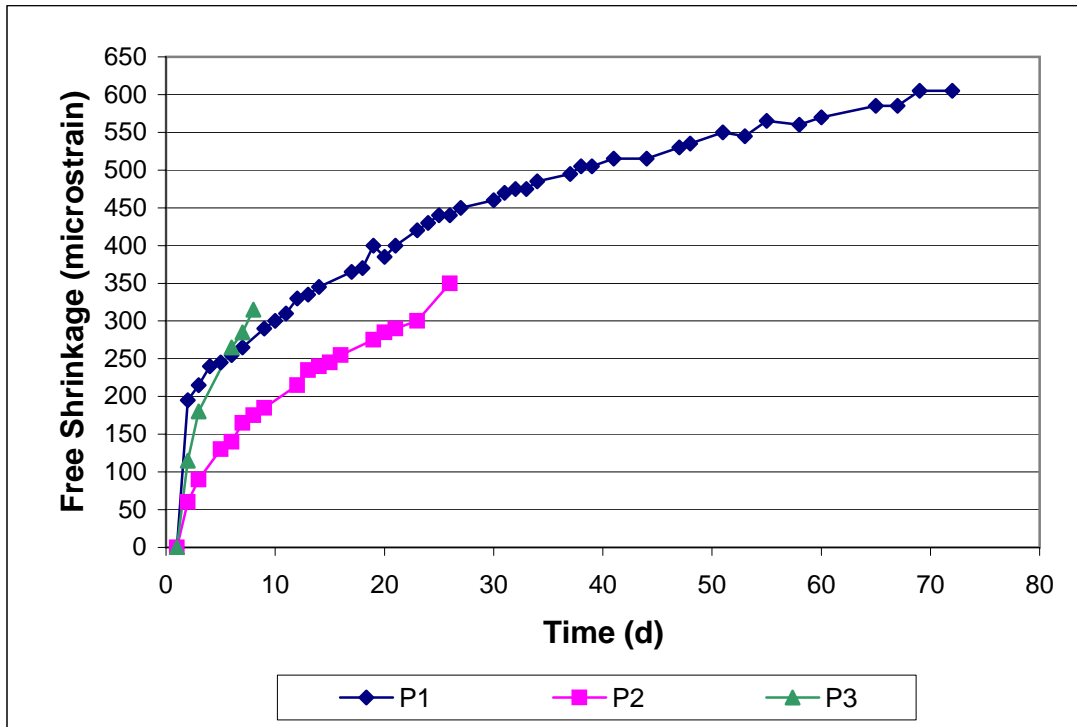


Figure 3.9 - Average free shrinkage curves for preliminary tests

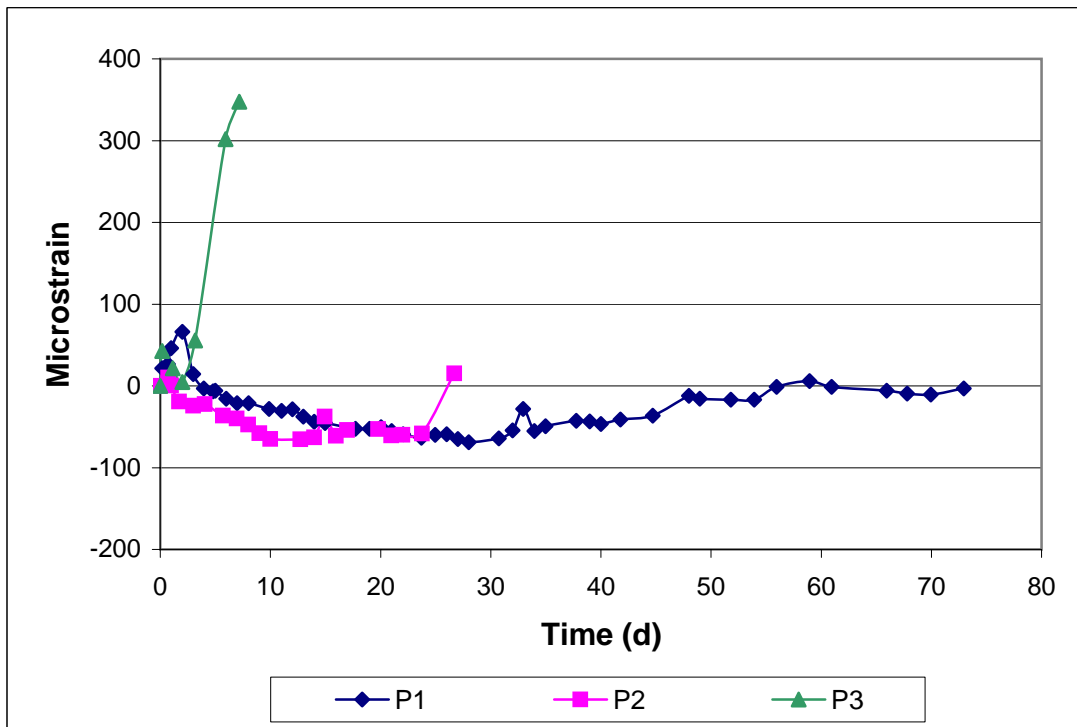


Figure 3.10 - Average restrained shrinkage curves for preliminary tests

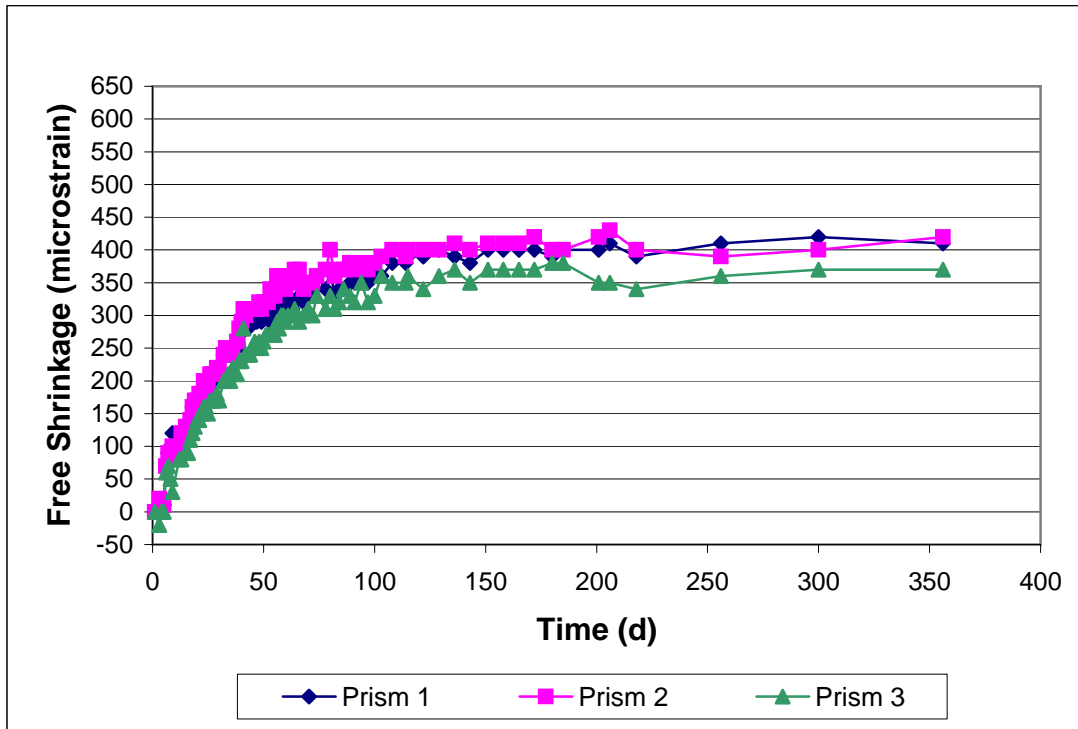


Figure 3.11 - Free Shrinkage Test, Program 1. Control mix, Batch 55. Drying begins on day 3.

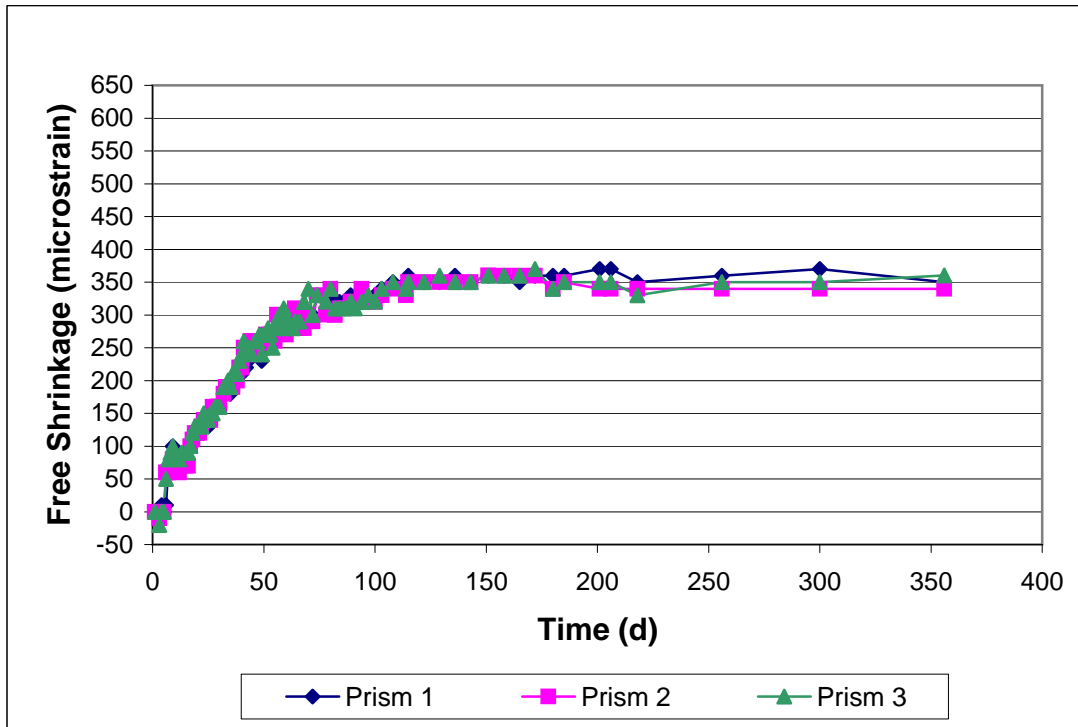


Figure 3.12 - Free Shrinkage Test, Program 1. Type II coarse-ground cement mix, Batch 56. Drying begins on day 3.

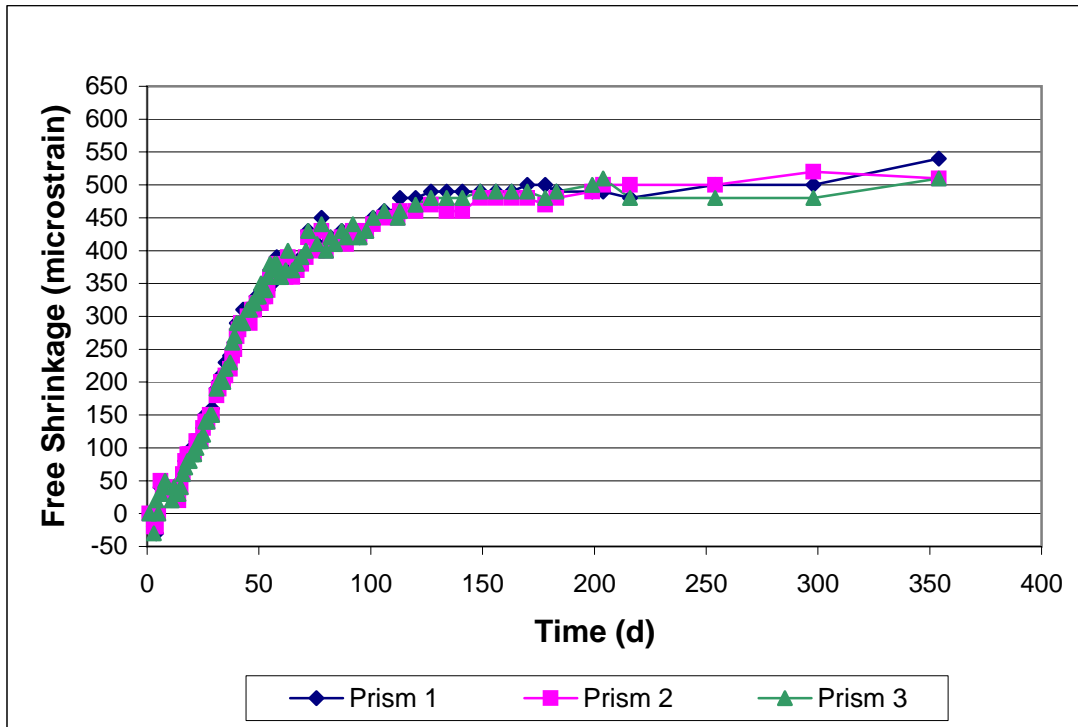


Figure 3.13 - Free Shrinkage Test, Program 1. MoDOT mix, Batch 57. Drying begins on day 3.

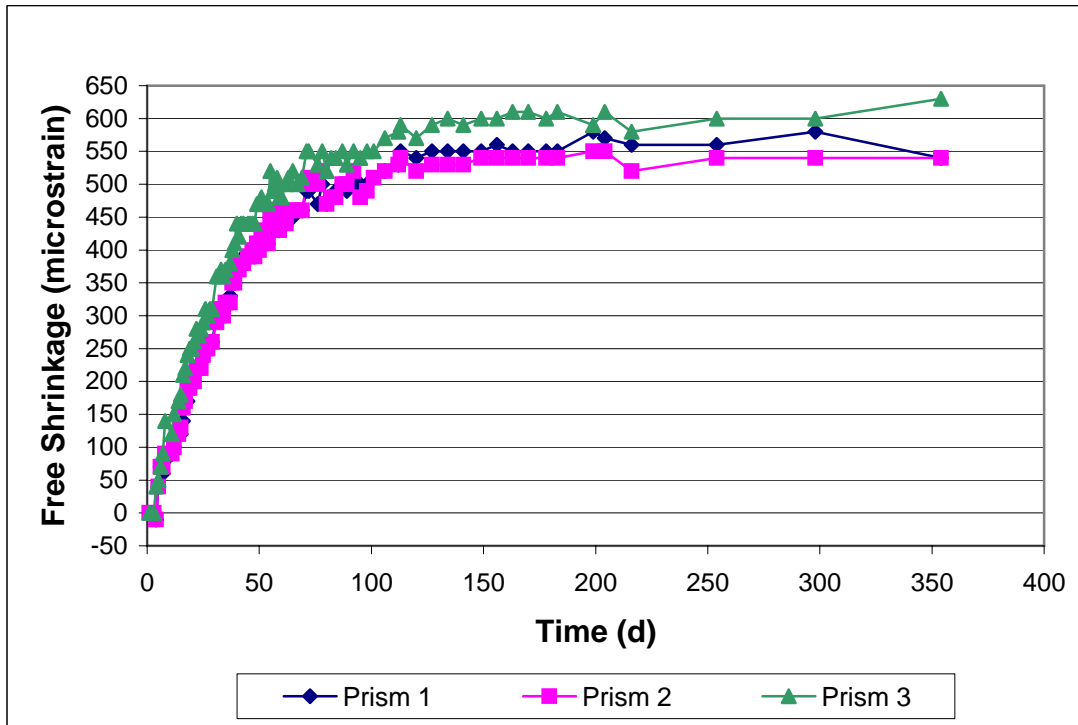


Figure 3.14 - Free Shrinkage Test, Program 1. KDOT mix, Batch 58. Drying begins on day 3. For prisms 1 and 2, zero reading occurs on day 3.

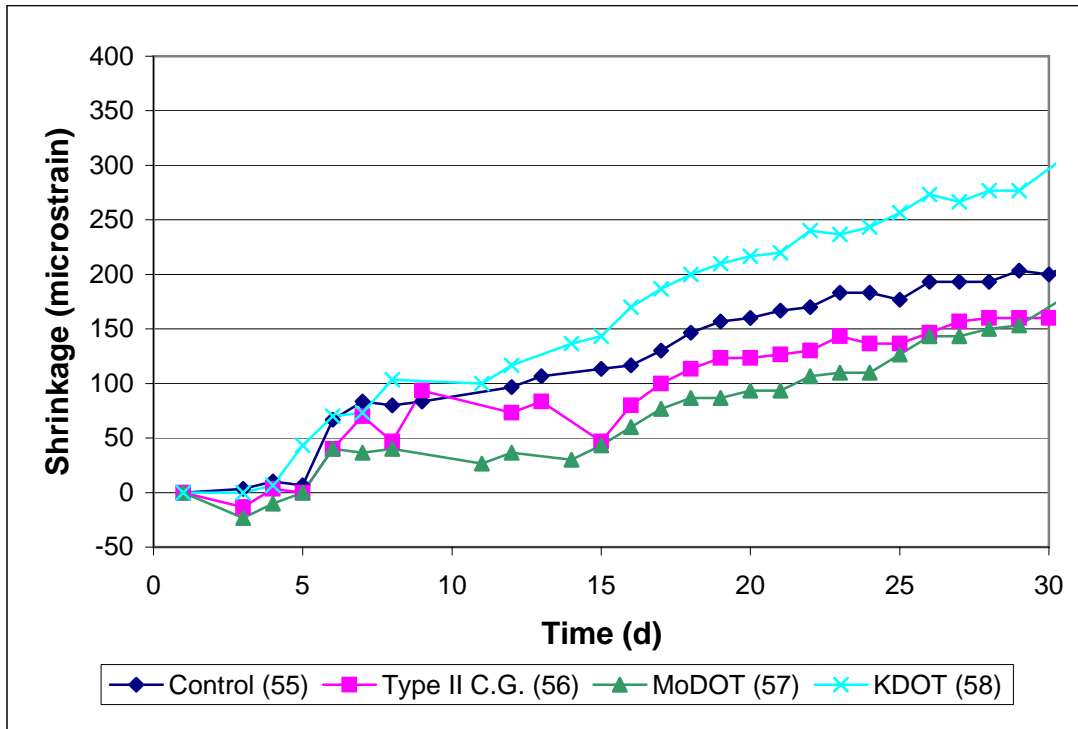


Figure 3.15 - Free Shrinkage Test, Program 1. Average free shrinkage curves for all specimens in a batch. First 30 days.

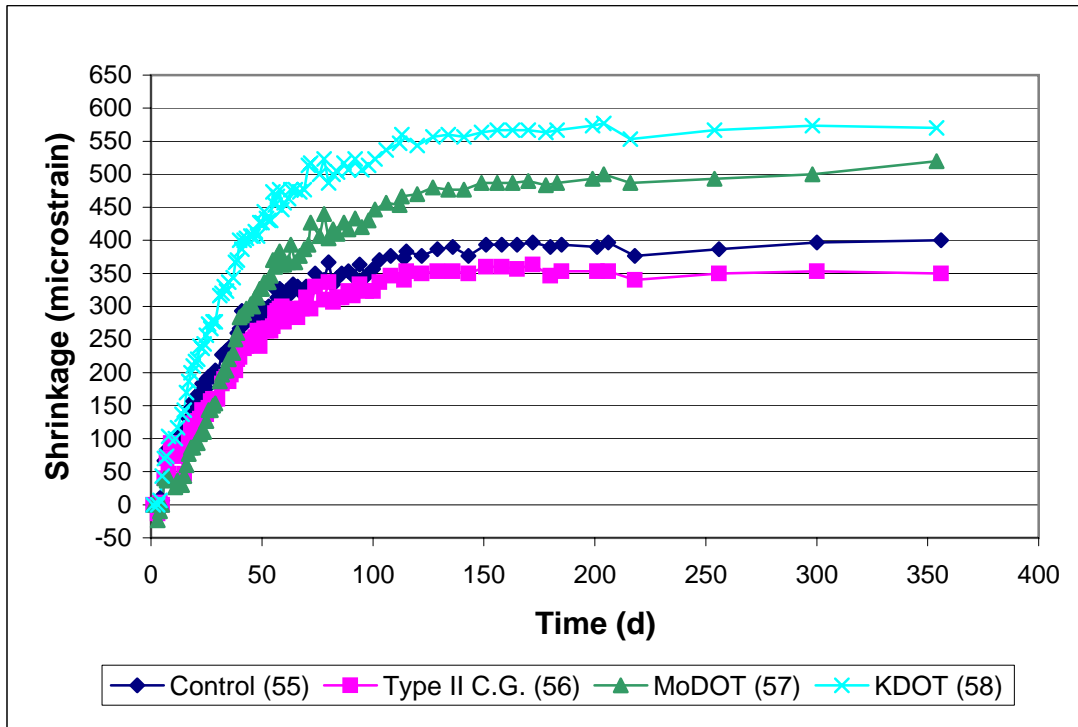


Figure 3.16 - Free Shrinkage Test, Program 1. Average free shrinkage curves for all specimens in a batch.

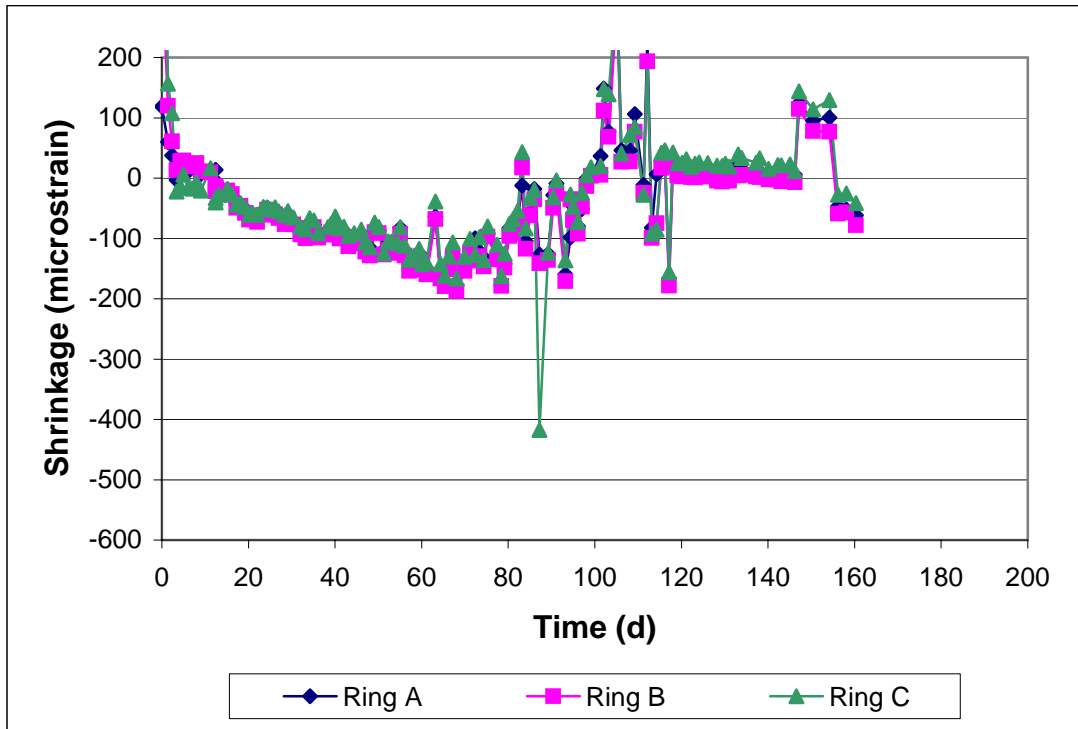


Figure 3.17 - Ring Test, Program 1. Control mix, Batch 55. Average adjusted curve for each ring.

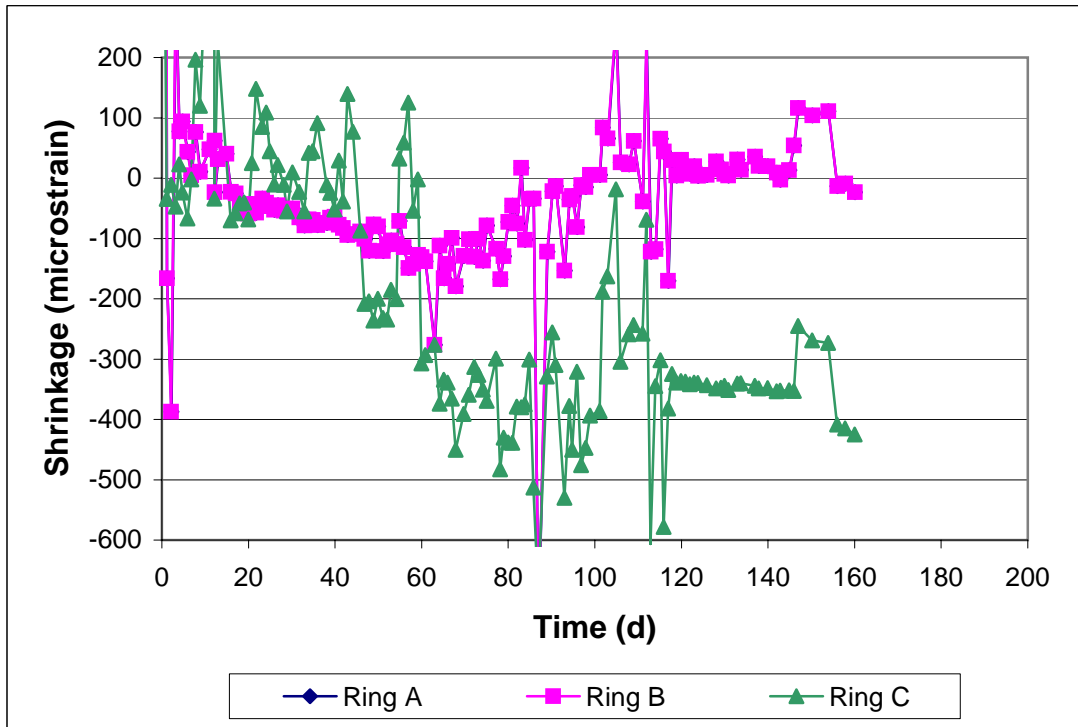


Figure 3.18 - Ring Test, Program 1. Type II C.G. mix, Batch 56. Average adjusted curve for each ring.

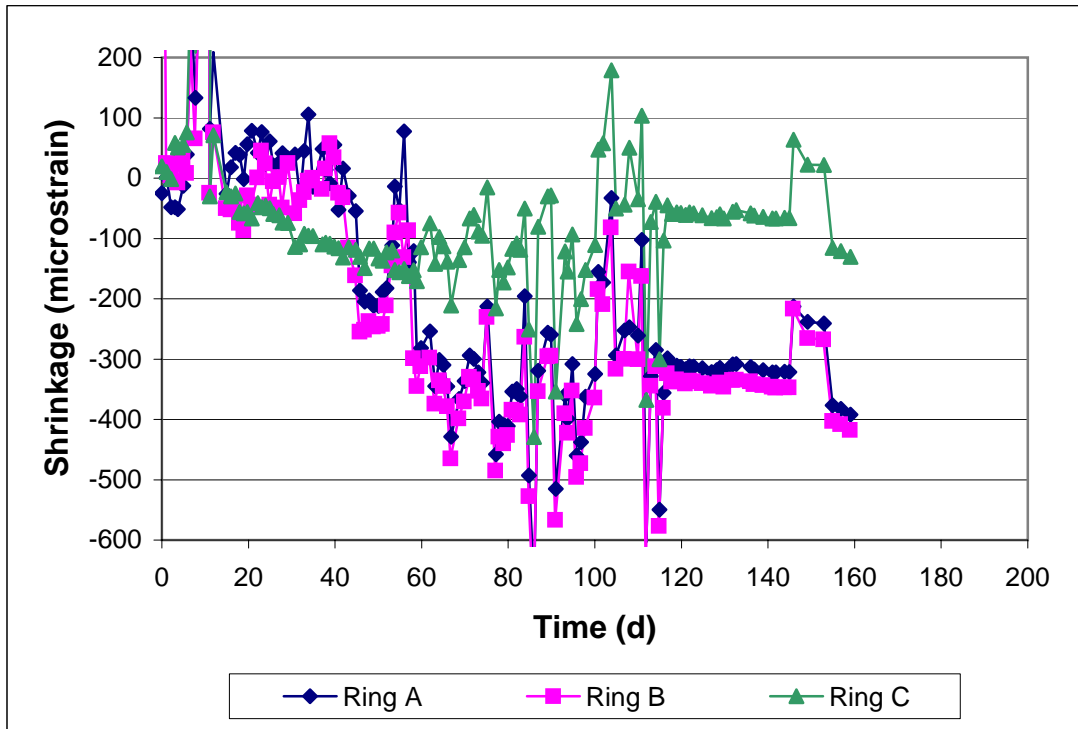


Figure 3.19 - Ring Test, Program 1. MoDOT mix, Batch 57. Average adjusted curve for each ring.

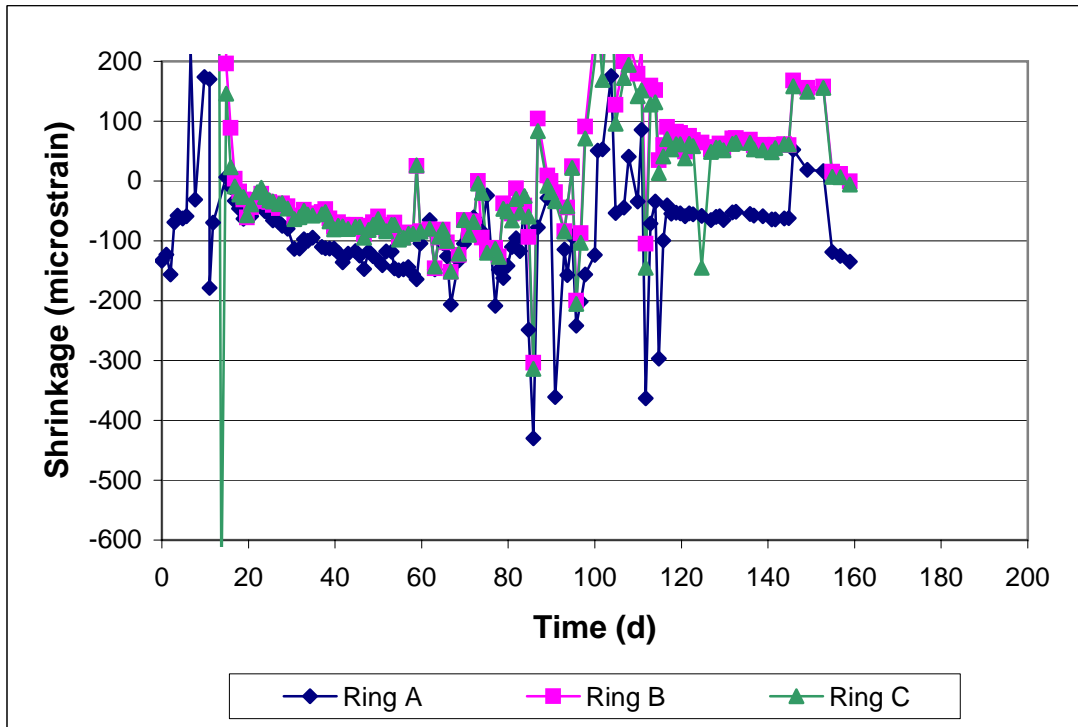


Figure 3.20 - Ring Test, Program 1. KDOT mix, Batch 58. Average adjusted curve for each ring.

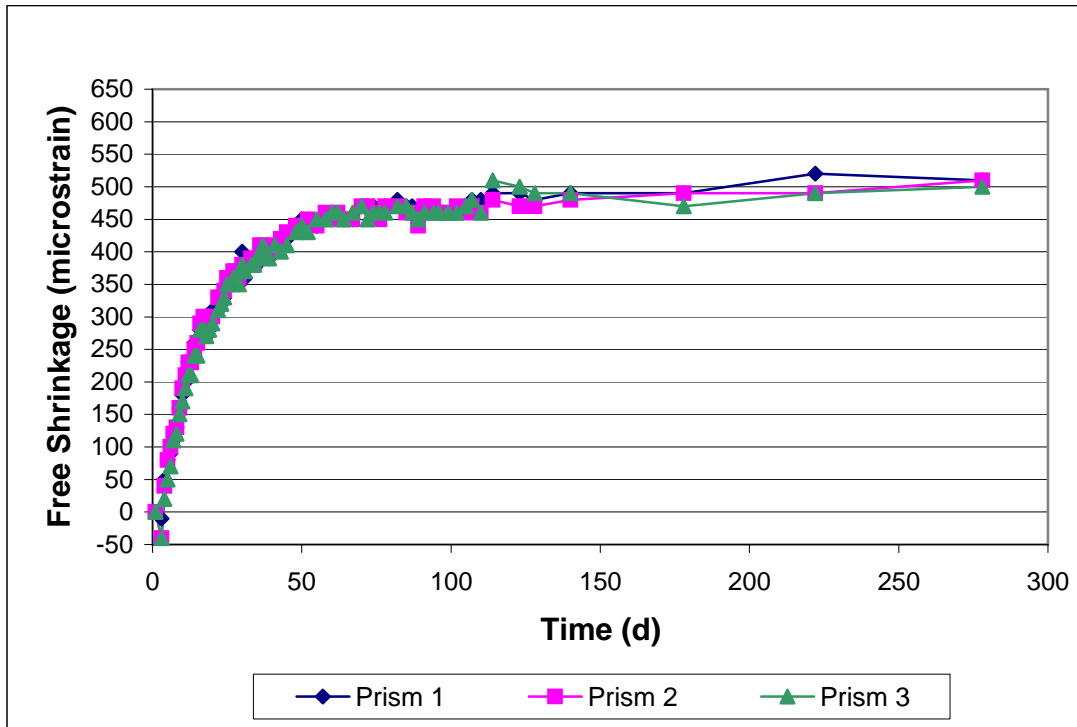


Figure 3.21 - Free Shrinkage Test, Replication of Program 1. Control mix, Batch 81. Drying begins on day 3.

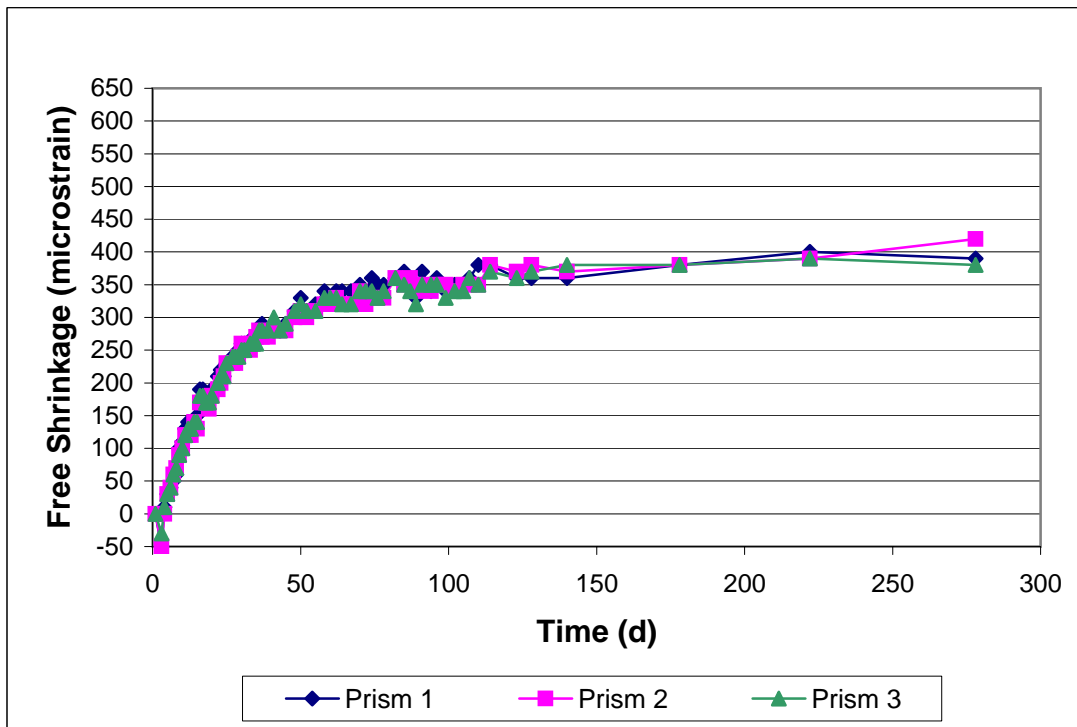


Figure 3.22 - Free Shrinkage Test, Replication of Program 1. Type II coarse-ground cement mix, Batch 82. Drying begins on day 3.

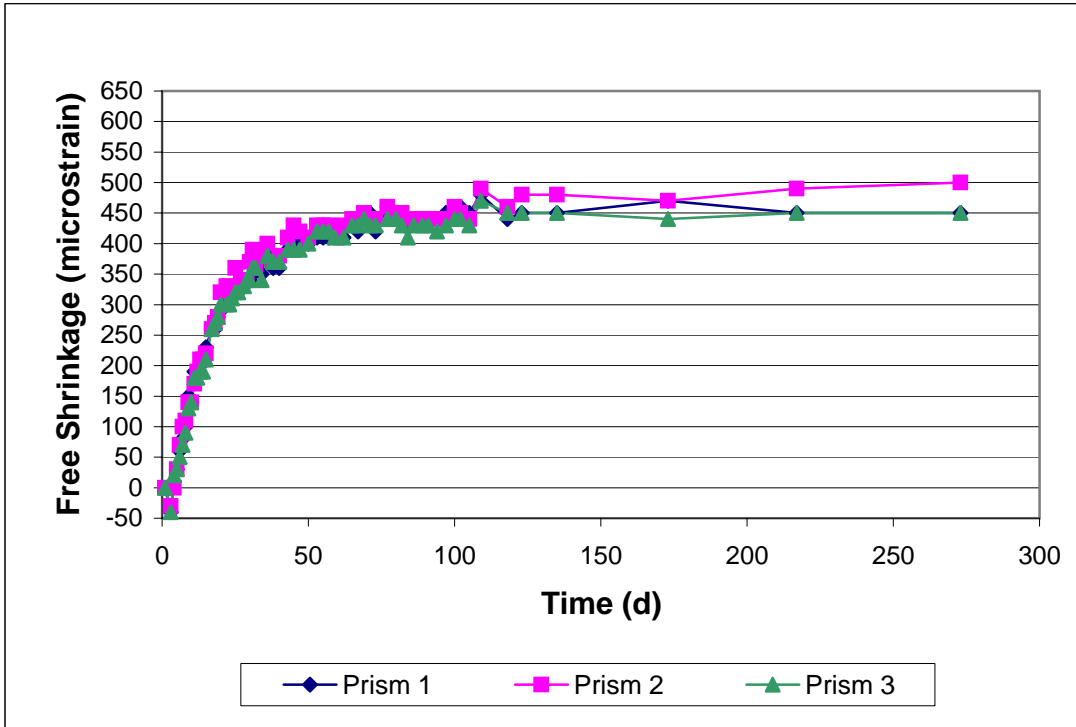


Figure 3.23 - Free Shrinkage Test, Replication of Program 1. MoDOT mix, Batch 83. Drying begins on day 3.

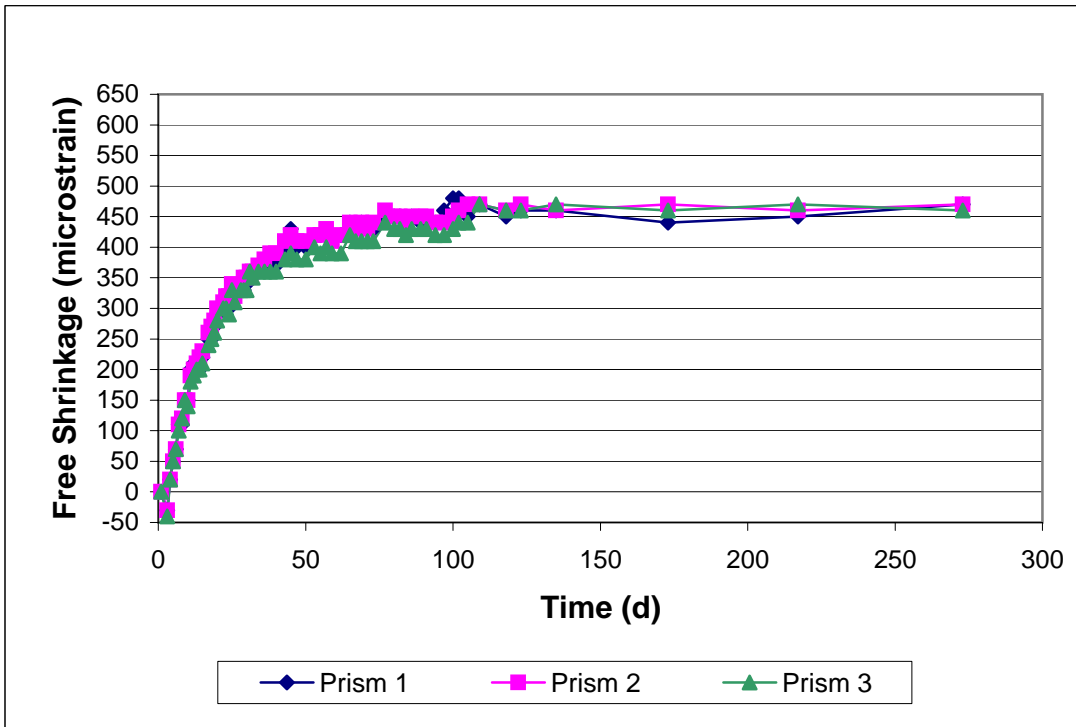


Figure 3.24 - Free Shrinkage Test, Replication of Program 1. KDOT mix, Batch 84. Drying begins on day 3.

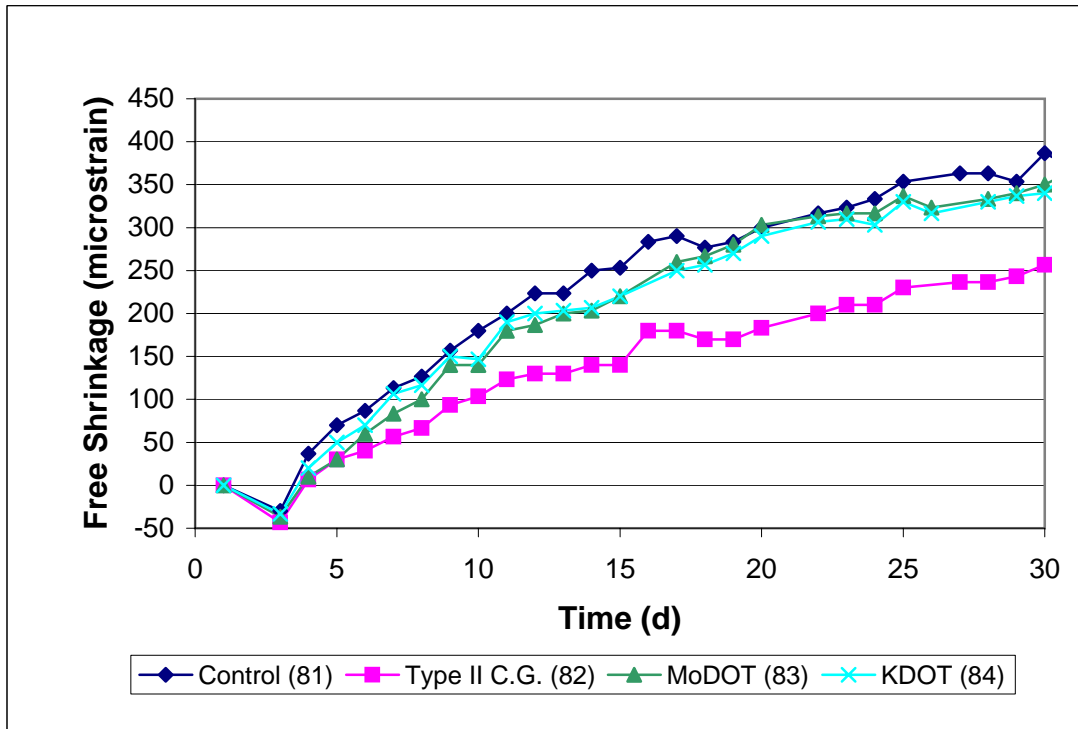


Figure 3.25 - Free Shrinkage Test, Replication of Program 1. Average free shrinkage curves for all specimens in a batch. First 30 days.

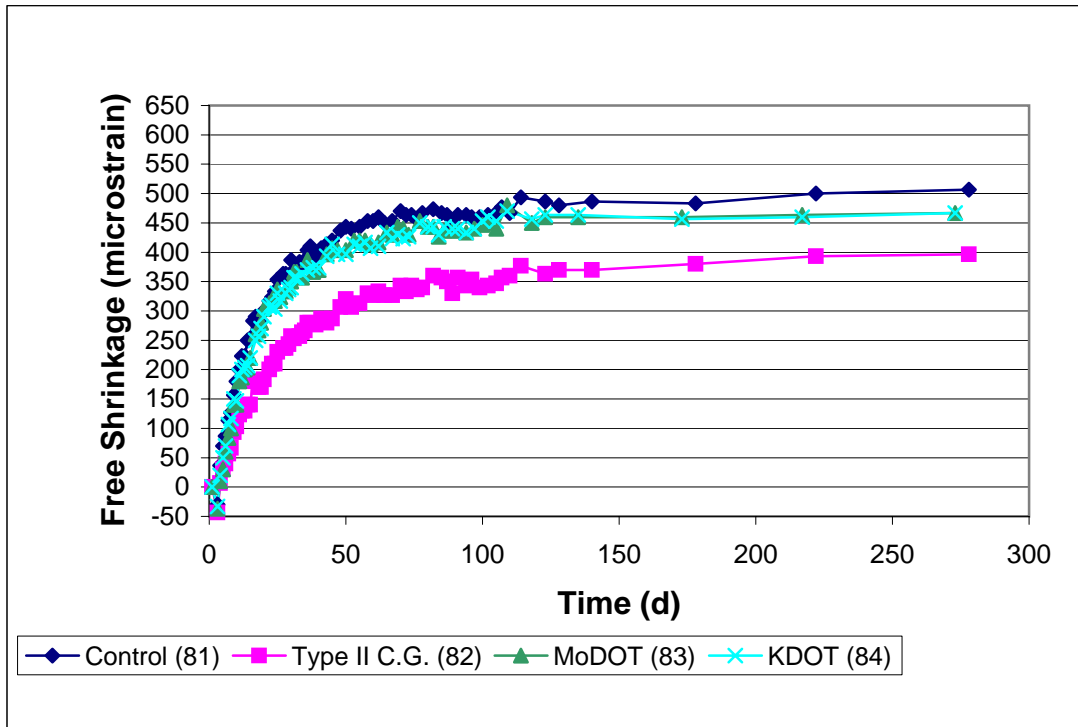


Figure 3.26 - Free Shrinkage Test, Replication of Program 1. Average free shrinkage curves for all specimens in a batch.

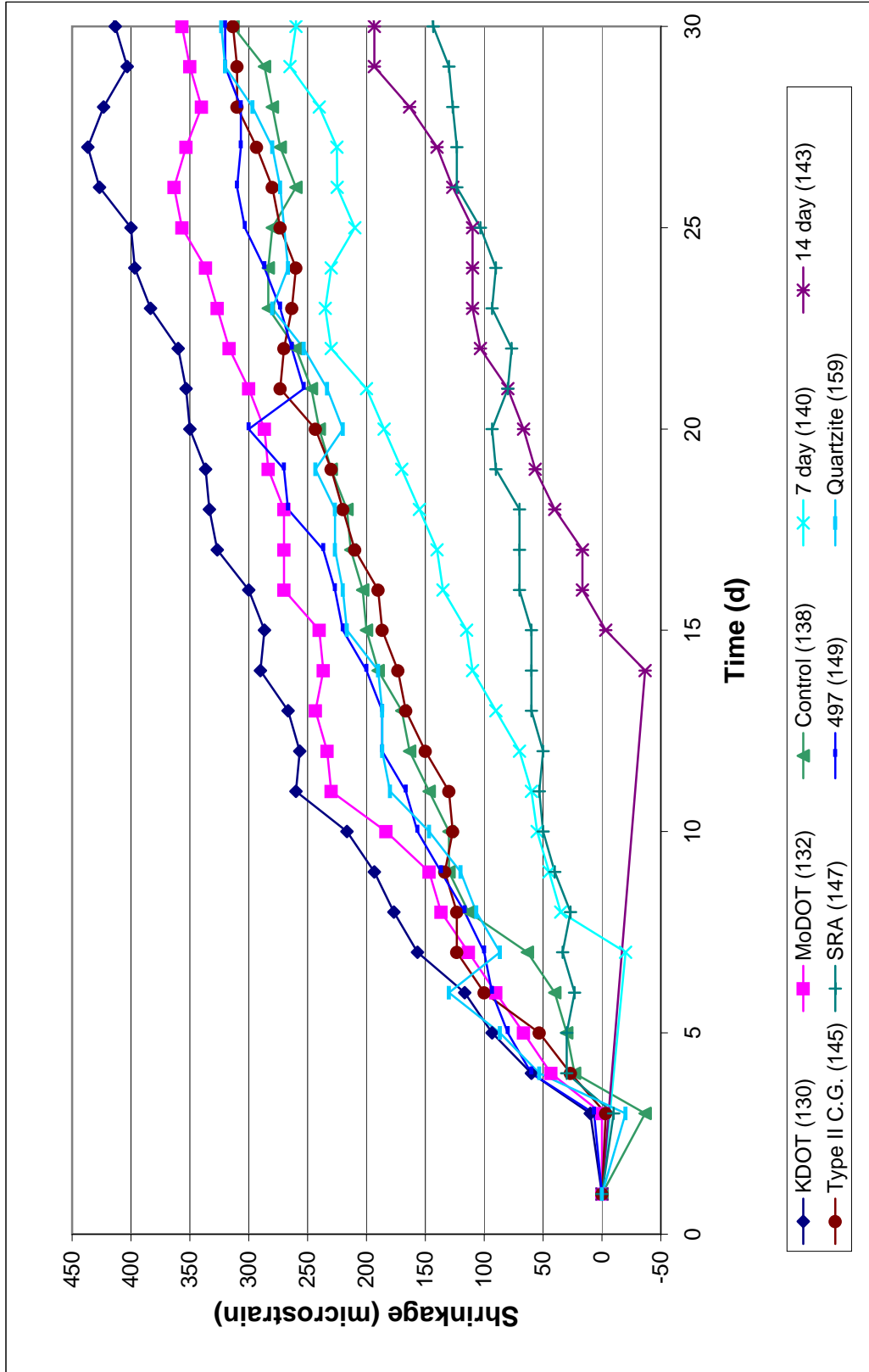


Figure 3.27 - Free Shrinkage Test, Program 2. Average free shrinkage curves for all specimens in a batch. Specimens were demolded on day 1.

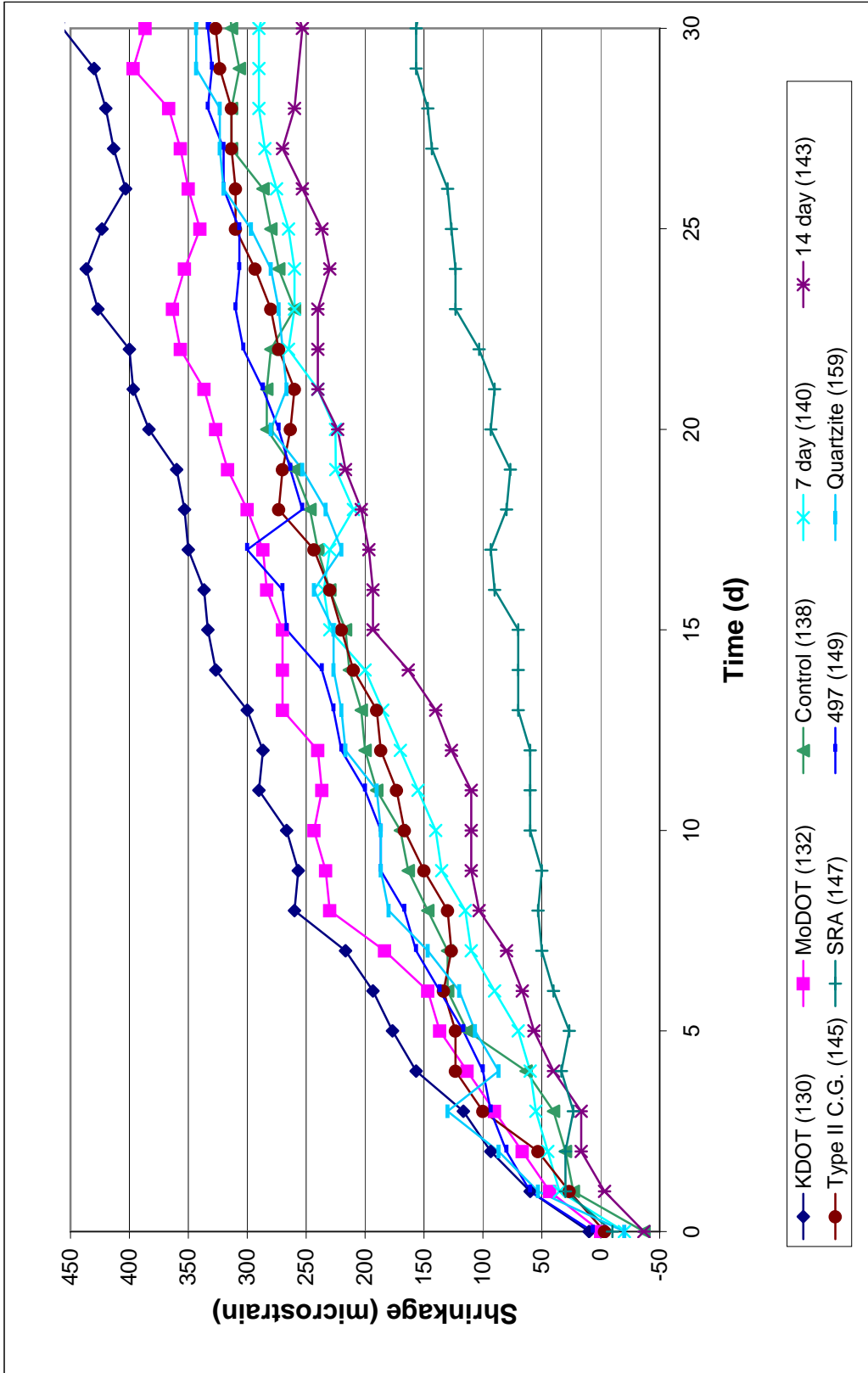


Figure 3.28 - Free Shrinkage Test, Program 2. Average free shrinkage curves for all specimens in a batch. First 30 days of drying.

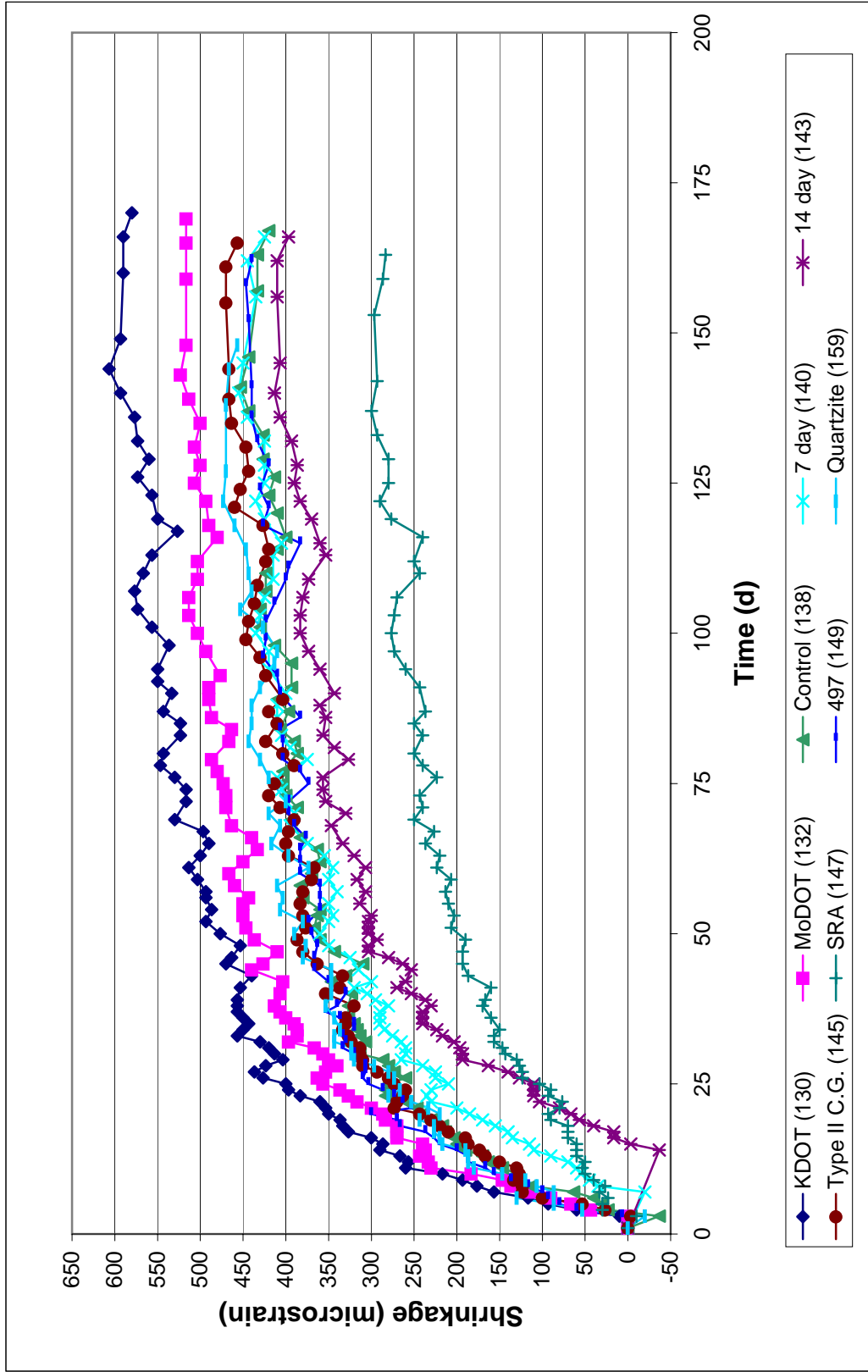


Figure 3.29 - Free Shrinkage Test, Program 2. Average free shrinkage curves for all specimens in a batch. Specimens were demolded on day 1.

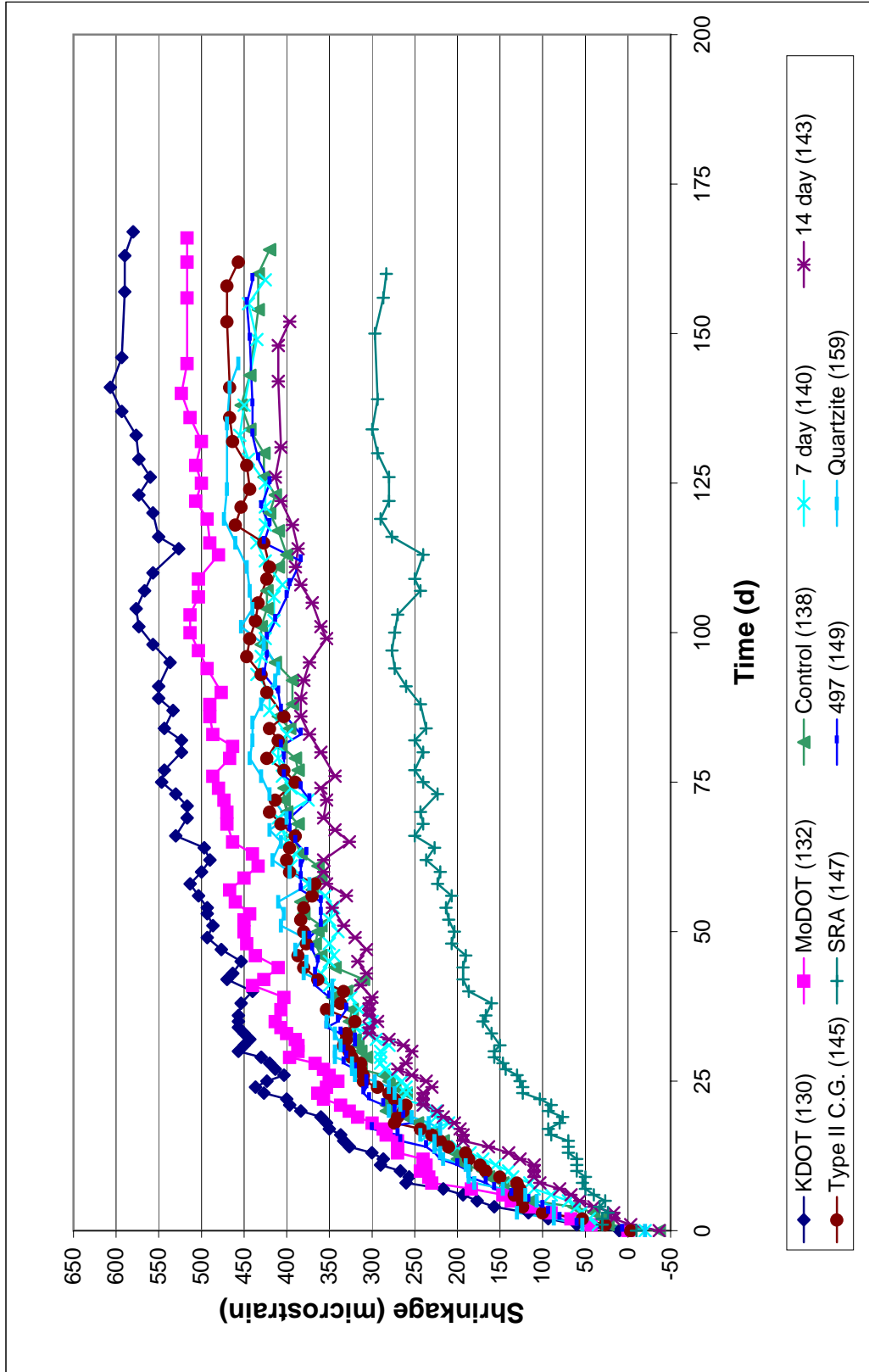


Figure 3.30 - Free Shrinkage Test, Program 2. Average free shrinkage curves for all specimens in a batch. Drying begins on day 0.

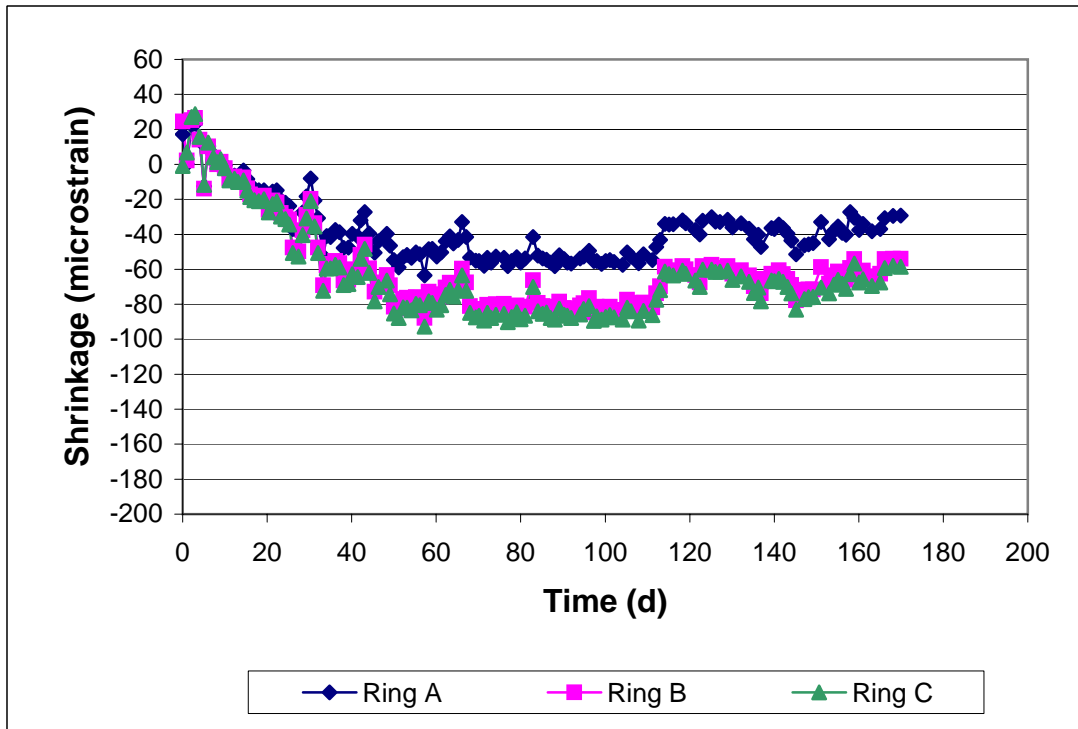


Figure 3.31 - Ring Test, Program 2. KDOT mix, Batch 130. Average adjusted curve for each ring.

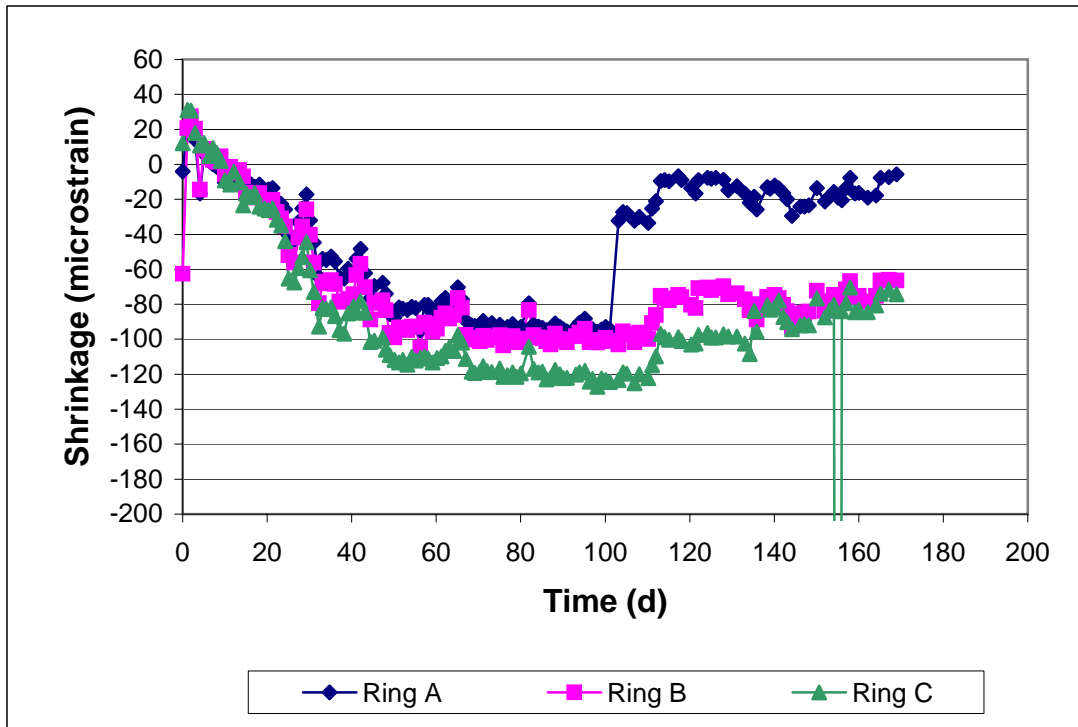


Figure 3.32 - Ring Test, Program 2. MoDOT mix, Batch 132. Average adjusted curve for each ring.

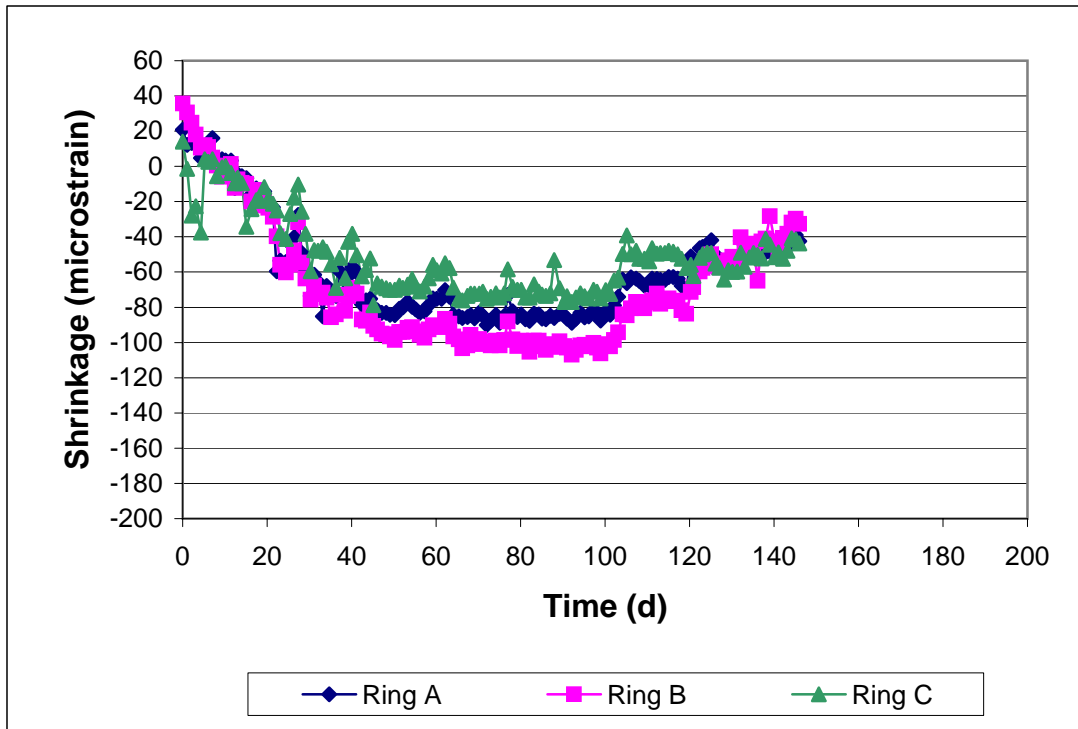


Figure 3.33 - Ring Test, Program 2. Control mix, Batch 138. Average adjusted curve for each ring.

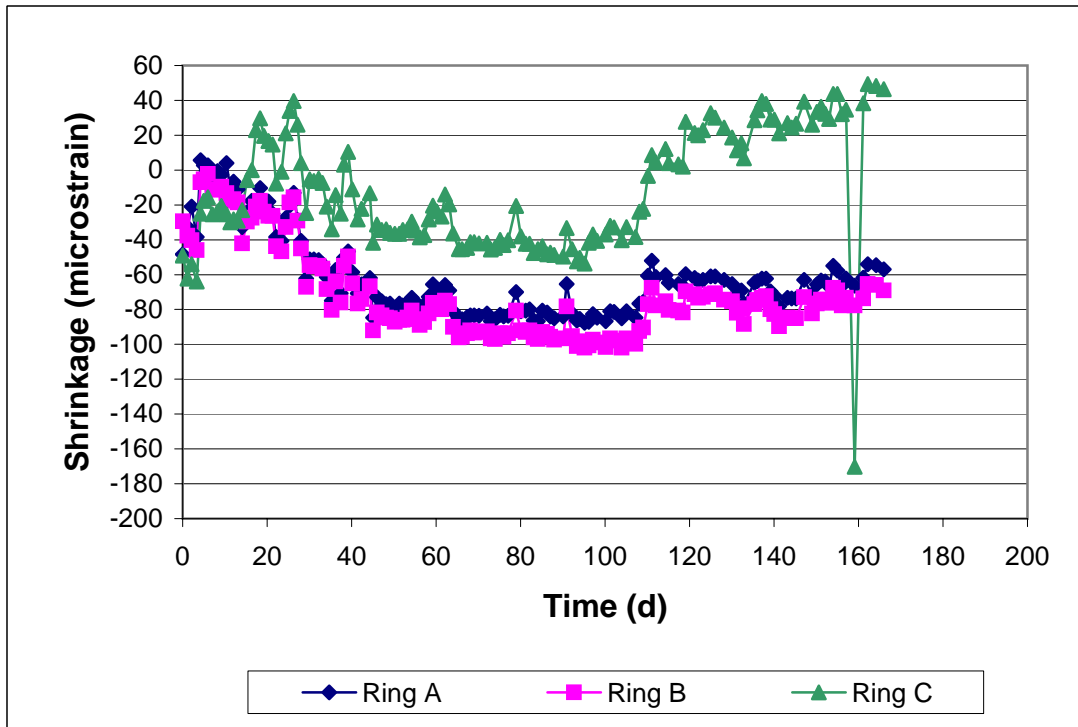


Figure 3.34 - Ring Test, Program 2. 7-day cure mix, Batch 140. Average adjusted curve for each ring.

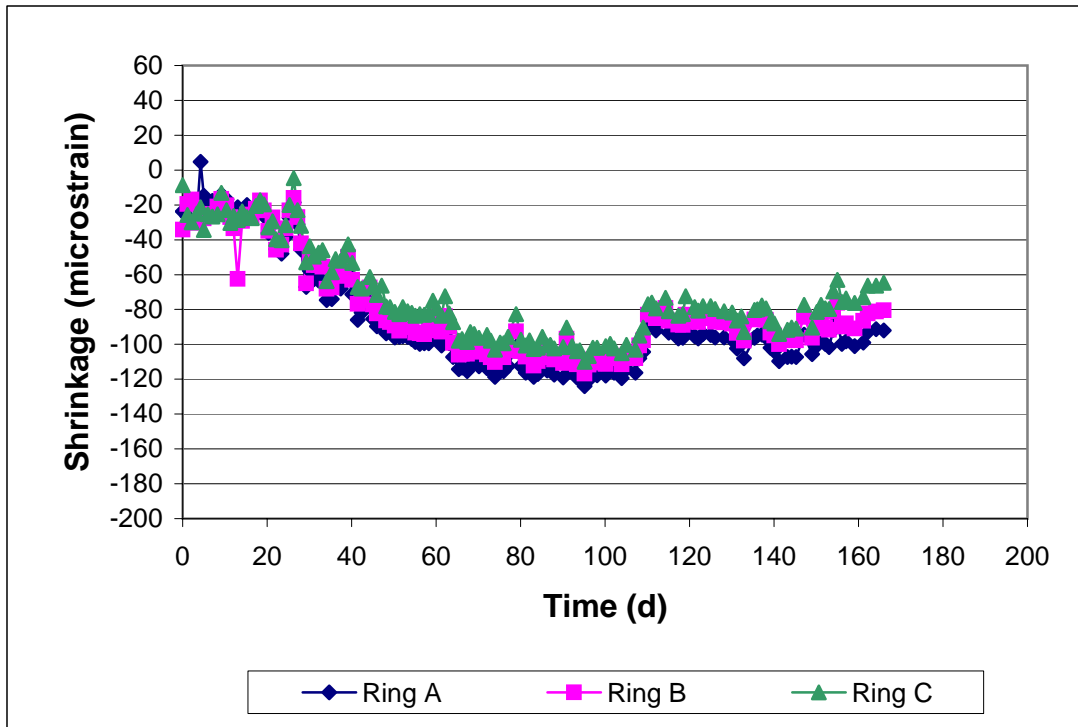


Figure 3.35 - Ring Test, Program 2. 14-day cure mix, Batch 143. Average adjusted curve for each ring.

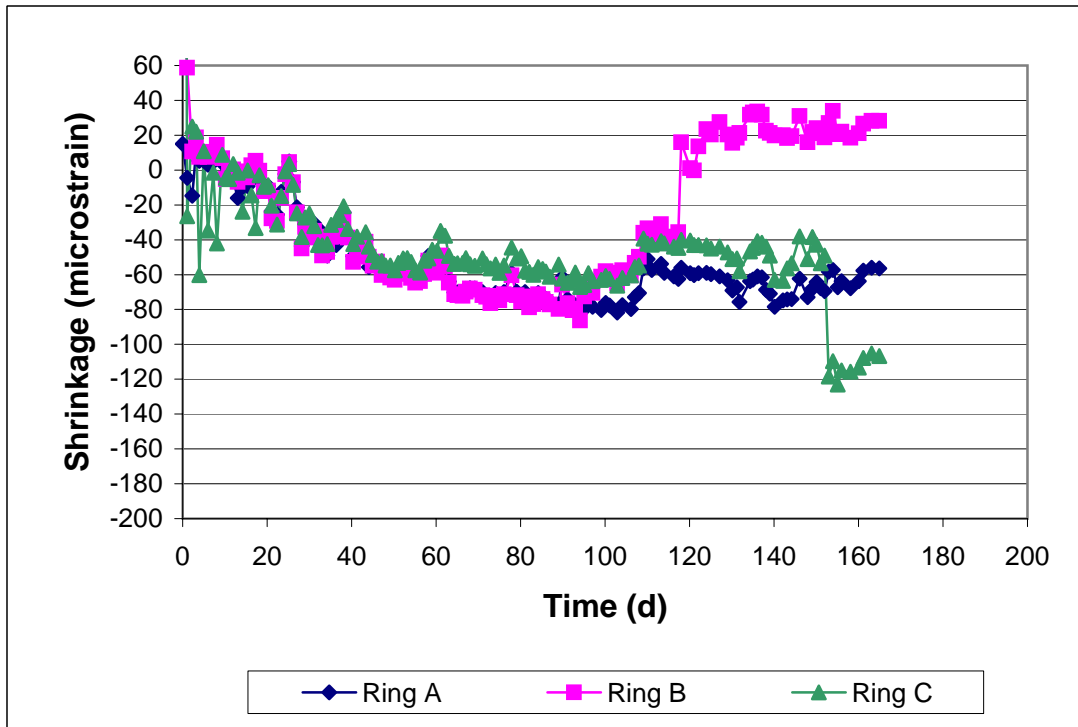


Figure 3.36 - Ring Test, Program 2. Type II C.G. mix, Batch 145. Average adjusted curve for each ring.

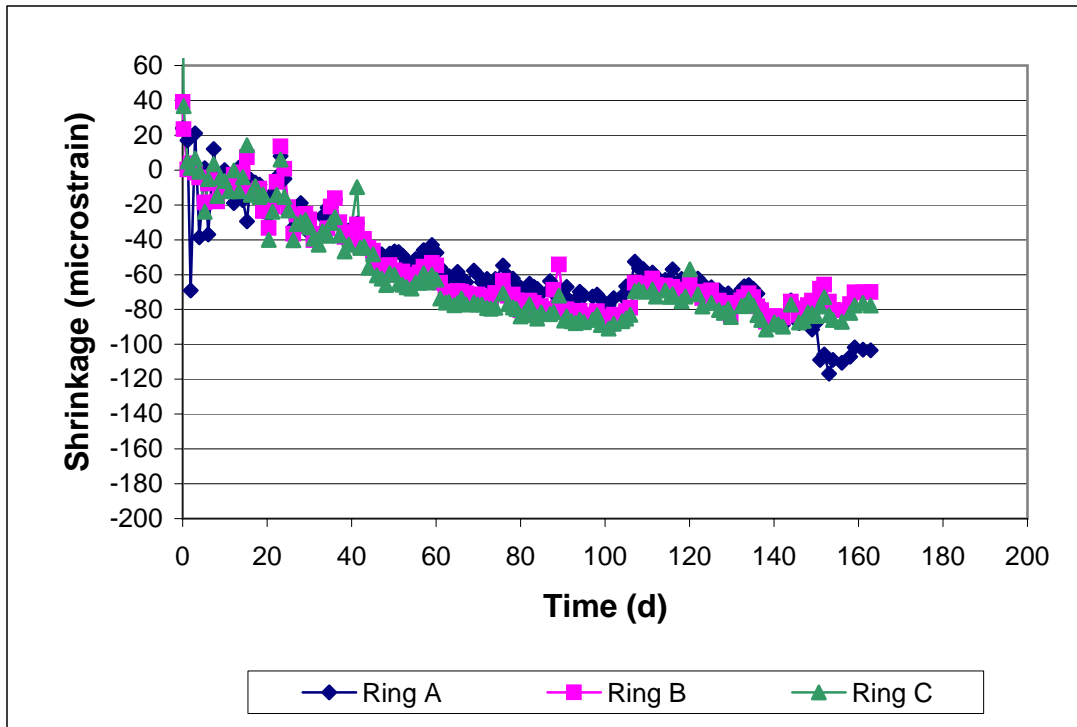


Figure 3.37 - Ring Test, Program 2. SRA mix, Batch 147. Average adjusted curve for each ring.

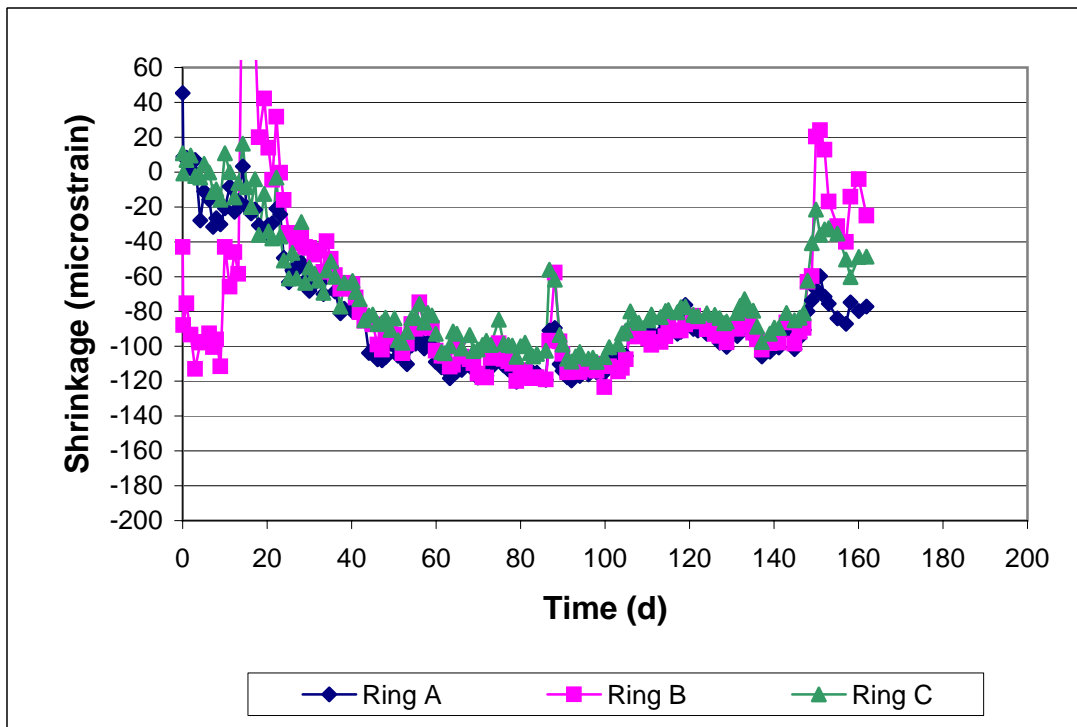


Figure 3.38 - Ring Test, Program 2. 497 mix, Batch 149. Average adjusted curve for each ring.

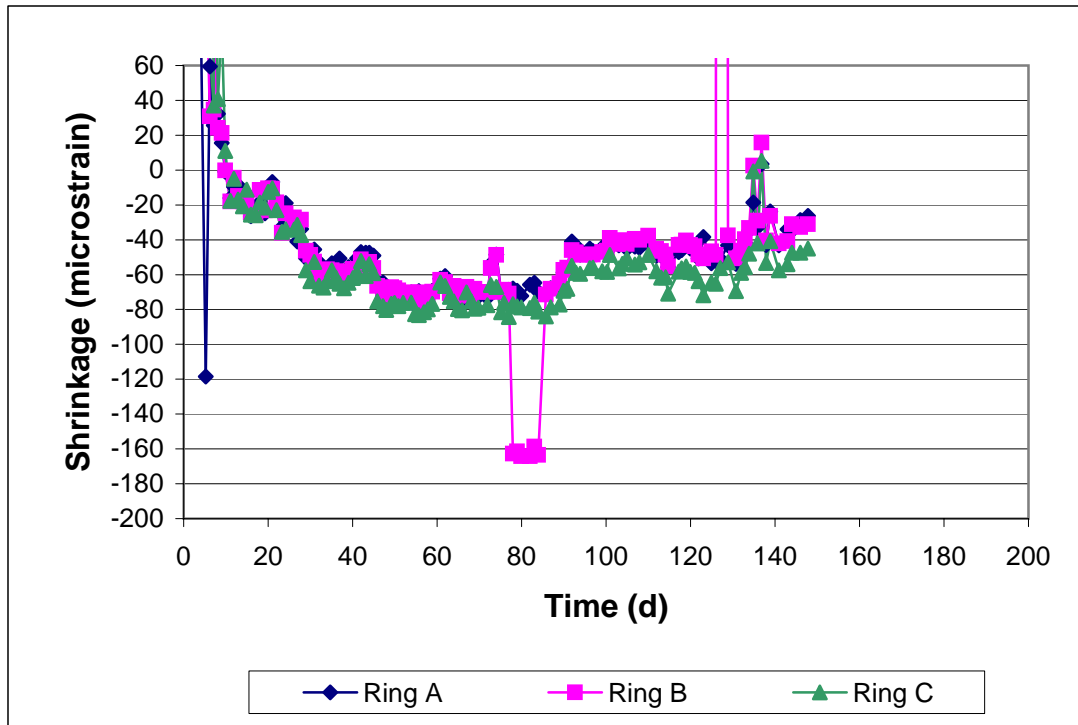


Figure 3.39 - Ring Test, Program 2. Quartzite mix, Batch 159. Average adjusted curve for each ring.



Figure 3.40 - Crack observed in MoDOT Ring A on day 103.

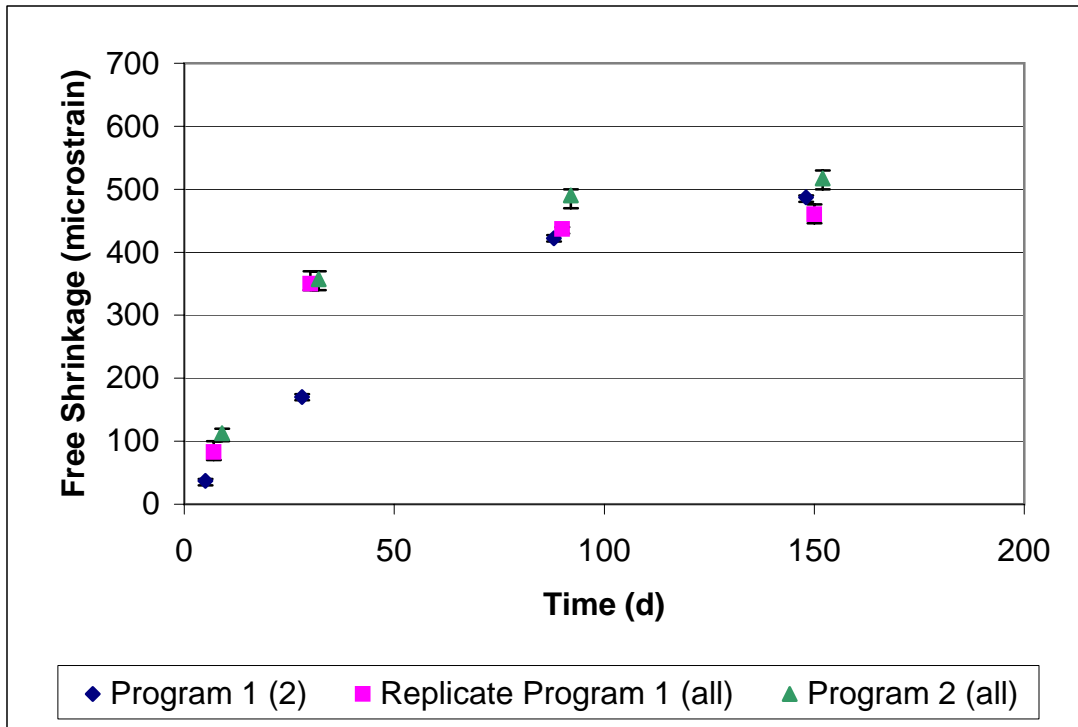


Figure 3.41 - Comparison of the number of drying sides (2 or all) versus free shrinkage at 7, 30, 90, and 150 days for the MoDOT mix.

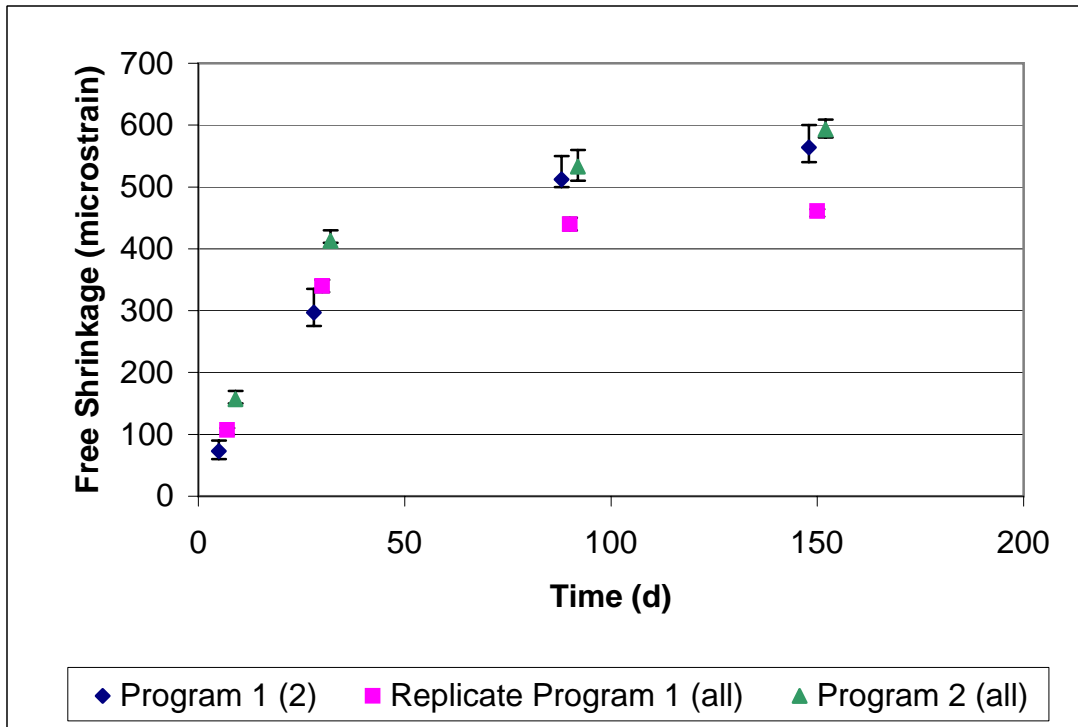


Figure 3.42 - Comparison of the number of drying sides (2 or all) versus free shrinkage at 7, 30, 90, and 150 days for the KDOT mix.

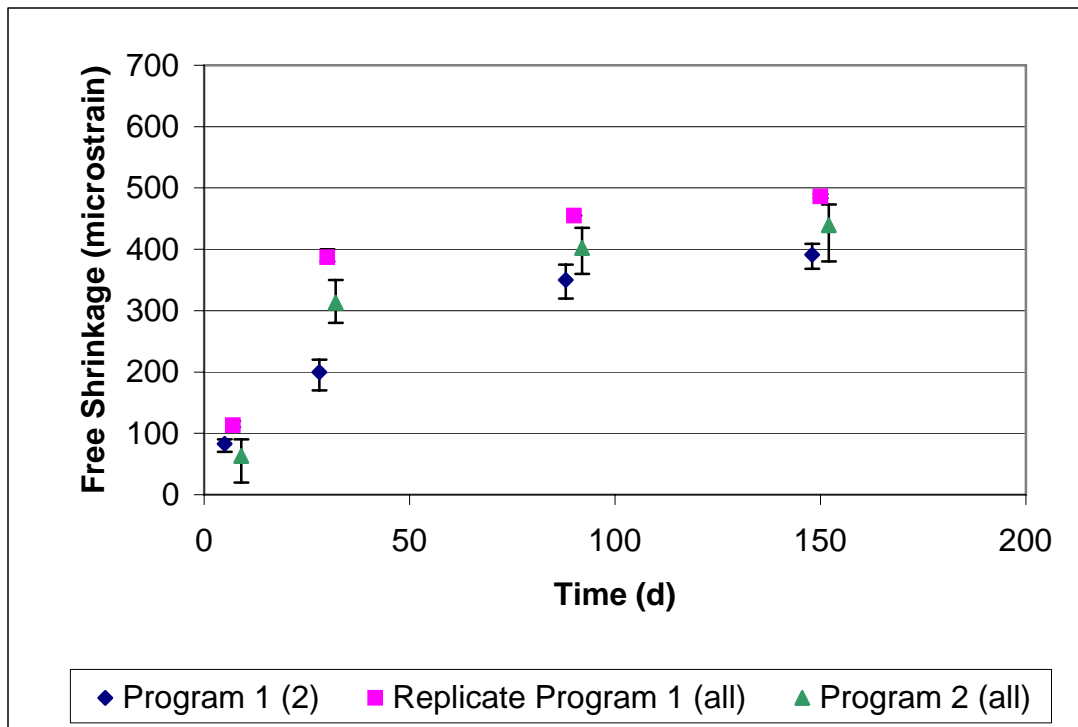


Figure 3.43 - Comparison of the number of drying sides (2 or all) versus free shrinkage at 7, 30, 90, and 150 days for the Control mix.

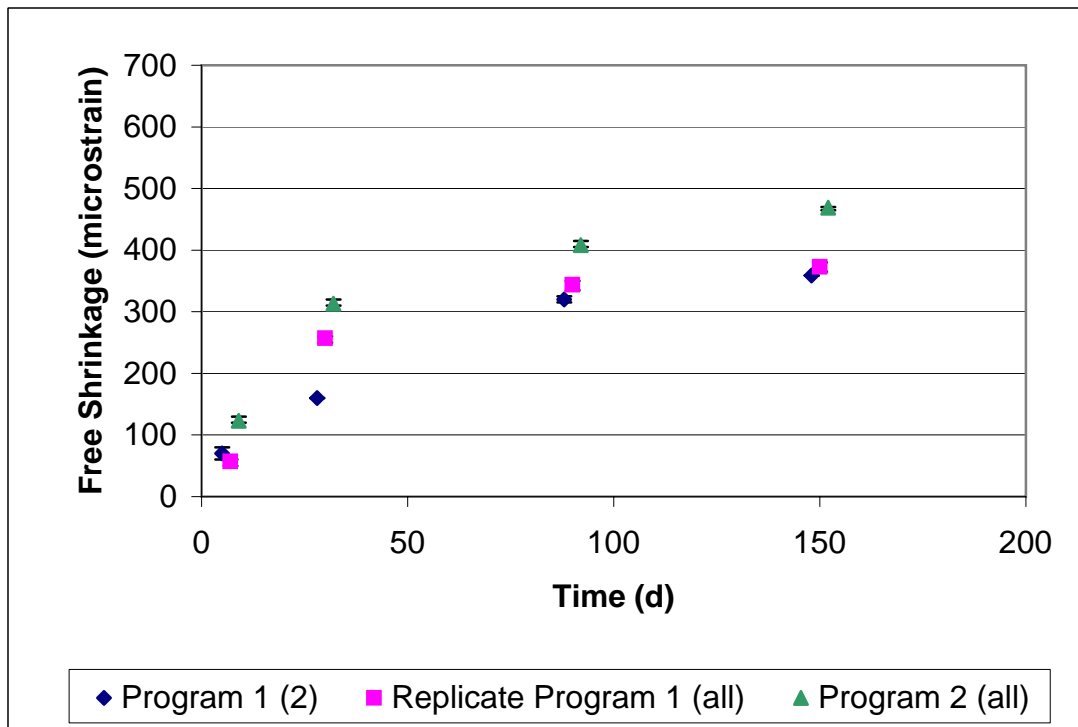


Figure 3.44 - Comparison of the number of drying sides (2 or all) versus free shrinkage at 7, 30, 90, and 150 days for the Type II coarse-ground mix.

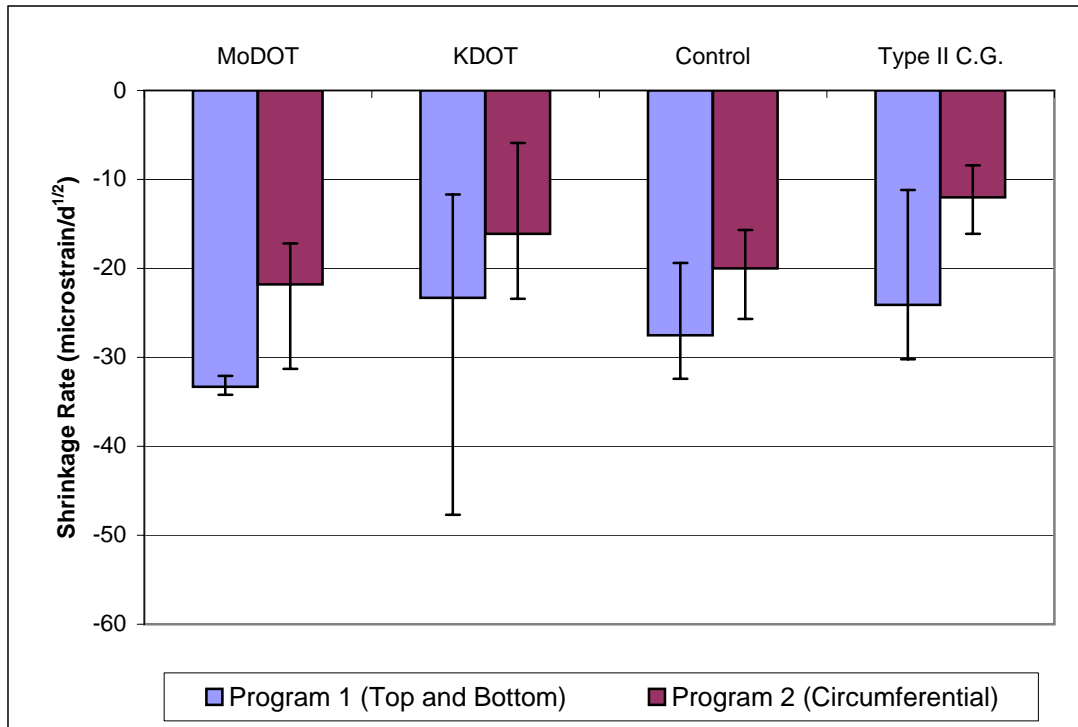


Figure 3.45 - Comparison of average shrinkage rate versus drying surfaces for the restrained ring test.

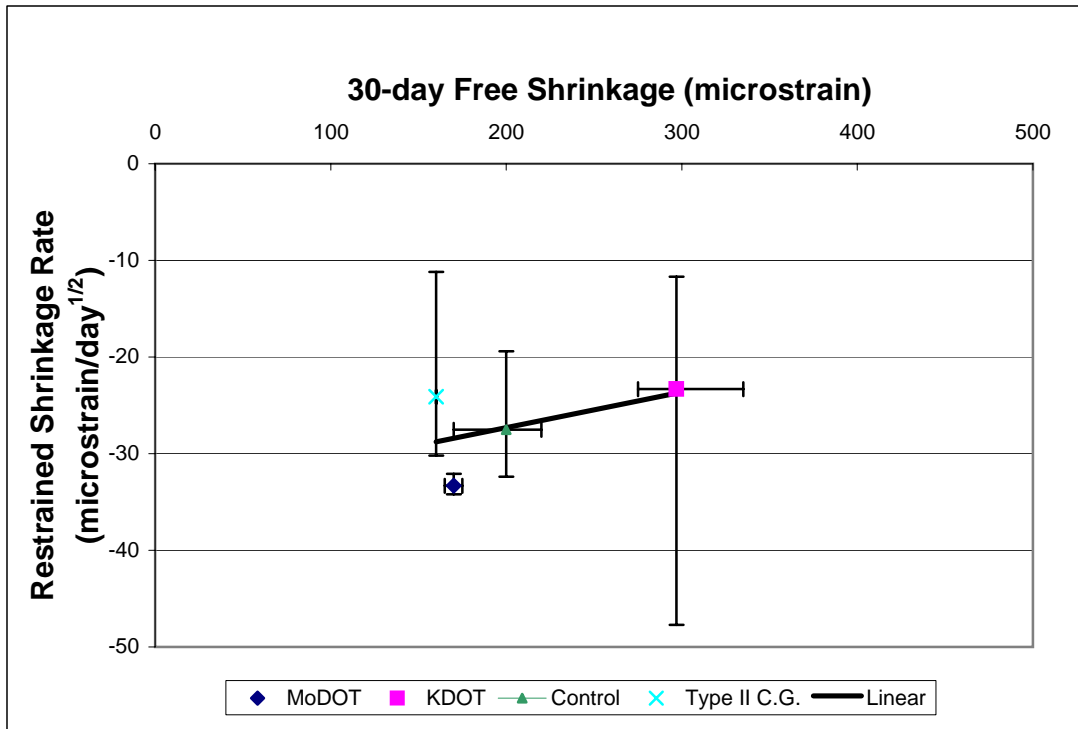


Figure 3.46 - Restricted shrinkage rate versus 30-day free shrinkage for Program 1. ($R^2 = 0.258$)

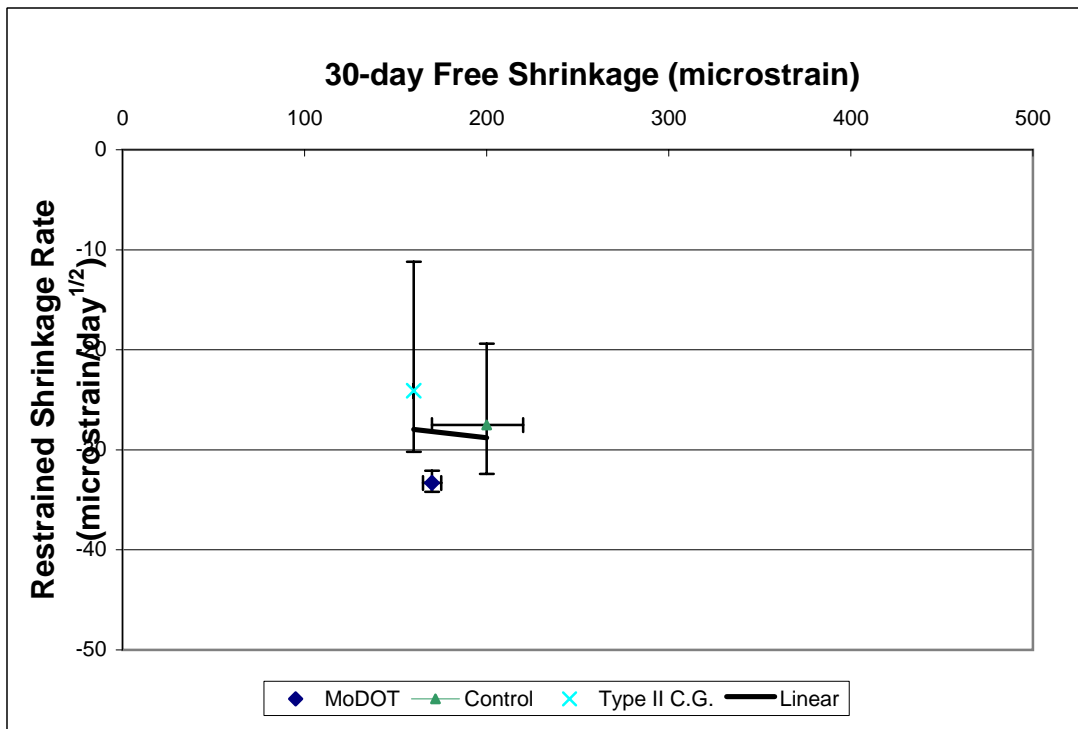


Figure 3.47 - Restricted shrinkage rate versus 30-day free shrinkage for Program 1. KDOT data excluded. ($R^2 = 0.0086$)

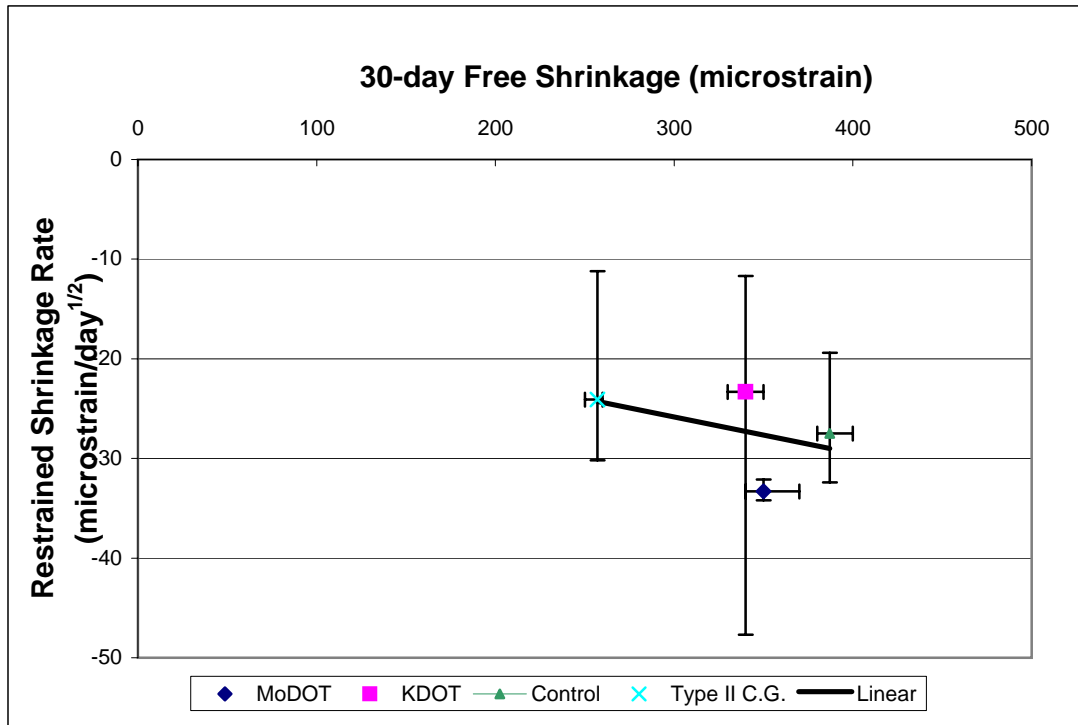


Figure 3.48 - Restrained shrinkage rate versus 30-day free shrinkage for Program 1 rings and the replication of Program 1 free shrinkage specimens. ($R^2 = 0.1927$)

APPENDIX A

Table A3.1 – Control, Batch 55: Slope Analysis of Shrinkage Versus Square Root of Time Data for Ring Tests

Ring	Gage	Slope, $\mu\epsilon/d^{1/2}$	Initial Day	Final Day
A	1	-25.9	4	61
	2	-27.6	4	61
	3	-27.6	4	61
	4	-27.6	4	61
B	1	-28.2	4	61
	2	-29.1	4	61
	3	-32.4	4	61
	4	-28.6	4	61
C	1	-28.3	4	61
	2	-30.1	4	61
	3	-19.4	23	61
	4	-25.0	4	61
Average Slope		-27	Std. Dev.	3.2

Table A3.2 – Type II coarse ground, Batch 56: Slope Analysis of Shrinkage Versus Square Root of Time Data for Ring Tests

Ring	Gage	Slope, $\mu\epsilon/d^{1/2}$	Initial Day	Final Day
A	1	-11.2	8	58
	2	-23.9	8	58
	3	-28.6	8	58
	4	-28.6	8	58
B	1	-23.7	18	60
	2	-30.2	18	60
	3	-23.4	18	60
	4	-23.3	18	60
C	1	-	-	-
	2	-	-	-
	3	-	-	-
	4	-	-	-
Average Slope		-24	Std. Dev.	5.9

Table A3.3 – MoDOT, Batch 57: Slope Analysis of Shrinkage Versus Square Root of Time Data for Ring Tests

Ring	Gage	Slope, $\mu\epsilon/d^{1/2}$	Initial Day	Final Day
A	1	-	-	-
	2	-	-	-
	3	-	-	-
	4	-	-	-
B	1	-	-	-
	2	-	-	-
	3	-	-	-
	4	-	-	-
C	1	-34.2	16	58
	2	-34.0	16	58
	3	-32.9	16	58
	4	-32.1	16	58
Average Slope		-33	Std. Dev.	1.0

Table A3.4 - KDOT, Batch 58: Slope Analysis of Shrinkage Versus Square Root of Time Data for Ring Tests

Ring	Gage	Slope, $\mu\epsilon/d^{1/2}$	Initial Day	Final Day
A	1	-28.4	16	57
	2	-47.7	16	57
	3	-28.7	16	57
	4	-28.5	16	57
B	1	-22.6	21	66
	2	-17.5	21	66
	3	-11.7	29	66
	4	-21.3	21	66
C	1	-21.3	16	60
	2	-16.4	16	60
	3	-19.5	16	60
	4	-16.3	16	60
Average Slope		-23	Std. Dev.	9.4

Table A3.5 – KDOT, Batch 130: Slope Analysis of Shrinkage Versus Square Root of Time Data for Ring Tests

Ring	Gage	Slope, $\mu\epsilon/d^{1/2}$	Initial Day	Final Day
A	1	-14.5	3	57
	2	-11.3	3	57
	3	-5.9	3	57
	4	-16.9	3	57
B	1	-18.0	3	57
	2	-17.2	3	57
	3	-18.6	3	57
	4	-16.5	3	57
C	1	-17.3	3	57
	2	-15.4	3	57
	3	-23.4	3	57
	4	-18.6	3	57
Average Slope		-16	Std. Dev.	4.3

Table A3.6 - MoDOT, Batch 132: Slope Analysis of Shrinkage Versus Square Root of Time Data for Ring Tests

Ring	Gage	Slope, $\mu\epsilon/d^{1/2}$	Initial Day	Final Day
A	1	-18.6	3	56
	2	-17.6	3	56
	3	-18.5	3	56
	4	-17.4	3	56
B	1	-31.3	3	56
	2	-19.2	3	56
	3	-17.9	3	56
	4	-17.2	3	56
C	1	-21.9	3	56
	2	-27.8	3	56
	3	-28.0	3	56
	4	-26.4	3	56
Average Slope		-22	Std. Dev.	5.1

Table A3.7 - Control, Batch 138: Slope Analysis of Shrinkage Versus Square Root of Time Data for Ring Tests

Ring	Gage	Slope, $\mu\epsilon/d^{1/2}$	Initial Day	Final Day
A	1	-21.1	3	50
	2	-19.7	3	50
	3	-22.7	3	50
	4	-21.9	3	50
B	1	-22.0	3	50
	2	-25.7	3	50
	3	-	-	-
	4	-24.6	3	50
C	1	-17.2	3	50
	2	-16.8	3	50
	3	-15.7	3	50
	4	-17.3	3	50
Average Slope		-20	Std. Dev.	3.4

Table A3.8 – 7-day cure, Batch 140: Slope Analysis of Shrinkage Versus Square Root of Time Data for Ring Tests

Ring	Gage	Slope, $\mu\epsilon/d^{1/2}$	Initial Day	Final Day
A	1	-18.3	7	53
	2	-	-	-
	3	-20.0	7	53
	4	-18.1	7	53
B	1	-	-	-
	2	-23.4	7	53
	3	-19.4	7	53
	4	-19.2	18	53
C	1	-	-	-
	2	-	-	-
	3	-17.4	18	53
	4	-	-	-
Average Slope		-19	Std. Dev.	2.0

Table A3.9 – 14-day cure, Batch 143: Slope Analysis of Shrinkage Versus Square Root of Time Data for Ring Tests

Ring	Gage	Slope, $\mu\epsilon/d^{1/2}$	Initial Day	Final Day
A	1	-21.1	14	70
	2	-	-	-
	3	-23.4	14	70
	4	-20.5	14	70
B	1	-20.3	14	70
	2	-20.5	14	70
	3	-20.1	14	70
	4	-18.8	14	70
C	1	-20.0	14	70
	2	-17.9	14	70
	3	-15.8	14	70
	4	-	-	-
Average Slope		-20	Std. Dev.	2.0

Table A3.10 – Type II coarse ground, Batch 145: Slope Analysis of Shrinkage Versus Square Root of Time Data for Ring Tests

Ring	Gage	Slope, $\mu\epsilon/d^{1/2}$	Initial Day	Final Day
A	1	-10.9	3	106
	2	-11.9	3	106
	3	-12.3	3	106
	4	-13.0	3	106
B	1	-16.1	3	106
	2	-14.3	3	106
	3	-8.4	3	106
	4	-8.4	3	106
C	1	-11.6	14	56
	2	-14.7	14	56
	3	-11.9	3	106
	4	-10.6	3	106
Average Slope		-12	Std. Dev.	2.3

Table A3.11 – SRA, Batch 147: Slope Analysis of Shrinkage Versus Square Root of Time Data for Ring Tests

Ring	Gage	Slope, $\mu\epsilon/d^{1/2}$	Initial Day	Final Day
A	1	-9.6	7	101
	2	-14.2	7	101
	3	-11.1	7	101
	4	-9.1	7	101
B	1	-11.9	7	101
	2	-12.2	7	101
	3	-13.3	7	101
	4	-12.8	7	101
C	1	-13.9	7	101
	2	-13.3	7	101
	3	-14.3	7	101
	4	-12.6	7	101
Average Slope		-12	Std. Dev.	1.7

Table A3.12 – 497, Batch 149: Slope Analysis of Shrinkage Versus Square Root of Time Data for Ring Tests

Ring	Gage	Slope, $\mu\epsilon/d^{1/2}$	Initial Day	Final Day
A	1	-17.7	14	71
	2	-17.4	14	71
	3	-28.3	14	71
	4	-29.9	14	71
B	1	-26.4	21	71
	2	-	-	-
	3	-20.5	21	71
	4	-16.7	21	71
C	1	-22.1	14	71
	2	-24.1	14	71
	3	-17.8	14	71
	4	-16.8	14	71
Average Slope		-22	Std. Dev.	4.9

Table A3.13 – Quartzite, Batch 159: Slope Analysis of Shrinkage Versus Square Root of Time Data for Ring Tests

Ring	Gage	Slope, $\mu\epsilon/d^{1/2}$	Initial Day	Final Day
A	1	-15.7	13	55
	2	-18.7	13	55
	3	-14.9	13	55
	4	-16.6	13	55
B	1	-15.6	13	55
	2	-17.3	13	55
	3	-19.0	13	55
	4	-16.7	13	55
C	1	-20.3	13	55
	2	-19.8	13	55
	3	-12.6	13	55
	4	-22.3	13	55
Average Slope		-17	Std. Dev.	2.7

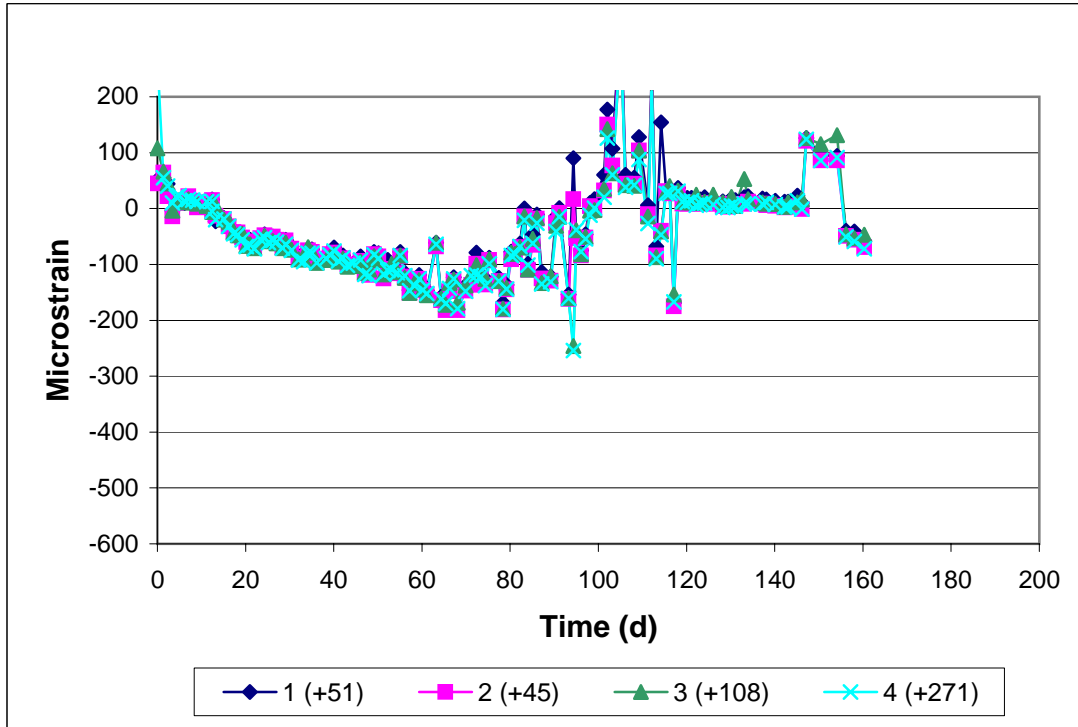


Figure A3.1a - Ring Test, Program 1. Control, Batch 55, Ring A. Drying begins on Day 2. Values in parentheses added to data to view all curves in the same window.

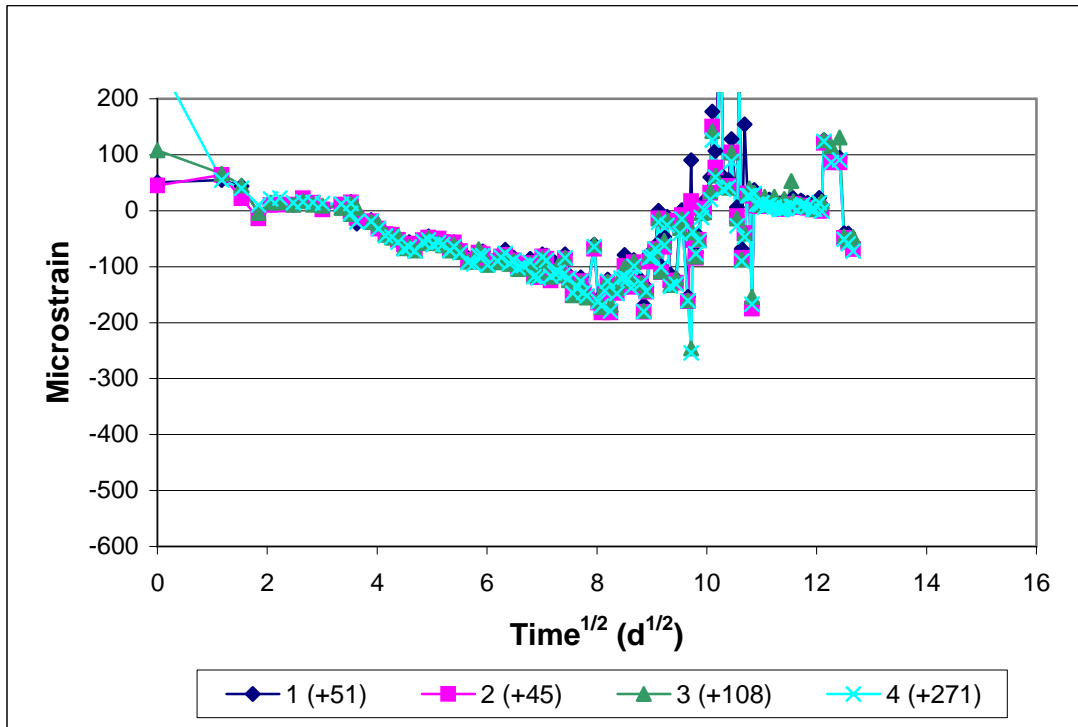


Figure A3.1b - Ring Test, Program 1. Control, Batch 55, Ring A. Shrinkage versus the square root of time.

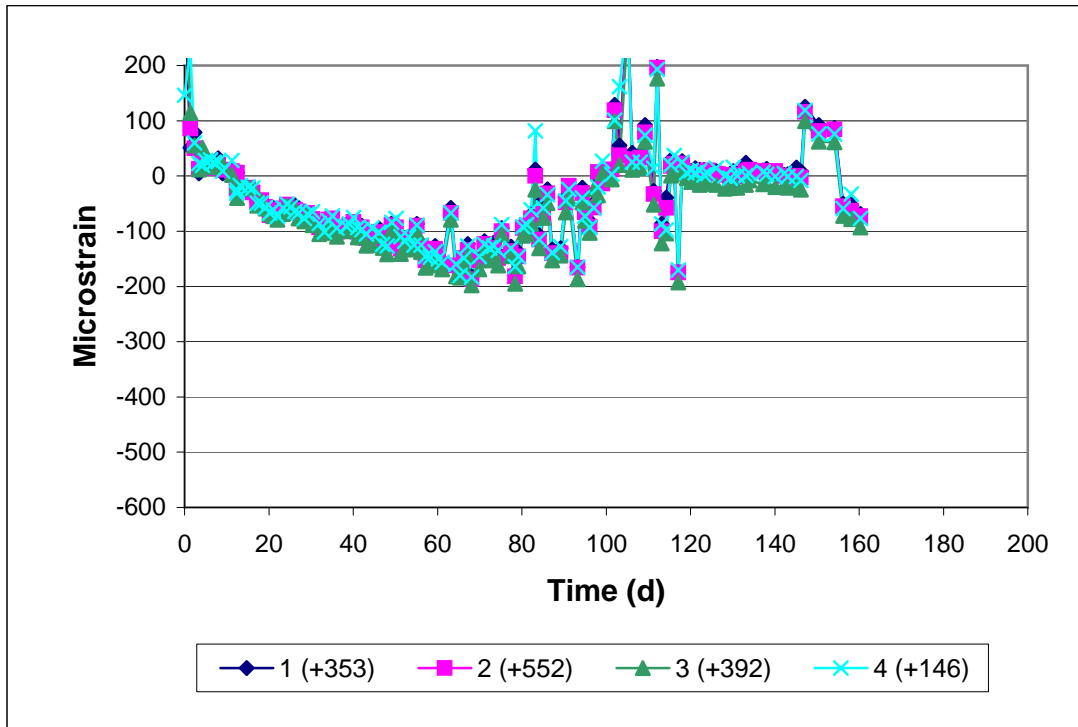


Figure A3.2a - Ring Test, Program 1. Control, Batch 55, Ring B. Drying begins on day 3. Values in parentheses added to data to view all curves in the same window.

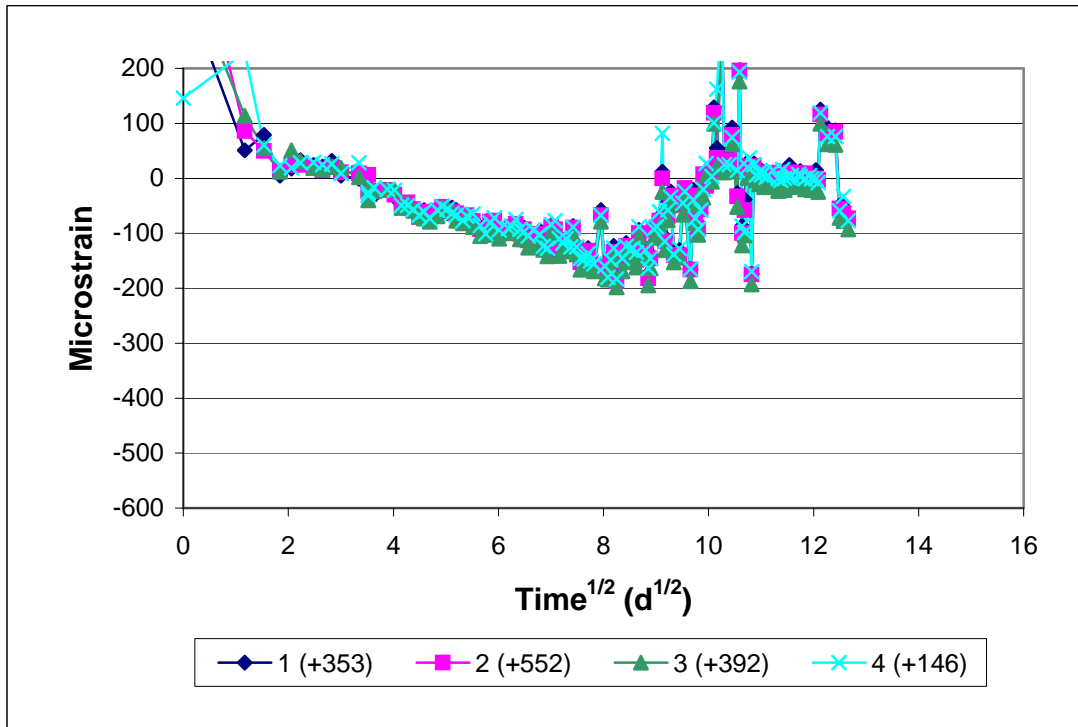


Figure A3.2b - Ring Test, Program 1. Control, Batch 55, Ring B. Shrinkage versus the square root of time.

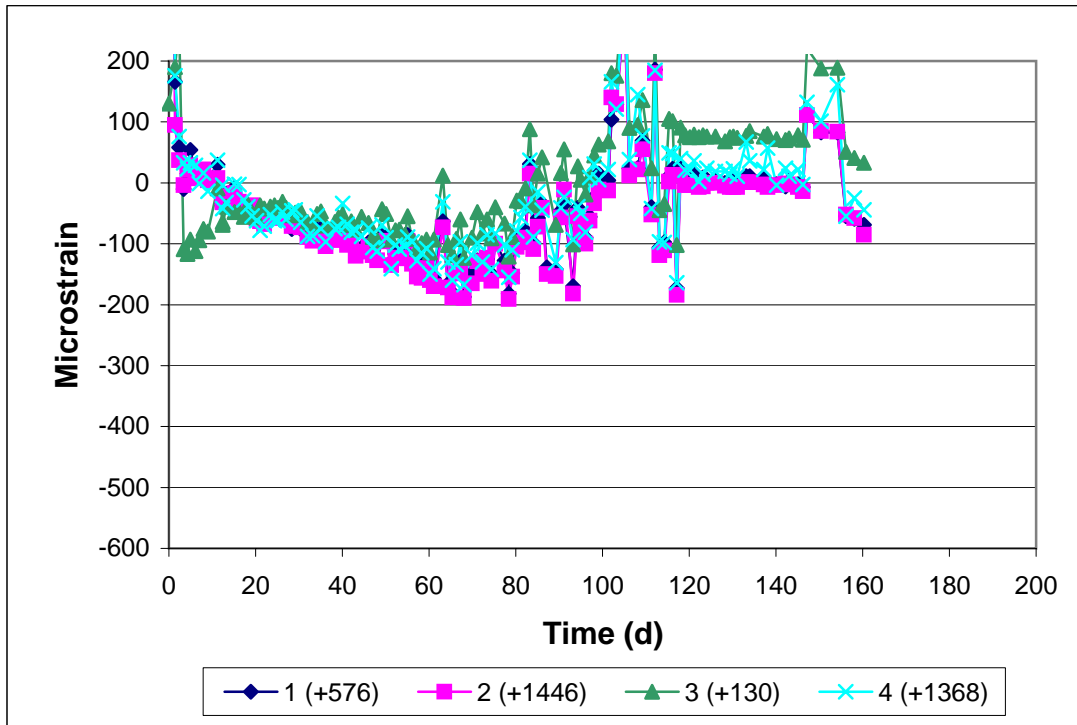


Figure A3.3a - Ring Test, Program 1. Control, Batch 55, Ring C. Drying begins on day 3. Values in parentheses added to data to view all curves in the same window.

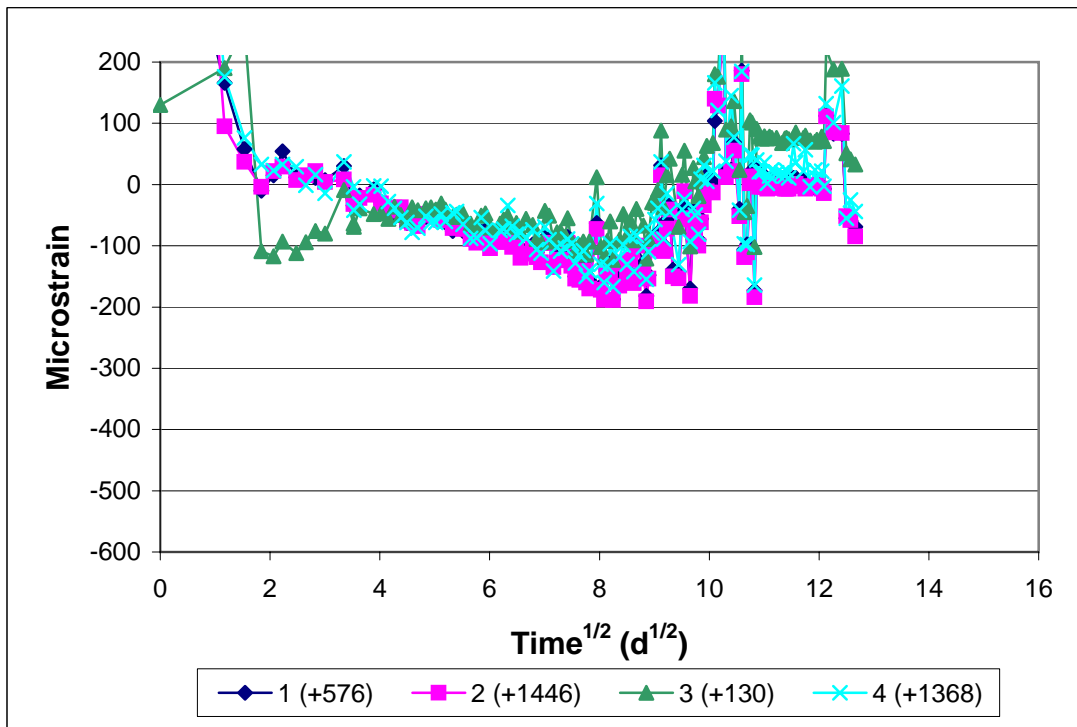


Figure A3.3b - Ring Test, Program 1. Control, Batch 55, Ring C. Shrinkage versus the square root of time.

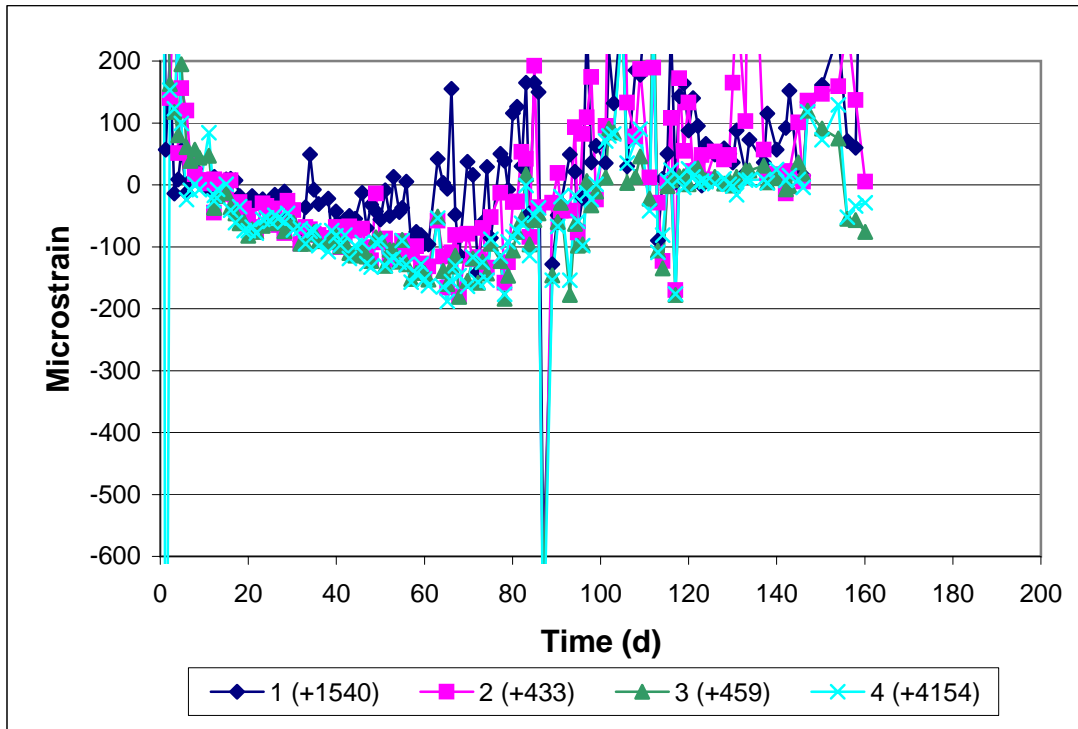


Figure A3.4a - Ring Test, Program 1. Type II C.G., Batch 56, Ring A. Drying begins on day 3. Values in parentheses added to data to view all curves in the same window.

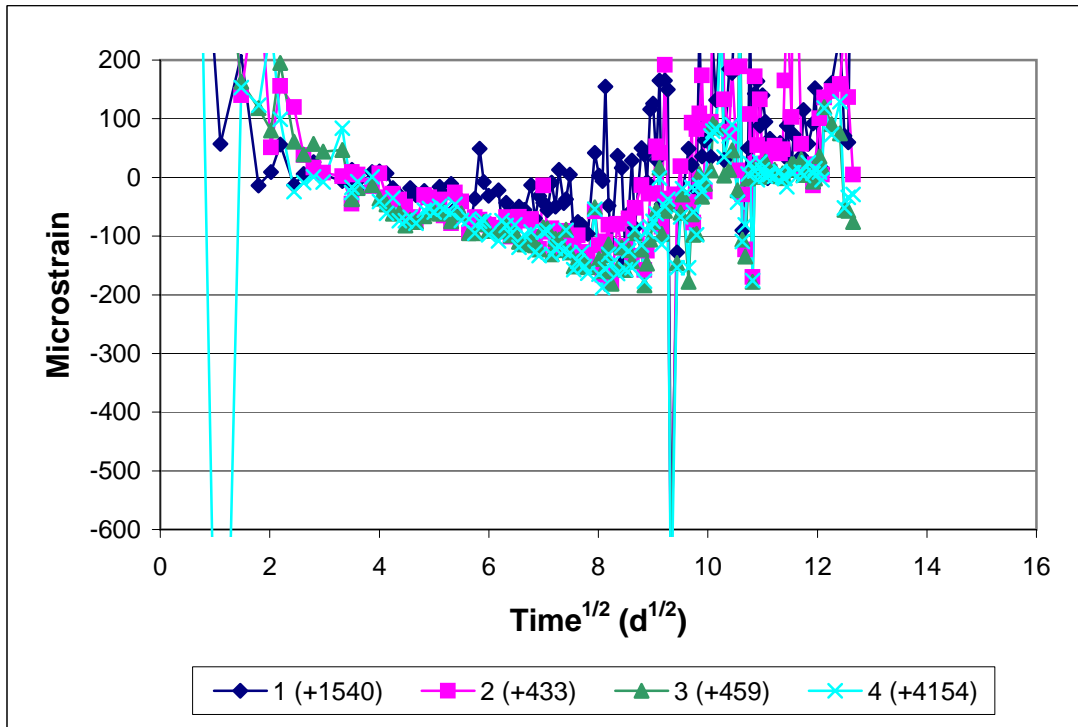


Figure A3.4b - Ring Test, Program 1. Type II C.G., Batch 56, Ring A. Shrinkage versus the square root of time.

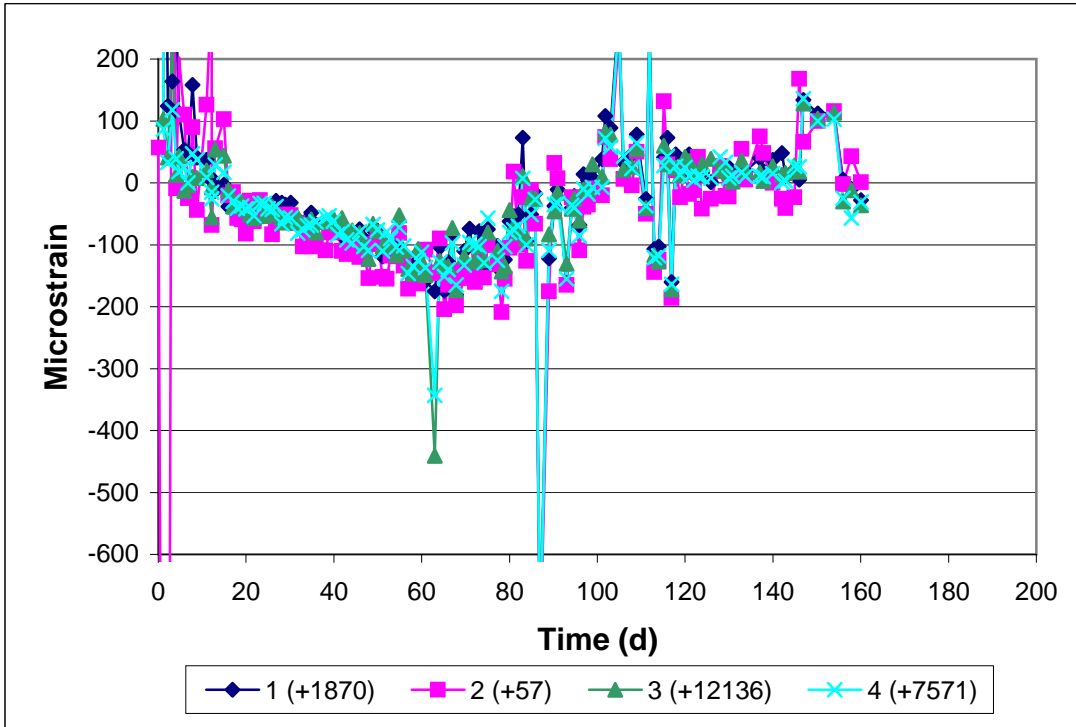


Figure A3.5a - Ring Test, Program 1. Type II C.G., Batch 56, Ring B. Drying begins on day 3. Values in parentheses added to data to view all curves in the same window.

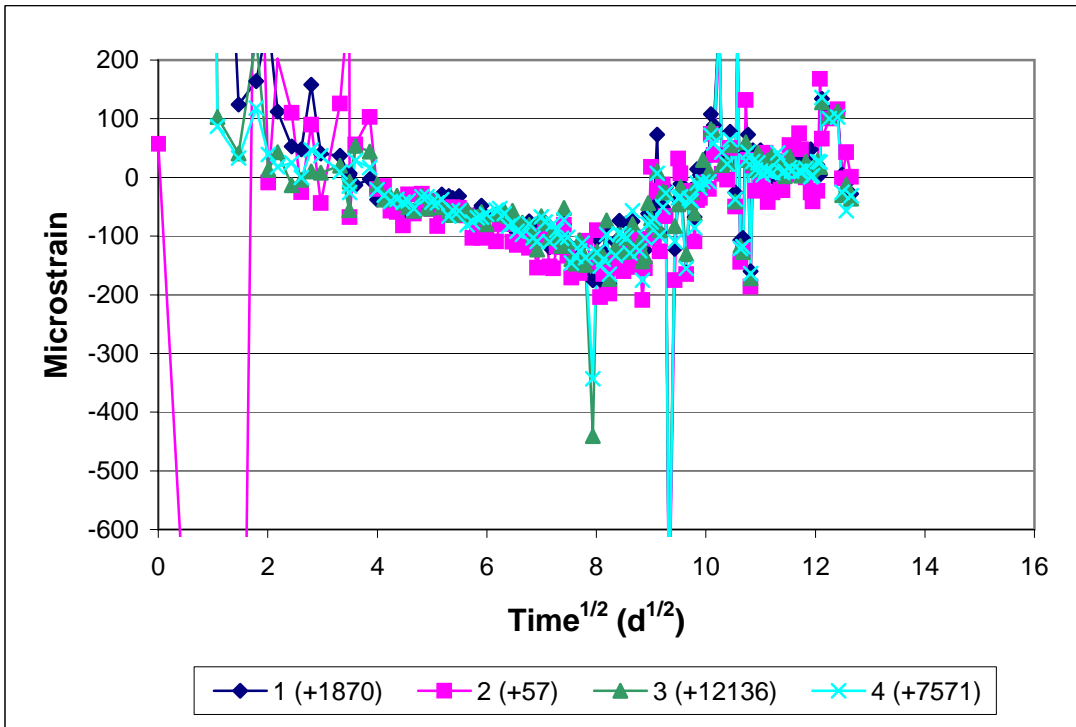


Figure A3.5b - Ring Test, Program 1. Type II C.G., Batch 56, Ring B. Shrinkage versus the square root of time.

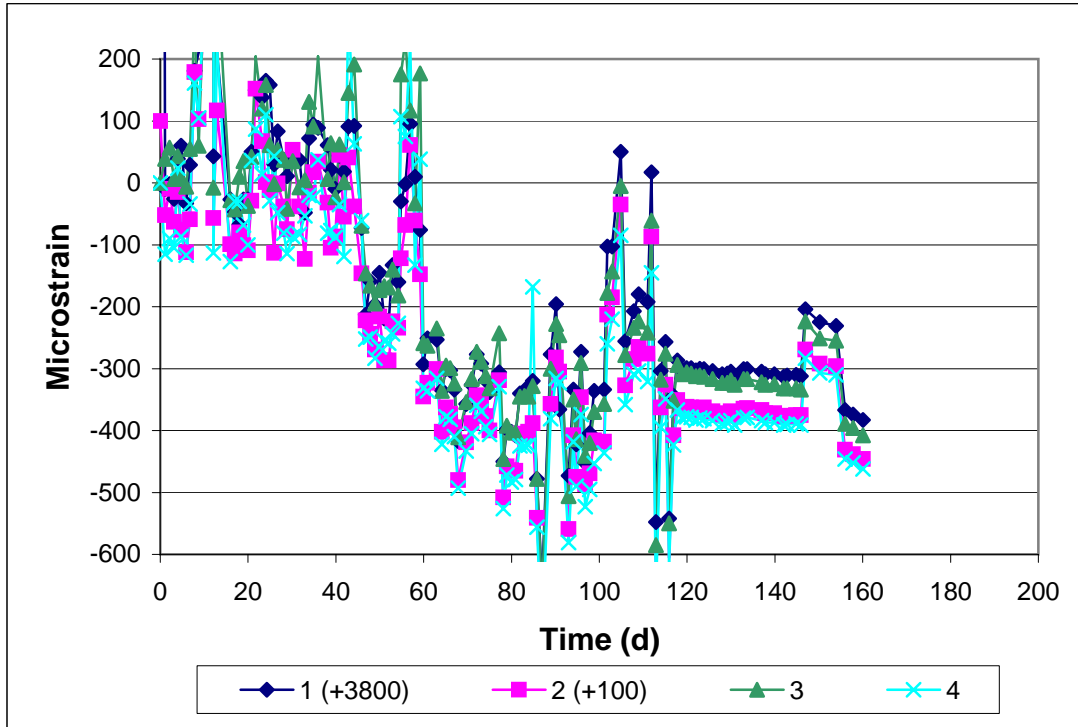


Figure A3.6a - Ring Test, Program 1. Type II C.G., Batch 56, Ring C. Drying begins on day 3. Values in parentheses added to data to view all curves in the same window.

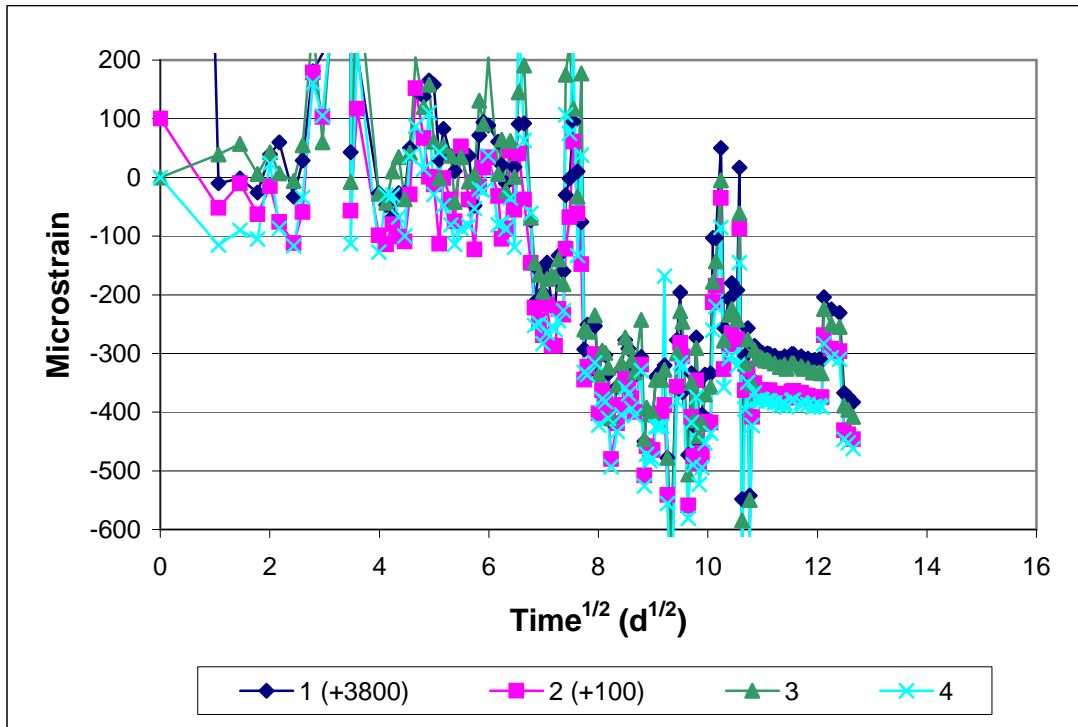


Figure A3.6b - Ring Test, Program 1. Type II C.G., Batch 56, Ring C. Shrinkage versus the square root of time.

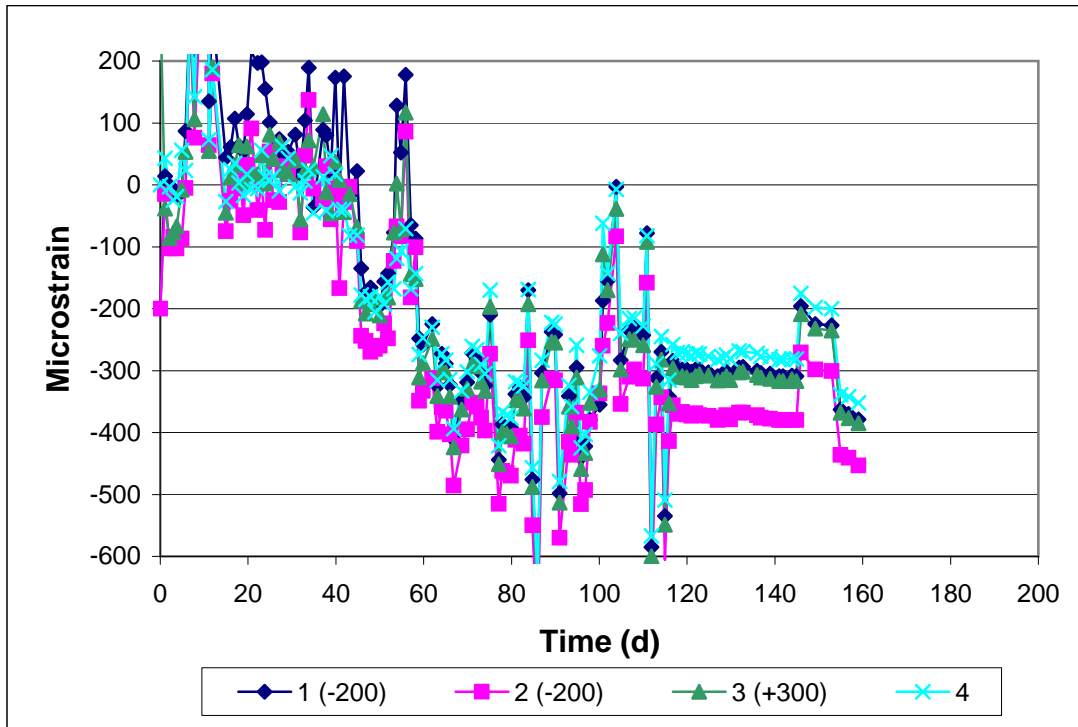


Figure A3.7a - Ring Test, Program 1. MoDOT, Batch 57, Ring A. Drying begins on day 3. Values in parentheses added to data to view all curves in the same window.

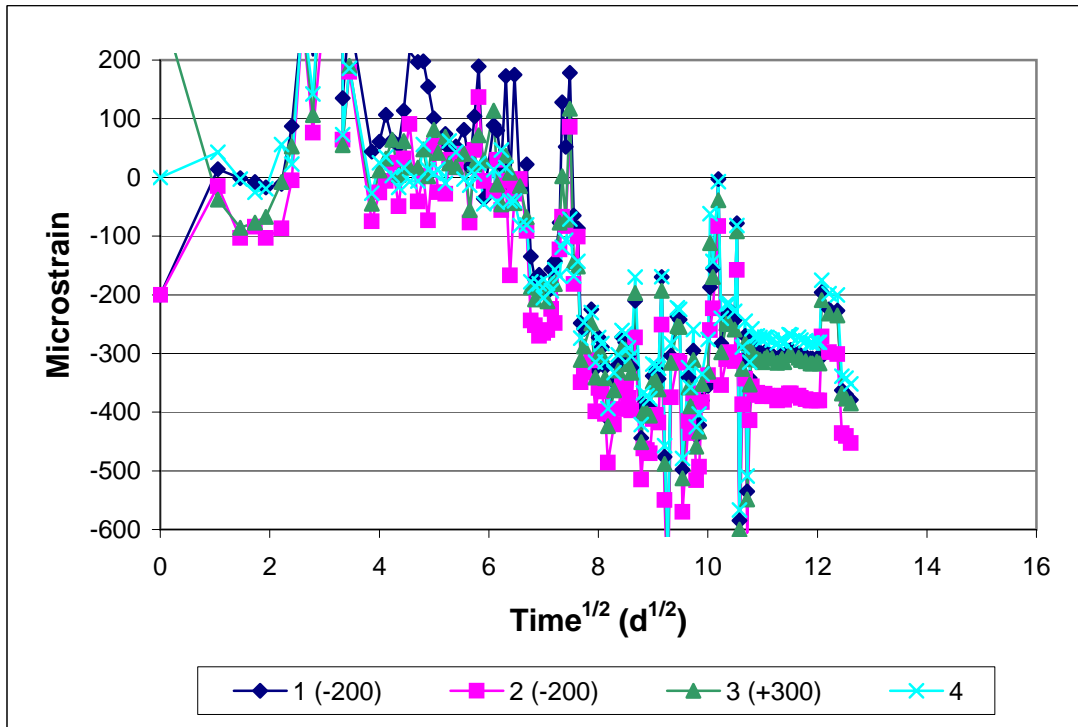


Figure A3.7b - Ring Test, Program 1. MoDOT, Batch 57, Ring A. Shrinkage versus the square root of time.

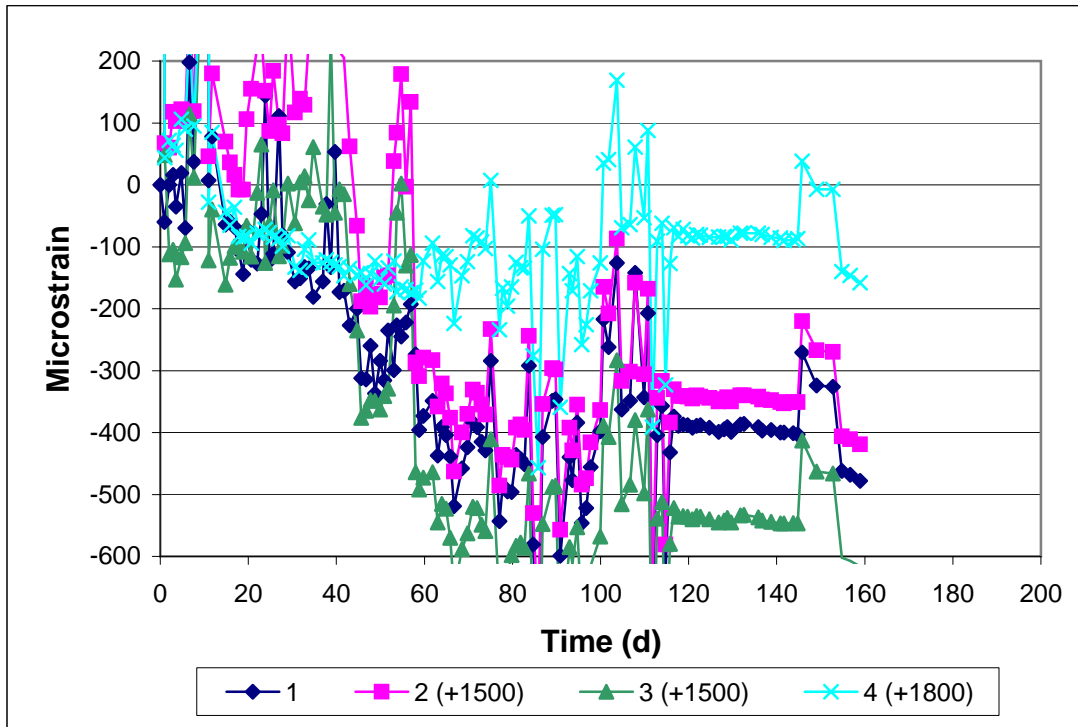


Figure A3.8a - Ring Test, Program 1. MoDOT, Batch 57, Ring B. Drying begins on day 3. Values in parentheses added to data to view all curves in the same window.

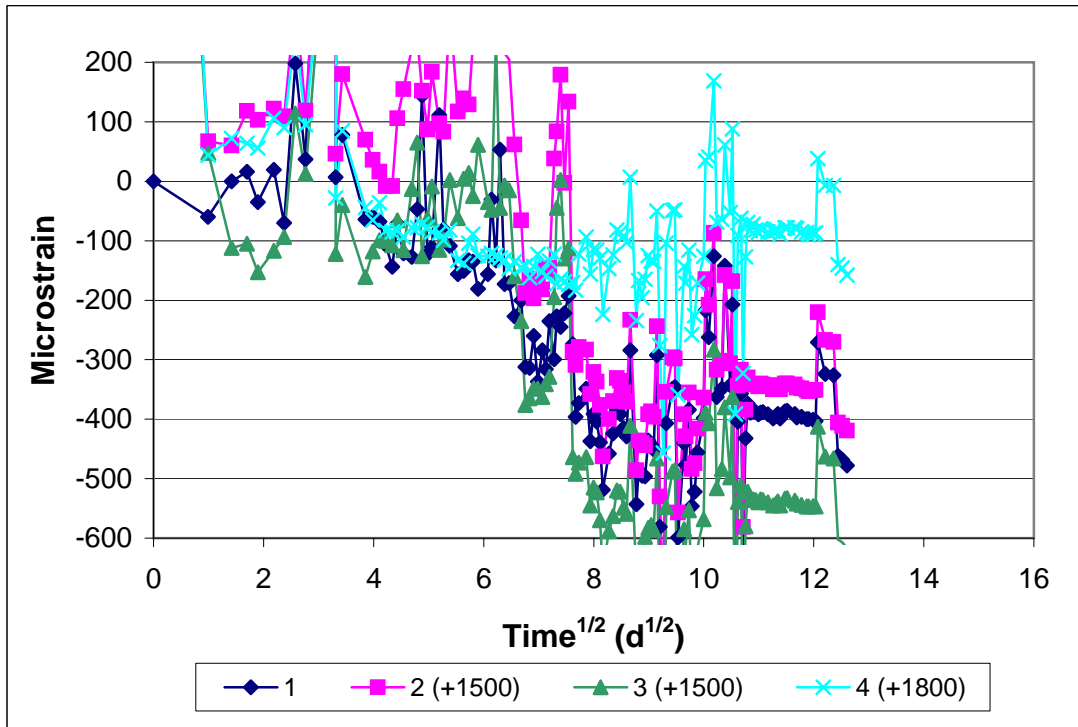


Figure A3.8b - Ring Test, Program 1. MoDOT, Batch 57, Ring B. Shrinkage versus the square root of time.

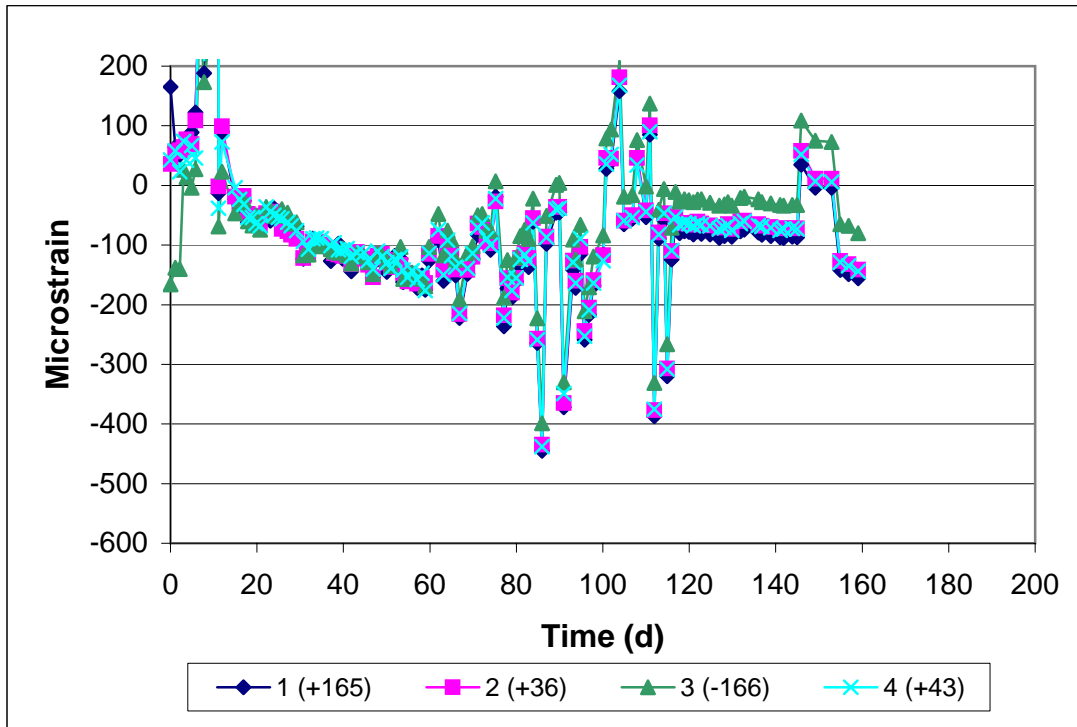


Figure A3.9a - Ring Test, Program 1. MoDOT, Batch 57, Ring C. Drying begins on day 3. Values in parentheses added to data to view all curves in the same window.

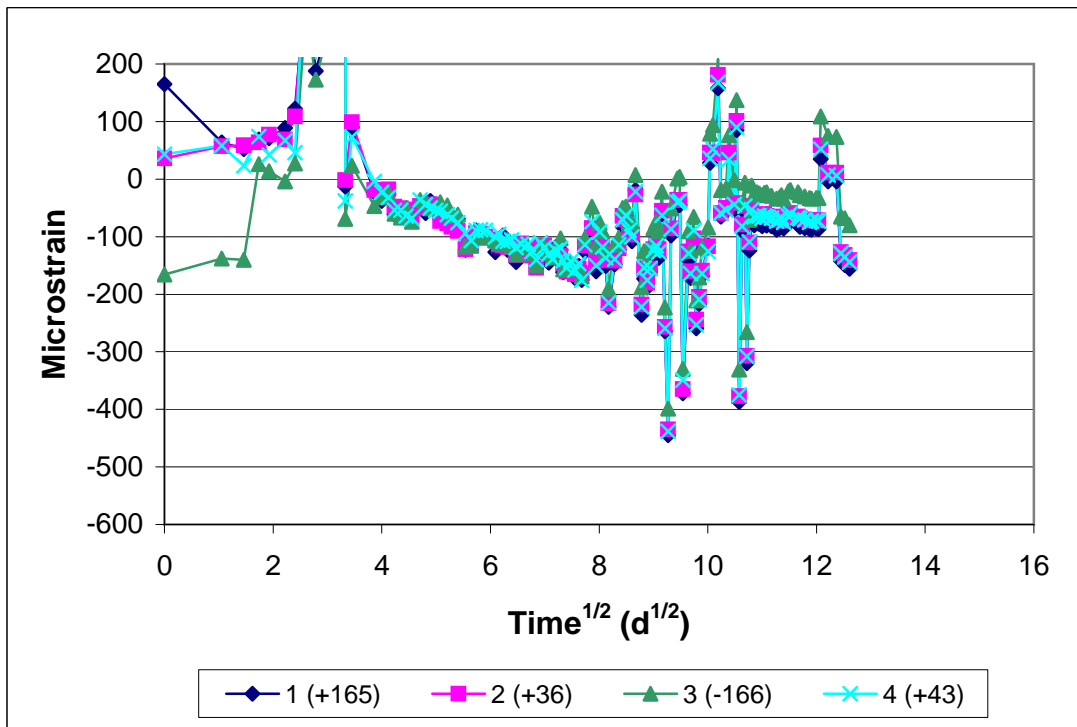


Figure A3.9b - Ring Test, Program 1. MoDOT, Batch 57, Ring C. Shrinkage versus the square root of time.

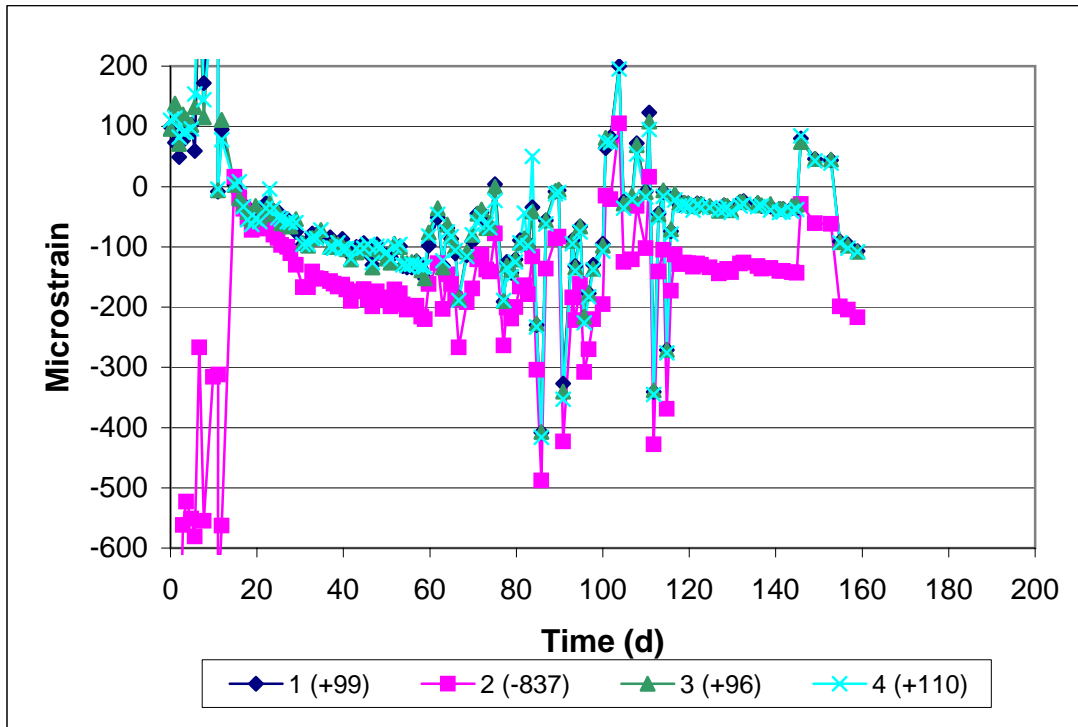


Figure A3.10a - Ring Test, Program 1. KDOT, Batch 58, Ring A. Drying begins on day 3. Values in parentheses added to data to view all curves in the same window.

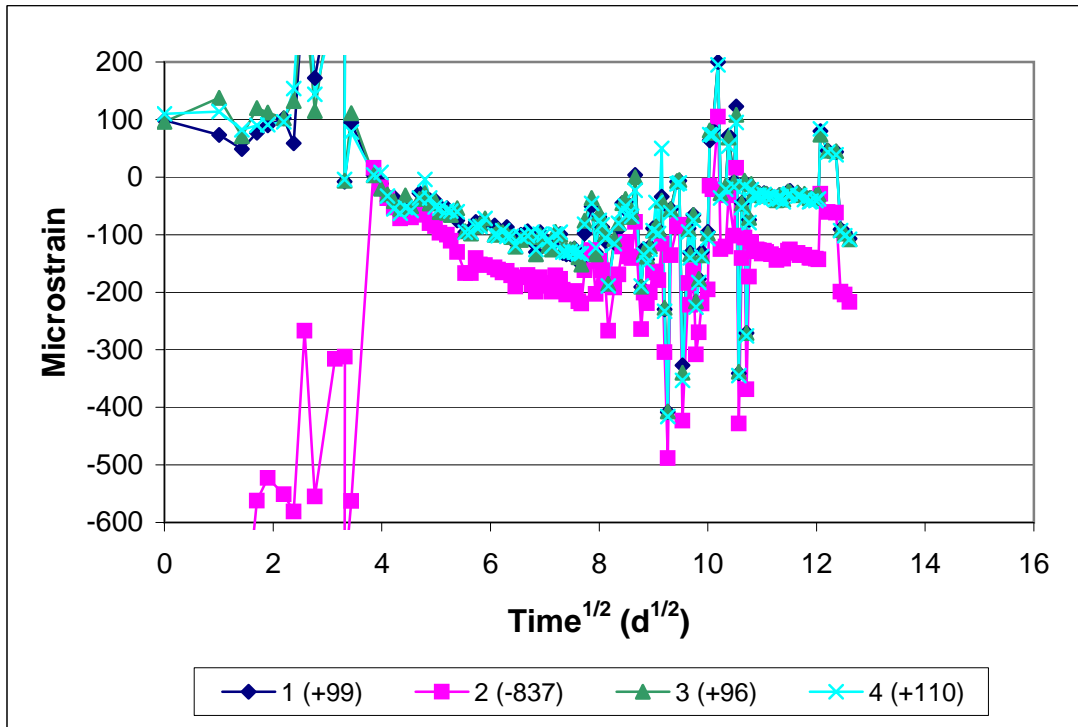


Figure A3.10b - Ring Test, Program 1. KDOT, Batch 58, Ring A. Shrinkage versus the square root of time.

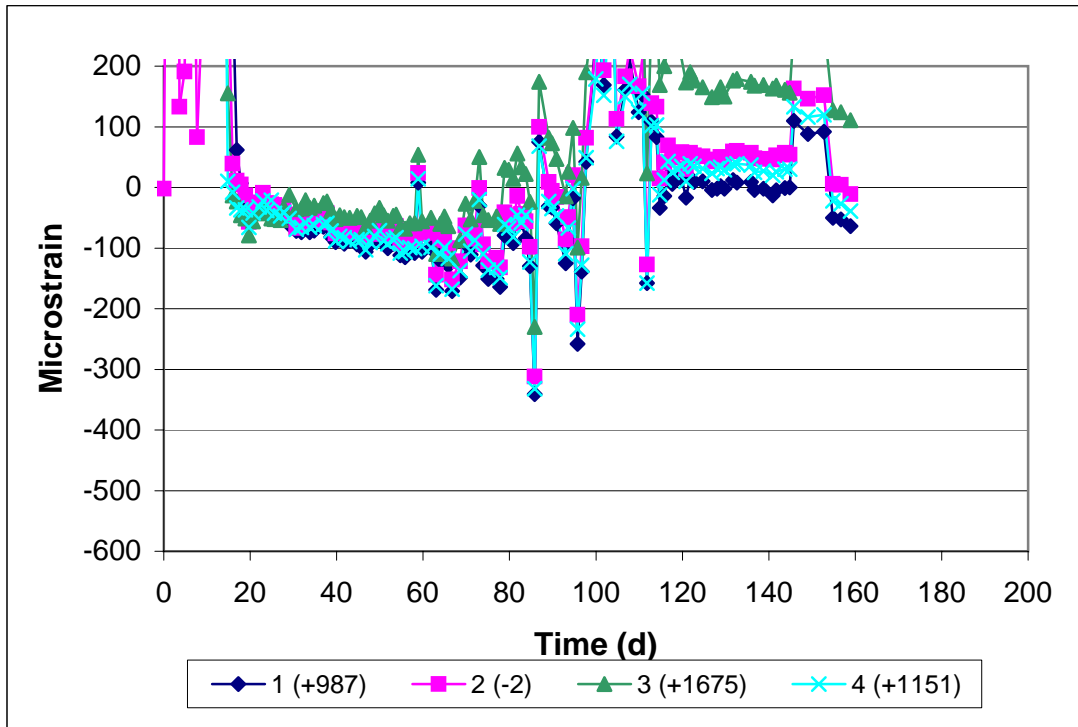


Figure A3.11a - Ring Test, Program 1. KDOT, Batch 58, Ring B. Drying begins on day 3. Values in parentheses added to data to view all curves in the same window.

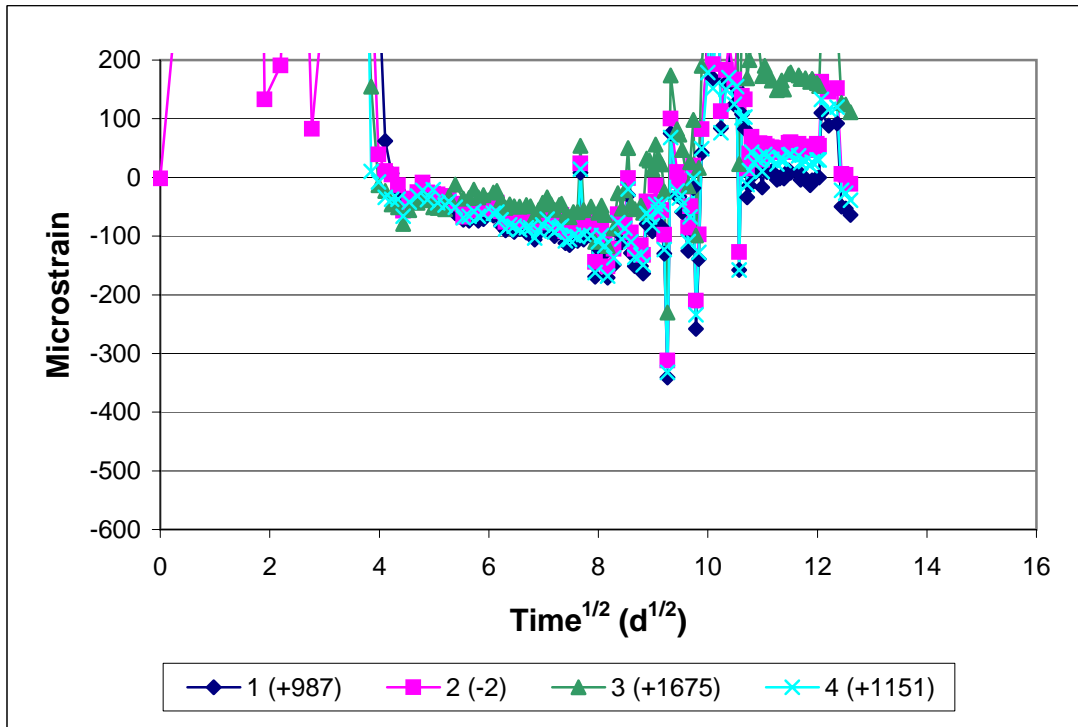


Figure A3.11b - Ring Test, Program 1. KDOT, Batch 58, Ring B. Shrinkage versus the square root of time.

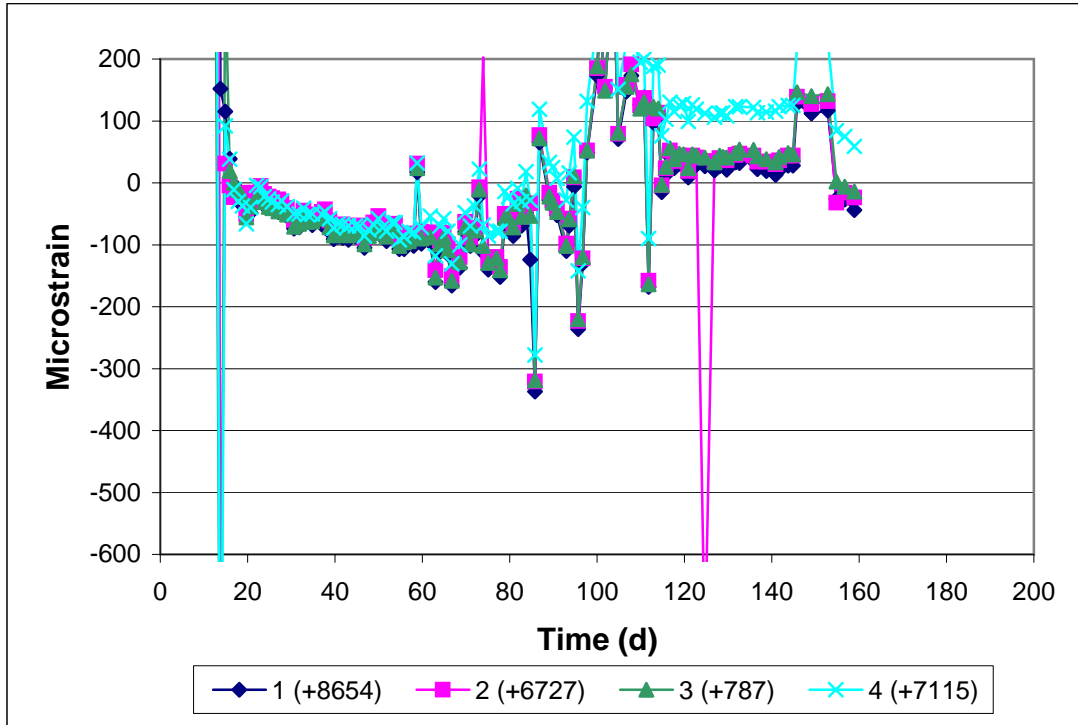


Figure A3.12a - Ring Test, Program 1. KDOT, Batch 58, Ring C. Drying begins on day 3. Values in parentheses added to data to view all curves in the same window.

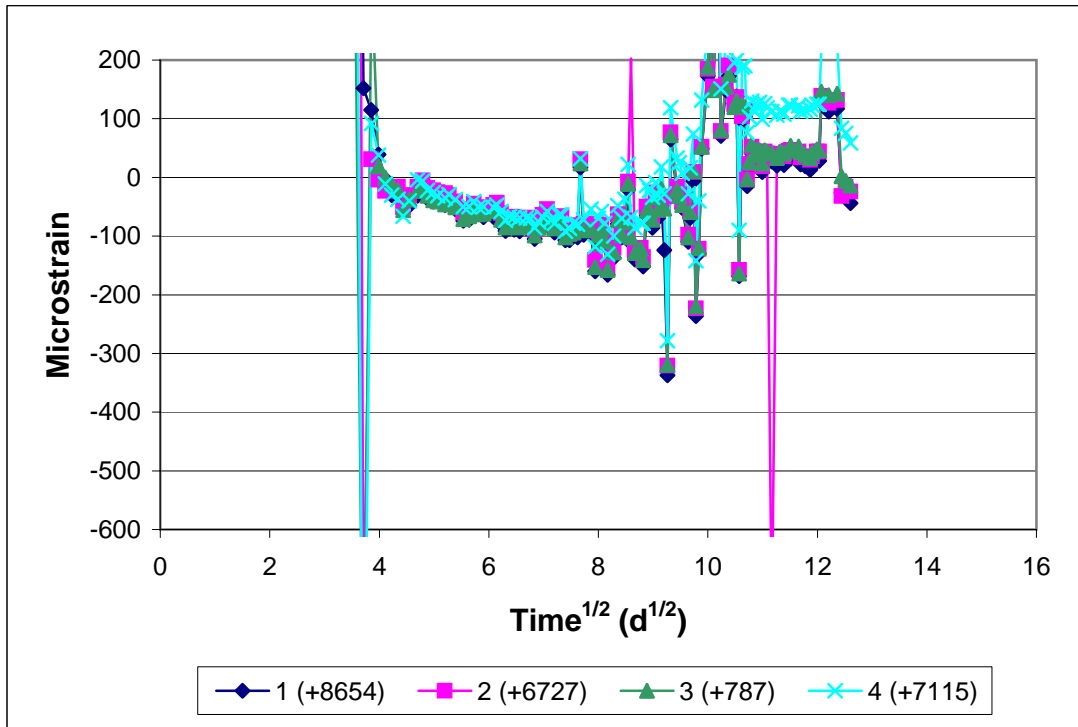


Figure A3.12b - Ring Test, Program 1. KDOT, Batch 58, Ring C. Shrinkage versus the square root of time.

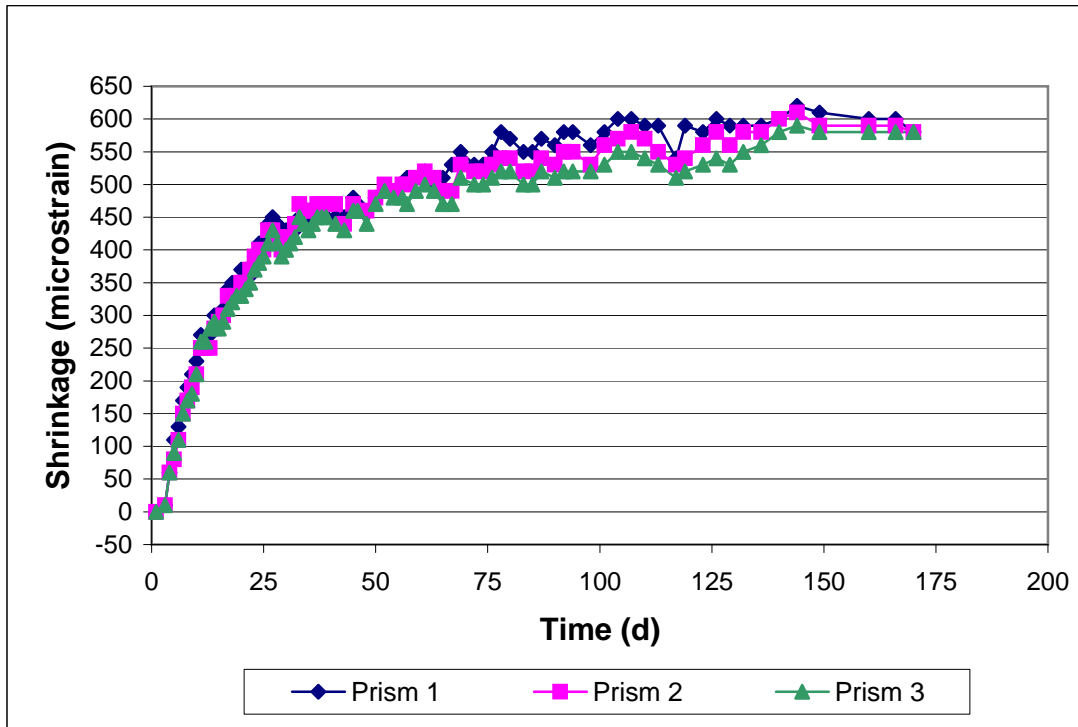


Figure A3.13 - Free Shrinkage Test, Program 2. KDOT mix, Batch 130. Drying begins on day 3.

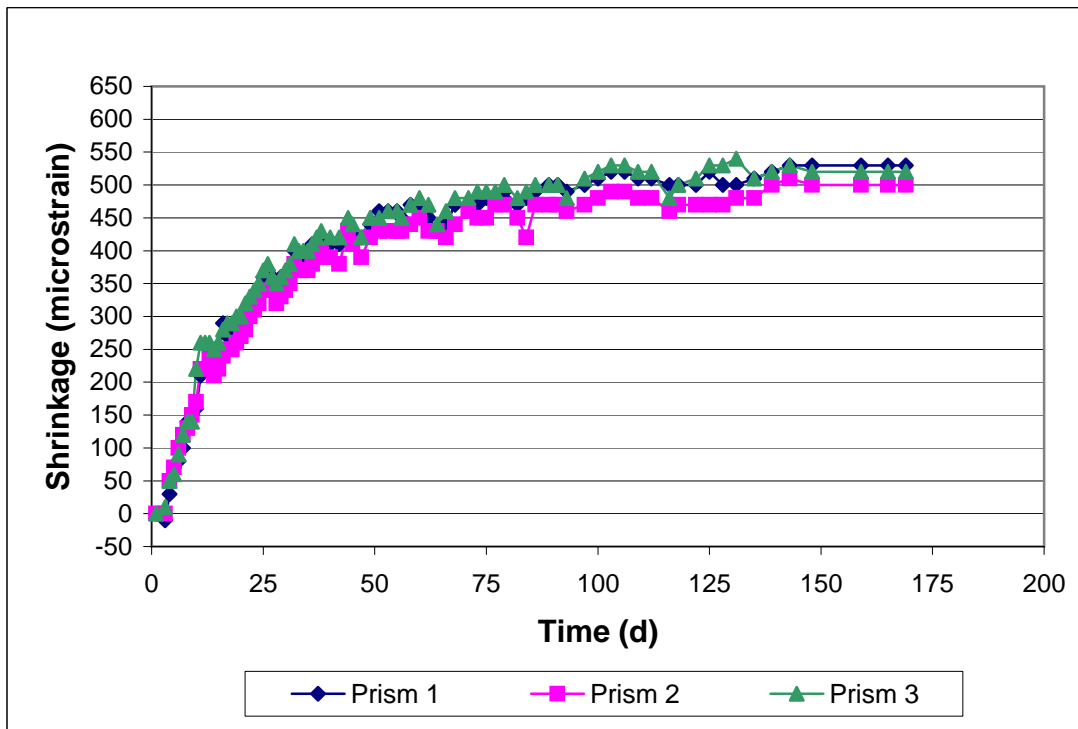


Figure A3.14 - Free Shrinkage Test, Program 2. MoDOT mix, Batch 132. Drying begins on day 3.

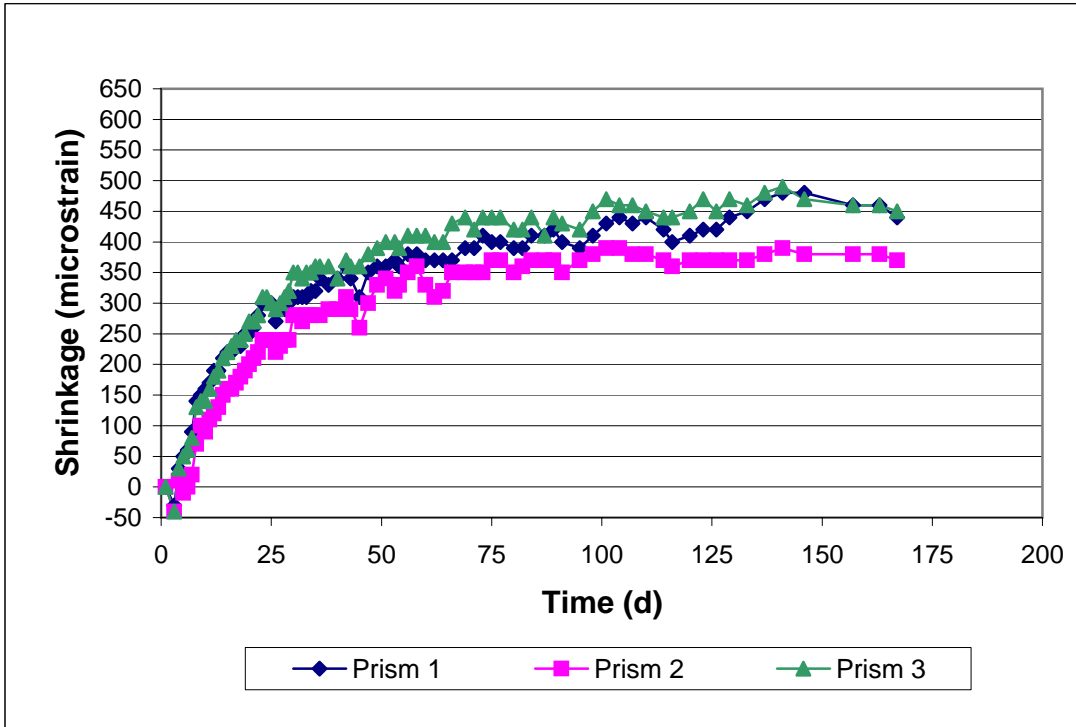


Figure A3.15 - Free Shrinkage Test, Program 2. Control mix, Batch 138. Drying begins on day 3.

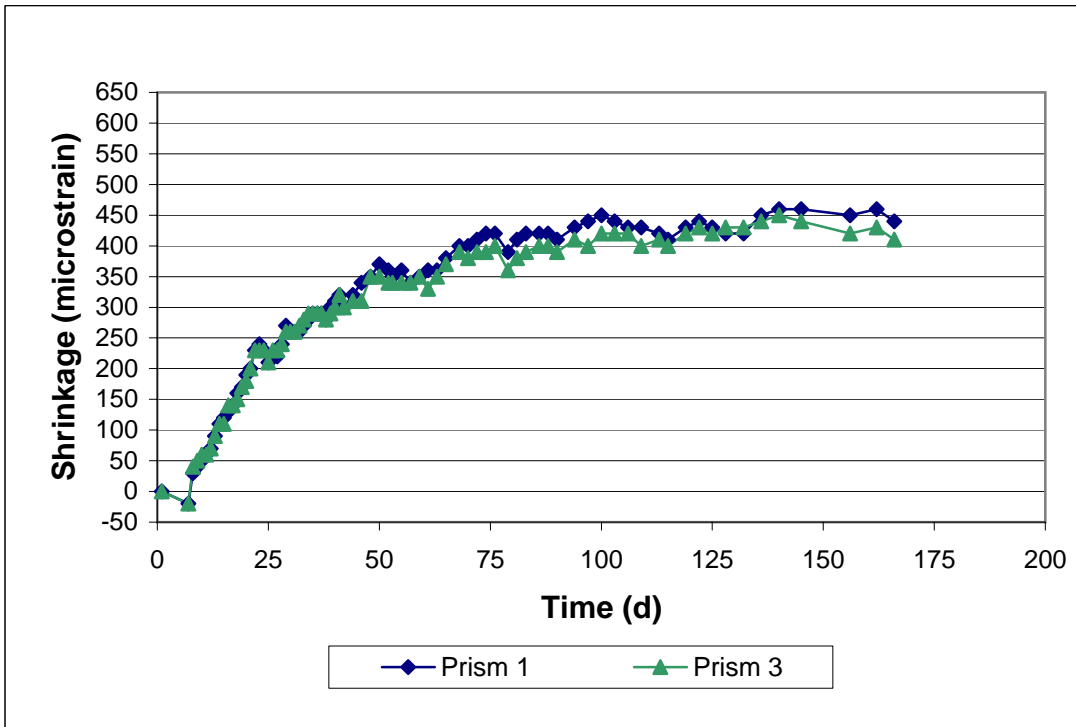


Figure A3.16 - Free Shrinkage Test, Program 2. 7 day cure mix, Batch 140. Drying begins on day 7.

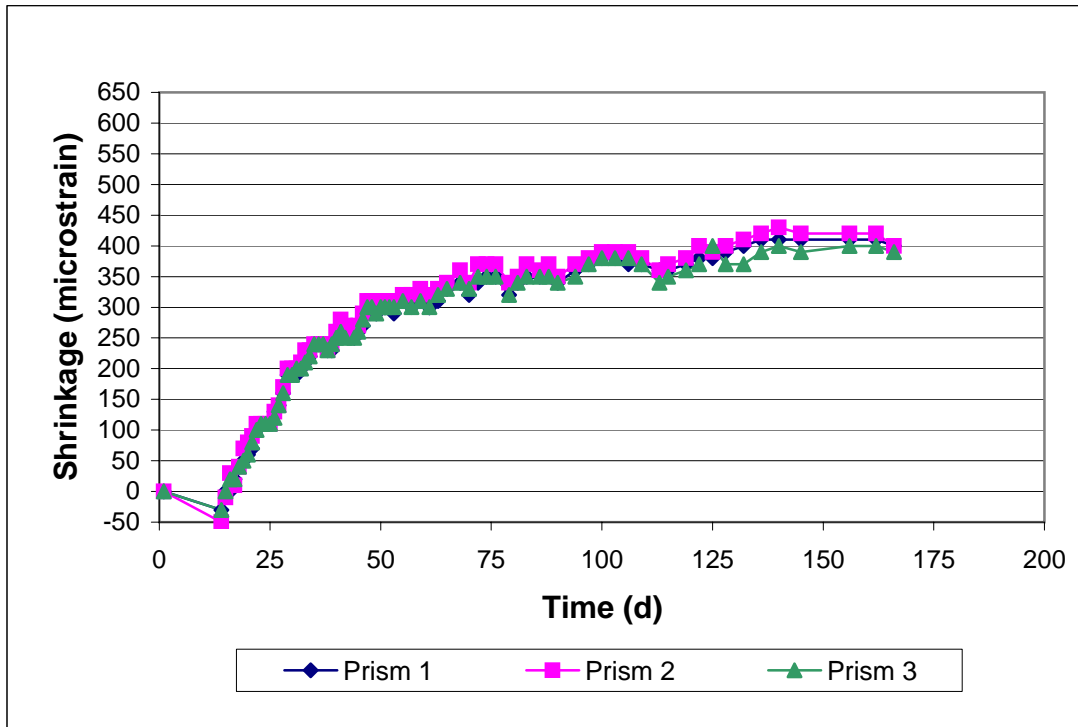


Figure A3.17 - Free Shrinkage Test, Program 2. 14 day cure mix, Batch 143. Drying begins on day 14.

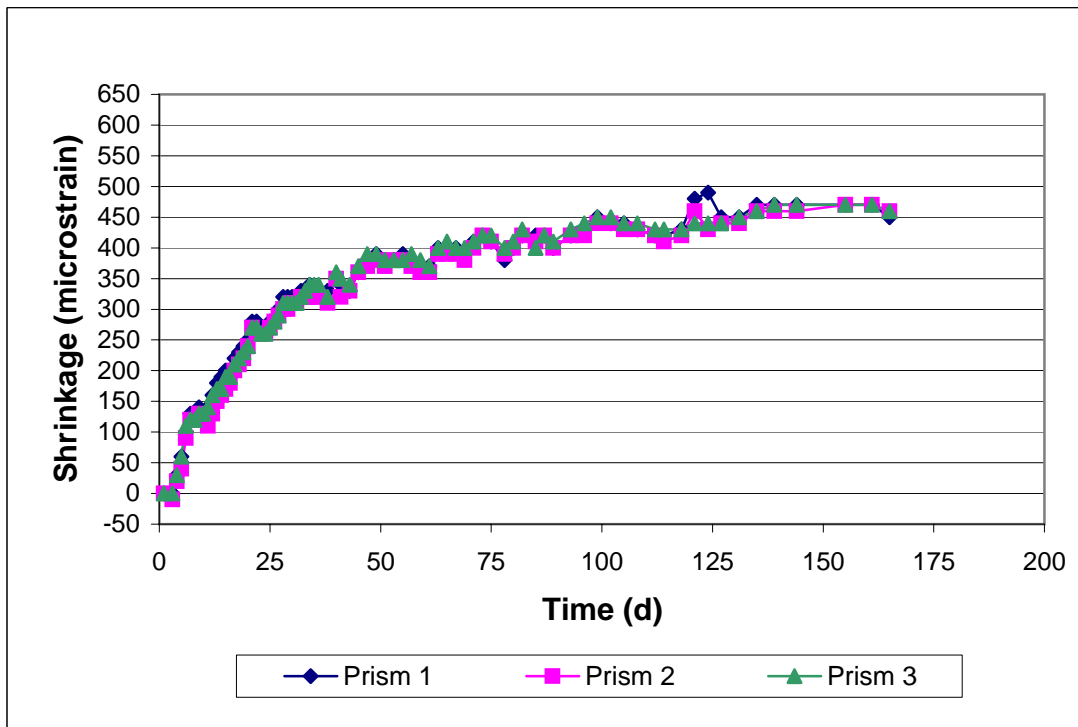


Figure A3.18 - Free Shrinkage Test, Program 2. Type II coarse-ground cement mix, Batch 135. Drying begins on day 3.

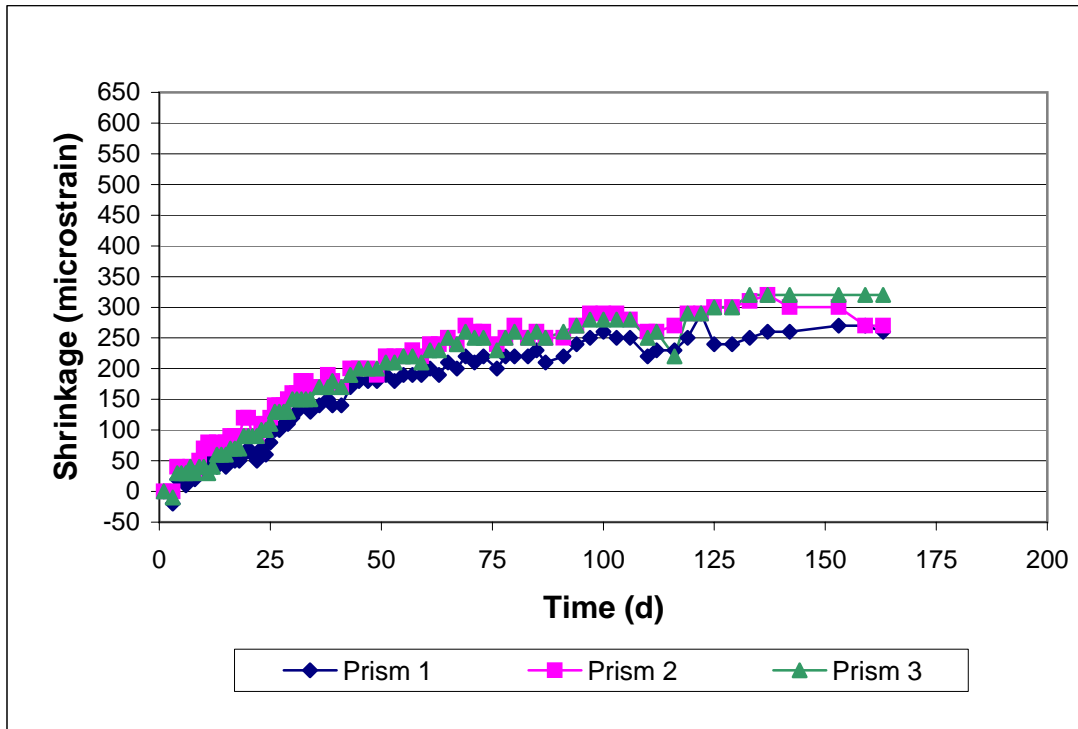


Figure A3.19 - Free Shrinkage Test, Program 2. SRA mix, Batch 147. Drying begins on day 3.

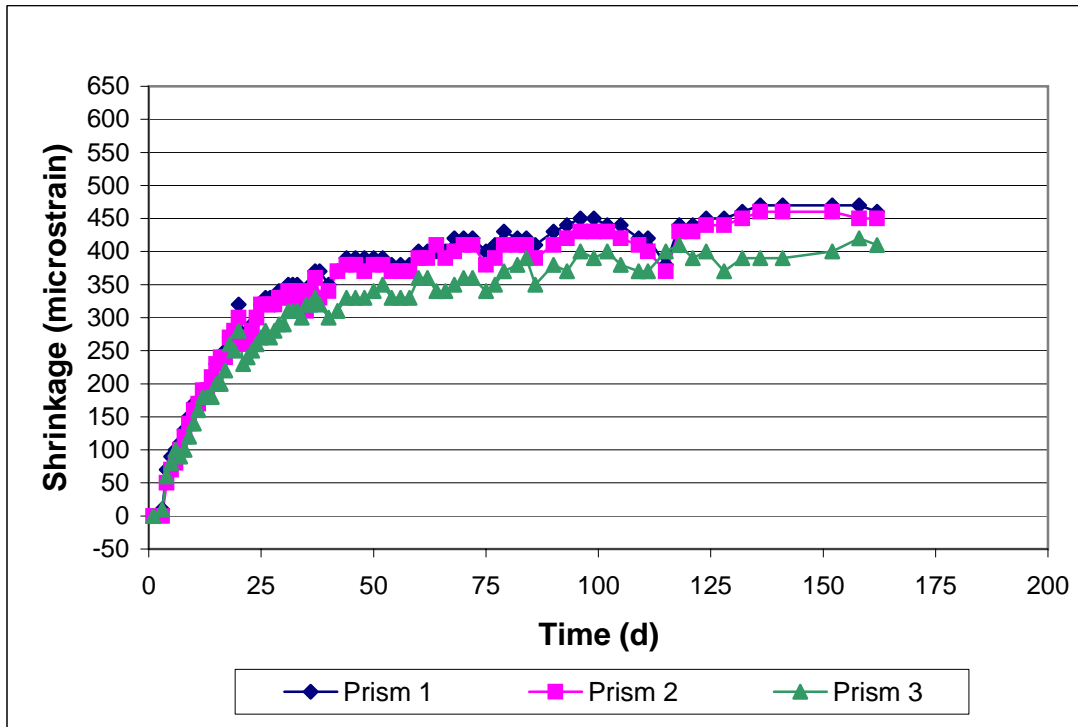


Figure A3.20 - Free Shrinkage Test, Program 2. 497 mix, Batch 149. Drying begins on day 3.

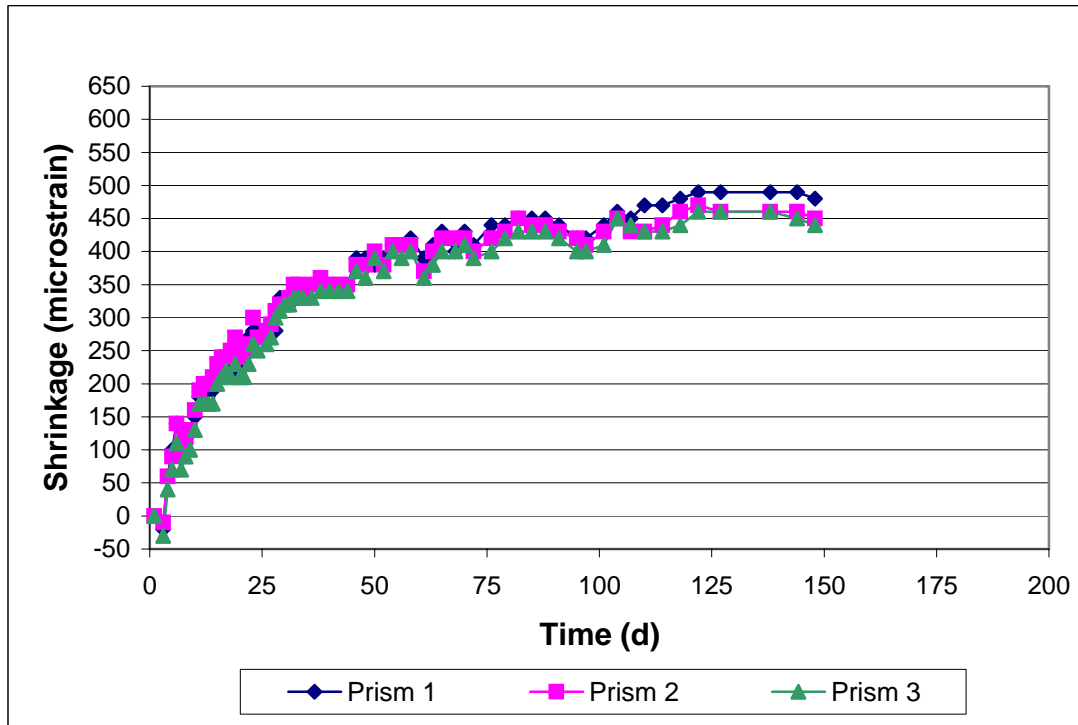


Figure A3.21 - Free Shrinkage Test, Program 2. Quartzite mix, Batch 159. Drying begins on day 3.

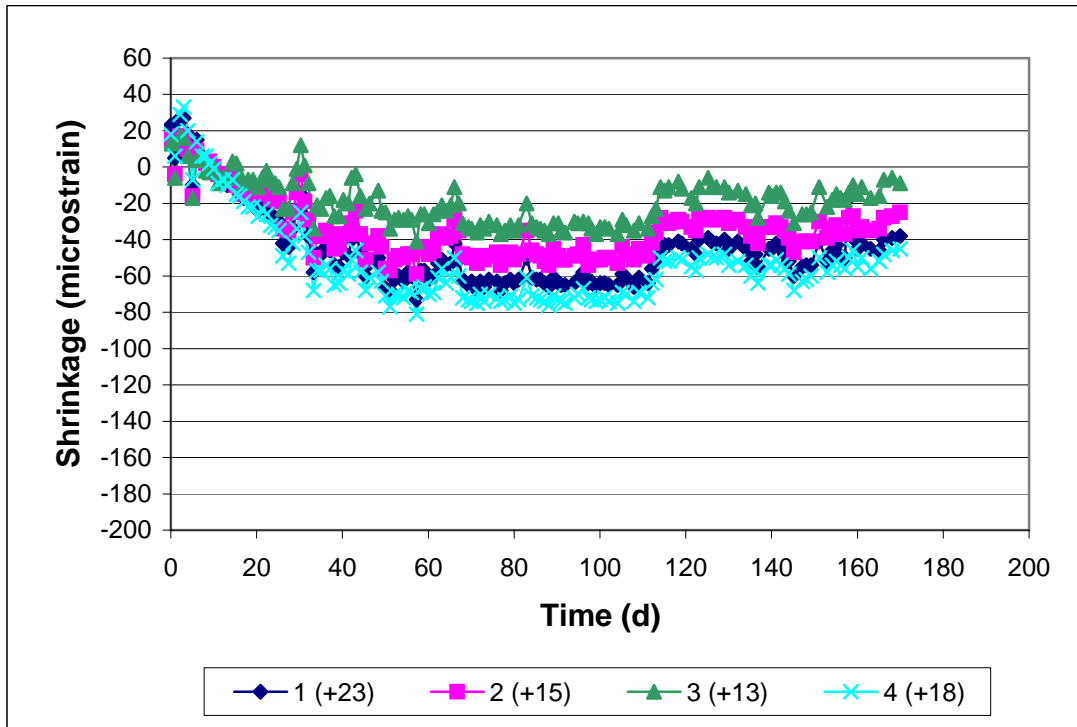


Figure A3.22a - Ring Test, Program 2. KDOT mix, Batch 130, Ring A. Drying begins on day 3.

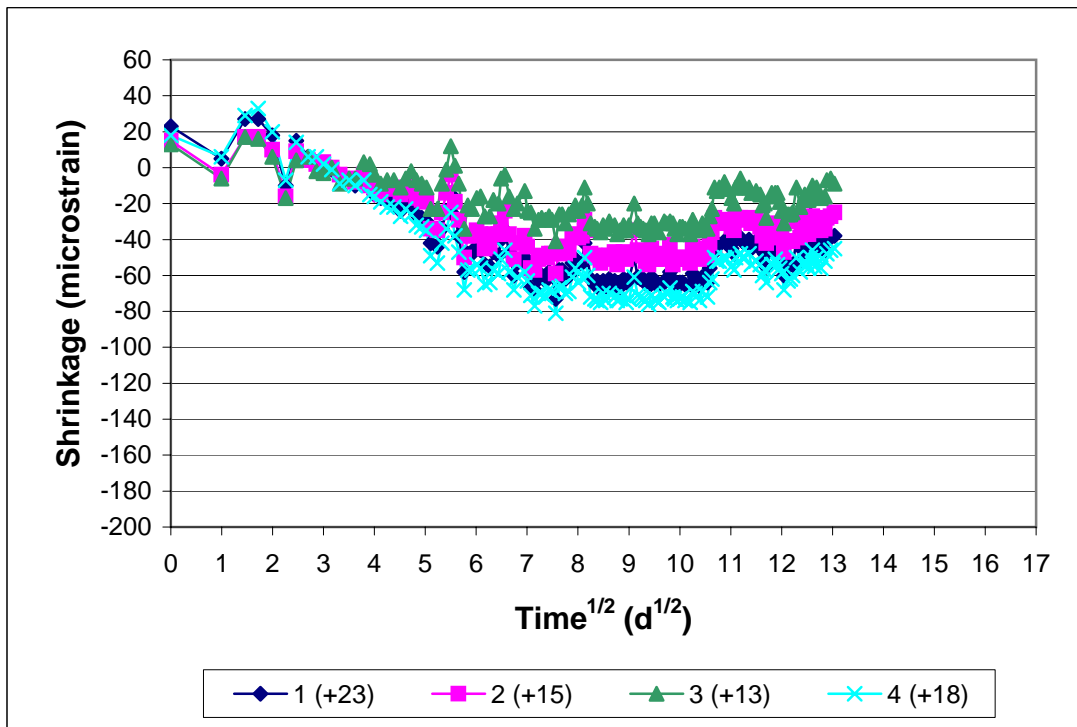


Figure A3.22b - Ring Test, Program 2. KDOT, Batch 130, Ring A. Shrinkage versus the square root of time.

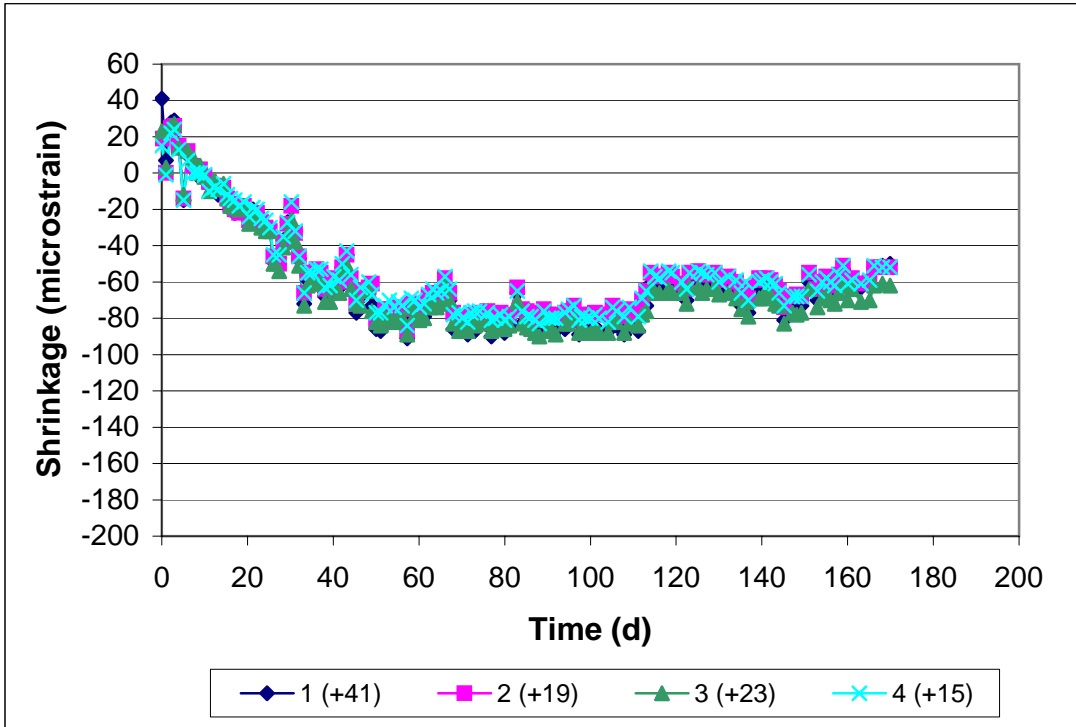


Figure A3.23a - Ring Test, Program 2. KDOT mix, Batch 130, Ring B. Drying begins on day 3.

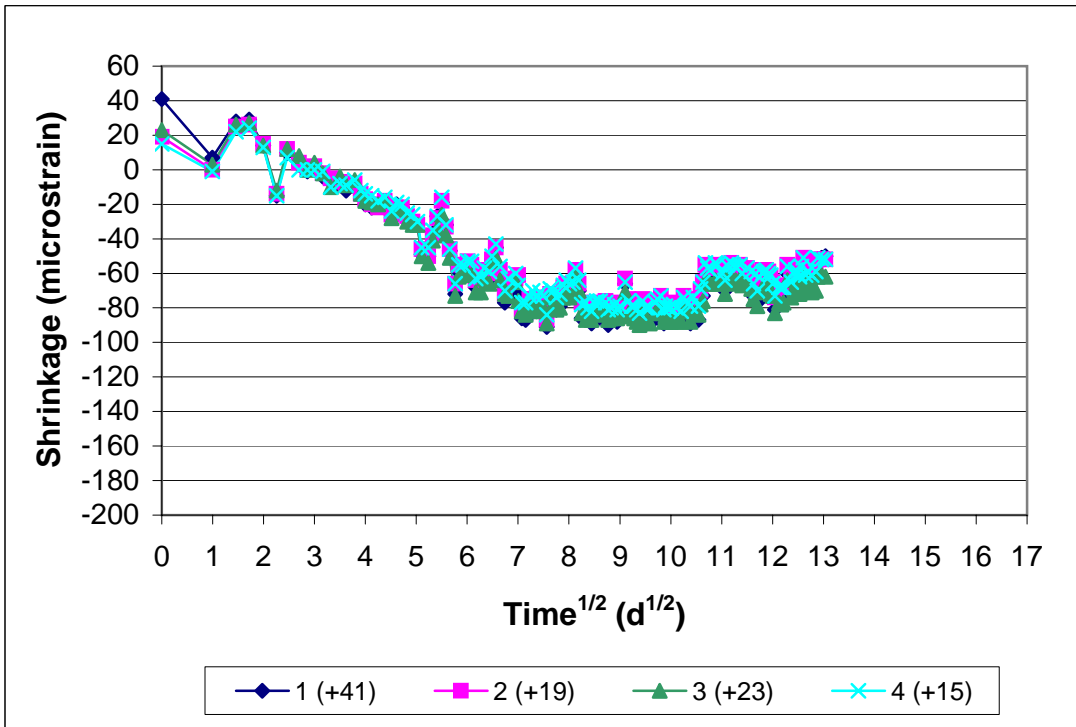


Figure A3.23b - Ring Test, Program 2. KDOT, Batch 130, Ring B. Shrinkage versus the square root of time.

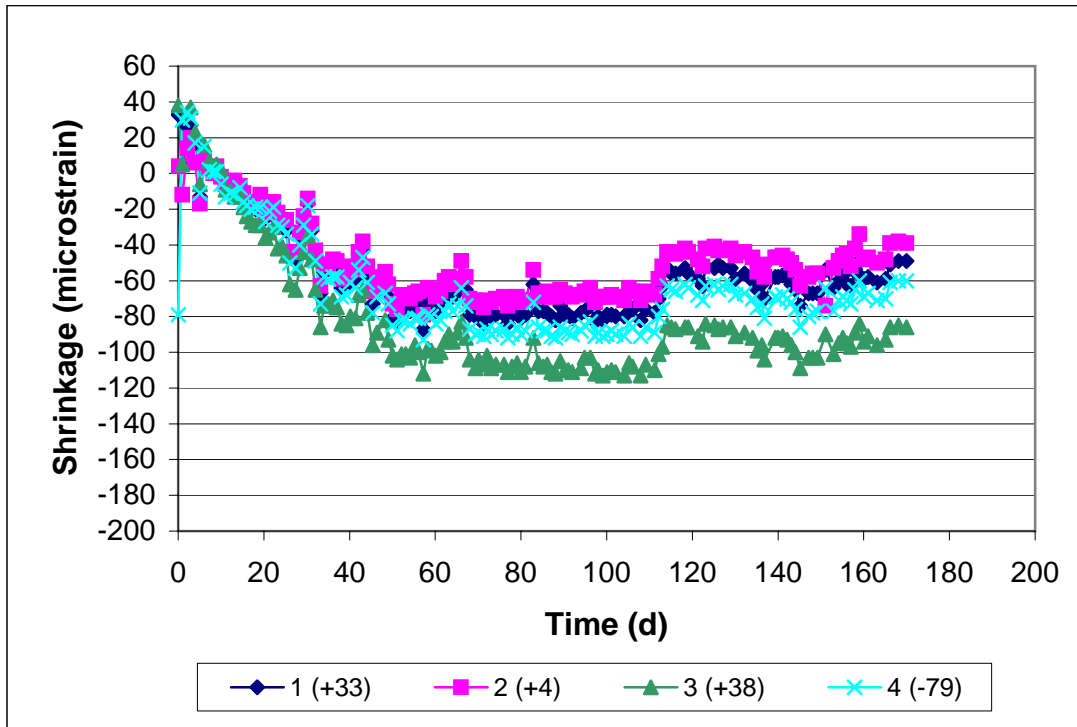


Figure A3.24a - Ring Test, Program 2. KDOT mix, Batch 130, Ring C. Drying begins on day 3. Value in parentheses added to data to view all curves in the same window.

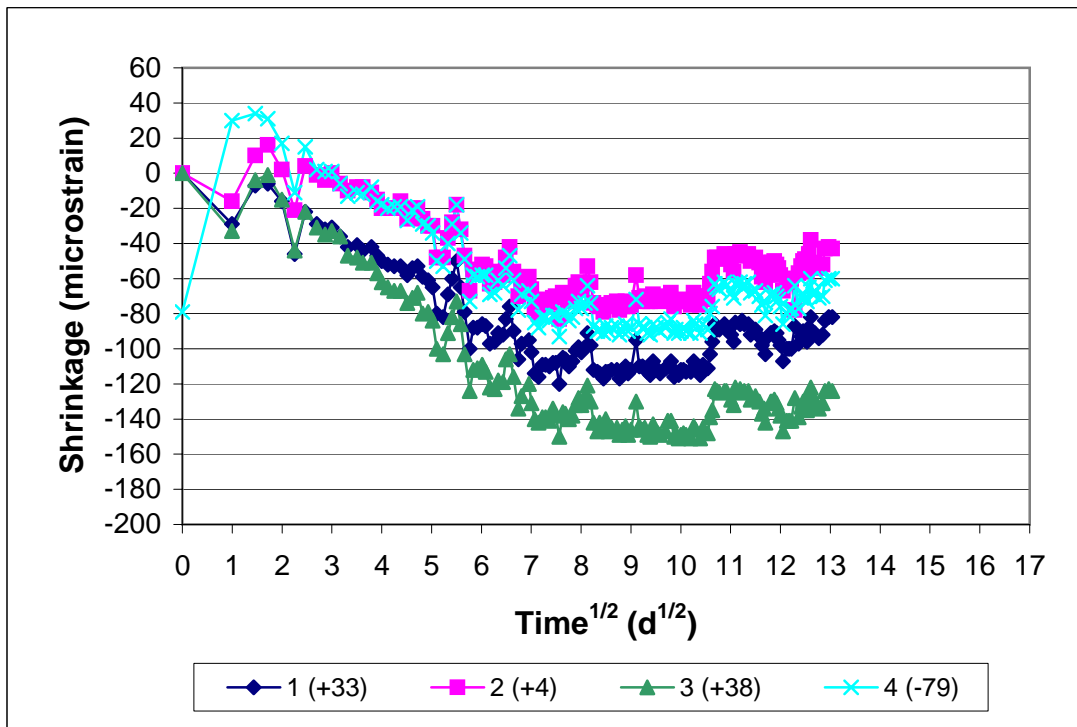


Figure A3.24b - Ring Test, Program 2. KDOT, Batch 130, Ring C. Shrinkage versus the square root of time.

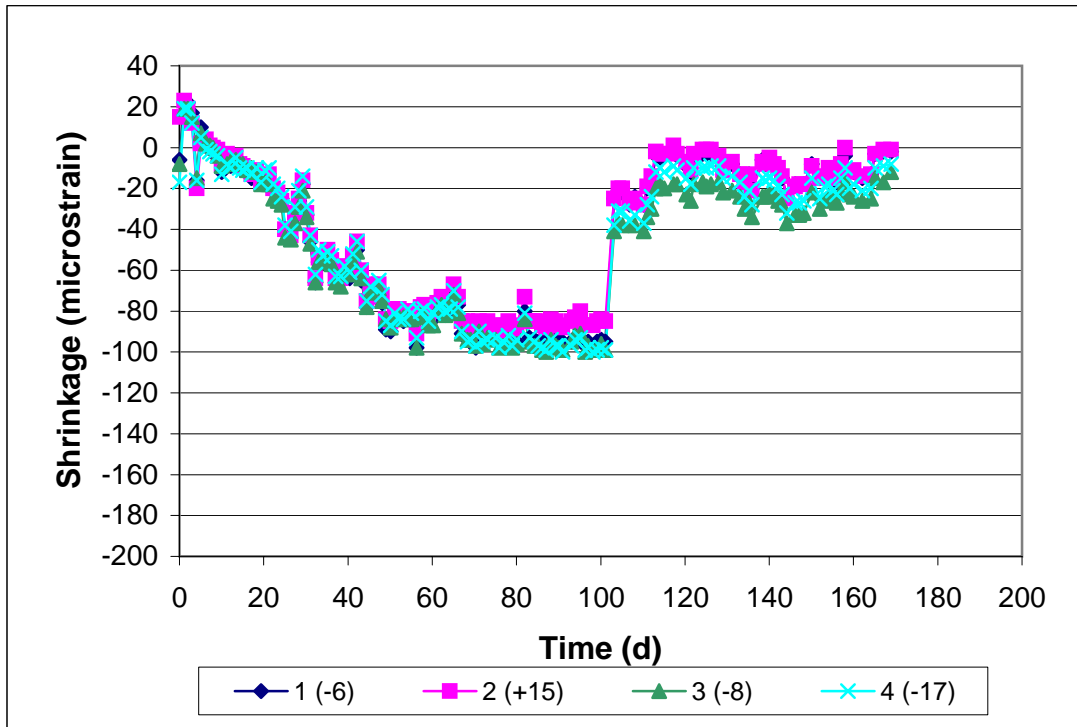


Figure A3.25a - Ring Test, Program 2. MoDOT mix, Batch 132, Ring A. Drying begins on day 3.

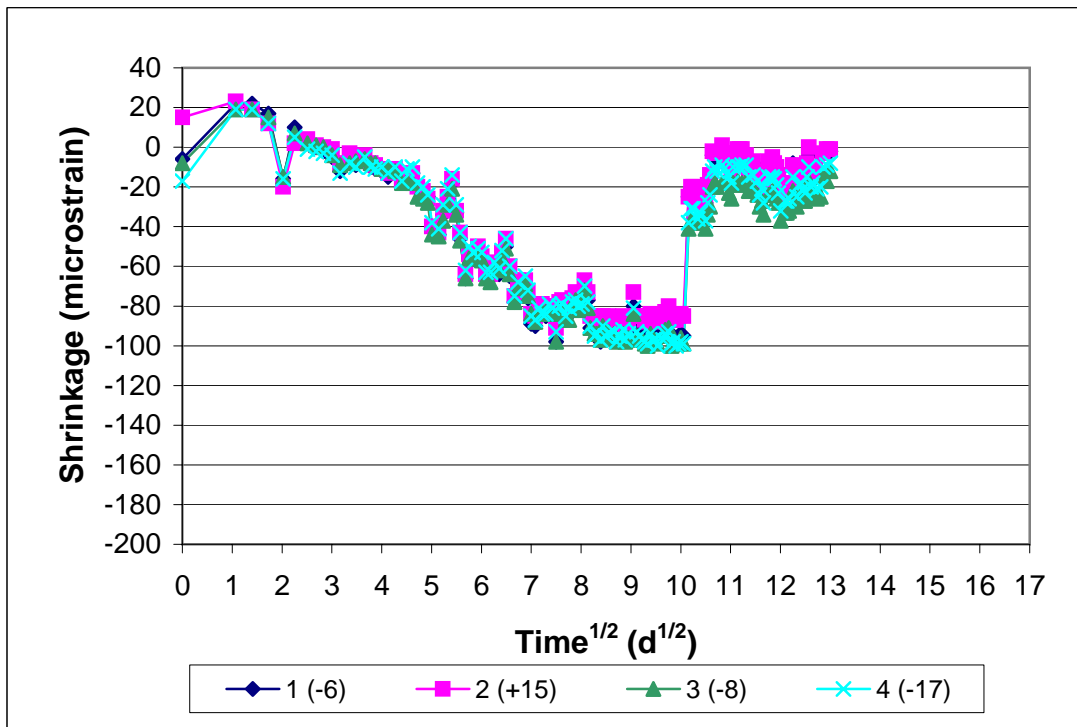


Figure A3.25b - Ring Test, Program 2. MoDOT, Batch 132, Ring A. Shrinkage versus the square root of time.

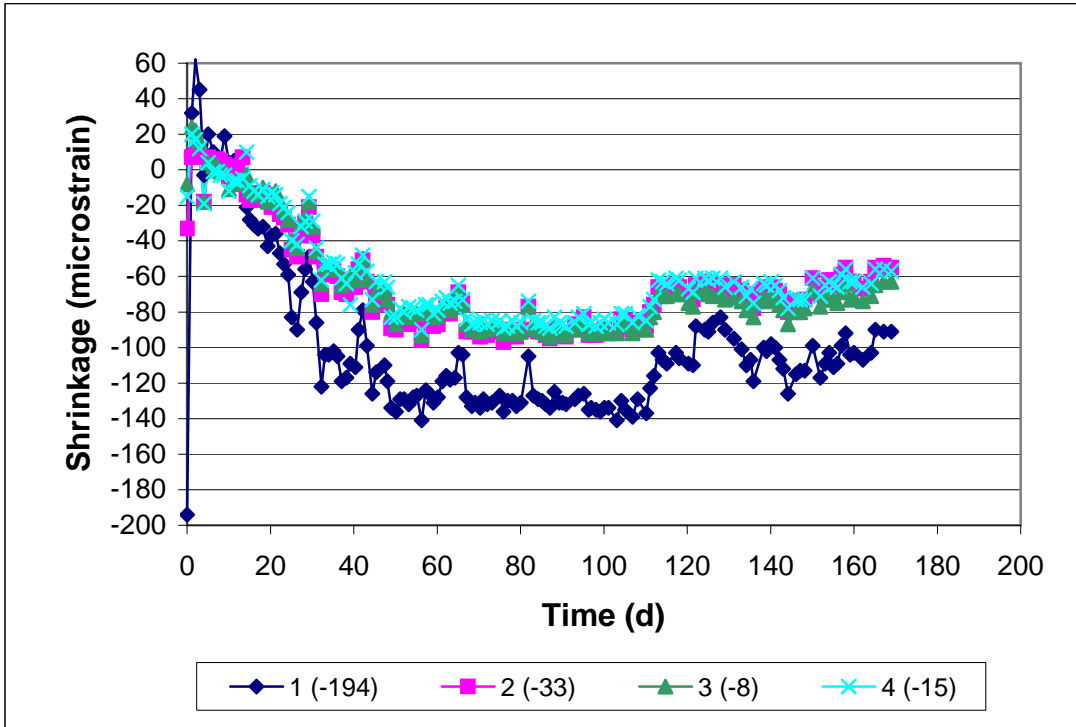


Figure A3.26a - Ring Test, Program 2. MoDOT mix, Batch 132, Ring B. Drying begins on day 3. Value in parentheses added to data to view all curves in the same window.

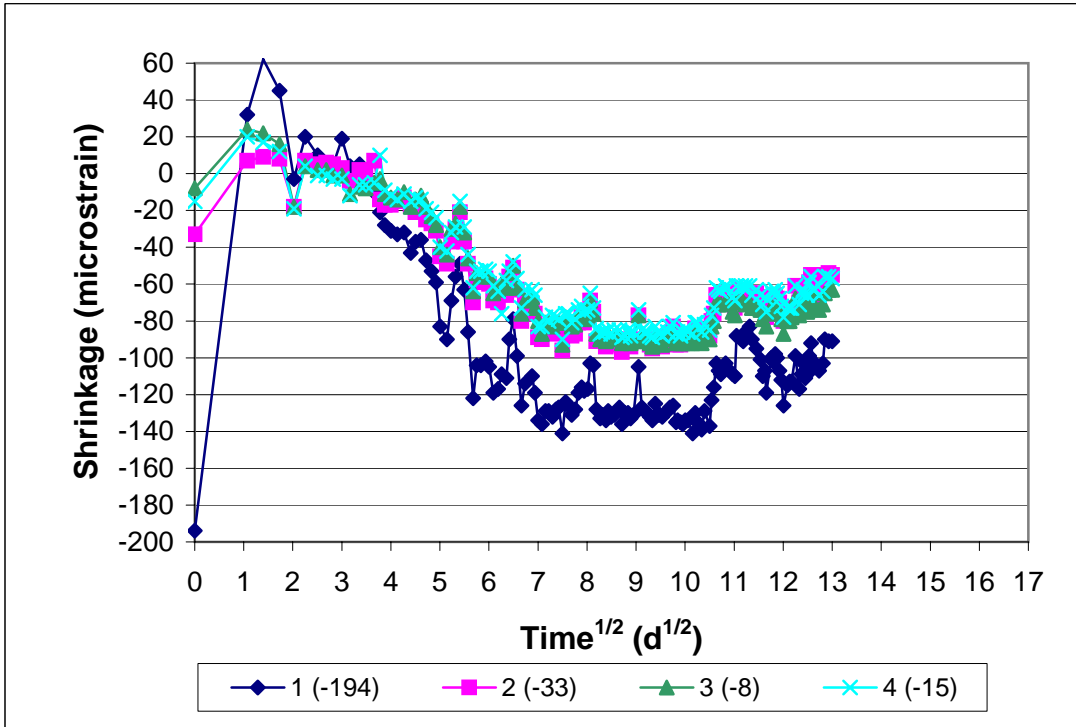


Figure A3.26b - Ring Test, Program 2. MoDOT, Batch 132, Ring B. Shrinkage versus the square root of time.

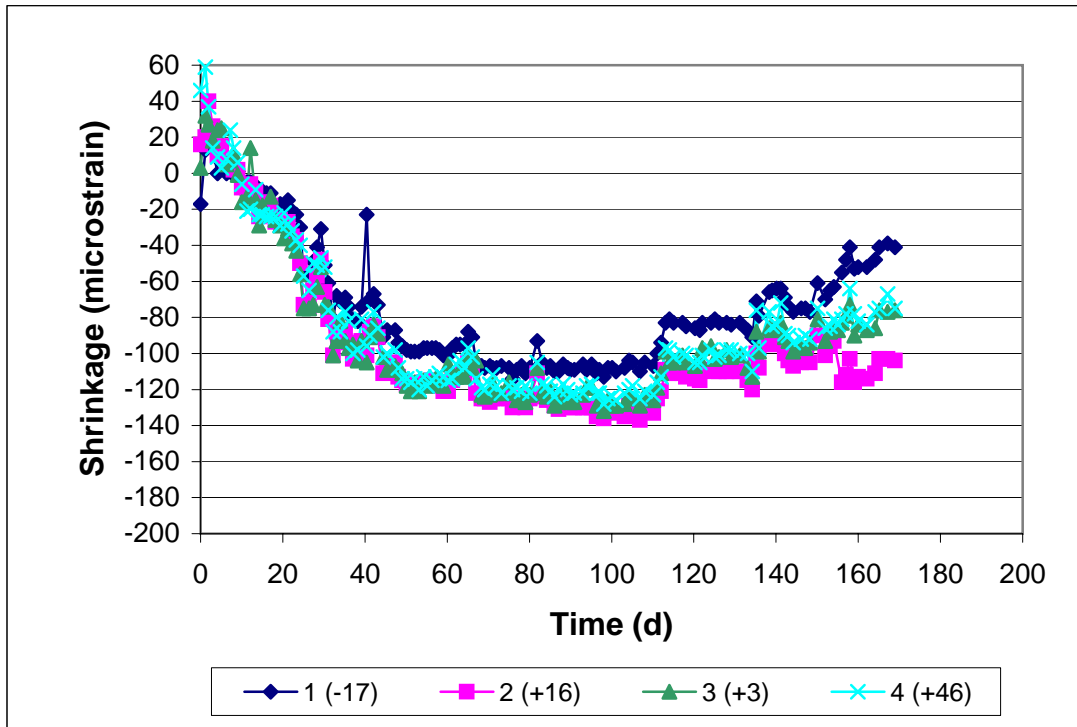


Figure A3.27a - Ring Test, Program 2. MoDOT mix, Batch 132, Ring C. Drying begins on day 3. Value in parentheses added to data to view all curves in the same window.

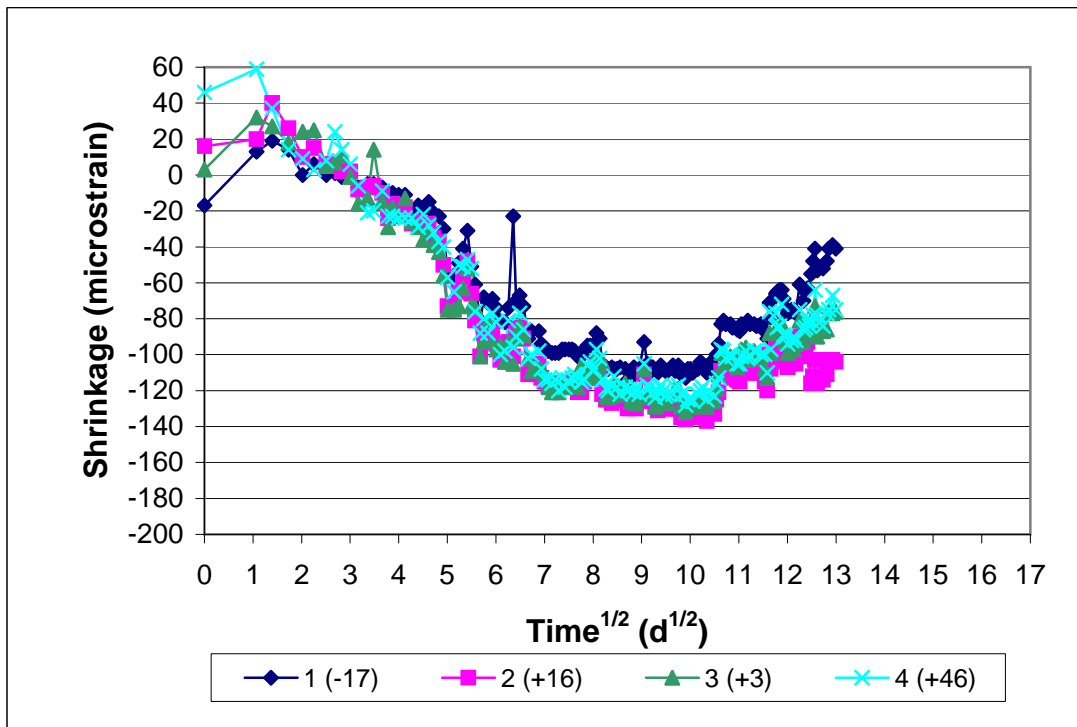


Figure A3.27b - Ring Test, Program 2. MoDOT, Batch 132, Ring C. Shrinkage versus the square root of time.

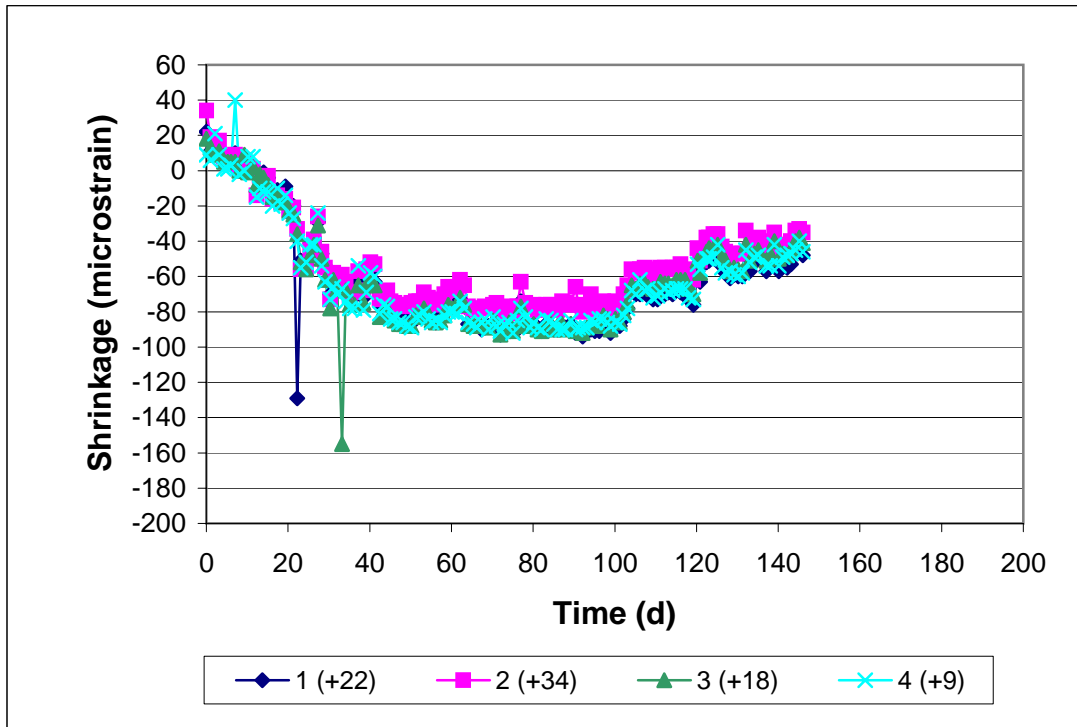


Figure A3.28a - Ring Test, Program 2. Control mix, Batch 138, Ring A. Drying begins on day 3.

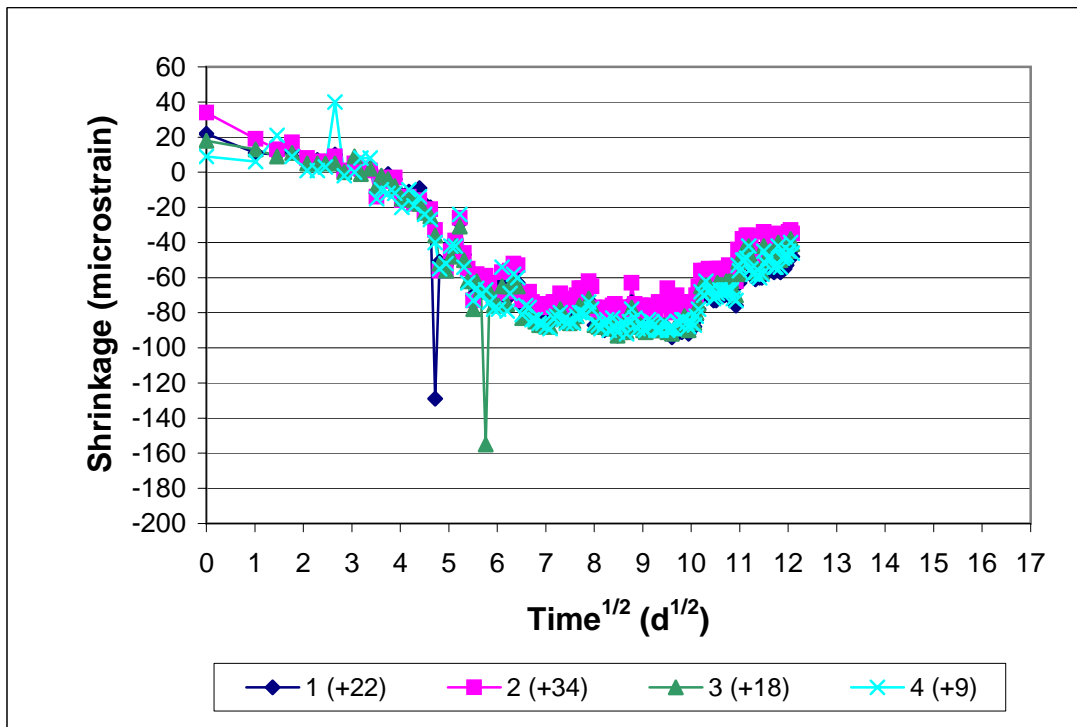


Figure A3.28b - Ring Test, Program 2. Control, Batch 138, Ring A. Shrinkage versus the square root of time.

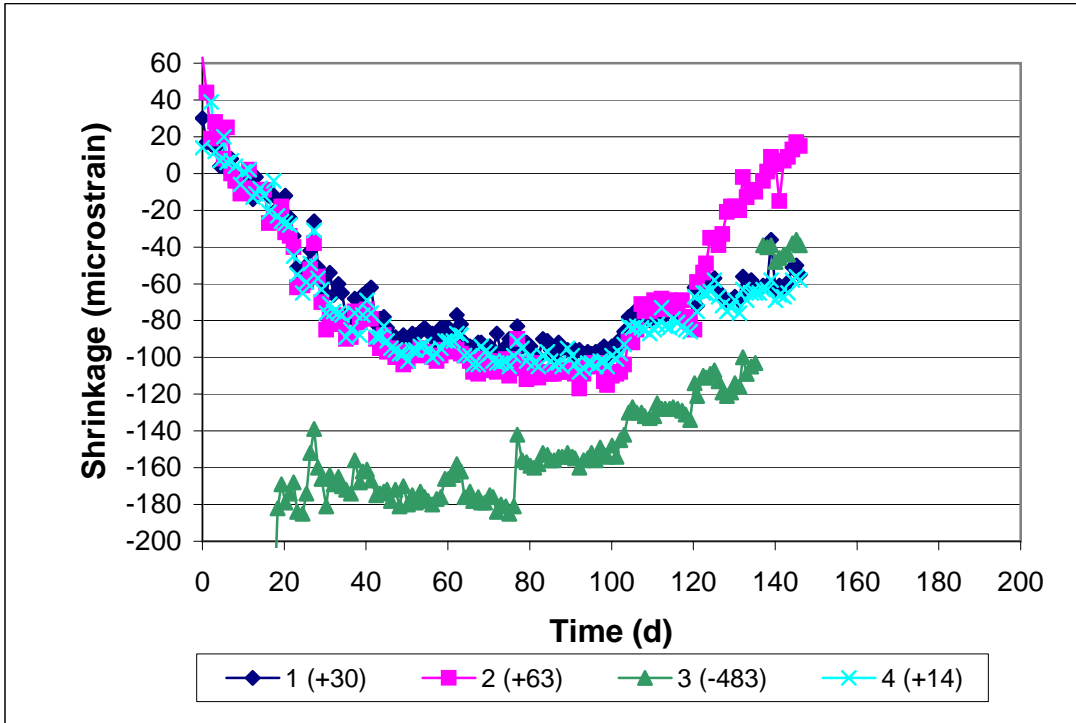


Figure A3.29a - Ring Test, Program 2. Control mix, Batch 138, Ring B. Drying begins on day 3.

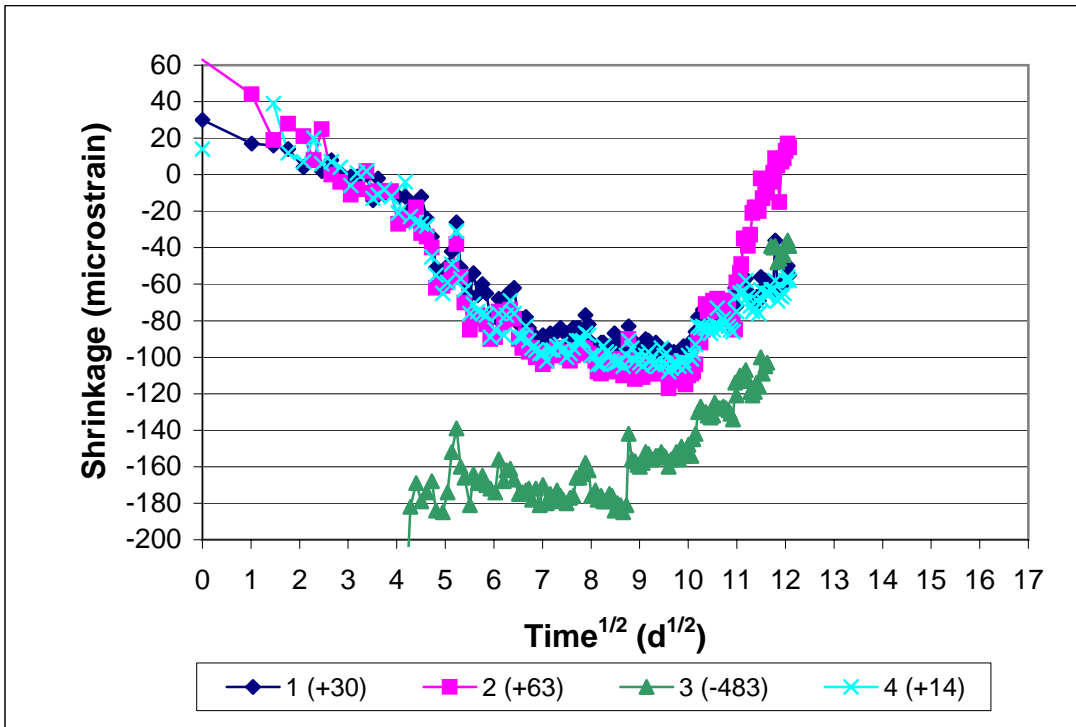


Figure A3.29b - Ring Test, Program 2. Control, Batch 138, Ring B. Shrinkage versus the square root of time.

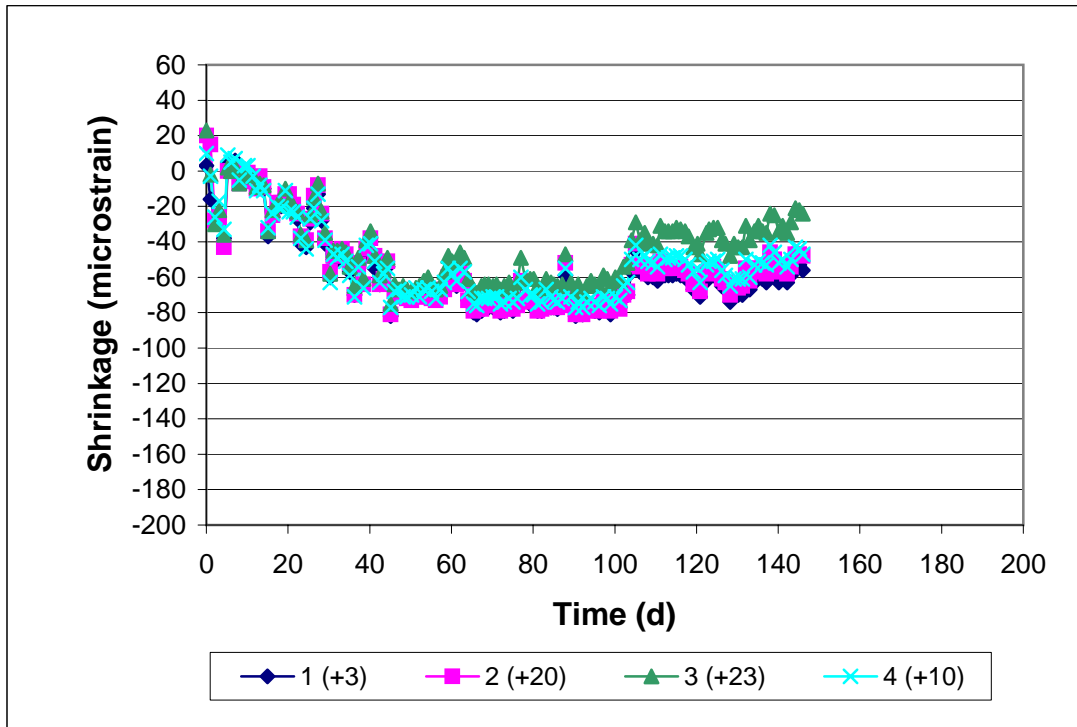


Figure A3.30a - Ring Test, Program 2. Control mix, Batch 138, Ring C. Drying begins on day 3.

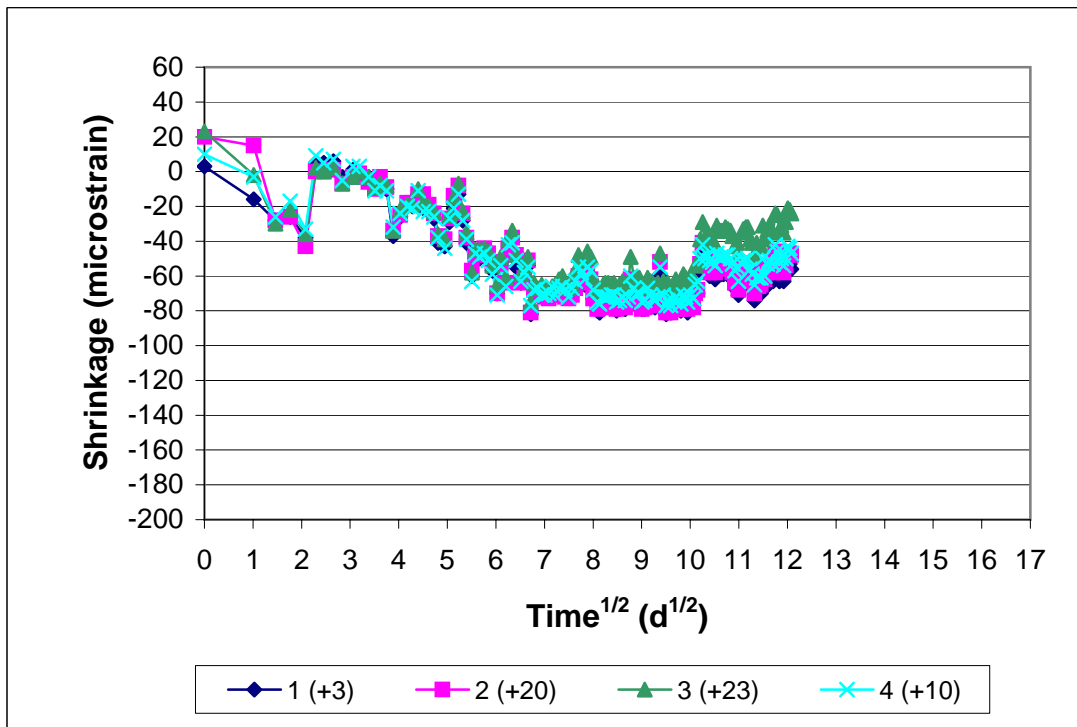


Figure A3.30b - Ring Test, Program 2. Control, Batch 138, Ring C. Shrinkage versus the square root of time.

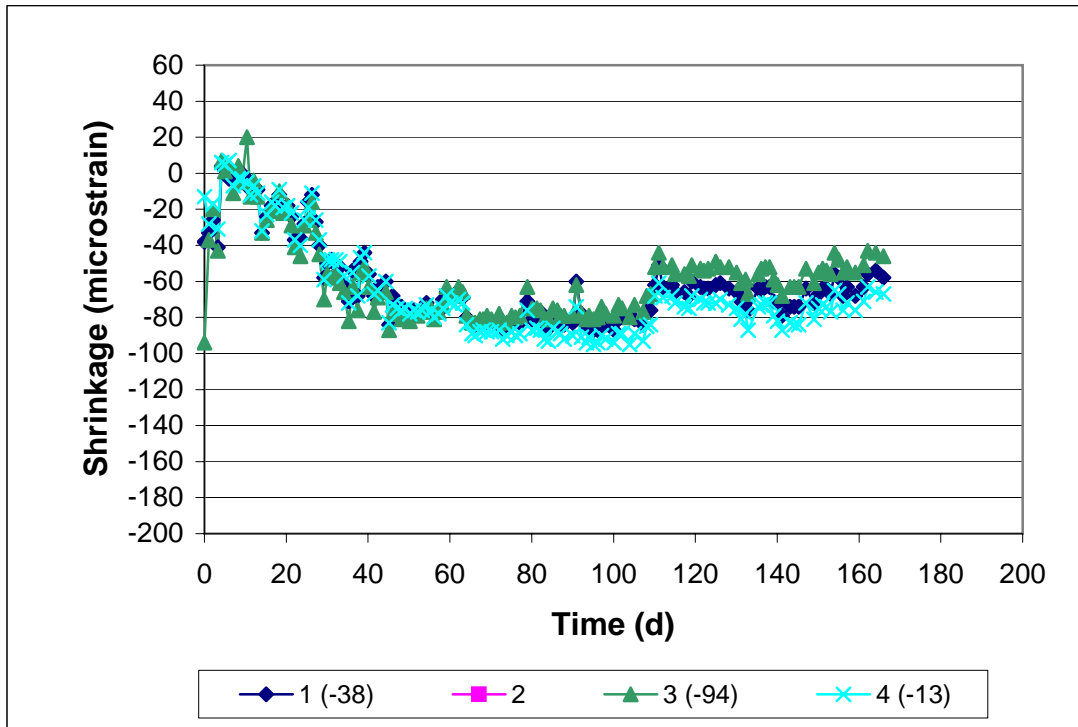


Figure A3.31a - Ring Test, Program 2. 7-day cure mix, Batch 140, Ring A. Drying begins on day 7.

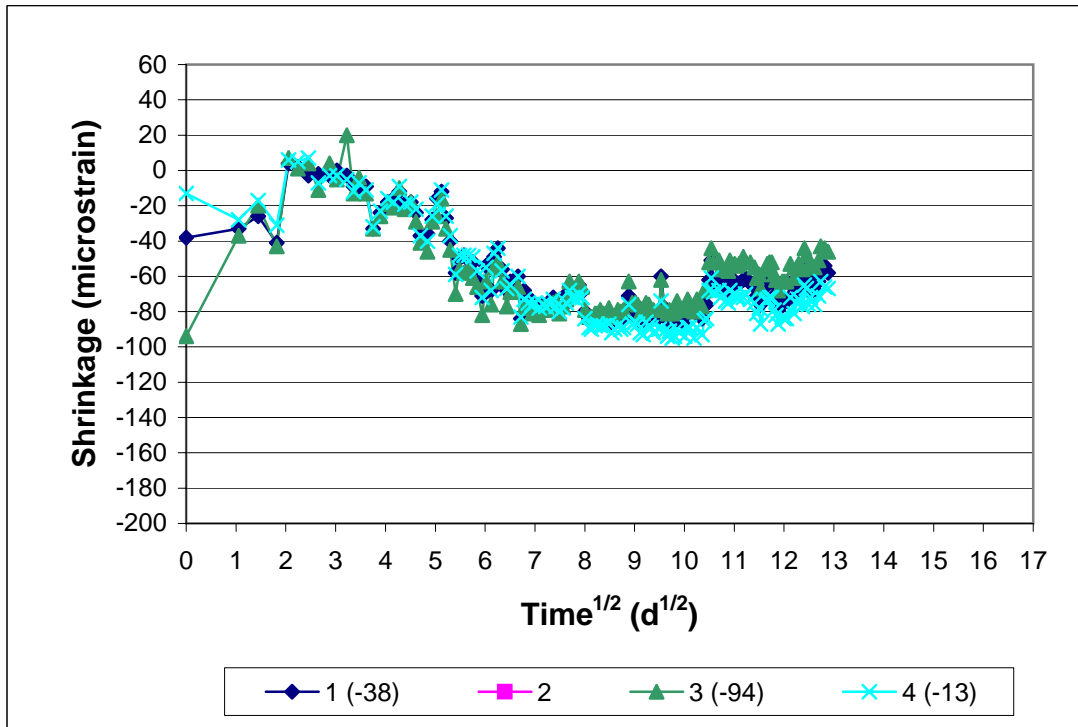


Figure A3.31b - Ring Test, Program 2. 7-day cure, Batch 140, Ring A. Shrinkage versus the square root of time.

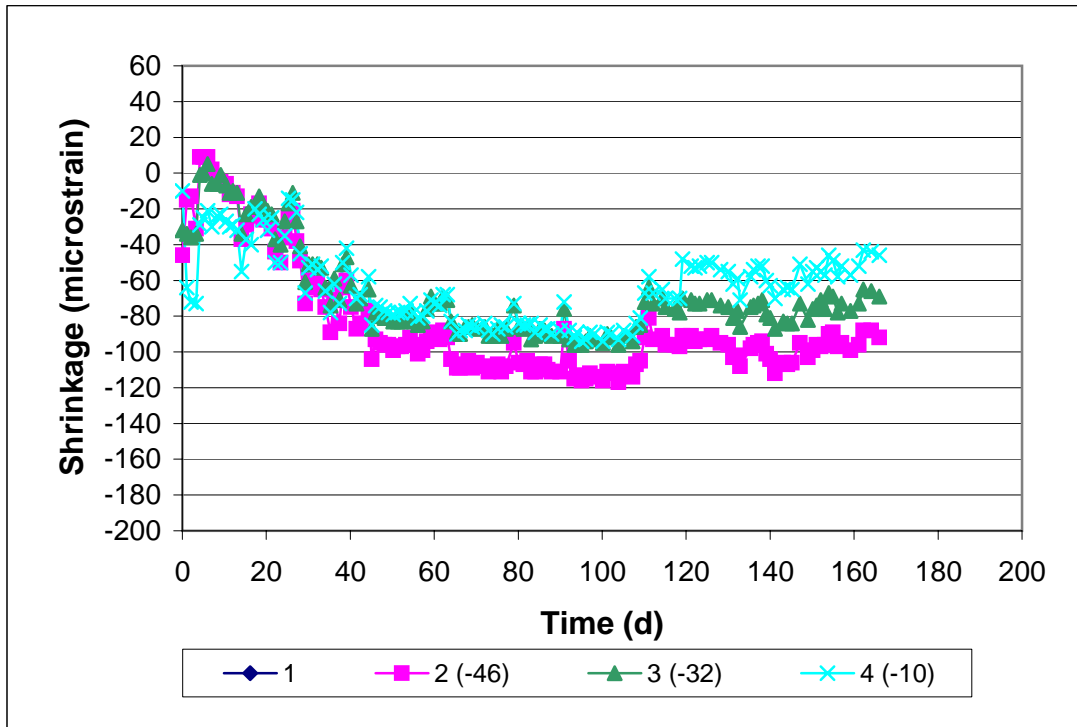


Figure A3.32a - Ring Test, Program 2. 7-day cure mix, Batch 140, Ring B. Drying begins on day 7.

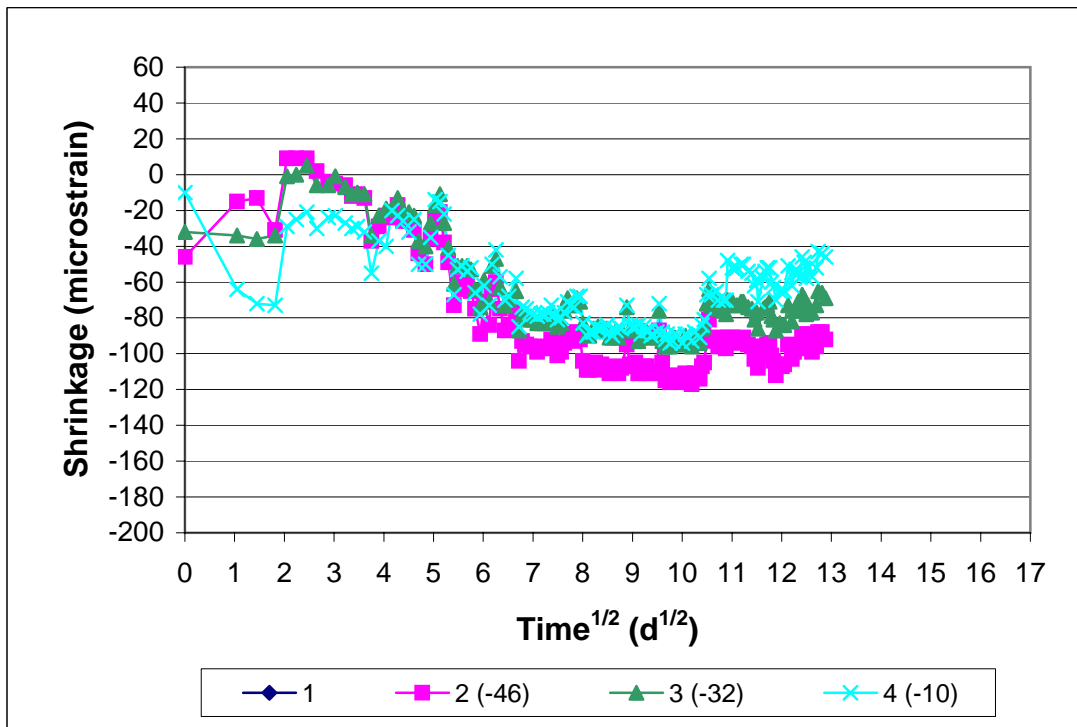


Figure A3.32b - Ring Test, Program 2. 7-day cure, Batch 140, Ring B. Shrinkage versus the square root of time.

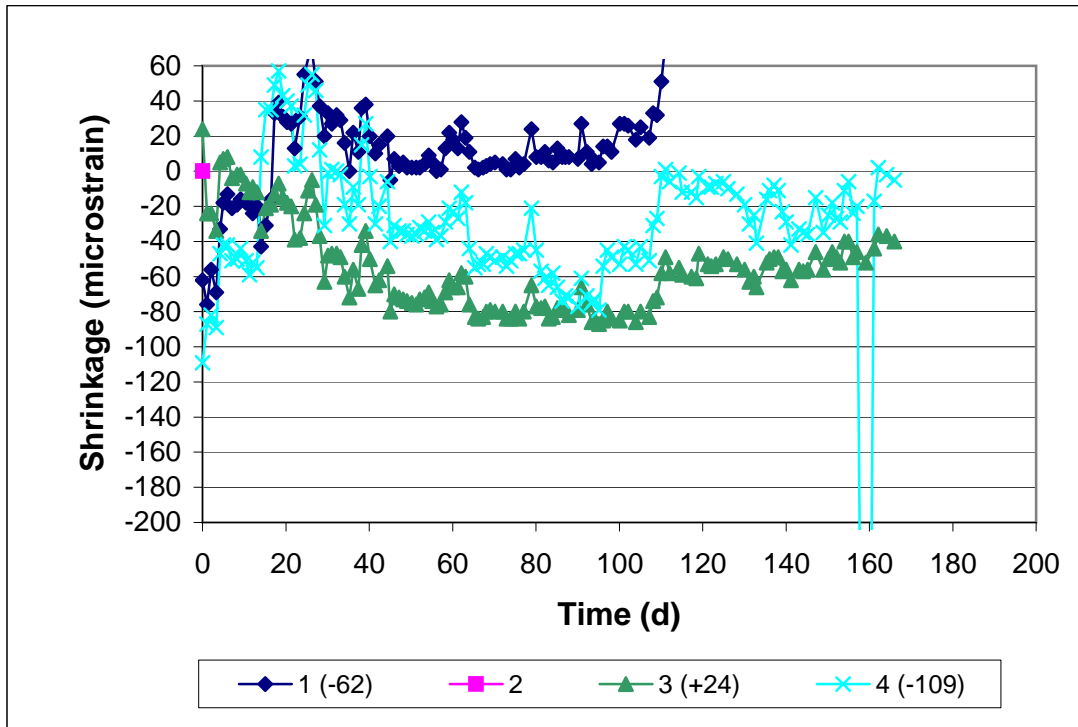


Figure A3.33a - Ring Test, Program 2. 7-day cure mix, Batch 140, Ring C. Drying begins on day 7. Values in parentheses added to data to view all curves in the same window.

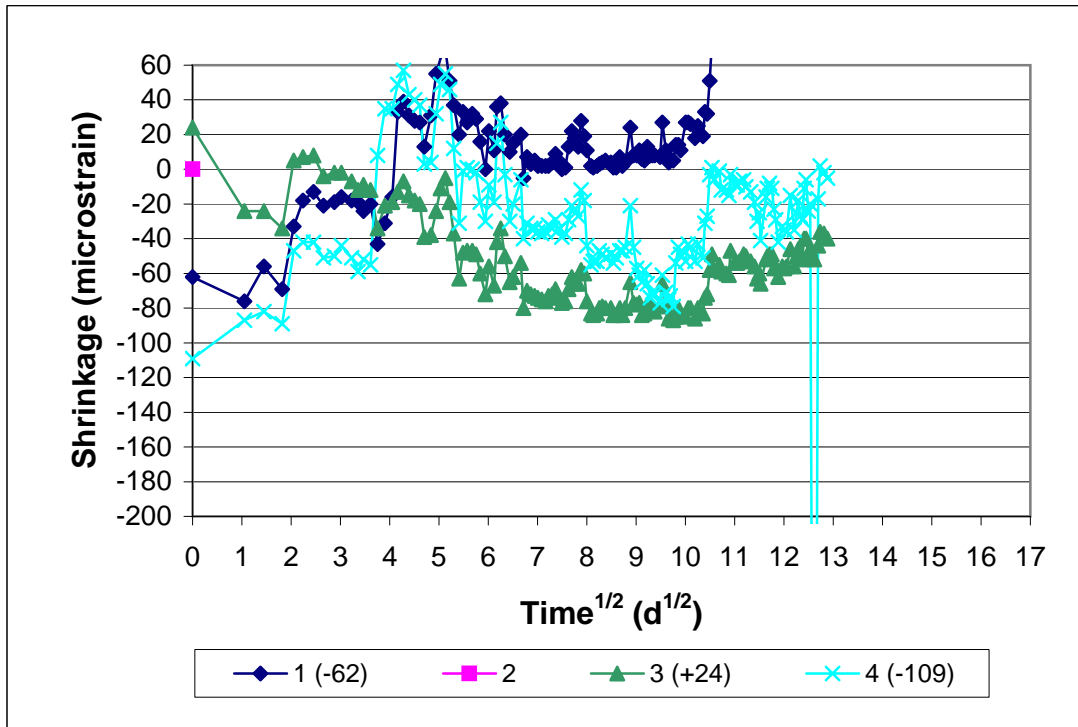


Figure A3.33b - Ring Test, Program 2. 7-day cure, Batch 140, Ring C. Shrinkage versus the square root of time.

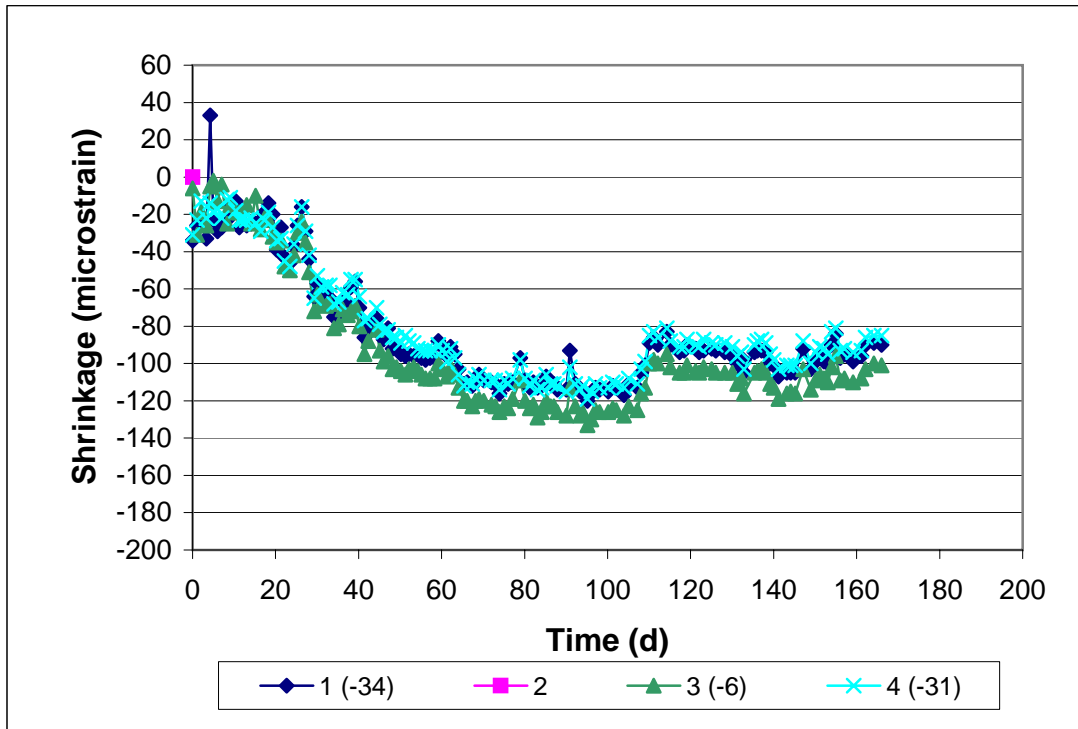


Figure A3.34a - Ring Test, Program 2. 14-day cure mix, Batch 143, Ring A. Drying begins on day 14.

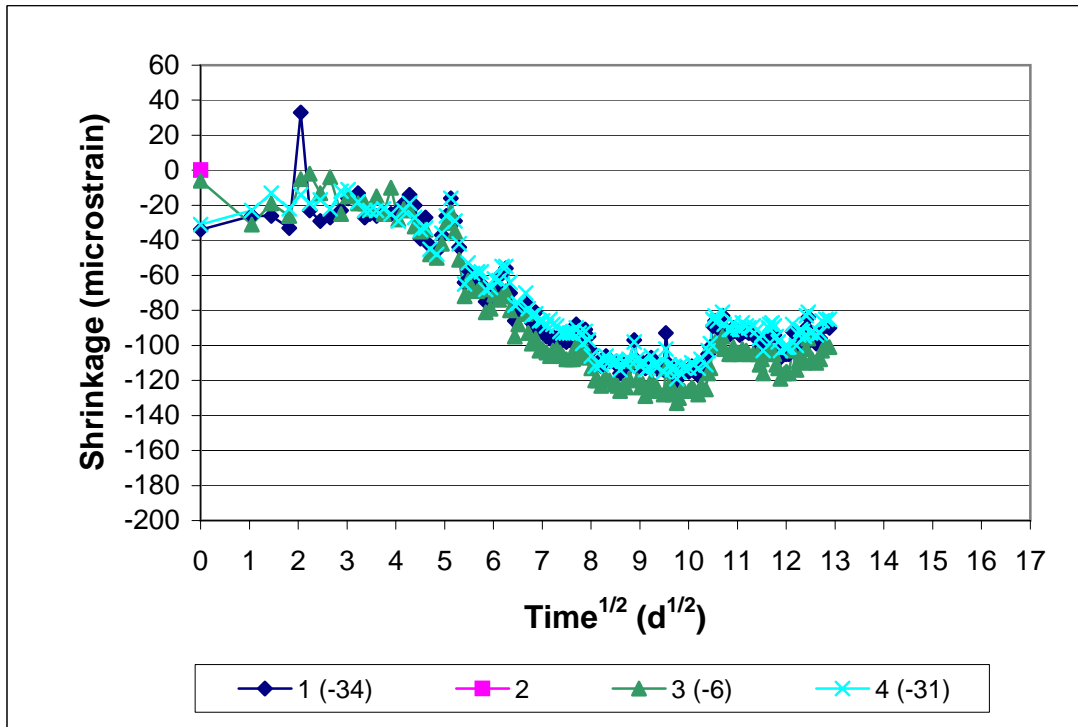


Figure A3.34b - Ring Test, Program 2. 14-day cure, Batch 143, Ring A. Shrinkage versus the square root of time.

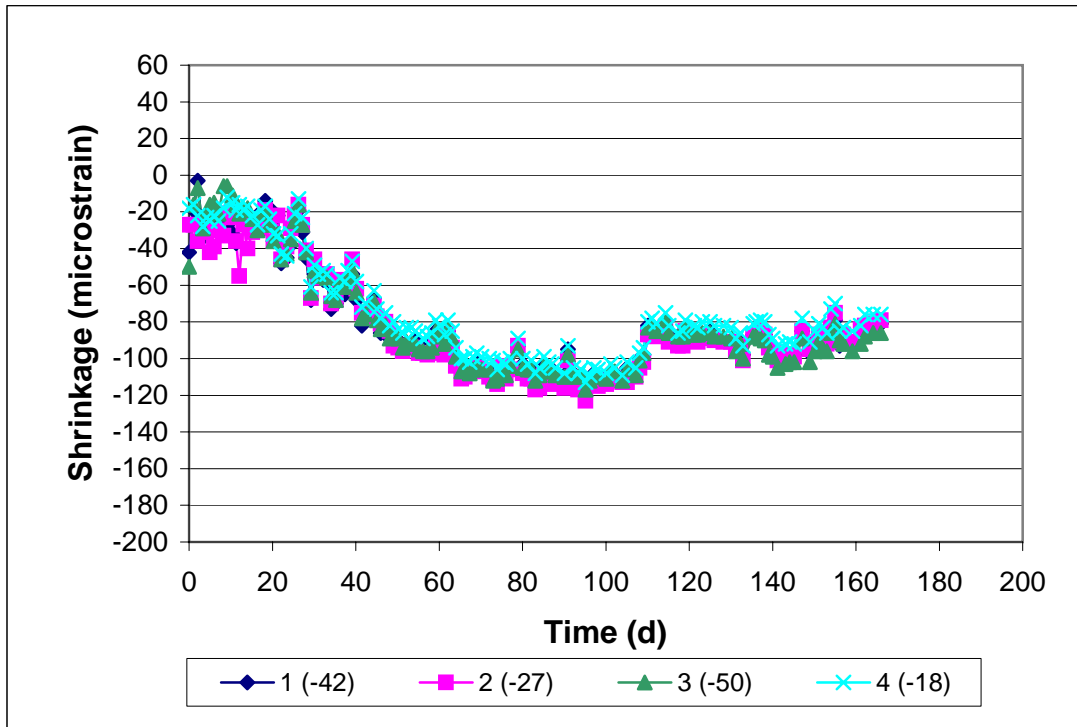


Figure A3.35a - Ring Test, Program 2. 14-day cure mix, Batch 143, Ring B. Drying begins on day 14.

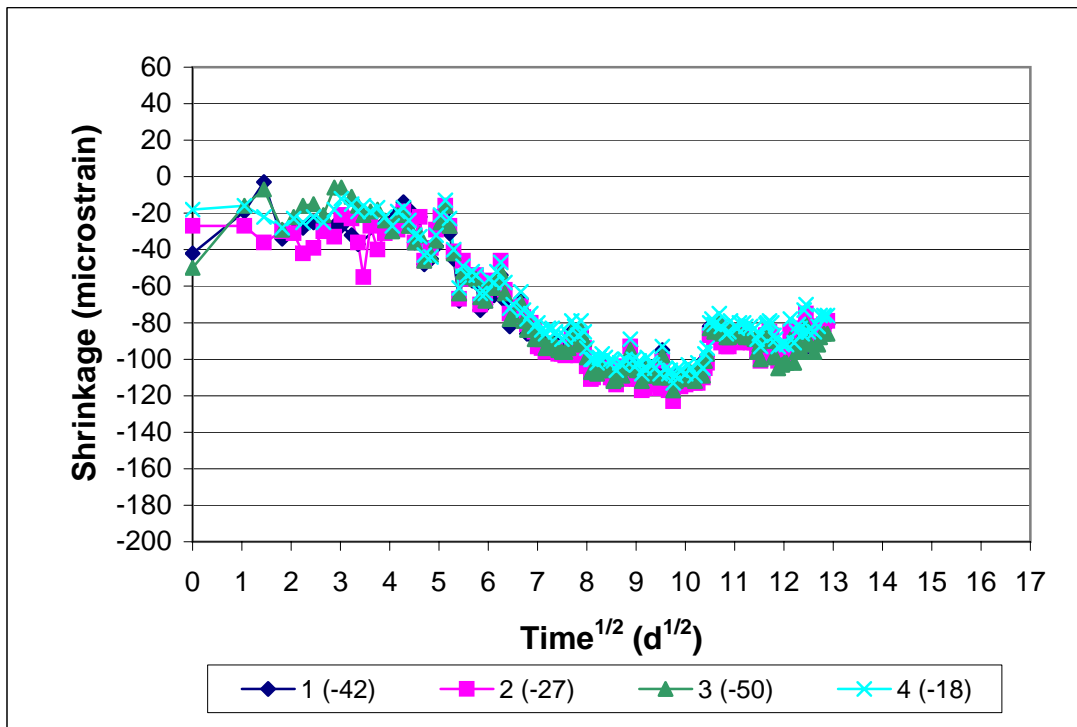


Figure A3.35b - Ring Test, Program 2. 14-day cure, Batch 143, Ring B. Shrinkage versus the square root of time.

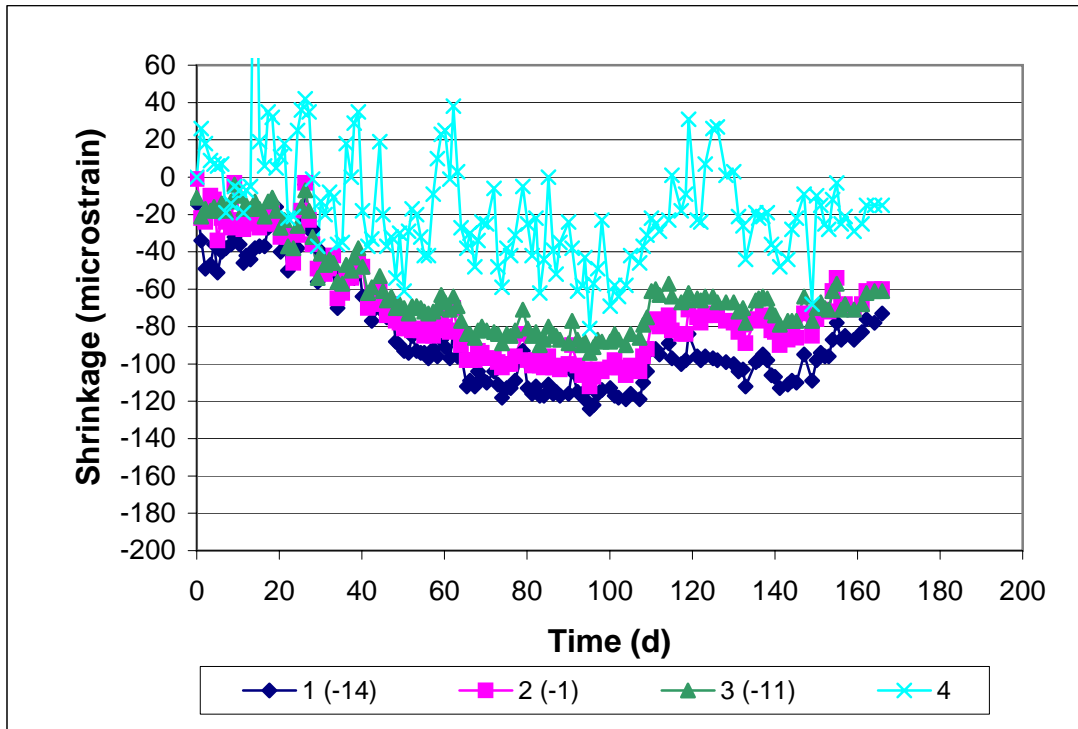


Figure A3.36a - Ring Test, Program 2. 14-day cure mix, Batch 143, Ring C. Drying begins on day 14.

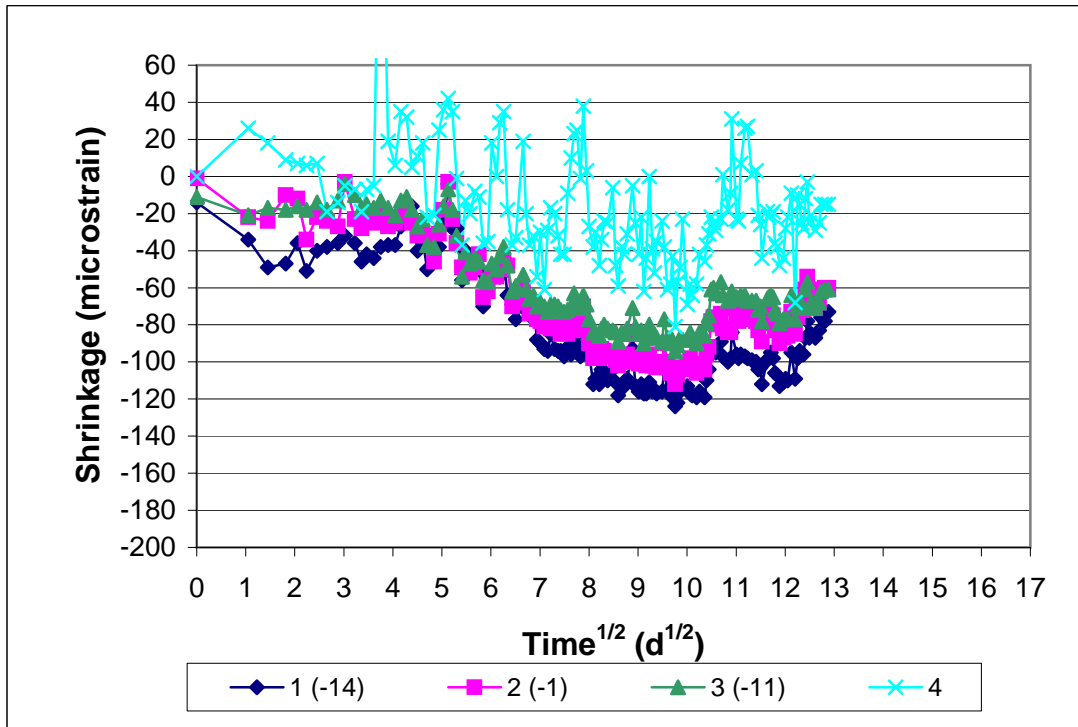


Figure A3.36b - Ring Test, Program 2. 14-day cure, Batch 143, Ring C. Shrinkage versus the square root of time.

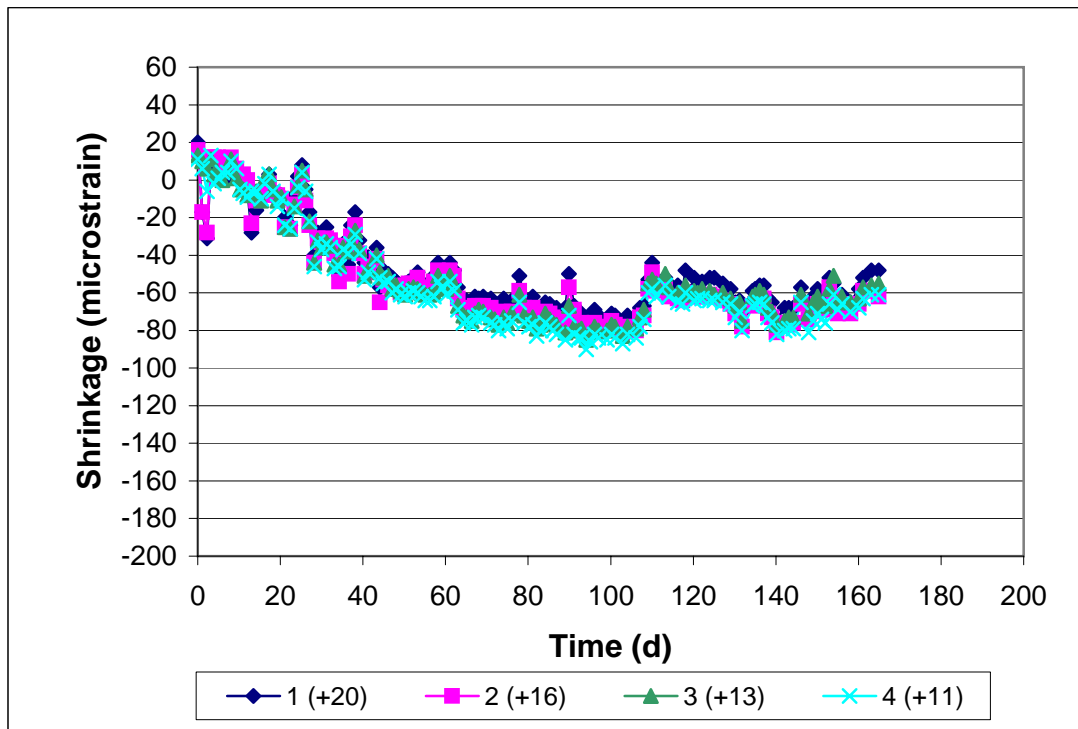


Figure A3.37a - Ring Test, Program 2. Type II C.G. mix, Batch 145, Ring A. Drying begins on day 3.

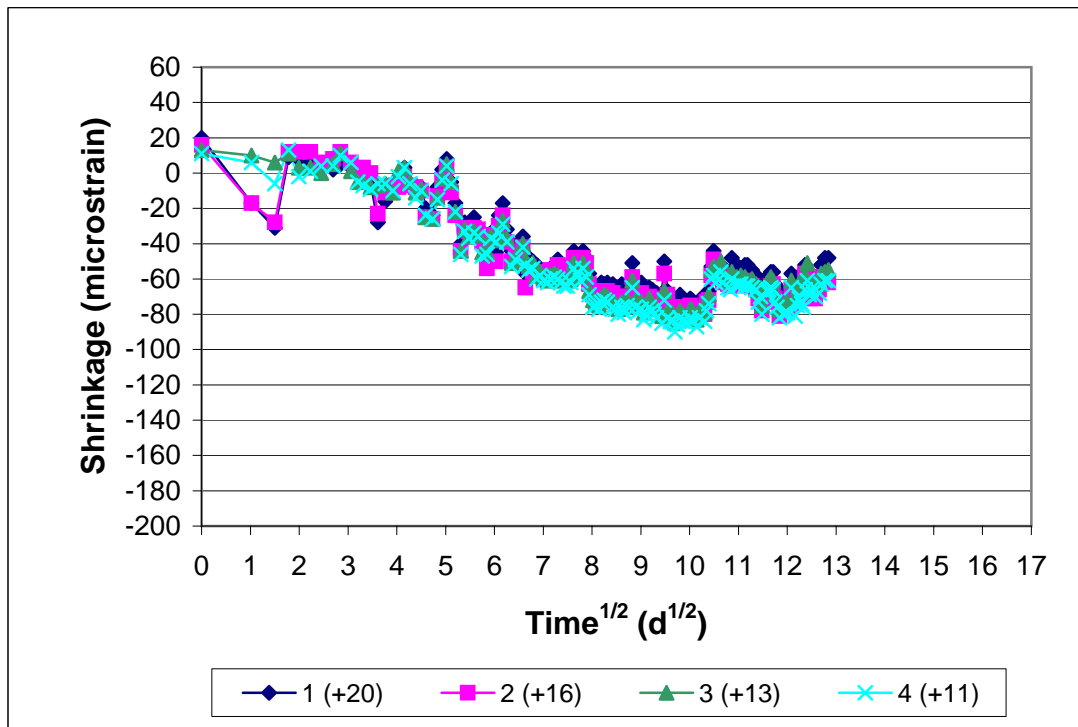


Figure A3.37b - Ring Test, Program 2. Type II C.G., Batch 145, Ring A. Shrinkage versus the square root of time.

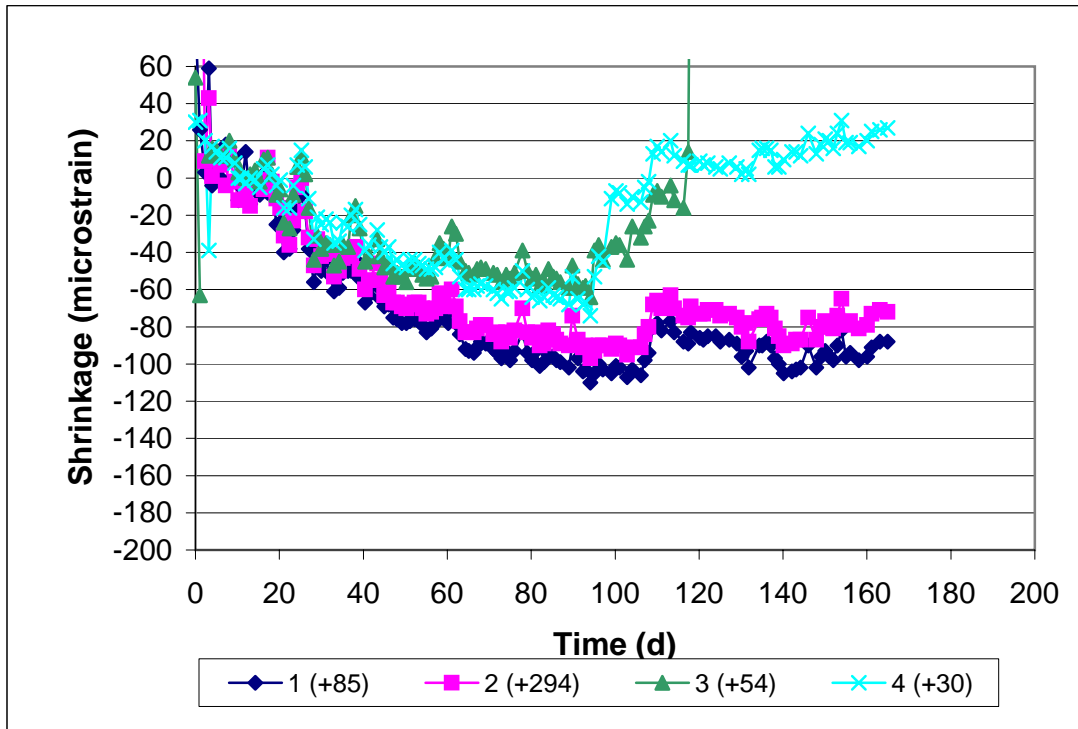


Figure A3.38a - Ring Test, Program 2. Type II C.G. mix, Batch 145, Ring B. Drying begins on day 3. Value in parentheses added to data to view all curves in the same window.

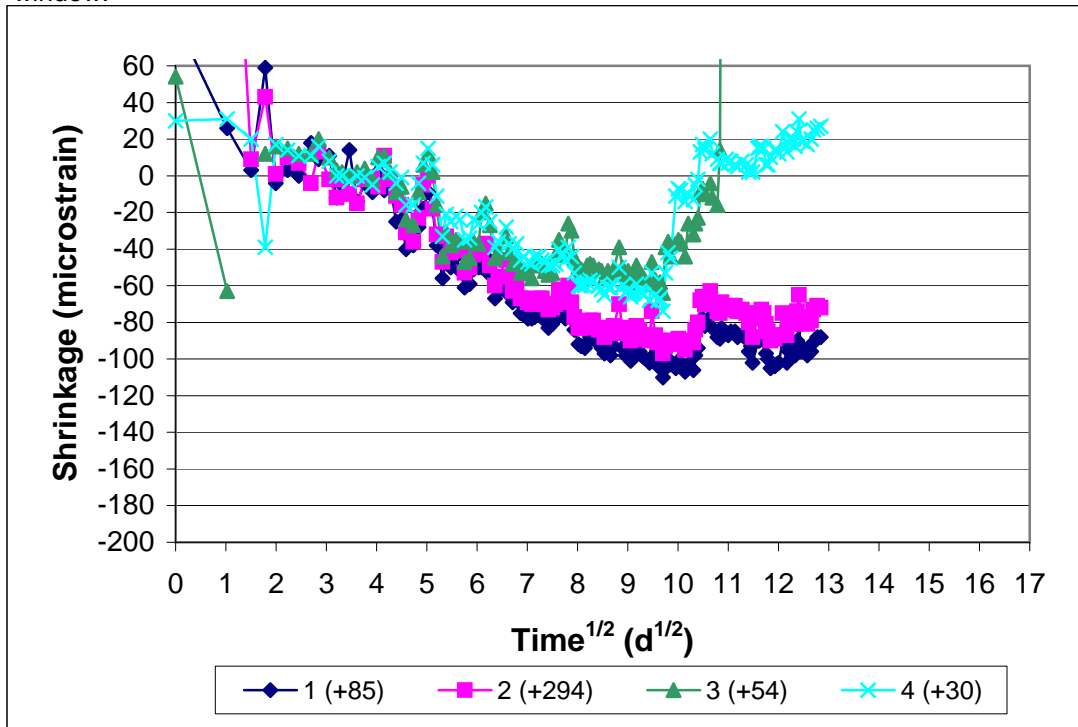


Figure A3.38b - Ring Test, Program 2. Type II C.G., Batch 145, Ring B. Shrinkage versus the square root of time.

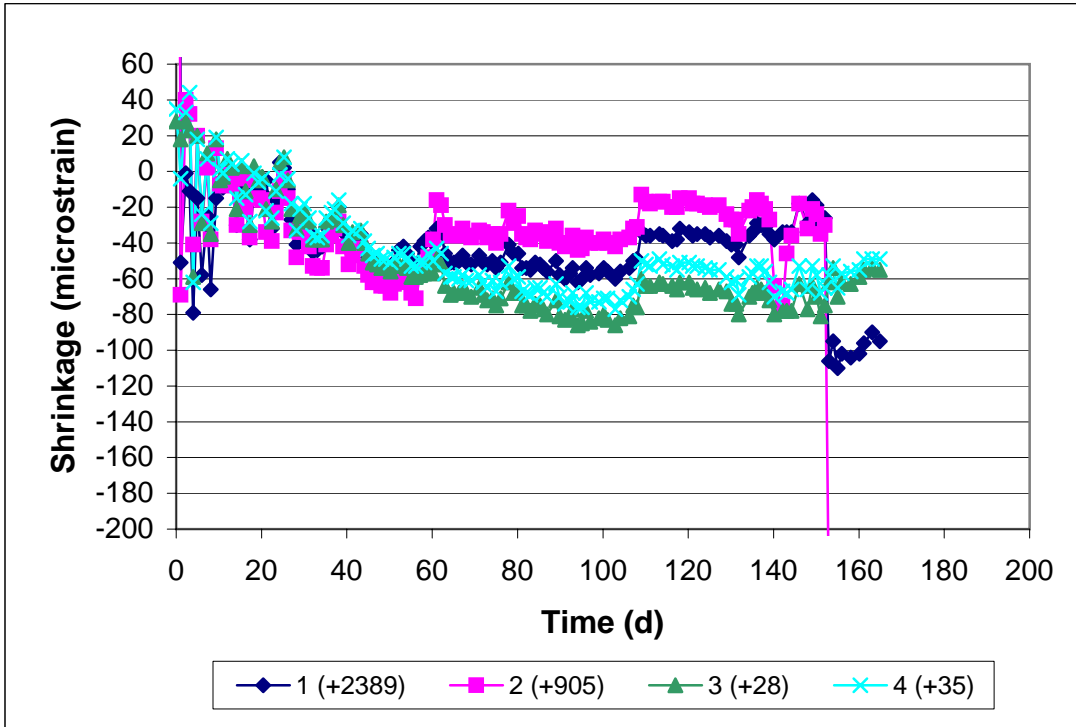


Figure A3.39a - Ring Test, Program 2. Type II C.G. mix, Batch 145, Ring C. Drying begins on day 3. Values in parentheses added to data to view all curves in the same window.

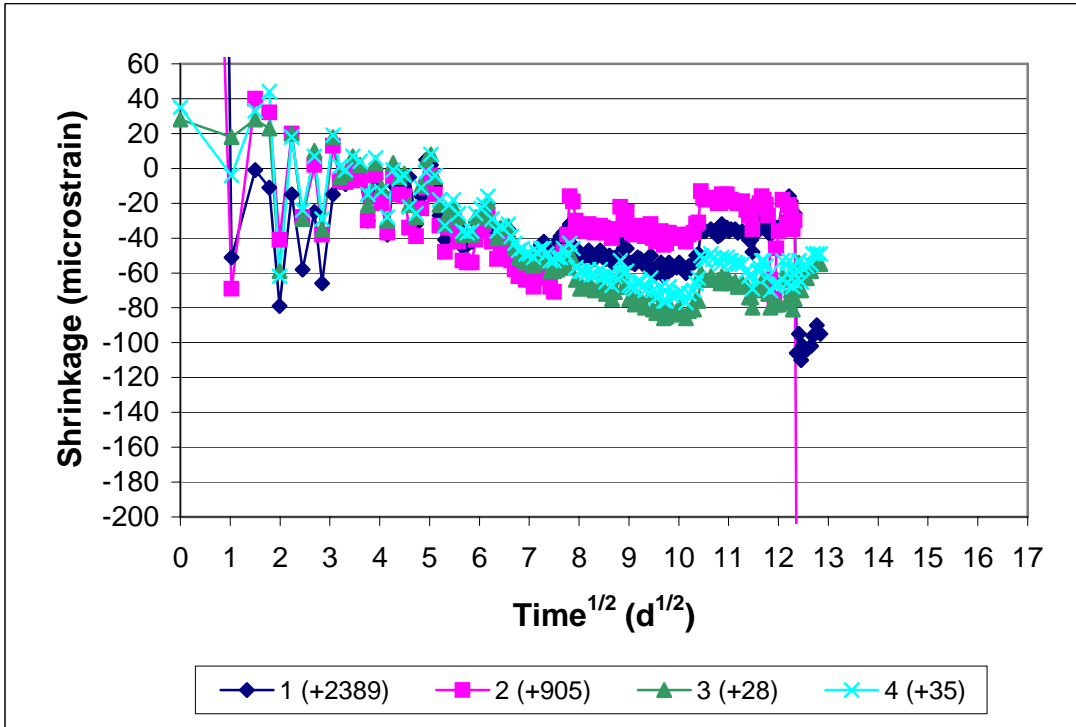


Figure A3.39b - Ring Test, Program 2. Type II C.G., Batch 145, Ring C. Shrinkage versus the square root of time.

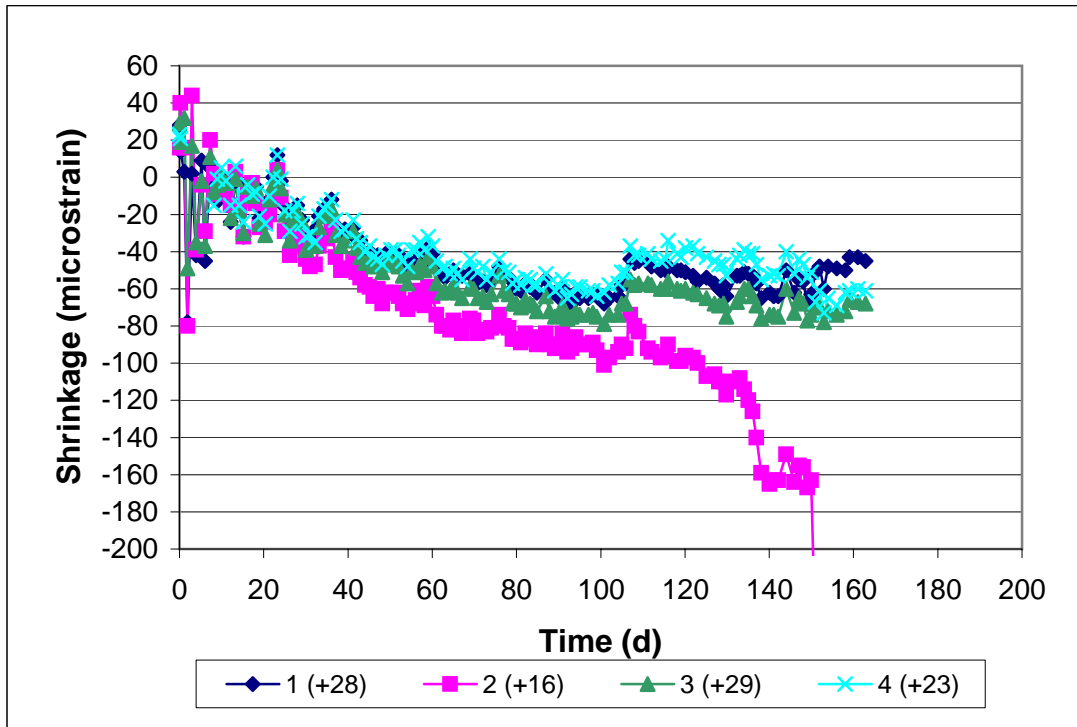


Figure A3.40a - Ring Test, Program 2. SRA mix, Batch 147, Ring A. Drying begins on day 3.

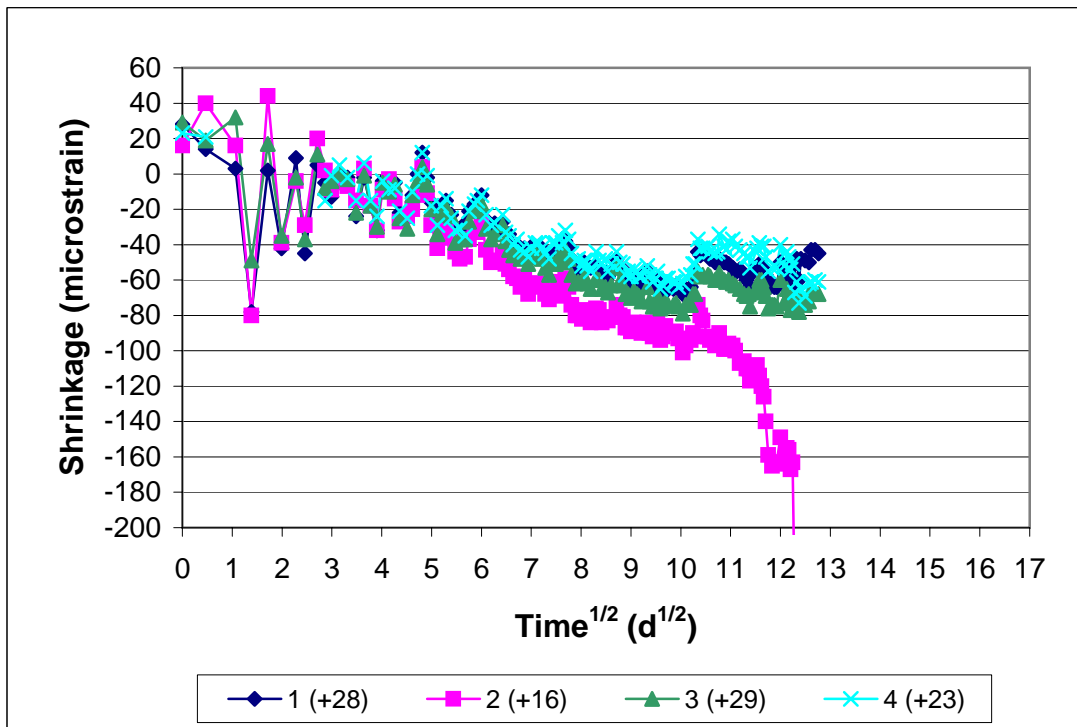


Figure A3.40b - Ring Test, Program 2. SRA, Batch 147, Ring A. Shrinkage versus the square root of time.

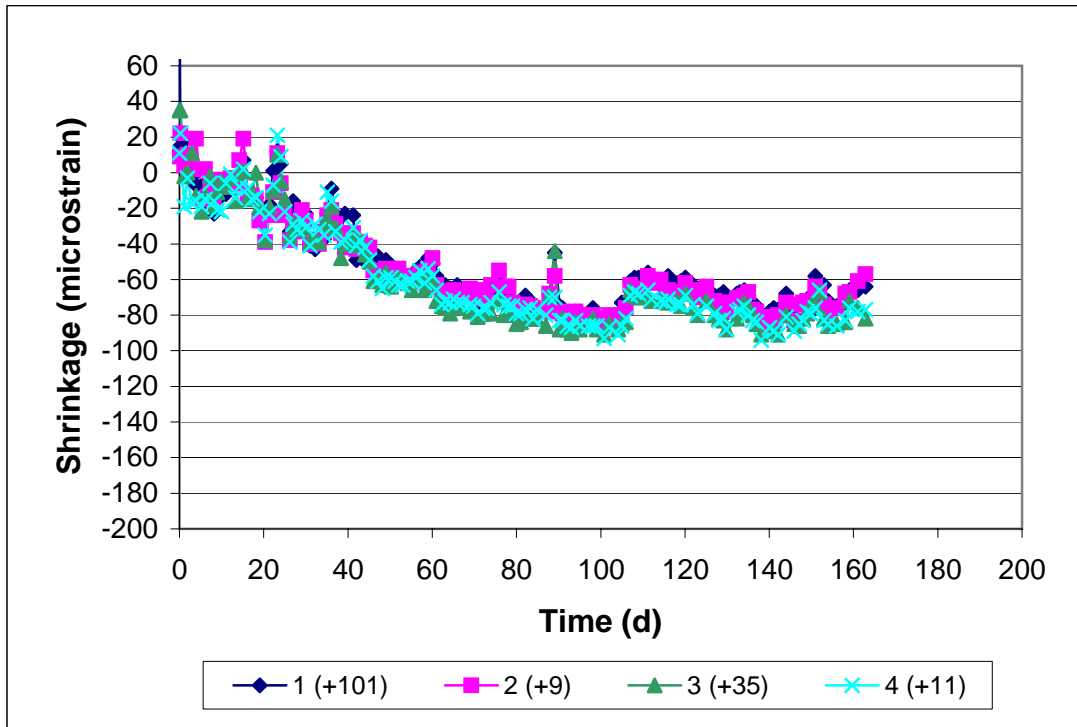


Figure A3.41a - Ring Test, Program 2. SRA mix, Batch 147, Ring B. Drying begins on day 3.

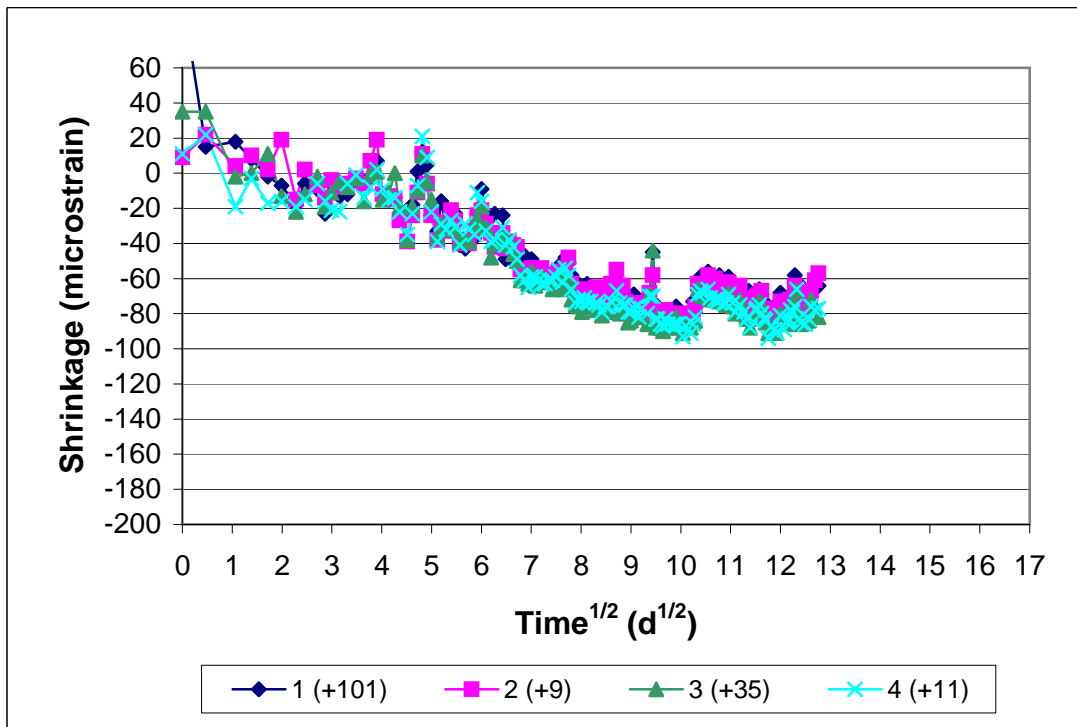


Figure A3.41b - Ring Test, Program 2. SRA, Batch 147, Ring B. Shrinkage versus the square root of time.

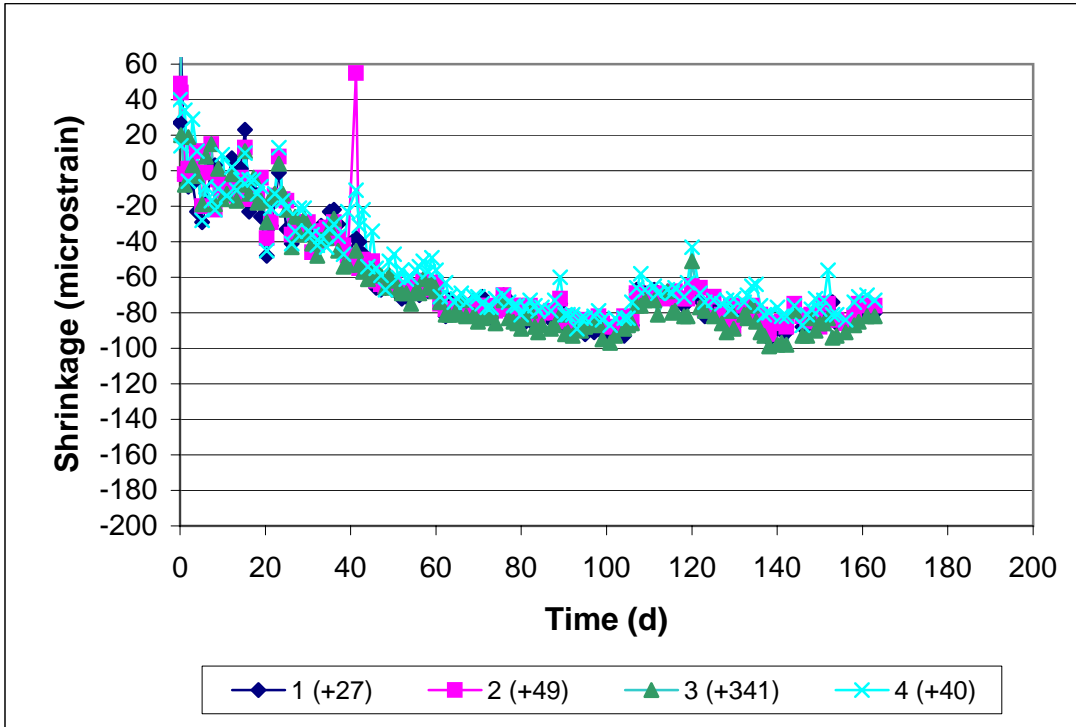


Figure A3.42a - Ring Test, Program 2. SRA mix, Batch 147, Ring C. Drying begins on day 3.

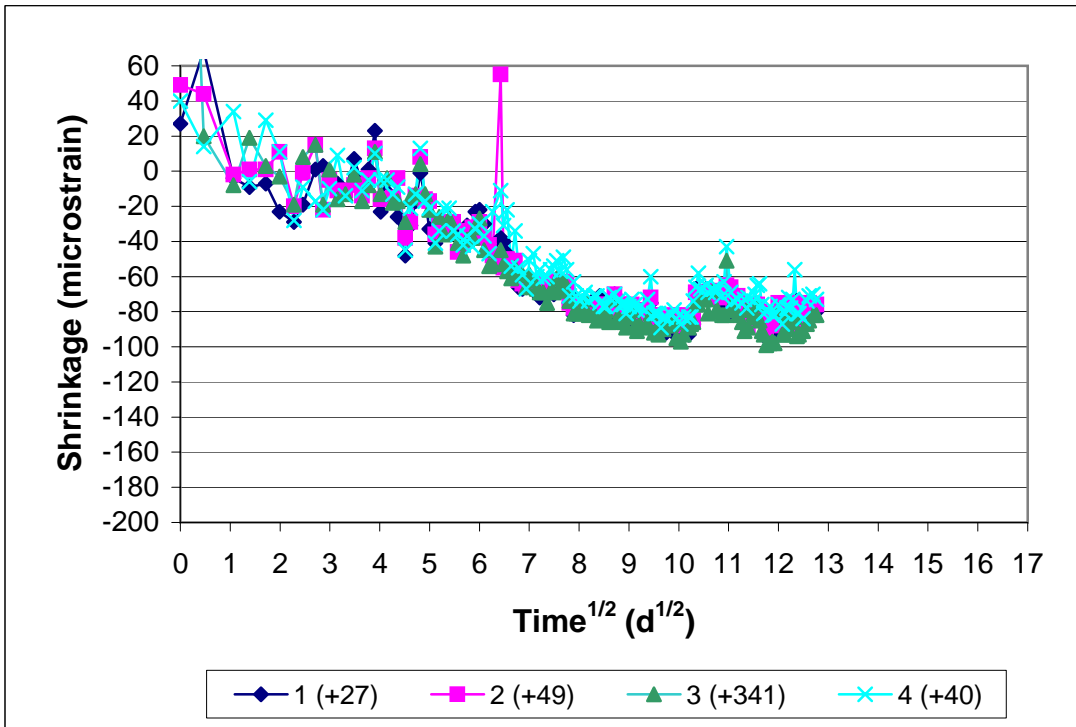


Figure A3.42b - Ring Test, Program 2. SRA, Batch 147, Ring C. Shrinkage versus the square root of time.

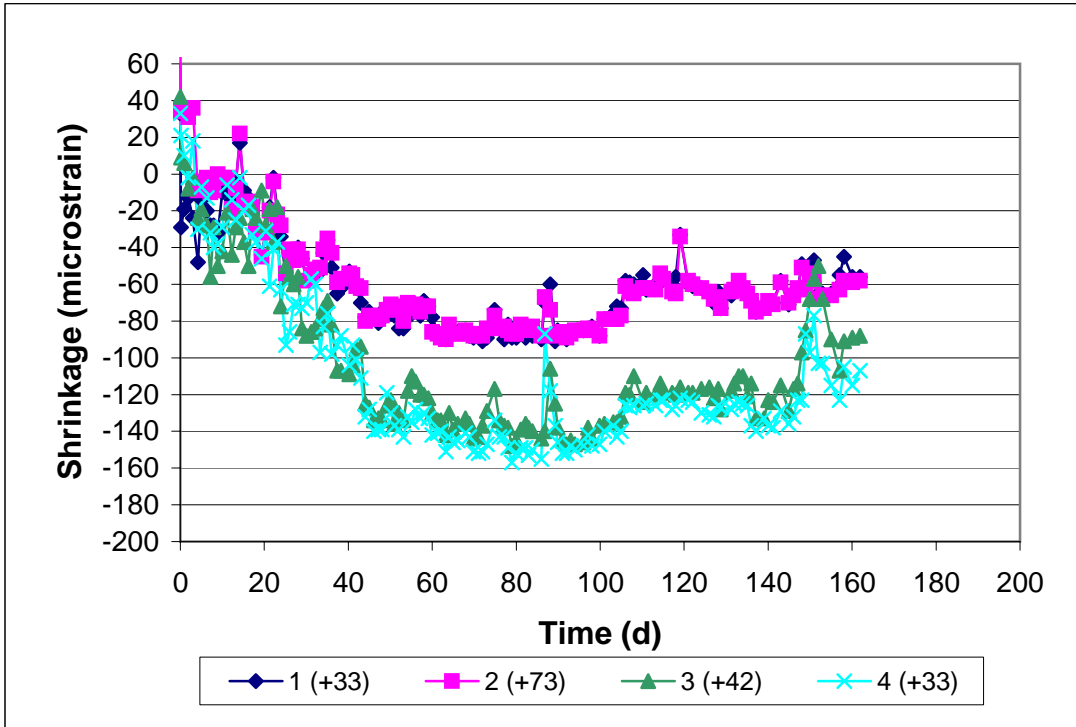


Figure A3.43a - Ring Test, Program 2. 497 mix, Batch 149, Ring A. Drying begins on day 3.

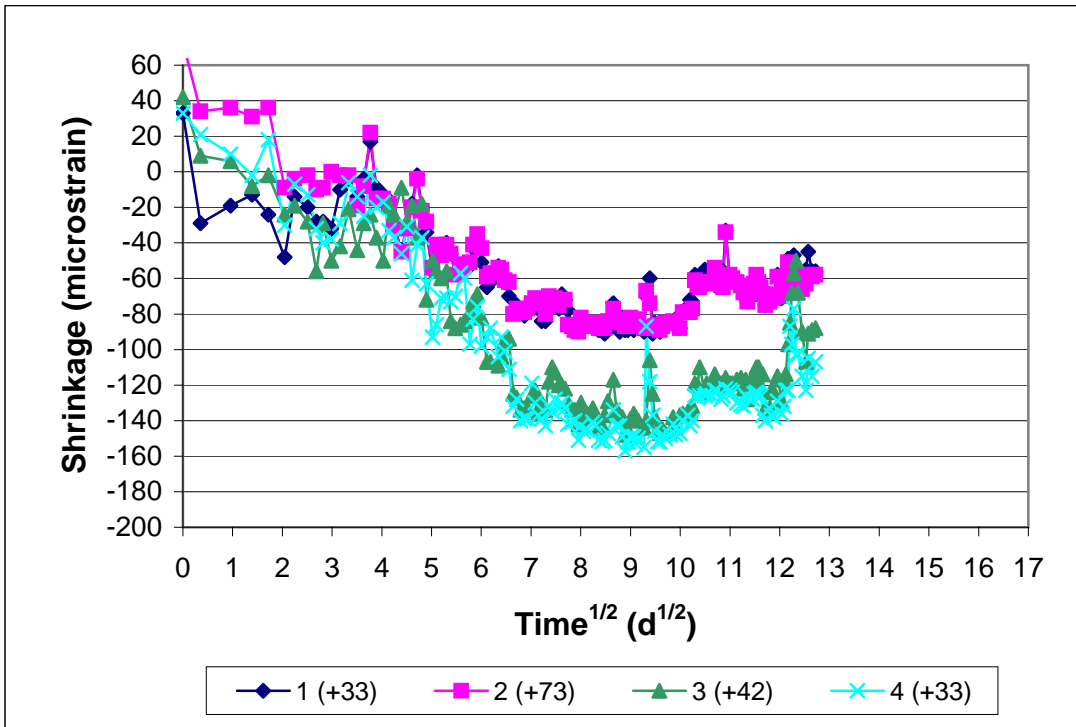


Figure A3.43b - Ring Test, Program 2. 497, Batch 149, Ring A. Shrinkage versus the square root of time.

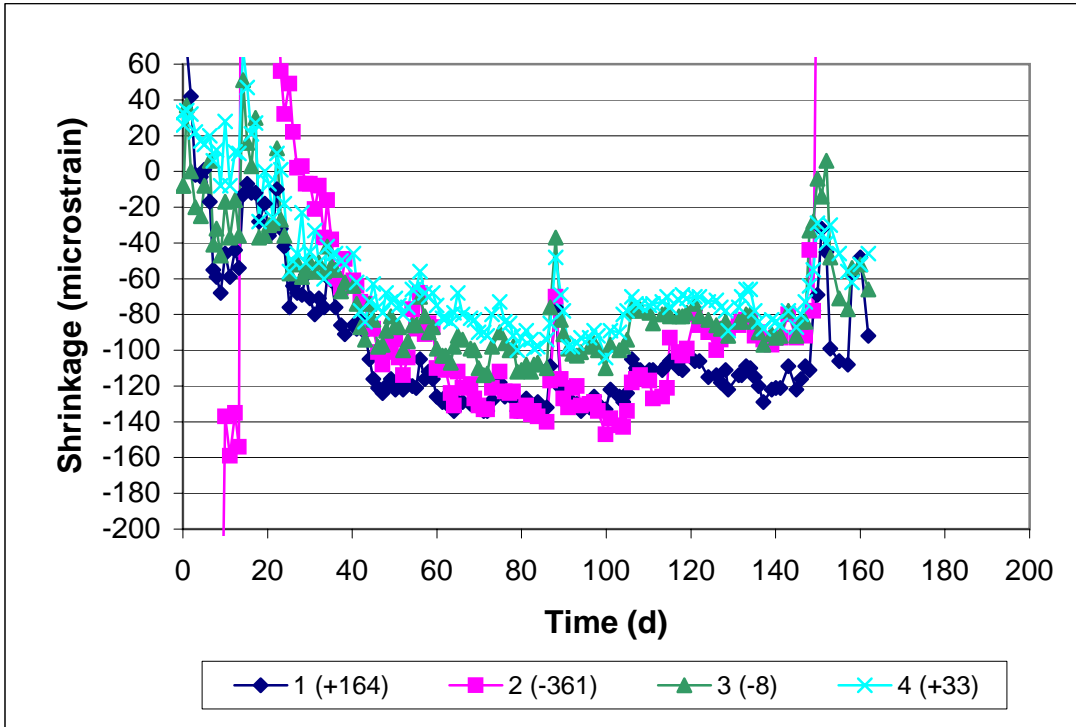


Figure A3.44a - Ring Test, Program 2. 497 mix, Batch 149, Ring B. Drying begins on day 3. Values in parentheses added to data to view all curves in the same window.

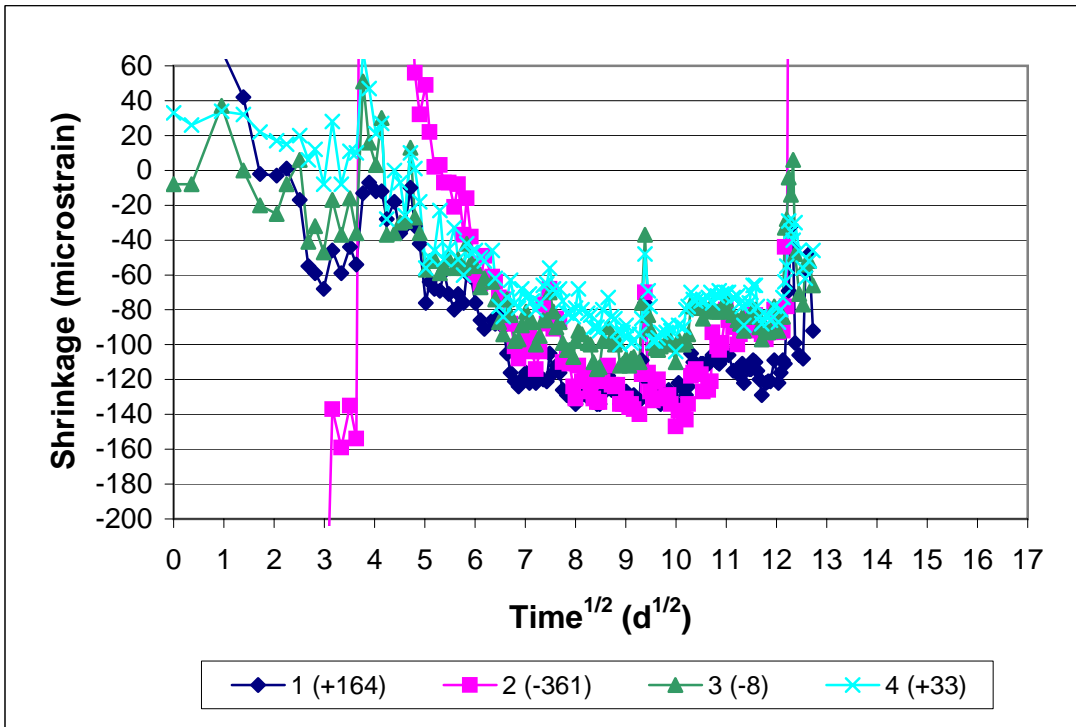


Figure A3.44b - Ring Test, Program 2. 497, Batch 149, Ring B. Shrinkage versus the square root of time.

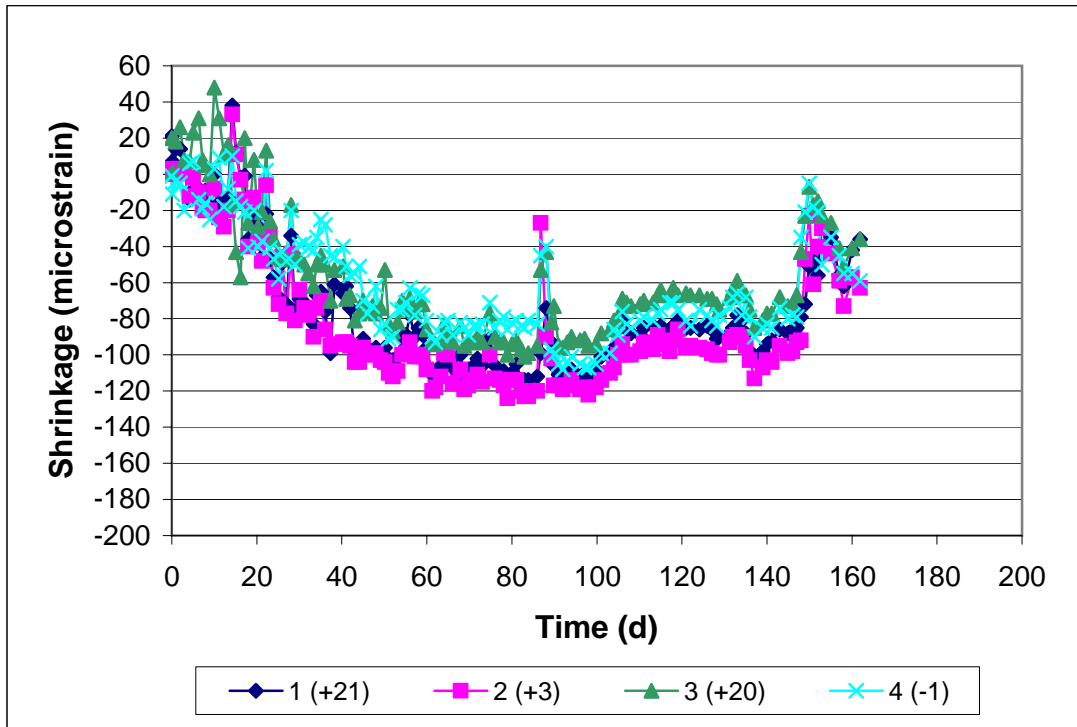


Figure A3.45a - Ring Test, Program 2. 497 mix, Batch 149, Ring C. Drying begins on day 3.

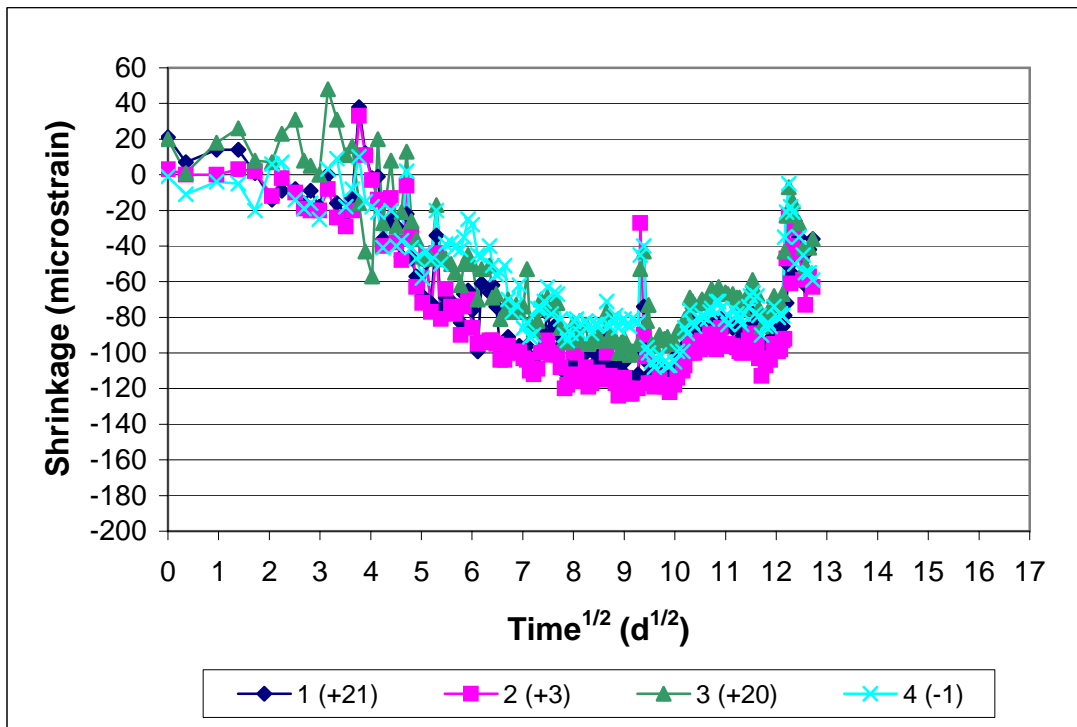


Figure A3.45b - Ring Test, Program 2. 497, Batch 149, Ring C. Shrinkage versus the square root of time.

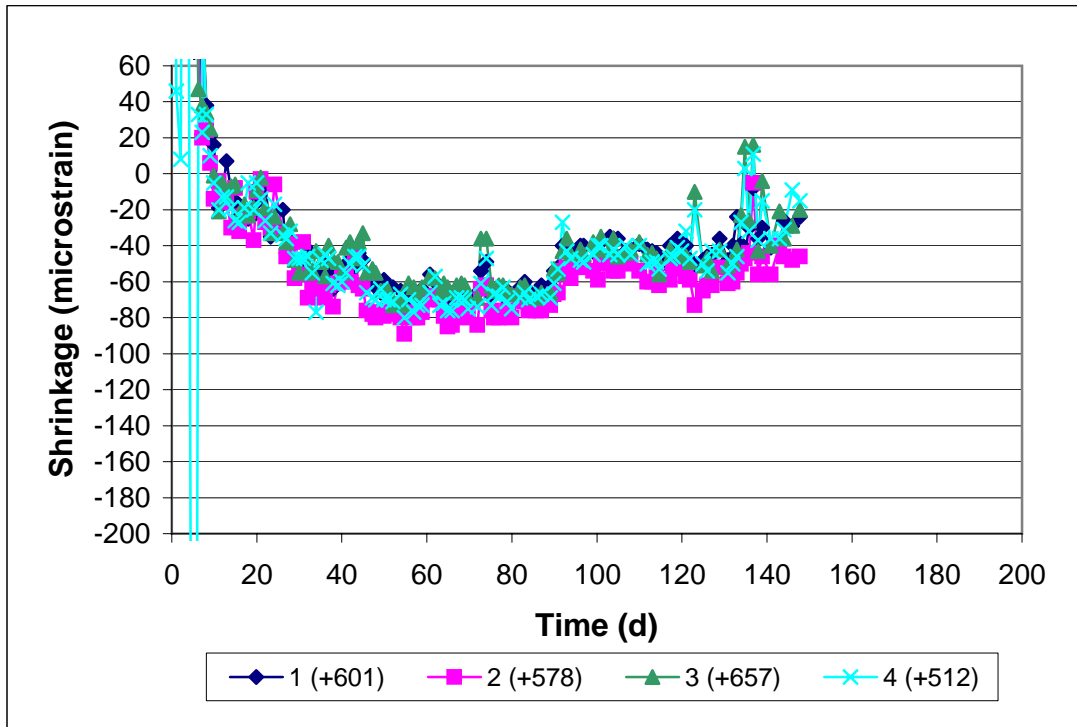


Figure A3.46a - Ring Test, Program 2. Quartzite mix, Batch 159, Ring A. Drying begins on day 3. Values in parentheses added to data to view all curves in the same window.

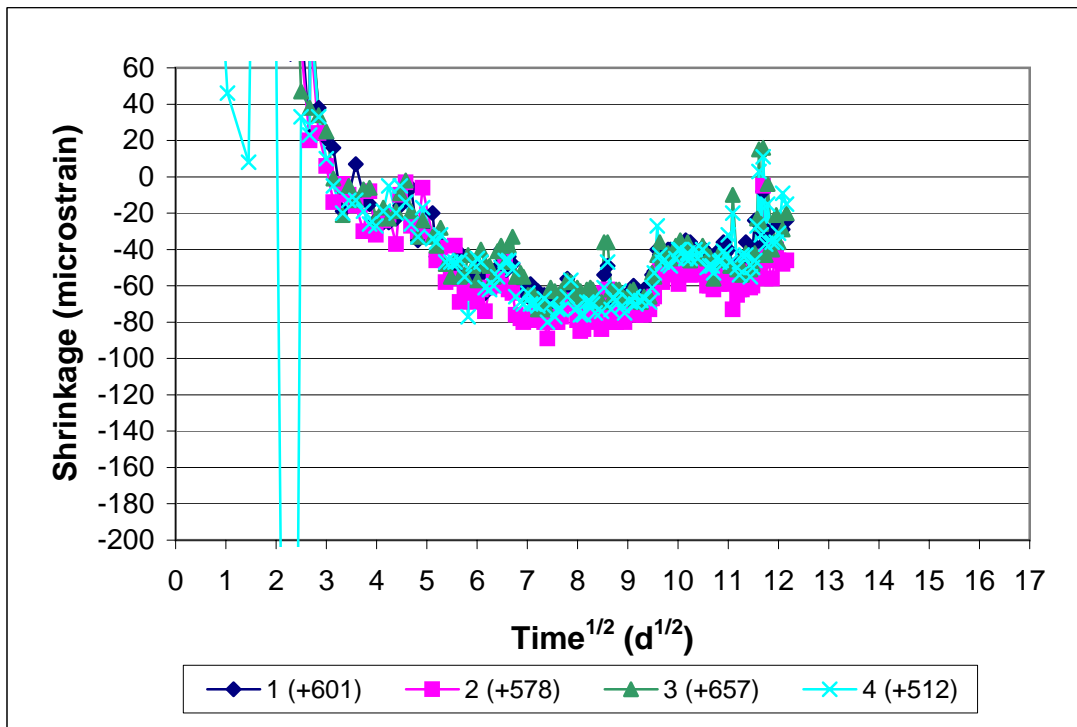


Figure A3.46b - Ring Test, Program 2. Quartzite, Batch 159, Ring A. Shrinkage versus the square root of time.

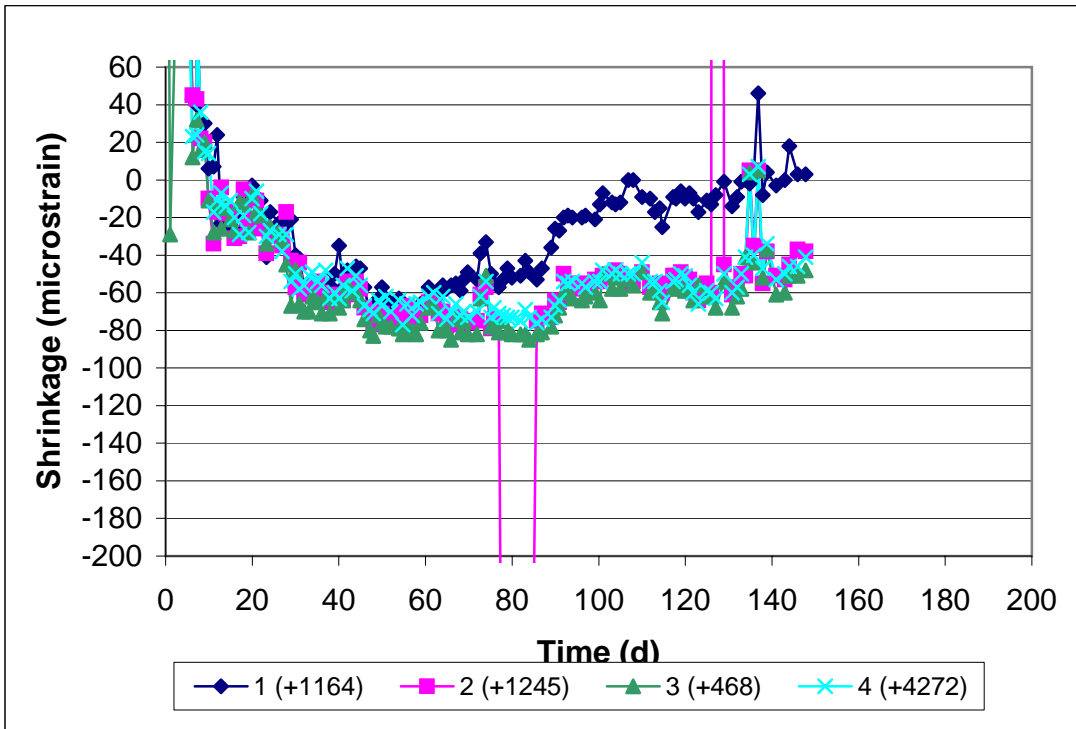


Figure A3.47a - Ring Test, Program 2. Quartzite mix, Batch 159, Ring B. Drying begins on day 3. Values in parentheses added to data to view all curves in the same window.

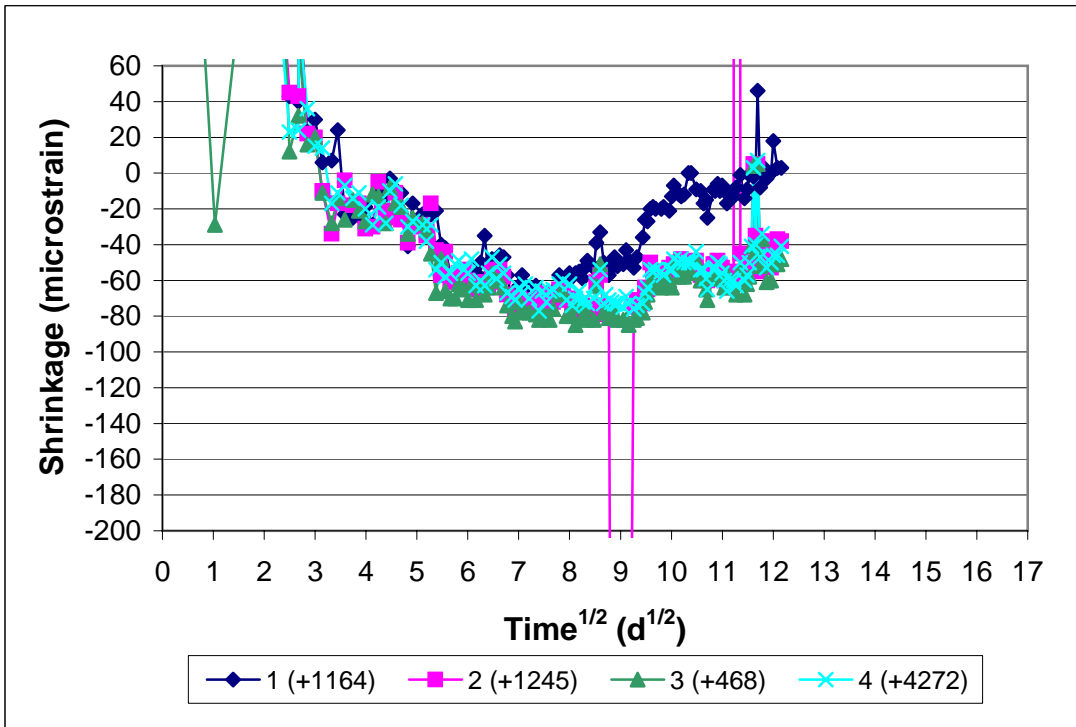


Figure A3.47b - Ring Test, Program 2. Quartzite, Batch 159, Ring B. Shrinkage versus the square root of time.

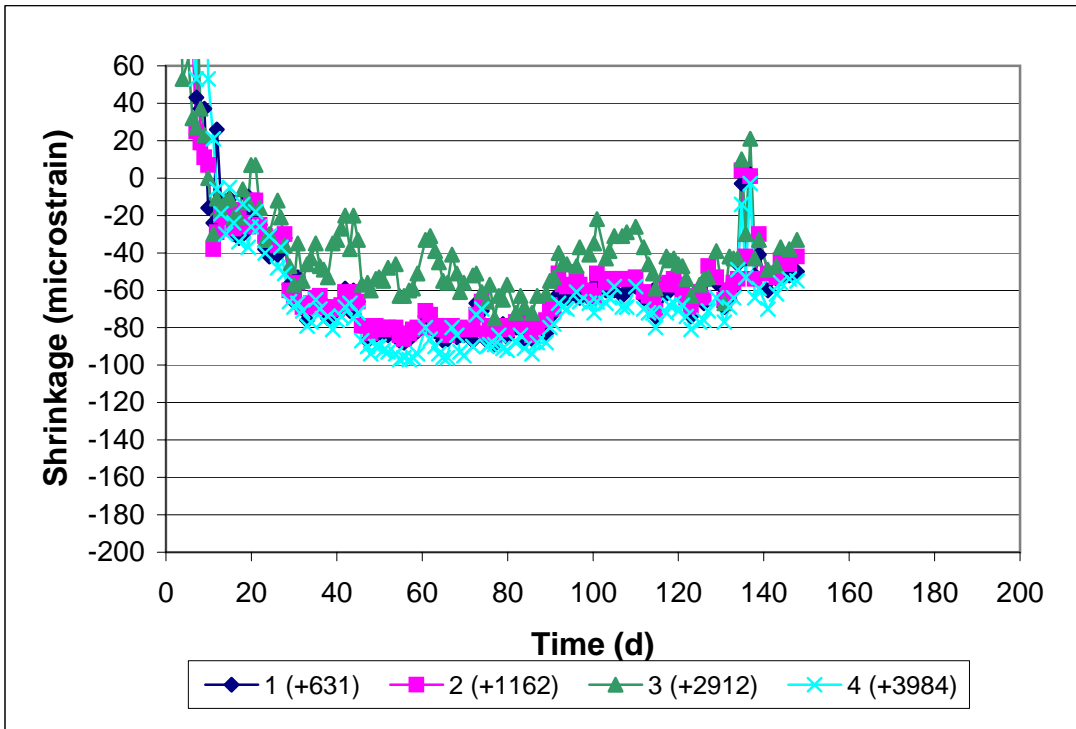


Figure A3.48a - Ring Test, Program 2. Quartzite mix, Batch 159, Ring C. Drying begins on day 3. Values in parentheses added to data to view all curves in the same window.

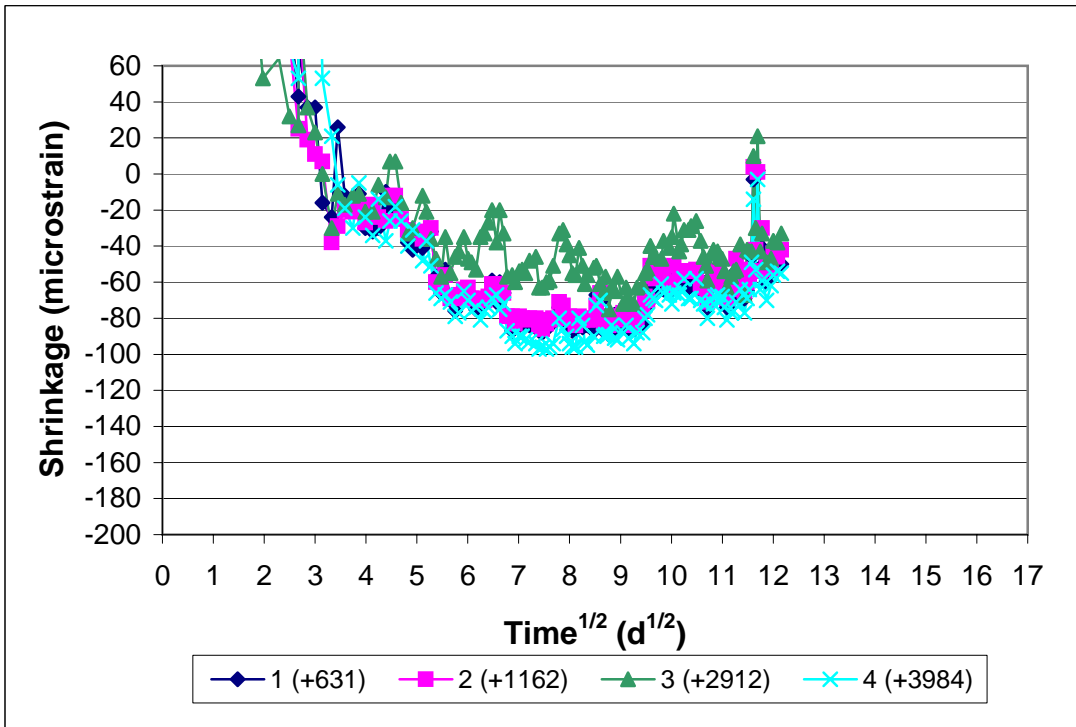


Figure A3.48b - Ring Test, Program 2. Quartzite, Batch 159, Ring C. Shrinkage versus the square root of time.